RIGA TECHNICAL UNIVERSITY

Faculty of Electrical and Environmental Engineering
Institute of Power Engineering

Zane Broka

Doctoral Student of the Study Programme "Power and Electrical Engineering"

HARNESSING THE VALUE
OF DEMAND-SIDE FLEXIBILITY
IN ELECTRICITY MARKETS

Doctoral Thesis

Scientific supervisor
Professor Dr. habil. sc. ing.
ANTANS SAUHATS

RTU Press
Riga 2020

ABSTRACT

During the last decade, Baltic electricity markets for wholesale trading in the day-ahead and intraday timeframe have been well-integrated with the Nordic power market. However, integration of balancing markets has been started only recently with the launch of the common Baltic balancing market in 2018 in line with the EU-wide trends on establishing regional balancing areas. As the 2025 deadline for synchronisation with the Continental Europe grid approaches, the Baltic transmission system operators have recognised the need to involve more local balancing resources. While currently the remaining Baltic imbalance is covered by regulation within the Integrated/Unified Power System (IPS/UPS) of Russia et al., the demand for balancing reserves will only continue to increase. Additionally, demand for balancing energy is expected to rise due to the growing share of intermittent generation sources. Abovementioned considerations require for increased flexibility of the Latvian power system.

This Doctoral Thesis is focussed on improvements of power system flexibility through employment of demand-side resources and optimisation of the overall balancing process. An optimised activation strategy of reserves is proposed which can be part of the Baltic TSOs' workflow where traditionally only human-based dispatching has been employed. Furthermore, assessment of the operating, planning and economic benefits obtainable from demand response (DR) in the Latvian power system is provided through detailed modelling of a DR-enabled technology for the Latvian case study. Finally, a robust tool for an economic assessment of DR from the end-user point-of-view has been developed. This can be useful for establishing a business case for DR and attracting new market participants to the Baltic balancing market, thus increasing market liquidity and improving the overall system flexibility. Hence, the Doctoral Thesis provides an array of tools and methods on establishing the value of demand response in the Latvian power system. Along with the optimised balancing process, this can aid in improving the flexibility of the Latvian and Baltic power systems.

ANOTĀCIJA

Pēdējo desmit gadu laikā Baltijas valstu elektroenerģijas tirgi, kas paredzēti vairumtirdzniecībai nākamās dienas un tekošās dienas ietvaros, ir veiksmīgi integrēti Ziemeļvalstu elektroenerģijas tirgū. Tomēr balansēšanas tirgus integrācija sākusies vien nesen līdz ar vienotā Baltijas balansēšanas tirgus atvēršanu 2018. gadā, kas atbilst arī reģionālo balansēšana apgabalu izveides tendencēm Eiropas Savienībā. Baltijas energosistēmu sinhronizācija ar kontinentālās Eiropas tīklu plānota 2025. gadā. Tuvojoties šim termiņam, pārvades sistēmas operatori ir atzinuši vajadzību pēc lielākas vietējo balansēšanas resursu iesaistes. Pagaidām Baltijas valstu atlikušā nebalansa regulēšana tiek nodrošināta Krievijas pārvaldītās IPS/UPS apvienotās energosistēmas ietvaros. Tāpēc pieprasījums pēc balansēšanas rezervēm turpinās arvien pieaugt. Turklāt ir sagaidāms, ka tas palielināsies arī tāpēc, ka pieaug pārtraukumaino ģenerācijas avotu īpatsvars. Iepriekš minētie apsvērumi prasa palielināt Latvijas energosistēmas elastību.

Promocijas darbā galvenā uzmanība pievērsta energosistēmas elastības uzlabošanai, izmantojot patēriņa resursu elastību un optimizējot balansēšanas procesu kopumā. Darbā piedāvāta optimāla balansēšanas rezervju aktivizācijas stratēģija, ko iespējams iekļaut Baltijas pārvades sistēmas operatoru darba procesā, kur tradicionāli dispečeru darbs balstīts galvenokārt uz cilvēkresursu izmantošanu. Turklāt darbā novērtēti ieguvumi, ko Latvijas energosistēmas darbībā, tās ekonomiskumā un plānošanā var sniegt patēriņa reakcijas (DR) izmantošana. Tas paveikts, detalizēti modelējot iekārtas ar patēriņa vadības iespējām Latvijas energosistēmas kontekstā. Visbeidzot, izstrādāts rīks DR ekonomiskajam novērtējumam no galalietotāja viedokļa. Tas var būt noderīgs, lai pamatotu DR izmantošanas ekonomisko lietderību un piesaistītu jaunus dalībniekus Baltijas balansēšanas tirgū. Līdz ar to tiktu palielināta tirgus likviditāte un uzlabota energosistēmas elastība kopumā. Tādējādi promocijas darbā izstrādāti vairāki rīki un metodes patēriņa reakcijas vērtības noteikšanai Latvijas energosistēmā. Līdztekus ar optimizētu balansēšanas procesu tas var palīdzēt uzlabot Latvijas un Baltijas energosistēmu elastību.

CONTENTS

LIST OF FIGURES

LIST OF TABLES

INTRODUCTION

Background and relevance of the research

The action plan for development of electricity market in the Baltic states and integrating it into the wider EU energy market was formally established by the **Baltic Energy Market Interconnection Plan** (BEMIP) in 2009 [1]. Lithuania, Latvia and Estonia was referred to as "the Baltic energy island" in the BEMIP action plan where it was recognised that sufficient interconnections should be developed to the grids of Finland, Sweden and Poland as well as the Baltic area should be integrated with the Nordic power market [2]. As a result of the BEMIP implementation, the **wholesale power markets** of the three Baltic states have been well coupled with the Nordic countries by joining the Nord Pool power exchange in 2010 (Estonia), 2012 (Lithuania) and 2013 (Latvia) respectively [3]. Now, electricity producers and traders from the Baltic states successfully operate in both **day-ahead** and **intraday** market of the Nord Pool where the majority of wholesale transactions take place.

Nevertheless, the Baltic power system still has some distinct characteristics from the rest of Europe due to its synchronous operation with the **Integrated/Unified Power System (IPS/UPS)** of Russia and Belarus. The Russian power system provides primary power reserves for frequency regulation and secure system operation within the BRELL (Belarus, Russia, Estonia, Latvia and Lithuania) ring [4]. The synchronous operation of the Baltic states with the IPS/UPS is planned to be terminated by **2025** which is the deadline to complete the synchronisation of the Baltic power grid with the Continental Europe network through two links between Lithuania and Poland: a 1000 MW alternating current link LitPol and a new 700 MW direct current submarine cable named Harmony Link [5].

However, in order to increase the energy independence of the Baltic states and involve more local balancing resources in power system regulation already several years before the planned desynchronisation, the TSOs of Latvia, Estonia and Lithuania (Augstsprieguma tīkls AS, Elering and Litgrid) have launched a **common Baltic balancing market** within which the three countries are able to share balancing energy [6]. The Baltic balancing market has been in operation since January 1, 2018, and the intention is to also integrate that in a joint Nordic-Baltic balancing market.

Furthermore, the growing share of intermittent generation sources, especially wind power plants, combined with the planned synchronisation of the Baltic power systems with the Continental Europe grid, only increases the demand for balancing resources and improved flexibility of the power system to be able to ensure frequency regulation not only during normal conditions but also in case of major outages and even in islanding mode [7].

Flexibility of the power system is its ability "to accommodate the variability and uncertainty in the load-generation balance" [8]. Generally, most of the flexibility today is provided by the **conventional power plants**, particularly, reservoir and pumped storage hydropower plants and gas-fired turbines which are traditionally considered as more flexible than, e.g., base load coal and nuclear plants [8]. Nevertheless, it is also possible to harvest flexibility from **demand-side resources**, the potential of which has been recognised, though still remains underexploited [8].

Demand response (DR) has become a particularly attractive option for increasing power system flexibility with the recent advances in IT, control and forecasting tools and techniques [9]. Moreover, the advancement of DR fortunately coincides with the increasing penetration of renewable generation largely composed of variable and intermittent energy sources calling for more and more flexibility in the power system.

It should be noted though that systematic load shedding is recognised as the **most obvious form of demand response** employed in various forms worldwide **for decades** as a last resort to avoid system blackout [9]. Automatic load shedding is a measure used to prevent a frequency collapse under emergency conditions or to prevent deep drops in system frequency. It is based on the philosophy that in case of emergency "selective restrictions in the energy supply are more acceptable than the consequences of an extended network breakdown resulting in a power cut lasting for several hours" [10]. Nevertheless, in order to narrow the amount of load to be shed, it is usually implemented in stages, starting with the least important loads [11].

However, the recent evolvement of a vast array of IT tools and techniques has enabled the advancement of much more sophisticated forms for demand response. Thus, nowadays in many power systems worldwide, **demand-side resources** can participate in balancing of the power system on a par with generation-side, including large-scale storage. It is acknowledged that, through provision of flexibility, demand response could bring a wide range of **benefits** and thus constitute one of the main components of the smart grid [12]. Notwithstanding, there are also a number of **challenges** related to the involvement of the still untapped demand-side resources in everyday control actions of the power systems.

European Commission Smart Grid Task Force has defined **demand-side flexibility** as "the changes in energy usage by end-use customers (domestic and industrial) from their current/normal consumption patterns in response to market signals, such as time-variable electricity prices or incentive payments, or in response to acceptance of the consumer's bid, alone or through aggregation, to sell demand reduction/increase at a price in organized electricity markets" [13]. Similarly, **demand response** (DR) is defined as "voluntary changes by end-consumers or producers or at storages of their usual electricity/gas flow patterns" [13].

On the one hand, the source of this flexibility is either industrial, commercial or domestic consumers [14] who may use their consumption elasticity or some form of distributed generation and storage. On the other hand, there is a range of possible procurers of flexibility services, including TSOs, DSOs and suppliers, who might use it for balancing of the power system (TSOs), congestion management of the grid (DSOs) or their own portfolio balancing (suppliers) [13]. As a result, three main types of benefits from DR can be distinguished [9]:

- **operating benefits** by balancing the fluctuations (forecast errors) of intermittent renewables, such as wind generation. It is considered that reliability of demand for provision of ancillary services may be even larger than that from conventional generators and, also, the effective ramping rate of aggregated demand might be much higher [9]. Moreover, effective use of DR can also decrease the dependence on power imported through interconnections from neighbouring regions [9]. This aspect is examined in a case study for Latvia in Chapter 3;

- **planning benefits** by reducing the capacity requirements of the system due to employment of DR so that investments in both network reinforcement or generation capacity are deferred or avoided [9], [14];
- **economic benefits** by decreasing the market power of producers and reducing the average wholesale electricity prices [9], [15].

However, in order to be able to actually receive those benefits, there are a number of challenges to be solved beforehand. Apart from other factors, the challenges involved depend on the **type of demand response**. To this end, two main categories of DR can be distinguished:

- **implicit DR** or indirect load control whereby consumers react to dynamic market price or network tariff signals [16]. These signals can be issued also in the form of, e.g., "time of use" rates with more expensive price during peak hours and cheaper price during the night or "critical peak pricing" [9];
- **explicit DR** or direct load control whereby (usually) aggregated demand-side resources are traded in the wholesale, balancing and capacity markets and consumers are rewarded when changing their consumption upon request for activation of balancing energy or congestion management in the network [16]. This type of DR is computationally and communicationally more intensive than implicit DR as it involves direct communication with individual appliances [16].

Important to note that **both forms of DR are needed** to accommodate different types of consumers and loads and "exploit the full spectrum of consumer and system benefits" [16]. Furthermore, since the amount of flexible load of individual consumers is often too low to be able to participate in the market, a new market participant, **aggregator**, is introduced who acts as an intermediary between smaller entities and the market [17], [18]. The role of aggregator can be fulfilled either by the customer's retailer or another third-party [16].

Some of the main **challenges** for implementation of both forms of DR [9] are as follows:

- lack of appropriate **market** mechanisms and **regulatory** framework;
- difficulty in establishing a **business case** for DR and/or DR aggregator;
- difficulties establishing DR as a **valuable resource**;
- end-user **behaviour**.

All these challenges can be directly related also to the Latvian power system where demand response, properly implemented and integrated into the system, could serve as a valuable resource in providing the required additional flexibility.

The concept of DR and its employment as a power system flexibility source has been reviewed in a large number of scientific papers addressing the overall benefits, challenges, barriers and enablers [19]–[22] as well as country-specific case studies [23]–[26]. However, this Doctoral Thesis provides an assessment of measures that could **increase the flexibility of power systems** by employing different types of **demand response** sources and, additionally, by improving the overall system **balancing process**. To that end, we start with the latter by proposing an optimised activation strategy of reserves and then move on with assessment of the obtainable operating, planning and economic benefits from demand response in the power system by providing detailed modelling of a residential DR-enabled power-to-heat (P2H)

technology for the Latvian case study. The specific type of technology has been selected considering that P2H exhibits "large and predictable capacities of DR" compared to smart electric appliances [27]. Furthermore, the Thesis contributes to establishing a business case of DR with a robust tool for an economic assessment of DR from the end-user point-of-view. The knowledge of possible benefits could potentially attract new market participants to the Baltic balancing market, thus increasing market liquidity and improving the overall system flexibility. Hence, the Doctoral Thesis provides a vast array of tools and methods on establishing the value of demand response in the Baltic power system.

Hypothesis, objective and tasks of the Thesis

Hypothesis

To sustain the growing needs for power system flexibility, demand response can be employed as a valuable resource able to bring benefits both for the power system as a whole and for the end-users providing it. Additionally, power system flexibility can be improved through optimisation of the balancing process, thus promoting efficient use of the available reserves both cost-wise and energy-wise.

Objective

Cost-benefit assessment of demand response deployment, considering its implications both on the power system, including distribution grid, and end-users providing it, and development of a strategy for optimal activation of balancing resources in the Baltic power system.

Tasks

1. To develop methodology and a software tool for optimising the activation process of balancing resources within the common Baltic balancing market framework.
2. To devise building thermal models for estimation of their heating demand (provided by DR-enabled electric heating).
3. To study the potential impact and benefits of large-scale deployment of DR-enabled technologies such as smart electric thermal storage in the Latvian power system.
4. To develop methodology and a software tool for probabilistic cost-benefit assessment of demand response provision from the DR asset owner point-of-view.

Research methods and tools

Research studies presented in the Doctoral Thesis were performed employing various bespoke modelling tools and algorithms developed in-house at the RTU Institute of Power Engineering by Thesis author together with other Institute staff members.

For defining and solving the optimisation problem of the *AOF parameter search* tool presented in **Chapter 1**, **MATLAB** scripting environment and **Global Optimization Toolbox** was used to take advantage of its data processing abilities and solver *patternsearch*.

Consequently, a stand-alone application was compiled which can be deployed on a standard computer with the royalty-free **MATLAB Runtime** environment. **Microsoft Excel** was used for data input and output due to its user-friendly interface. Additionally, validation and analysis of the results obtained by the optimiser also take place in Excel to enable the user to manually inspect the dynamics of ACE forecast and the course of regulation activations in any particular hour in the test dataset.

Building thermal network models introduced in **Chapter 2** were devised in **MATLAB Simscape** which enables creation of models of physical systems (buildings in our case) and simulation of their thermal performance using **MATLAB Simulink**. Thus, MATLAB environment was used both for identification of equivalent thermal network parameters and building simulations to derive their heating demand timeseries for power system modelling in the next chapter. Performance of the simplified thermal network was compared against the results of a more complex *EnergyPlus*-calibrated model developed by our partners within the RealValue project. For physical experiments in the buildings, temperature loggers were used to derive the cooling and heating curves of the houses.

In **Chapter 3**, **MATLAB** was used for power flow modelling in the distribution grid. Solvers from its **Optimization Toolbox** were employed for optimal load scheduling based on different objectives. Namely, for minimisation of load variance and minimising the cost of losses, *fmincon* solver (employing the *interior-point* algorithm) was used which is intended for constrained nonlinear optimisation problems. However, energy cost minimisation, being a linear problem, was performed with the *linprog* solver using the *dual-simplex* algorithm.

Furthermore, for power system modelling, the RTU's in-house developed scheduling tool **OptiBidus-TEC** was employed to derive electricity production schedules for two major cogeneration plants. When modelling the different future scenarios, **MATLAB** was employed to prepare the input data by scaling and adjusting the data according to the scenario assumptions. Furthermore, the concluding power system benefit assessment was implemented in **Excel**. It also involved employment of the **method of least squares** for linear regression.

Similarly to the approach used in Chapter 1, *DR Assess* tool presented in **Chapter 4** was developed using the MATLAB scripting environment. To make it usable for any interested person, a stand-alone application was compiled which can be deployed on a standard computer with the royalty-free **MATLAB Runtime** environment. Additionally, due to its user-friendly interface, **Microsoft Excel** was used for data input and output of detailed results for exemplary scenarios. They allow studying each demand response activation of the scenario and related cash flows in high detail.

Scientific novelty

To facilitate optimal activation of balancing resources by the transmission system operator, a **bespoke tool, *AOF parameter search***, has been developed. It includes a complex algorithm mimicking the activities of a TSO dispatch operator in ordering mFRR products to sustain the power system balance. However, in contrast to solely human-based dispatching of reserves, the proposed algorithm allows automated processing of a large amount of historic data to devise an

optimal strategy for the power system regulation process. The optimised regulation parameters provide **more efficient power system balancing** both energy- and cost-wise and allows reducing the area control error of the Baltic power system towards the Open Balance Provider, thus improving the energy independence of the Baltic states.

Subsequent research efforts have been dedicated to the **cost-benefit assessment of various demand-side flexibility resources** that can be used not only for power system balancing (via explicit demand response) but also for other services or purposes such as implicit demand response. To carry out this evaluation from different angles and consider the benefits both from the power system and end-user point-of-view, several mathematical models have been devised.

Firstly, an **efficient data-driven modelling approach** has been implemented for thermal modelling of buildings in order to estimate their heating demand. This is vital to enable cost-benefit assessment of DR-enabled electric heating equipment with thermal storage (smart electric thermal storage heaters, SETS), which is a technology potentially able to provide a number of benefits both for the power system at large and the end-users. The simulated timeseries of building heating demand are then fed into **distribution grid** and **power system models** tailored particularly for studying the impact of SETS deployment on the Latvian power system. While this type of heating has been in use in several European countries for decades, it has been virtually unknown in the Latvian market before. To that end, the conducted study is the first one providing insights into the implications of SETS deployment in Latvia. Furthermore, the study was informed by the data obtained through real-life demonstration of SETS in 50 different buildings around Latvia.

Finally, to inform the potential DR-providing end-users of the related costs and benefits, the *DR Assess* **tool** has been developed. It is based on **Monte-Carlo simulations** to properly consider the uncertainties characteristic to electricity markets and provide **probabilistic results** on benefits the end-user can gain through provision of explicit DR to the market or via implementing implicit DR. While the tool has been tailored for the Latvian case, considering the existing common Baltic balancing market and Nord Pool day-ahead market frameworks, it could be easily applied also to other case studies with similar market setup.

Practical significance of the research

Research studies carried out by the author during development of the Doctoral Thesis have contributed to several research and innovation projects. Listed below, they include not only national and international scientific projects but also contract work for a major industry stakeholder.

1. National Research Programme project "Energy-efficient and low-carbon solutions for a secure, sustainable and climate variability reducing energy supply (**LATENERGI**)" (2014–2017).
2. Project "Realising Value from Electricity Markets with Local Smart Electric Thermal Storage Technology (**RealValue**)" (2015–2018), funded within the European Union's Horizon 2020 research and innovation programme.

3. Research contract "Development of mathematical models for an economic assessment of demand-side flexibility resources and activation optimisation of balancing reserves" (2017–2018), commissioned by "Augstsprieguma tīkls" AS (**the Latvian TSO**).
4. Project "Management and Operation of an Intelligent Power System (**I-POWER**)" (2018–2021), funded by the Latvian Council of Science.
5. Project "Future-proof development of the Latvian power system in an integrated Europe (**FutureProof**)" (2018–2021), funded by the Ministry of Economics of the Republic of Latvia within the National Research Programme "Energy".
6. Project "Innovative smart grid technologies and their optimization (**INGRIDO**)" (2018–2021), funded by the Ministry of Economics of the Republic of Latvia within the National Research Programme "Energy".
7. Project "TSO-DSO-Consumer INTERFACE aRchitecture to provide innovative grid services for an efficient power system (**INTERRFACE**)" (2019–2022), funded within the European Union's Horizon 2020 research and innovation programme.

Author's personal contribution

During development of the Doctoral Thesis, its author participated in several collaborative projects implying tight cooperation with other staff members of the RTU Institute of Power Engineering.

Namely, the *AOF parameter search* tool was developed by the author together with Researcher K. Baltputnis, under the supervision of Prof. A. Sauhats. The author contributed to all stages of work and specifically to state-of-the-art analysis, conceptualisation and definition of the mathematical model, data collection and analysis, took part in programming and testing of the tool, performed the case studies and analysed their results.

Modelling of DR-enabled electric heating and its value estimation for the Latvian power system was performed by the author together with Researcher K. Baltputnis, Senior Researchers J. Kozadajevs and L. Petrichenko, under supervision of Prof. A. Sauhats and coordinated by Senior Researcher D. Zalostiba. The author contributed to the state-of-the-art analysis, conceptualisation of the models and methodology, took part in programming and testing of the models as well as in data collection and analysis. The author also interpreted and analysed the results of performed case studies.

Finally, the *DR Assess* tool was developed by the author in close collaboration with Researcher K. Baltputnis, under the supervision of Prof. A. Sauhats. The author contributed to the state-of-the-art analysis, conceptualisation and definition of the mathematical model, took part in programming and testing of the tool, and analysed the case study results.

Approbation of the results

Research results of the Doctoral Thesis have been included in **eight peer-reviewed scientific papers** which have been published in the proceedings of **six international conferences**, all indexed in *Scopus*.

Scientific paper related to Chapter 1

1. **Broka, Z.**, Baltputnis, K., Sauhats, A., Junghāns, G., Sadoviča, L., Lavrinovičs, V. Towards Optimal Activation of Balancing Energy to Minimize Regulation from Neighboring Control Areas. In: *2018 15th International Conference on the European Energy Market (EEM 2018)*, Poland, Lodz, 27–29 June 2018. Piscataway: IEEE, 2018, pp.1042–1046. ISBN 978-1-5386-1489-1. e-ISBN 978-1-5386-1488-4. e-ISSN 2165-4093. doi:10.1109/EEM.2018.8469935.

Scientific papers related to Chapter 2

2. **Broka, Z.**, Kozadajevs, J., Sauhats, A., Finn, D., Turner, W. Modelling Residential Heat Demand Supplied by a Local Smart Electric Thermal Storage System. In: *2016 57th International Scientific Conference on Power and Electrical Engineering of Riga Technical University (RTUCON 2016): Proceedings*, Latvia, Riga, 13–14 October 2016. Piscataway, NJ: IEEE, 2016, pp.259–266. ISBN 978-1-5090-3732-2. e-ISBN 978-1-5090-3731-5. doi:10.1109/RTUCON.2016.7763128.

3. Kozadajevs, J., **Broka, Z.**, Sauhats, A. Modelling Heat Demand in Buildings with an Experimental Approach. In: *2017 IEEE International Conference on Environment and Electrical Engineering and 2017 IEEE Industrial and Commercial Power Systems Europe (EEEIC / I&CPS Europe)*, Italy, Milan, 6–9 June 2017. Piscataway: IEEE, 2017, pp.1308–1311. ISBN 978-1-5386-3918-4. e-ISBN 978-1-5386-3917-7. doi:10.1109/EEEIC.2017.7977621.

Scientific paper related to Chapter 3

4. Petričenko, Ļ., **Broka, Z.**, Sauhats, A. Impact of Smart Electric Thermal Storage on Distribution Grid. In: *2017 IEEE International Conference on Environment and Electrical Engineering and 2017 IEEE Industrial and Commercial Power Systems Europe (EEEIC / I&CPS Europe)*, Italy, Milan, 6–9 June 2017. Piscataway, NJ: IEEE, 2017, pp.1330–1335. ISBN 978-1-5386-3918-4. e-ISBN 978-1-5386-3917-7. doi:10.1109/EEEIC.2017.7977625.

Scientific papers related to Chapter 4

5. **Broka, Z.**, Baltputnis, K., Sauhats, A., Sadoviča, L., Junghāns, G. Stochastic Model for Profitability Evaluation of Demand Response by Electric Thermal Storage. In: *2018 IEEE 59th International Scientific Conference on Power and Electrical Engineering of Riga Technical University (RTUCON 2018)*, Latvia, Riga, 12–14 November 2018. Piscataway, NJ: IEEE, 2018, pp.449–454. ISBN 978-1-5386-6904-4. e-ISBN 978-1-5386-6903-7. doi:10.1109/RTUCON.2018.8659837.

6. Sadoviča, L., Junghāns, G., Sauhats, A., **Broka, Z.**, Baltputnis, K., Lavrinovičs, V. Case Study – Assessing Economic Potential for Demand Response in Baltic Balancing Market. In: *2018 IEEE 59th International Scientific Conference on Power and Electrical Engineering of Riga Technical University (RTUCON 2018)*, Latvia, Riga, 12–14 November 2018. Piscataway, NJ: IEEE, 2018, pp.257–261. ISBN 978-1-5386-6904-4. e-ISBN 978-1-5386-6903-7. doi:10.1109/RTUCON.2018.8659901.

7. Baltputnis, K., **Broka, Z.**, Sauhats, A. Influence of Flexibility Modeling Parameters on Residential-Scale Demand Response Assessment. In: *2019 IEEE Milan PowerTech*, Italy, Milan, 23–27 June 2019. Piscataway: IEEE, 2019, pp.2053–2058. ISBN 978-1-5386-4723-3. e-ISBN 978-1-5386-4722-6. doi:10.1109/PTC.2019.8810947.

8. Baltputnis, K., **Broka, Z.**, Sauhats, A. Analysis of the Potential Benefits from Participation in Explicit and Implicit Demand Response. In: *2019 54th International Universities Power Engineering Conference (UPEC 2019)*, Romania, Bucharest, 3–6 September 2019. Piscataway: IEEE, 2019, pp.72–76. ISBN 978-1-7281-3350-8. e-ISBN 978-1-7281-3349-2. doi:10.1109/UPEC.2019.8893589.

Research results included in the Doctoral Thesis have been discussed at **six international scientific conferences**.

1. 57th International Scientific Conference on Power and Electrical Engineering of Riga Technical University (RTUCON 2016) in Latvia, Riga on October 13–14, 2016.

2. 17th IEEE International Conference on Environment and Electrical Engineering & 1st IEEE Industrial and Commercial Power Systems Europe (EEEIC / I&CPS Europe) in Italy, Milan on June 6–9, 2017.

3. 15th International Conference on the European Energy Market (EEM 2018) in Poland, Lodz on June 27–29, 2018.

4. 59th IEEE International Scientific Conference on Power and Electrical Engineering of Riga Technical University (RTUCON 2018) in Latvia, Riga on November 12–14, 2018.

5. 13th IEEE PowerTech in Italy, Milan on June 23–27, 2019.

6. 54th International Universities Power Engineering Conference (UPEC 2019) in Romania, Bucharest on September 3–6, 2019.

Selected **additional peer-reviewed scientific papers** developed during the Doctoral Studies but not included in the Thesis are listed below (all indexed in *Scopus*).

1. Sauhats, A., Coban, H., Baltputnis, K., **Broka, Z.**, Petričenko, R., Varfolomejeva, R. Optimal Investment and Operational Planning of a Storage Power Plant. *International Journal of Hydrogen Energy*, 2016, Vol.41, Iss.29, pp.12443–12453. ISSN 0360-3199. doi:10.1016/j.ijhydene.2016.03.078.

2. Baltputnis, K., **Broka, Z.**, Sauhats, A., Petričenko, R. Short-Term Optimization of Storage Power Plant Operation under Market Conditions. In: *2016 IEEE 16th International Conference on Environment and Electrical Engineering (EEEIC 2016)*, Italy, Florence, 7–10 June 2016. Piscataway, NJ: IEEE, 2016, pp.250–255. ISBN 978-1-5090-2321-9. e-ISBN 978-1-5090-2320-2. doi:10.1109/EEEIC.2016.7555466.

3. Sauhats, A., Petričenko, R., Baltputnis, K., **Broka, Z.**, Varfolomejeva, R. A Multi-Objective Stochastic Approach to Hydroelectric Power Generation Scheduling. In: *2016 Power Systems Computation Conference (PSCC 2016)*, Italy, Genoa, 20–24 June 2016. Piscataway, NJ: IEEE, 2016, pp.56–62. ISBN 978-1-4673-8151-2. e-ISBN 978-88-941051-2-4. doi:10.1109/PSCC.2016.7540821.

4. Sauhats, A., Petričenko, R., **Broka, Z.**, Baltputnis, K., Soboļevskis, D. ANN-Based Forecasting of Hydropower Reservoir Inflow. In: *2016 57th International Scientific Conference on Power and Electrical Engineering of Riga Technical University (RTUCON 2016): Proceedings*, Latvia, Riga, 13–14 October 2016. Piscataway, NJ: IEEE, 2016, pp.267–272. ISBN 978-1-5090-3732-2. e-ISBN 978-1-5090-3731-5. doi:10.1109/RTUCON.2016.7763129.

5. Baltputnis, K., **Broka, Z.**, Sauhats, A. Assessing the Value of Subsidizing Large CHP Plants. In: *2018 15th International Conference on the European Energy Market (EEM 2018)*, Poland, Lodz, 27–29 June 2018. Piscataway: IEEE, 2018, pp.488–492. ISBN 978-1-5386-1489-1. e-ISBN 978-1-5386-1488-4. e-ISSN 2165-4093. doi:10.1109/EEM.2018.8469816.

6. Petričenko, Ļ., **Broka, Z.**, Sauhats, A., Bezrukovs, D. Cost-Benefit Analysis of Li-Ion Batteries in a Distribution Network. In: *2018 15th International Conference on the European Energy Market (EEM 2018)*, Poland, Lodz, 27–29 June 2018. Piscataway, NJ: IEEE, 2018, pp.1–5. ISBN 978-1-5386-1489-1. e-ISBN 978-1-5386-1488-4. e-ISSN 2165-4093. doi:10.1109/EEM.2018.8469782.

7. **Broka, Z.**, Baltputnis, K. Handling of the Rebound Effect in Independent Aggregator Framework. *17th International Conference on the European Energy Market (EEM 2020)*, Sweden, Stockholm, 16–18 September 2020. Piscataway: IEEE (*accepted*).

Structure of the Thesis

The Doctoral Thesis is written in English. It is composed of an introduction, four main chapters, conclusions and bibliography with **117** references. The Thesis, containing **84** figures, **21** tables and **5** appendices, consists of **170** pages.

Chapter 1 proposes an optimisation procedure of the balancing process of the Baltic power system. This is both an economically and politically important topic for cost-reduction of power system regulation and increase of the energy independence of the three Baltic countries. The developed optimisation algorithm allows automated establishing of the regulation parameters as opposed to human decision-based regulation procedure only. Thus, it can serve as a part of the "activation optimisation function" set forth by the EC regulation on electricity balancing. Furthermore, improvements in the balancing process can also aid in the technically challenging synchronisation with the Continental Europe network due in 2025.

To ensure a balanced power system operation, it is important the TSO has enough flexibility resources at hand. As such, demand-side flexibility has been generally admitted being an underused resource, especially in the common Baltic balancing market with sometimes lacking balancing reserve providers. Therefore, subsequent chapters are dedicated to employment of demand response sources and their cost-benefit assessment to inform both the system operators or policymakers and the end-users of related effects when unlocking the demand-side flexibility.

Smart electric thermal storage is selected as one potential demand-side flexibility resource which, until now, has been generally unknown in the Latvian market. Thus, **Chapter 2**

describes the technology and modelling approach employed to estimate the heating demand of buildings with a data-driven black-box approach. The derived consumption of DR-enabled electric heating devices is then used for their value and impact estimation both at the distribution grid and power system scale in **Chapter 3**.

Finally, **Chapter 4** presents methodology and a tool for a probabilistic economic assessment of DR provision from the end-user point of view with a focus on their participation in the balancing market. The tool informs the potential DR providers on their probable cash flows considering uncertainties related to electricity wholesale and balancing prices and also market demand for the balancing resources. Thus, it can facilitate the entrance of new balancing market participants and increase the overall flexibility of the Baltic power systems.

1. OPTIMAL ACTIVATION OF BALANCING RESERVES

1.1. Motivation and background

The European Commission Regulation on electricity balancing aims to foster the formation of integrated balancing markets to enable a cost-efficient and reliable exchange of balancing services among the European countries [28]. To implement this, relevant ICT tools need to be developed, as until now the balancing of power systems is still often human operator dependent. Balancing bids for activation should be selected from merit order lists containing bids of standardised balancing products.

This chapter is focused on a software tool, *AOF parameter search*, developed in 2017 in preparation for the launch of the common Baltic balancing market established in 2018 by the Latvian, Lithuanian and Estonian transmission system operators (TSOs) with the overarching objective to develop a common Nordic-Baltic balancing market for manually activated frequency restoration reserves (mFRR) [29]. It presents practical research based on a real-life case study of the Baltic power system for optimal activation of manual frequency restoration reserves.

The tool for determination of the activation volume and time schedule for balancing reserves was developed to facilitate the decision-making process of the transmission system operator in balancing of the power system within a coordinated balancing area. The study is important in light of the ongoing integration of balancing markets within the European Union (EU) and the subsequent need to develop an activation optimisation function. Recently, regular balancing needs of the Baltic countries were covered mostly by the neighbouring Russian power system. The motivation for this study was moving towards local regulation as much as possible for energy dependence related and economic reasons.

The Baltic power system has some distinct characteristics due to its synchronous operation with the Integrated/Unified Power System (IPS/UPS) of Russia and Belarus. The Russian power system provides primary power reserves for frequency regulation and secure system operation within the BRELL (Belarus, Russia, Estonia, Latvia and Lithuania) ring [4]. As of 2018, the TSOs of Latvia, Estonia and Lithuania (Augstsprieguma tīkls AS, Elering and Litgrid) have established a common Baltic balancing market within which the three countries are able to share balancing energy. However, the remaining not netted imbalance is settled by an Open Balance Provider (OBP) (Fig. 1.1) which provides balancing energy from the Russian power system via seven transmission lines. The imbalance settlement period (ISP) currently is one hour, and the not netted imbalance with the OBP is defined as the total Baltic area control error (ACE), or the overall system imbalance. It is calculated as the difference between the scheduled and the actual power flow each minute, integrated over the whole ISP to obtain the final ACE in MWh. Thus, the payment for the Baltic ACE covers the cost of the Russian frequency control service [30].

Formally, the three Baltic countries are required to keep their imbalance within certain limits (±30 MWh/h for Estonia and Latvia each and ±50 MWh/h for Lithuania [29]). In practice, until the end of 2017 minor imbalances were handled by the imports from Russia on

a regular basis while local activations were used to cover larger imbalances on comparatively rare occasions. As a result, the ACE energy constituted a major part of the total Baltic balancing energy and contributed a significant share of balancing costs in the Baltic markets (e.g., some 40% of total balancing costs in Latvia in 2014 [30]). Handling ACE with energy from the Russian power system is costly due to the specific pricing policy employed by the OBP: a low sell price fixed at 5 €/MWh and a high buy price which may exceed 100 €/MWh (data of 2015) [30]. For context, the average day-ahead market electricity price in the three Nord Pool bidding areas of the Baltic countries was 35.23 €/MWh in 2016.
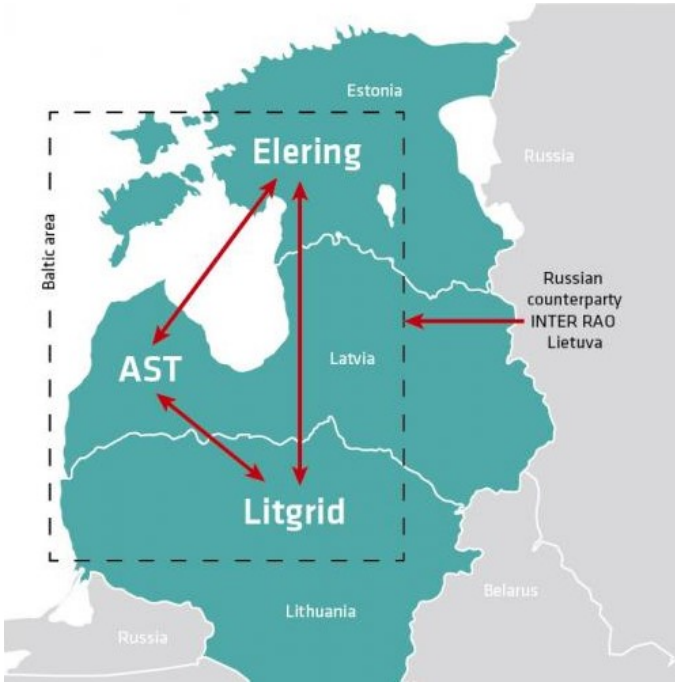
Fig. 1.1. Imbalance netting of the Baltic TSOs under the Open Balance Agreement [30].

The aforementioned considerations along with the political decision to cease synchronous operation with the IPS/UPS by 2025 [31] encouraged the Baltic TSOs to develop a Baltic balancing IT system with the primary function to ensure sustainable physical cross-border balancing. This system facilitates sharing balancing energy among the three countries with the aim to increase reliance on mFRR provided by local producers, the bids of which are included in the Baltic common merit order list (CMOL). It is expected to reduce the overall balancing costs incurred by the three Baltic TSOs while contributing to the energy independence of Latvia, Estonia and Lithuania.

One of the building blocks of the common balancing system is the **Activation Optimisation Function** (AOF). As stipulated in the guidelines [28] developed by ENTSO-E, the AOF determines the most efficient activation of the incoming balancing request while respecting some capacity and operational restrictions. The Baltic TSOs intend to implement the AOF as an automatic algorithm the main inputs to which are the available bids from the CMOL (considering transmission constraints) and activation volume proposal [29], the latter being the focus of this study. Specifically, it implies an algorithm for determination of optimal activation volume of balancing reserves along with a time schedule based on the historic ACE data with

minute resolution and the current ACE forecast. It is meant to support the decision-making by the dispatch operator of the transmission system, which thus serves as the first step towards building a fully automatic system for the activation of balancing reserves.

As of now, the ordering of the balancing energy is left solely to the dispatch operator with a very short timeframe for decision-making. Combining the time restriction with the large number of variable and uncertain parameters of the power system, it stands to reason that an automated tool should provide operational advantages. However, the significant hands-on experience of dispatch operators, which is challenging if not outright impossible to translate into an automated algorithm [32], cannot be dismissed or ignored. Thus, one of the tasks of this study has been to investigate the pros and cons of automated vs manual regulation activation.

Literature search in 2017, when this study was still ongoing, yielded only a few scientific papers referring to the AOF. This term was first introduced in the EC guidelines on electricity balancing approved in 2017 [28]. One of the studies [33] proposes balancing optimisation based on stochastic unit commitment principles using imbalance forecast scenarios. The objective of optimisation in [33] is to minimise expected activation costs, which is demonstrated using Norwegian imbalance and market data. As a result, bid activation schedules are proposed. The imbalance forecasts are generated from probability distributions of historical data series, and balancing activation bids are created based on prices and volumes in the Norwegian balancing energy market. Utilisation of both mFRR and aFRR is considered.

Case studies of optimal scheduling of ancillary services (AS) for the Czech Republic are presented in [34] and [35]. In [34], five different types of AS used by the Czech TSO are considered to minimise the cost of balancing. Power imbalances and the resulting ACE is obtained from Monte Carlo simulations to imitate the random behaviour of the power system, while the AS prices are assumed as estimated by experts due to the complexities related to modelling the entire AS market. In [35], an evolutionary algorithm for cost-optimal dispatch of AS is used and regulation reserves are modelled for a 6-hour horizon. Comparison of the historical vs optimised activations shows that the ACE and regulation energy costs decrease in the latter case.

1.2. Methodology

Within this study, we developed a software tool for deriving **optimal activation parameters of mFRR** for balancing of the Baltic power system. The main objective of the algorithm implemented is to identify close to optimal regulation parameters and to evaluate the performance of balancing operations carried out in accordance with these parameters. The optimisation problem is formulated and solved in MATLAB to take advantage of its data processing abilities and solvers. MS Excel is used for input and output due to its user-friendly interface.

Development of the *AOF parameter search* tool took place in 2017. It was commissioned by the Lavian TSO, "Augstsprieguma tīkls" AS, within the research contract work "Development of mathematical models for an economic assessment of demand-side flexibility resources and activation optimisation of balancing reserves". The scope of the tool is the

activation of balancing reserves (namely, mFRR) provided within the common Baltic balancing market to minimise the ACE covered by OBP (Fig. 1.2).
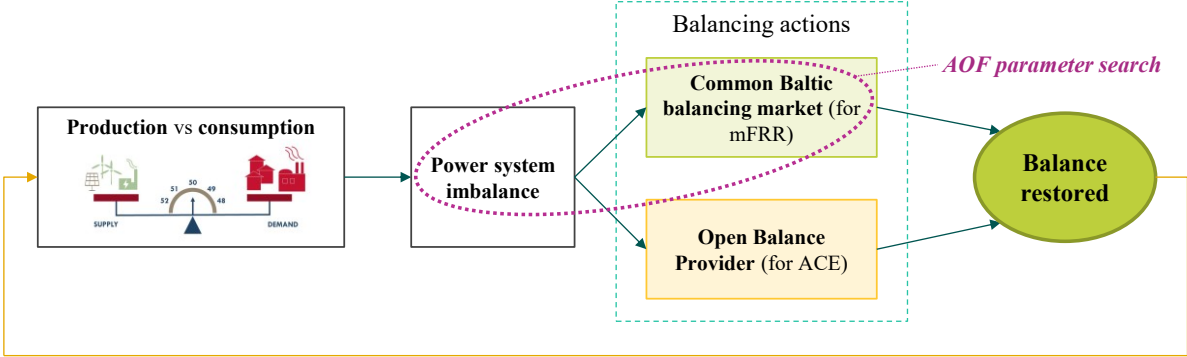
Fig. 1.2. The role of *AOF parameter search* tool within the Baltic balancing process.

The core of *AOF parameter search* is an algorithm for activation volume and time suggestion. It is implemented as a stand-alone application to inform the dispatch operator whether, at a certain point within an ISP, balancing activation must be ordered and, if so, in which direction and to what extent. The algorithm receives as its input minutely data of the Baltic area control error (ACE) forecast along with the final ACE at the end of each ISP (currently, an hour). Then, an optimisation procedure is employed (Fig. 1.3) to determine the most efficient balancing schedule based on the historic ACE data.
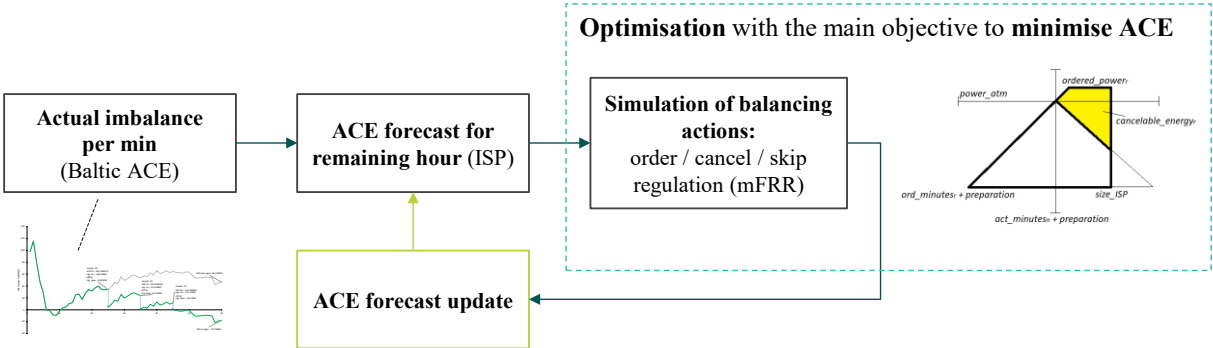
Fig. 1.3. A simplified illustration of *AOF parameter search* operation.

The balancing energy is dispatched based on three distinct sets of parameters:

- **time of activation** (minutes from the beginning of each ISP);
- **percentage of the ACE forecast** to be regulated against;
- **ignorance level** which is the threshold the ACE forecast must meet for regulation to be activated.

In this study, the optimisation and balancing simulations are performed on the **historical ACE data of 2016**, with 2/3 of that data used for training and the remaining 1/3 – for testing purposes. The values of the regulation parameters are found by employing a direct search optimisation procedure which, within its evaluations, simulates the balancing actions during each ISP applied to the training dataset. The objective function encompasses a **multi-objective problem** which mainly aims to **minimise the ACE** with some other additional criteria such as

balancing energy and **ordered power**, the importance of which can be adjusted by means of weight coefficients. Finally, the parameters identified by the optimiser are once again fed to the balancing simulation algorithm to generate results and their summary. By default, the simulation with the optimised parameters is carried out on the testing dataset to assess the generalisability of the procedure.

1.2.1. Overall structure of the algorithm

The **structure of the overall algorithm** is illustrated in Appendix 1. The parts of it dealing with the formulation and solution of the optimisation problem are implemented in the MATLAB scripting environment to take advantage of its data processing abilities and solvers. Thus, a stand-alone application has been compiled to be deployed with the royalty-free MATLAB Runtime environment. MS Excel is used for input and output. Additionally, validation and analysis of the results obtained by the optimiser are carried out in Excel to enable the user with an ability to manually inspect the dynamics of ACE forecast and the course of regulation activations in any particular hour in the test dataset.

The most important parts of the algorithm are as follows:

1) **reading input data** of ACE forecast in 1-minute resolution and user-selected settings for regulation and optimisation, such as ISP duration, max number of activations per ISP, preparation time before mFRR activation, ramping rate, the minimum interval between two subsequent activations and bounds on optimisation variables (i.e., regulation parameters);

2) **data preprocessing** – the initial dataset is partitioned in two subsets and all further operations with them happen independently. One of these subsets comprises working days, whereas the other one – non-working days which include weekends and public holidays. While Saturdays and Sundays are detected automatically (provided the date and time information in the initial dataset is included in a distinguishable format), the dates of public holidays are determined from an additional editable external list since they can be subject to policy changes.

    Further on, the datasets are subjected to a **filtration procedure** the aim of which is removing those hours from the datasets that contain sudden jumps in their ACE forecasts in a short time span possibly indicating either a fault in data collection or failure to subtract historical regulation activities (the input dataset ought to be in a form where regulation is not included, i.e., it should be subtracted from the time series to ensure that the algorithm is applied to data without regulation). Generally, the procedure of filtering can be tuned, but by default, it discards the hours where a change in the absolute value of ACE forecast equal or greater than 50 MWh/h happens in a time span of 5 minutes or less (but not accounting for the first 10 minutes of the hour as notable changes in the ACE forecast are expected at the beginning of ISP following the current forecasting techniques);

3) finally, the datasets are divided into **training** and **testing subsets**; by default, they comprise 2/3 and 1/3 of the filtered data respectively, but this can be adjusted or

altogether disabled in the configuration of the tool. By default, regulation parameters are optimised on the training dataset. Then, to test the performance of the optimised balancing schedule, the estimated parameters are applied to the testing dataset to simulate all activities of regulation. Consequently, the results then show the performance of regulation only for the testing set and allow us to evaluate the generalisation ability of the activation parameters found by the optimisation problem solver;

4) **optimisation problem solver** – it iteratively finds a solution (a set of regulation parameters) which provides a good (close to minimum) objective function value. Given that the objective function is very complicated (it includes passing the entirety of the training dataset through regulation activation logical instructions including both ordering of regulating power and its partial or full cancellation taking into account ramping), traditional gradient-based solvers cannot be used. Instead, more versatile solvers, e.g., MATLAB *patternsearch*, should be employed. Another issue caused by the complexity of the objective function is the risk of stopping in local minima, which can be partially alleviated by implementing a multi-start call to the solver (i.e., beginning the search at different initial points). The greater the number of calls to the solver, the greater the chance of finding a better solution at the cost of higher computational time. Nevertheless, absolute certainty of obtaining the global minimum cannot be established by definition, hence a precaution in the terminology used – hereinafter the term *optimum solution* refers to the output of the solver and generally describes the best solution the solver was able to find under the particular circumstances and time allocated to it;

5) the objective function receives the set parameters of activation (minutes, percentages and ignorance levels) at every solver iteration where it calculates the corresponding value to be minimised (Appendix 2). The calculation procedure of the objective function comprises mainly **two nested loops** where the **outer** one passes ACE forecast data of every ISP in the training dataset to the **inner** loop, which in turn applies the activation parameters chronologically by simulating the ordering, partial and full cancellation of regulating power. Essentially, the form of the objective function is that of a set of logical operators meant to mimic as realistically as possible an automated decision making of such a balancing system which would perfectly obey the pre-selected activation parameters;

6) finally, the **activation parameters** found by the solver are **applied to** the **testing dataset** (at this stage, in Excel instead of MATLAB) where the same regulation logic as in the objective function is employed to analyse the performance of these parameters. Some of the most important metrics to pay attention to during the testing stage are the average absolute ACE, ordered and supplied regulation energy, the share of cancelled or *wrong* energy, the share of ISPs where the regulation has increased the final imbalance instead of improving it etc.

1.2.2. ACE forecast

In general, timeseries of ACE forecast that are provided as input data for optimisation can be either a historical record of ACE forecasts or simulated timeseries created for simulation purposes. In this study, we used real-life historic data of 2016 with a minute resolution from the SCADA/EMS provided by the TSO. Since forecasting per se was out of the scope of this study, we employed an already existing naïve ACE forecasting approach used by the TSO:

$$ACE_{\text{forec.}}^{m} = \left(P_{\text{actual}}^{m} \cdot \left(M - m + 1 \right) + \sum_{k=1}^{m-1} P_{\text{actual}}^{k} - \sum_{k=1}^{M} P_{\text{plan}}^{k} \right) \cdot \frac{\Delta t}{60} \, , \tag{1.1}$$

where m – index of the particular minute;

M – length of the ISP in minutes;

$ACE_{\text{forec.}}^{m}$ – forecast of the hourly ACE (MWh) at minute m;

P_{actual}^{m} – actual power flow measured at minute m.

The two summation operators calculate the total actual power flow P_{actual} from the beginning of ISP till the previous minute, $m - 1$, and the planned power flow, P_{plan}, for the whole ISP, where k indexes through the time steps Δt. Since the time step, in our case, is equal to one minute, we divide the equation by 60 to obtain energy (ACE forecast) in MWh. The power flows here refer to the total scheduled Baltic power flow balance (after Nord Pool day-ahead and intraday market clearing) and the actual Baltic balance. The results of the case study presented further on demonstrate overall good applicability of this ACE forecasting approach. Nevertheless, it is also one of the possible directions for improvement of the AOF algorithm in future work. Some of the approaches suggesting more sophisticated forecasting of system imbalance volumes are provided in [36] and [37].

1.2.3. Objective function

In Appendix 2, a general outline for calculation of the objective function value can be found. As previously mentioned, it iterates through the ISPs (hours in the current implementation) and simulates the process of regulation activation within each ISP with a set of given parameters. For multi-objective optimisation, we employ the **weighted sum method** to scalarise a set of objectives into a **single-objective function,** which is the subject of minimisation. Its value is made up of several metrics, the most important of which usually is the sum of the absolute values of **ACE** at the end of each ISP. The other two metrics considered in the software tool are the sum of the **provided balancing energy** and the sum of the **balancing power orders** during each ISP. The combination of these metrics is made possible by imposing user-selected **weight coefficients** to each criterion of the problem statement. Their primary purpose is to set the importance of each of the components within the objective function, but they also aid in ensuring that the various components can agree dimensionally. Thus, the objective function can be expressed as

$$w_{1a} \cdot \sum_{ISP=1}^{ISPs} ACE_{pos}^{ISP} + w_{1b} \cdot \sum_{ISP=1}^{ISPs} \left| ACE_{neg}^{ISP} \right| + w_2 \cdot \sum_{ISP=1}^{ISPs} \left| E_{reg.suppl.}^{ISP} \right| + w_3 \cdot \sum_{ISP=1}^{ISPs} \left| P_{reg.ord.}^{ISP} \right| \rightarrow \min \ , \quad (1.2)$$

where w_{1a}, w_{1b}, w_2, w_3 – weight coefficients for the various criteria of the problem statement;

ACE_{pos}^{ISP} – positive ACE, or net balancing energy exported to the Russian power system (MWh/h) during the ISP;

ACE_{neg}^{ISP} – negative ACE, or net balancing energy imported from the Russian power system (MWh/h) during the ISP;

$E_{reg.suppl.}^{ISP}$ – total provided balancing energy (MWh) during the ISP;

$P_{reg.ord.}^{ISP}$ – sum of the ordered regulation power (MW) during the ISP;

$ISPs$ – number of ISPs in the training dataset.

The **weight coefficients** can be adjusted by the user depending on their priorities. In our case studies, the primary goal was to minimise the ACE at the end of each ISP, while also trying to efficiently reduce the amount of balancing energy used and the ordered regulation power.

Optimisation variables comprise a set of parameters a dispatch operator would use for the actual balancing actions, namely: (1) **time** of activation (minutes from the beginning of each ISP); (2) **percentage** of the ACE forecast to be regulated against; (3) **ignorance level** which is the threshold the ACE forecast must meet for regulation to be activated. The constraints for these variables are set by the user. Additionally, the user selects the maximum number of activations per hour (1..5), the preparation time for activation of reserves and the ramp rate. All these settings serve as constraints during the optimisation and are used for simulating the regulation actions.

1.2.4. Regulation simulation logic

To simulate the regulation actions, we assume that three distinct decisions can be made at each decision point (time of activation): order regulation; request a change (incl. cancellation) of a previously ordered regulation; do nothing. The set of instructions which carries out the task of simulating regulations within the inner loop of the objective function calculation (Appendix 2) has a fairly complex structure. It takes into account factors like **preparation** time (from making the decision to order/change regulation to the beginning of its implementation), **ramping** rate (from one power state to another), and **feasibility** of the necessary regulation energy to actually be delivered in the remaining time within the ISP (this, in combination with the ramp rate, also defines the ceiling of power that can be ordered at a given activation time). The algorithm for activation of balancing reserves is described in more detail in Appendix 3.

The decision to call for regulation activation is made if at a given activation minute the ACE forecast meets or exceeds the **ignorance level**. The ACE forecast is updated correspondingly. The decision to cancel a previous regulation also requires a violation of the ignorance level, but additionally, the sign of the ACE forecast needs to have changed. The **cancellation**, in this case, allows avoiding a situation where two activations in opposite directions are online at the same

time, thus minimising the amount of regulation energy which has ultimately been *wasted* by shifting the ACE in the wrong direction, requiring additional regulation to alleviate this.

The operation of the activation logic can be better explained by referring to visual representations of ACE dynamics in particular hours in the following figures. In these figures, the simulated regulation activities during some arbitrarily selected hours are illustrated. The cases displayed refer to a scenario where the maximum number of activations (i.e., time setpoints) is equal to five. If the upper bound on activation minutes is 45, the lower bound – 5, and the minimum distance between two activations – 10 minutes, then a decision on whether to activate has to be made at minutes 5, 15, 25, 35 and 45. In the first example (Fig. 1.4), only one of these times was the corresponding ignorance level overcome (minute 35/ 13.8 MWh/h) and, subsequently, down-regulation (–76.5 MW) was ordered.
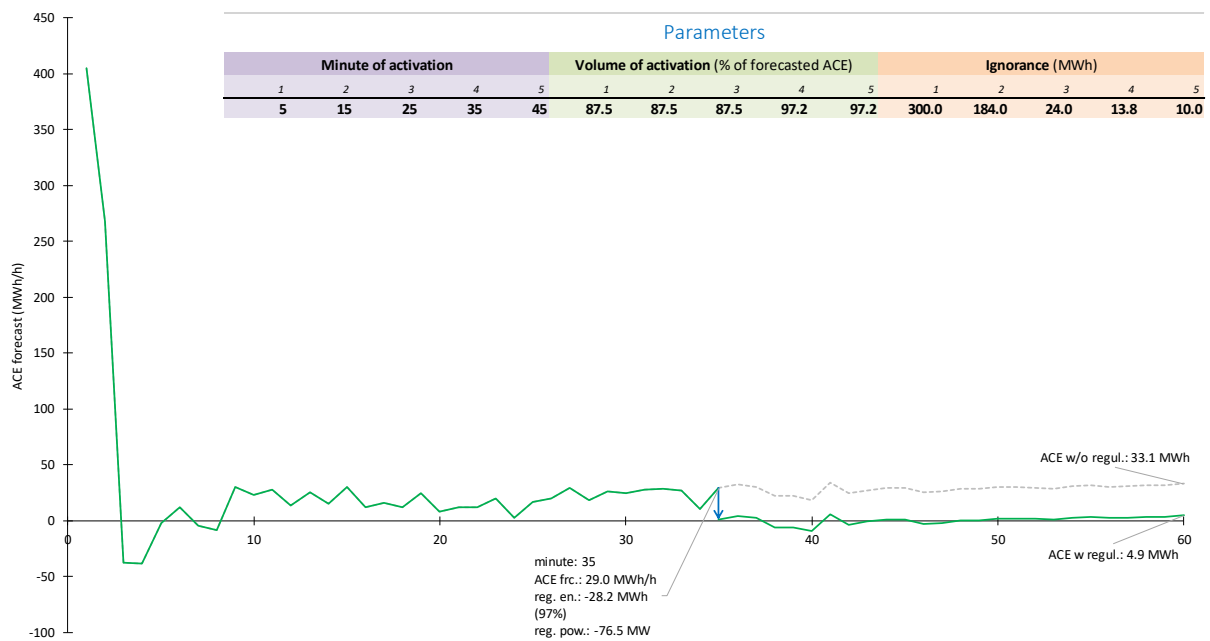
Fig. 1.4. Regulation example with one activation.

In the next example (Fig. 1.5), the ignorance level was violated at minute 25 (|–31.0| > > 24.0 MWh/h) which given an 87.5% activation volume resulted in ordered up-regulation power of 49.6 MW. However, during the next minute setpoint (minute 35) it was found that the ACE forecast once again exceeds the current threshold (16.0 > 13.8 MWh/h), but now in the opposite direction. This implies that at least part of the previously ordered regulating power might actually not be necessary, hence, the previous order is decreased by 41.8 MW. Nevertheless, the final ACE with regulation has a different sign than without it signifying overregulation.
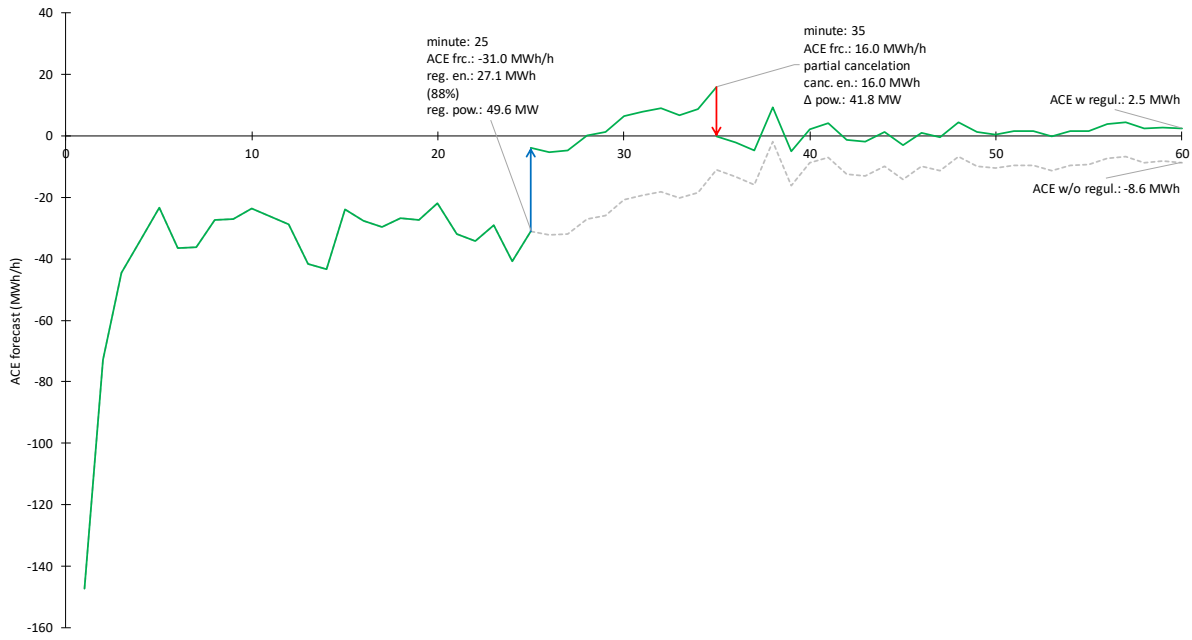
Fig. 1.5. Regulation example with one activation and its partial cancellation.

Example of another hour (Fig. 1.6) illustrates well the perils of overly early activations. At minute 5 a very high ACE forecast is obtained, which exceeds even the very large threshold for this set time (317.7 MWh > 300 MWh) resulting in a large regulation volume. However, the order had to be partially decreased at minutes 25 and 35 and fully cancelled at minute 45. Furthermore, at minute 45 a new activation in the opposite direction had to be ordered equal to 11.4 MWh of regulating energy. The significance of this lies in the regulation procurer having to pay twice for this energy without it having any tangible benefit.
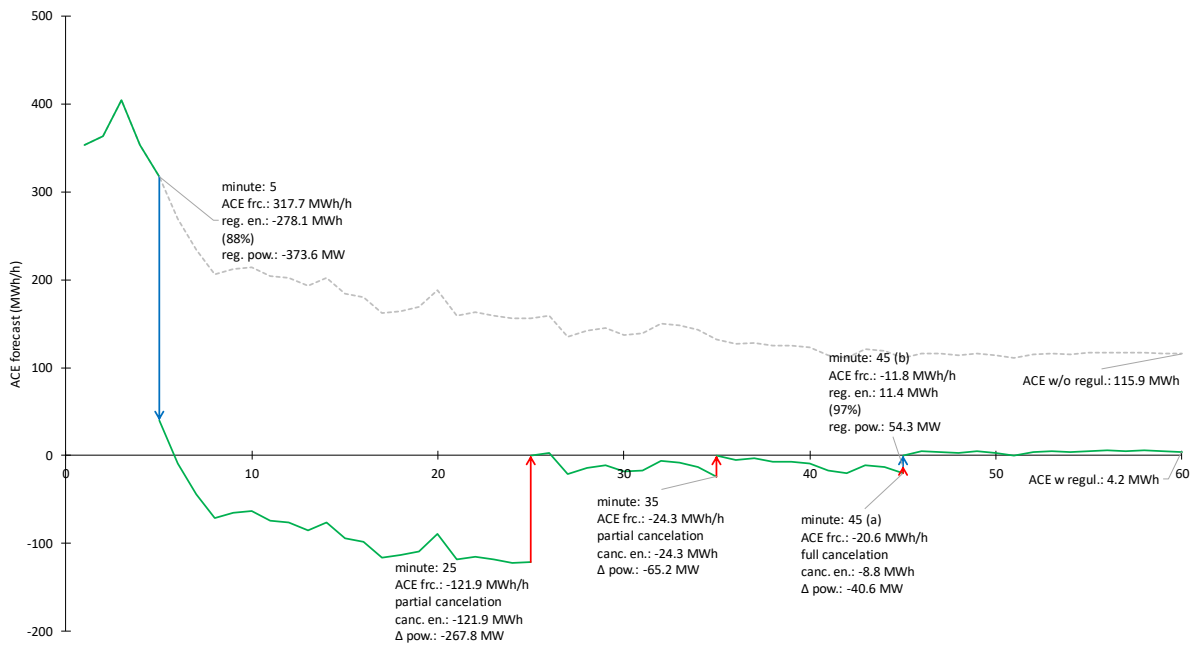
Fig. 1.6. Example with regulation in opposite directions.

Similarly to the previous example, in the next case (Fig. 1.7) regulation in the wrong direction has been detected which had to first be fully cancelled, secondly – mitigated and finally – regulation in the right direction had to be ordered to decrease the final ACE. However, overall the operations were a success as the ACE for this hour decreased from 37.1 MWh without regulation to 4.5 MWh with. The cases of opposite regulation are a consequence of the fairly notable changes in ACE forecasts during some particular hours and they can be avoided mainly by improving forecasting techniques.
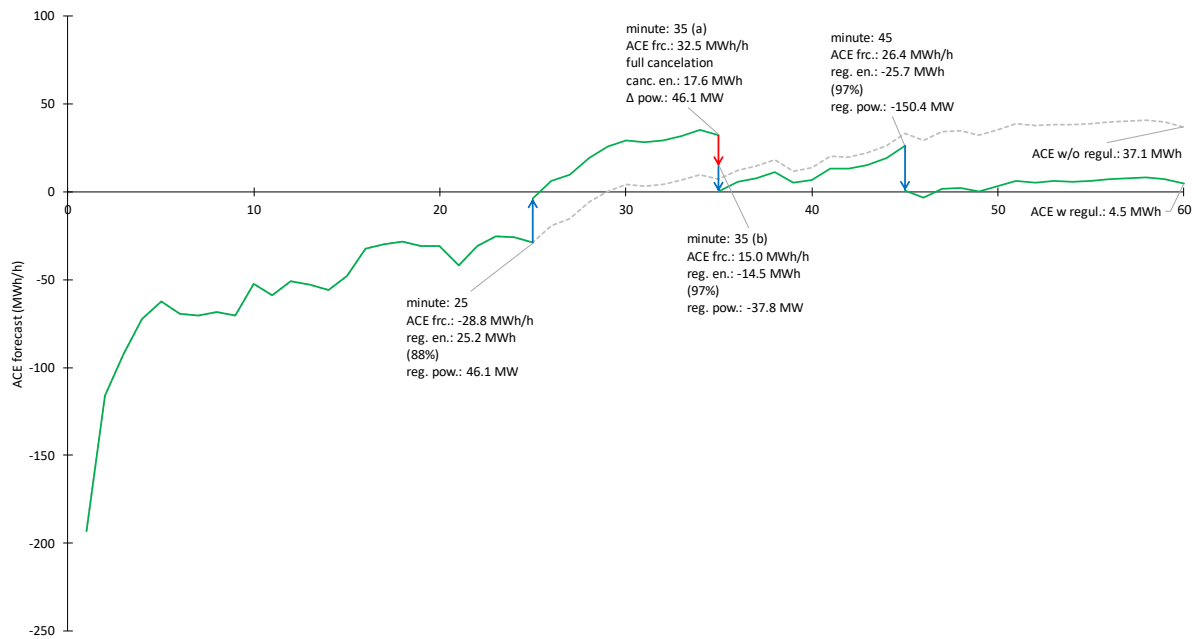
Fig. 1.7. Another example with regulation in the opposite direction.

Further on, in Fig. 1.8 regulation has been activated for a total of three times, besides at none of the set times a necessity to fully or partially cancel the previous activations was identified. Still, this particular example is of interest due to the overregulation evident from the final ACE values (46.3 MWh without and –17.9 MWh with regulation). The third activation happened at the last allowed set time (minute 45) and at that point, the adjusted ACE forecast reached a mere 0.4 MWh, but drop in the ACE trajectory during the last fifteen minutes by 18.3 MWh results in –17.9 MWh overregulation once again illustrating the importance of accurate forecasting. The other takeaway from these examples is the necessity to exercise caution if the operator is indeed committed to begin regulation very early in the hour.
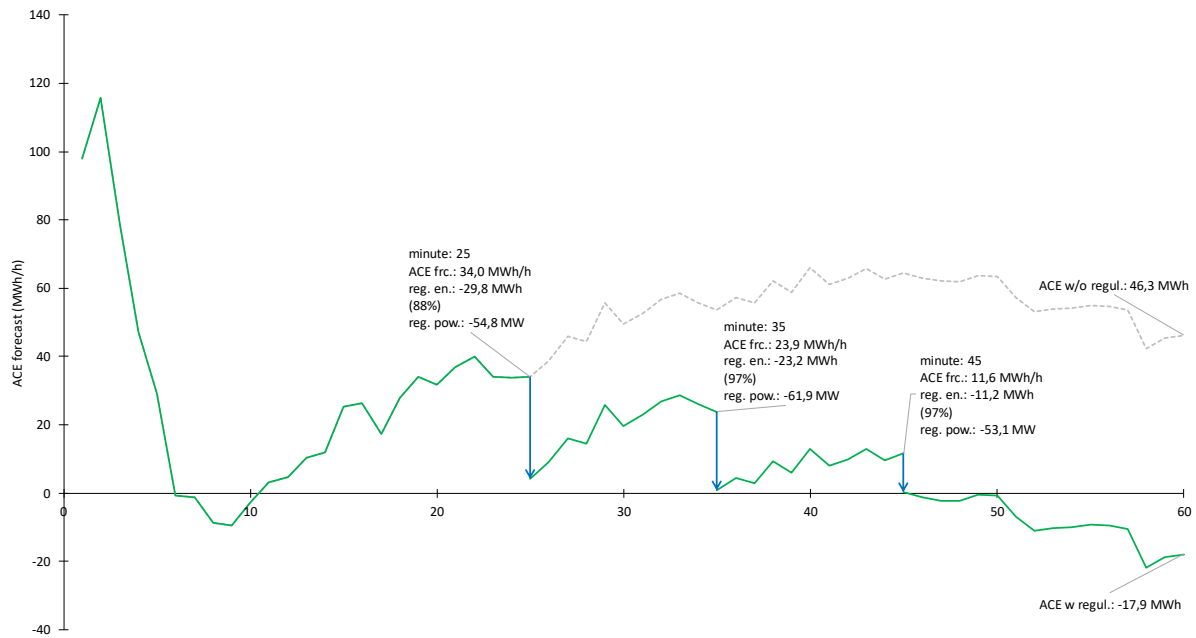
Fig. 1.8. Example with several activations over the hour.

1.3. Results and discussion

To obtain (close to) optimum mFRR activation parameters, the optimisation procedure was applied to historical data of the year 2016 provided by the TSO which was divided into training and testing subsets. Data series of the ACE forecast (1.1) and the actual ACE with minute resolution was split into three-month periods in an attempt to capture seasonal differences in data. This approach also reflects the intended use of the algorithm by the Baltic TSOs, namely, its application on historic data of one or a few months to obtain activation parameters which are then used to assist the operators in balancing the power system for upcoming periods (e.g., one or a few months). Regulation parameters were optimised on the training dataset comprising the first 2/3 of the whole preprocessed set. To test the performance of the optimised balancing schedule, the estimated parameters were applied on the testing dataset (i.e., the remaining 1/3) to simulate all activities of regulation as performed by the TSO. Consequently, the results presented show the performance of regulation only for the testing set and allow us to evaluate the generalisation ability of the optimisation procedure.

The calculations were performed with different day-type differentiation settings: (1) *all days* – optimisation and testing done without distinguishing weekdays and holidays; (2) *weekdays* – optimisation and testing done for weekdays only; and (3) for only *holidays*, which include weekends and public holidays. For space-saving purposes, the results shown below refer to the optimisation of *all days*.

1.3.1. Optimised regulation parameters

The optimised activation parameters and resulting ACE for one of the three-month datasets (July–September 2016) are shown in Table 1.1. While the maximum number of activations per

ISP was varied from 1 to 5, in all cases but with only 1 activation the last selected activation minute is 45 which is the upper bound imposed during the optimisation. This is due to the initially highly uncertain nature of the ACE forecast the accuracy of which significantly increases towards the end of each hour (Fig. 1.10). Since premature activation can lead to redundant regulation orders (i.e., opposite reg. energy) and the subsequent cancellation of regulations that happen to be in the opposite direction, the algorithm evidently tends to postpone activations for as long as possible.

In the case of **1 max. activation**, the selected activation minute is 35 with a volume of activation 90.5% relative to the ACE forecast. Ignorance level of the ACE forecast is 10 MWh/h which is actually equal to the lower bound set for optimisation. This implies that decreasing this bound might possibly provide a slightly lower ACE at the end of hour because a larger amount of imbalance would be eliminated. The final |ACE|[1] for 1 max. activation reaches an average of 12.5 MWh/h which is 38–62% larger than that with a greater number of activations. Thus, we can conclude that more than one activation should be preferred. Nevertheless, even one activation improves the final ACE by 25.5 MWh/h and significantly reduces its positive bias. Similar conclusions follow also from the optimisation results when *weekdays* and *holidays* are differentiated.

For **2 to 5 max. activations**, even more evident is the tendency to postpone activations to as late as possible. Moreover, for 5 activations the only feasible activation minutes due to the imposed constraints are 5, 15, 25, 35 and 45. In all instances, the percentage volume to be activated increases towards the end of hour which is related to the increasing accuracy of the ACE forecast, since the amount of imbalance to be regulated is calculated as percentage volume of the ACE forecast. Conversely, the ignorance level decreases towards the end of hour eventually reaching the lowest bound (10 MWh/h). In a few instances, for **4 and 5 max. activations** the ignorance level for the two first activations is set to a fairly high value close to 200 MWh. This implies that early activations should happen only in rare occasions where the ACE forecast is particularly large.

The **resulting ACE** after simulating the balancing activities according to the optimised schedule for the same period is illustrated also in Fig. 1.9. The ACE is noticeably reduced (up to 4.9 times) from **37.95** MWh/h before any regulation to **7.71–12.50** MWh/h. It is important to note that the average absolute error of the ACE forecast at the last selected activation minute is 6.34–10.67 MWh/h (Table 1.1). This is very close to the lowest average ACE value achieved (7.71 MWh/h) clearly demonstrates a very good overall performance of the algorithm and its generalisation ability when distinct sets are used for training and testing. The number of hours where ACE has increased as compared to that without regulation is rather small and varies from 2.9% to 10.4%.

---

[1] For comparability of positive and negative values, the absolute value of ACE and regulation energy is referred to hereinafter.

Table 1.1. Optimised regulation parameters and resulting imbalance for 1 to 5 max. activations

Data period		July–September 2016 (day type: all days)				
Reg. parameters		*optimised for all days*				
max number of activations		**1**	**2**	**3**	**4**	**5**
activation minutes		35	23; 45	22; 34; 45	15; 25; 35; 45	5; 15; 25; 35; 45
volume of activation relative to ACE forecast	%	90.5	75.4; 97.4	65.9; 81.9; 98.5	50.1; 50.7; 80.6; 93.7	31.1; 31.1; 31.1; 76.7; 94.3
ignorance level	MWh	10.0	22.1; 10.0	33.0; 27.5; 10.0	192.0; 107.0; 31.0; 10.0	182.0; 137.5; 81.8; 33.0; 10.0
Average |ACE| w/o reg.	MWh/h	**37.95**				
Average ACE w/o reg.	MWh/h	21.85				
Sum |ACE| w/o reg.	MWh	**19 315**				
Sum ACE w/o reg.	MWh	11 121				
Average |ACE| w reg.	MWh/h	**12.50**	**9.04**	**7.71**	**7.71**	**7.78**
Average ACE w reg.	MWh/h	4.42	3.63	2.47	2.73	2.55
Sum |ACE| w reg.	MWh	**6364**	**4601**	**3924**	**3923**	**3961**
Sum ACE w reg.	MWh	2252	1847	1255	1391	1298
|ACE forec. error| @ last act.	MWh/h	10.67	6.34	6.34	6.34	6.34
|ACE| change after reg.	MWh/h	**−25.44**	**−28.91**	**−30.24**	**−30.24**	**−30.16**
Sum |ACE| ch. after reg.	MWh	−12 950	−14 714	−15 390	−15 392	−15 354
Hours in total		**509**				
% of hours w reg.		82.7%	88.0%	85.7%	81.1%	81.1%
% of hours with increased |ACE|		10.4%	5.9%	4.3%	2.9%	2.9%
Ordered bal. energy	GWh	**16.419**	**20.490**	**20.507**	**17.776**	**17.915**
ordered per hour	MWh	**32.258**	**40.255**	**40.288**	**34.924**	**35.196**
orders for activation		421	624	658	548	581
Cancelled bal. energy	GWh	**−**	**1.374**	**1.113**	**0.249**	**0.309**
% of ord. en.		−	6.7%	5.4%	1.4%	1.7%
cancelled orders		−	105	83	17	19
Supplied bal. energy	GWh	**16.419**	**19.116**	**19.394**	**17.527**	**17.605**
supplied per hour	MWh	**32.258**	**37.556**	**38.102**	**34.435**	**34.588**
% of ord. en.		100.0%	93.3%	94.6%	98.6%	98.3%
regulation up	GWh	3.775	4.921	4.764	3.899	3.891
regulation down	GWh	12.644	14.195	14.630	13.629	13.714
Overregulated energy	GWh	**1.735**	**1.287**	**1.309**	**1.068**	**1.102**
% of suppl. en.		10.6%	6.7%	6.7%	6.1%	6.3%
orders causing overreg.		177	183	194	172	166

The stacked chart in Fig. 1.9 allows assessing the **efficiency of regulation** in terms of the provided balancing energy and improvement of the ACE. The sum of the ACE after regulation and provided balancing energy is always more than the ACE without any regulation because of the ACE uncertainty which sometimes causes redundant orders (leading to the cancellation of previous balancing orders or overregulation). During the specific period, the most efficient regulation happens when the max number of activations is 4–5. Then, cancellation is needed

for only 1.4%–1.7% of the ordered energy respectively (Table 1.1). Also, less balancing energy is used to reduce the ACE compared to cases with 2–3 activations. This is due to more gradual and cautious regulation which is possible with a larger number of activations within the ISP.
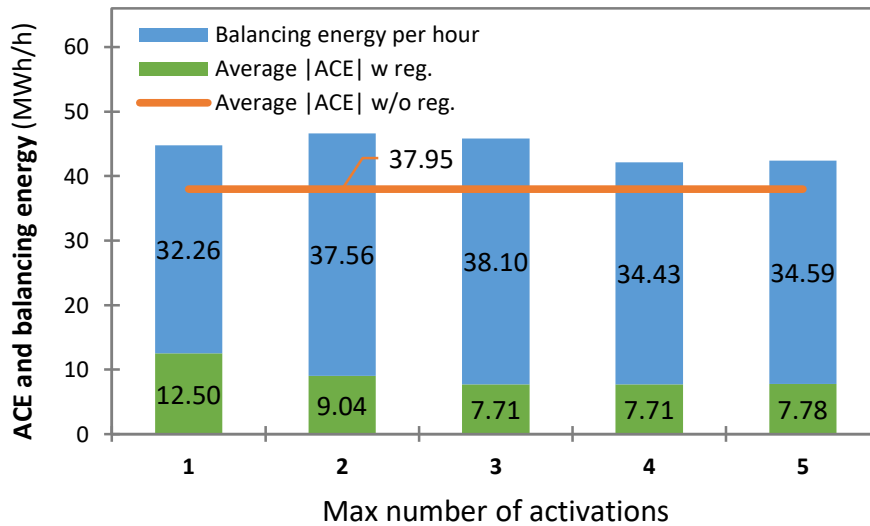
Fig. 1.9. Average |ACE| w/o and w reg. and provided balancing energy.
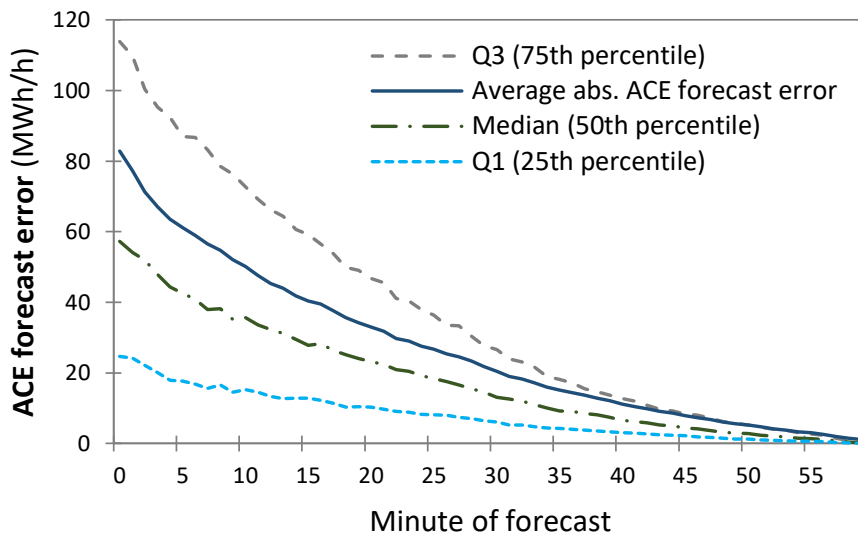
Fig. 1.10. Statistics of the absolute ACE forecast error depending on the minute of forecasting within the ISP of one hour.

Fig. 1.11 presents the frequency distribution of the hourly ACE without and with regulation applied to the testing subset of July–September 2016 dataset (509 hours in total). The ACE without regulation (blue bars) is moderately skewed to the right with an average value of +21.9 MWh/h. This can be explained by the behaviour of balance responsible parties (BRP) who tend to prefer long rather than short positions because the potential financial risk for 'short' prices is inclined to be more extreme than for 'long' prices [30]. As a result, the Baltic countries, in general, sell more energy to the OBP than they buy.

After applying the optimised regulation parameters to the test set of July–September 2016, the average ACE decreases from +21.9 MWh/h to +2.5 MWh/h (Fig. 1.11, orange bars). Thus,

the noticeable positive bias of the ACE is almost eliminated. This clearly demonstrates not only good performance of regulation with the optimised parameters but also the generalisability of the obtained parameters when applied to the testing data.
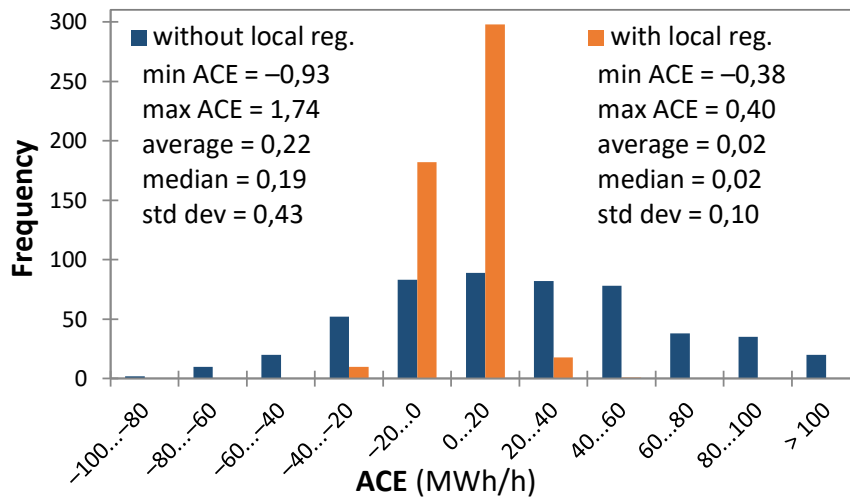
Fig. 1.11. ACE histogram w/o local reg. and w reg. (3 max activations).

Apart from the main results discussed previously, Table 1.1 includes additional data for evaluation of more granular aspects of power system balancing that are of interest to the TSO dispatch operators in charge of this process. **Ordered balancing energy** can be further divided into actually supplied energy and cancelled energy (i.e., ordered regulations that were later reduced or cancelled). Obviously, no cancellations are possible in case of 1 max. activation. The **supplied balancing energy** tends to grow as the number of max. activations increases from 1 to 3. However, 4 and 5 max. activations require nearly 10% less energy supply than 3 max. activations. Given the large positive bias of the ACE, several times more **downward regulation** is supplied compared to upward. This is true for all data periods analysed and any number of activations.

The proportion of regulation **energy cancellations** varies between 1.4–6.7% of ordered balancing energy (Table 1.1). The largest amount of cancellations is observed with 2 max. activations. Analysing the respective regulation parameters, the main reason for larger cancellations is rather early activations with relatively large regulation volumes. Since, almost surely, the ACE forecast at early stages is highly inaccurate, activation of large volumes will definitely result in later cancellations as the ACE forecast reaches more accurate values and fluctuates less. Therefore, if one desires to reduce the possible cancellations, early activations should be very restrained and, probably, reserved for only exceptionally large forecasted ACE values.

A situation when, at the end of hour, the ACE changes its sign due to the regulation, is distinguished as **overregulation** and presented in terms of overregulated energy and number of orders causing that. This proportion of energy varies between 6.1–10.6% of supplied balancing energy and is generally slightly more than the share of hours where ACE has increased as compared to that without any regulation.

1.3.2. Trade-offs between the minimal ACE vs other indicators

Besides minimising the ACE, a TSO is also interested in decreasing the amount of supplied energy as well as preventing cancellation of the orders or avoiding system overregulation that would otherwise imply additional costs to transmission system users. Therefore, while the *AOF parameter search* algorithm does not guarantee to find the globally optimal regulation parameters, it is useful to consider the possible trade-offs between minimisation of ACE versus minimisation of other important regulation indicators as illustrated by the charts in Fig. 1.12–Fig. 1.15. The results refer to balancing of the weekdays of July–September 2016 with 1 to 5 max. activations according to the regulation parameters optimised with seven different sets of weights and applying default constraints. By adjusting the weights assigned to the four components of the multi-objective function (1.2), it is possible to shift the priorities from ACE minimisation to decreasing the supplied balancing energy or ordered regulation power. The orange markers in the charts below represent the **Pareto front**, i.e., the most 'optimal' results of the whole set in terms of a smaller ACE or lesser amount of balancing energy. Markers are labelled by numbers indicating the selected max number of activations per. By definition, none of the Pareto-optimal points strictly dominates over any other in terms of both indicators.

While only 1 max. activation evidently ensures the lowest amount of provided balancing energy per hour (Fig. 1.12), it results in the largest ACE values due to early regulation (minute 35). When aiming to minimise the ACE, the Pareto-optimal results are achieved with 3 (two instances), 4 (one inst.) or 5 (two inst.) max. activations, though this is not always the case. However, the points with 2 max. activations are located far away from the Pareto set and therefore are not efficient.
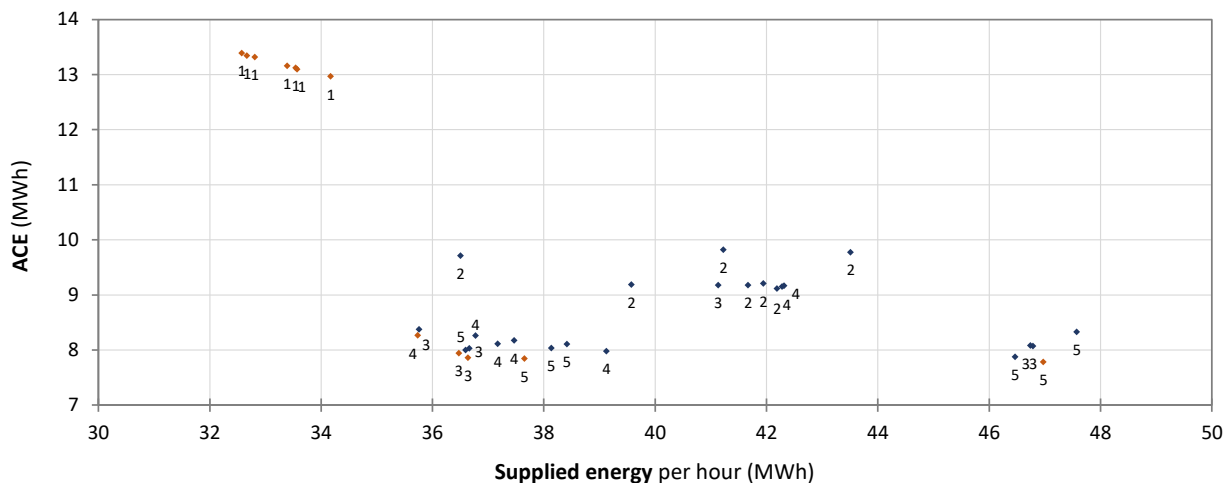
Fig. 1.12. Trade-off between minimisation of the ACE and supplied.

If we look at the trade-off between the minimal ACE and the amount of cancelled balancing energy (Fig. 1.13), the Pareto front again starts with 1 max. activation where it is not possible to cancel any of the regulation orders and is followed by 3 (three instances), 4 (one inst.) and 5 max. activations (two inst.).

Similarly, we can analyse the trade-off between the ACE versus the overregulated energy per ISP (Fig. 1.14) or the average ordered power per activation (Fig. 1.15). In contrast to the

two previous cases, none of the points with 1 max. activation belong to the Pareto set and they are located much further from it compared to 2 or more max. activations. For overregulated energy, the efficient solutions are achieved with 4 or 3 (one inst. each) and 5 max. activations (three inst.), whereas for average ordered power per activation, the Pareto front is formed of points with only 5 max. activations (four inst.).

To sum up the possible trade-offs, all the charts demonstrate that, besides the Pareto-optimal results, there are also quite many other points close to the front. As a rule of thumb, the furthest points mostly represent 1 or 2 max. activations, suggesting that more activations should be preferred. More so important, the results are largely dependent on the input data used, so they should not be generalised to any possible time series before testing each particular dataset.
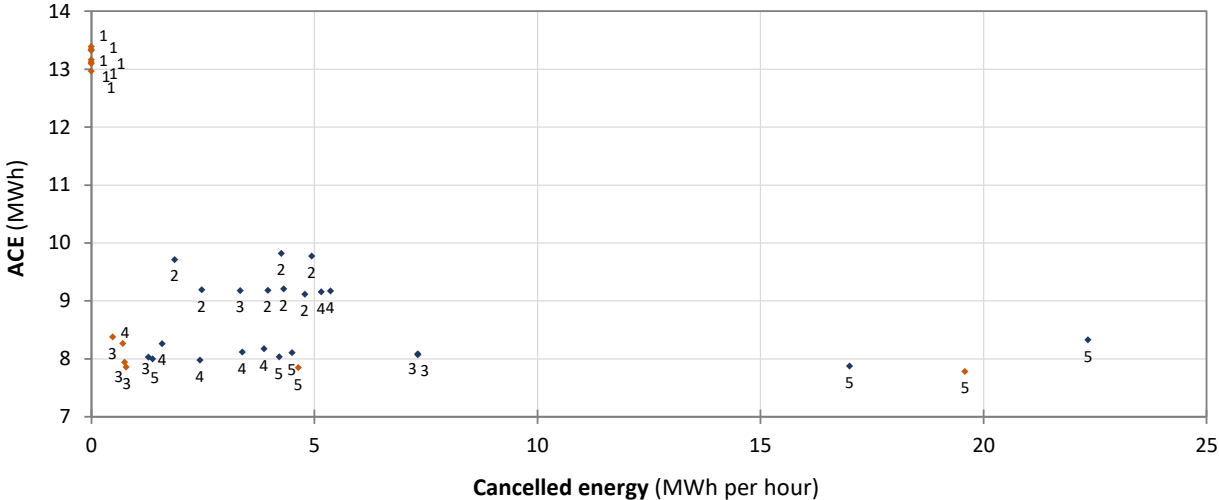
Fig. 1.13. Trade-off between minimisation of the ACE and that of cancelled energy.
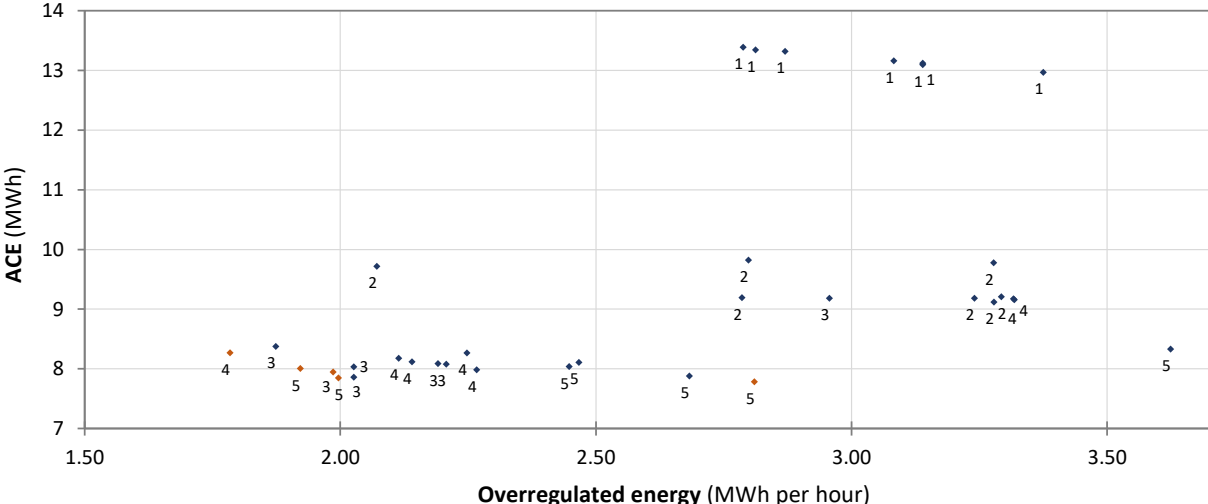
Fig. 1.14. Trade-off between minimisation of the ACE and overregulated energy.
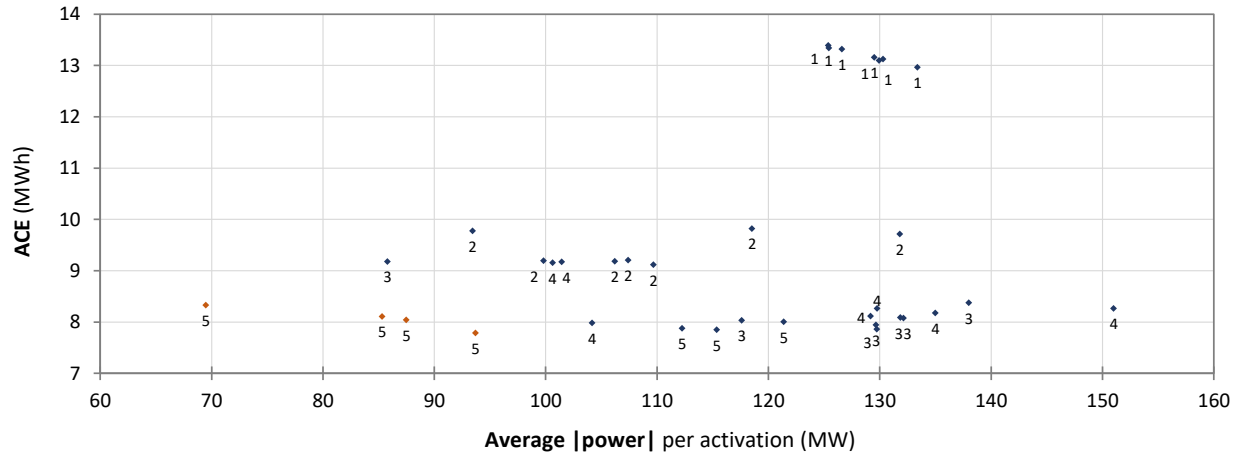
Fig. 1.15. Trade-off between minimisation of the ACE and ordered power.

1.3.3. Cost comparison of regulation energy

Though cost minimisation of balancing services was not at the focus of this study, it is useful to quantify the economic benefits of common Baltic balancing operations compared to sole reliance on the neighbouring Russian power system for balancing needs (Table 1.2).

Table 1.2. Estimated cost of regulation energy

Max. number of activations	1	2	3	4	5
(a)	*Cost of ACE with local regulation (€)*				
Energy bought @ 100 €/MWh	205 643.77	137 685.42	133 461.79	126 568.68	133 142.01
Surplus sold @ 5 €/MWh	–21 540.16	–16 118.70	–12 948.91	–13 285.65	–13 148.32
Cost of ACE	*184 103.60*	*121 566.72*	*120 512.88*	*113 283.03*	*119 993.69*
(b)	*Cost of supplied local regulation energy (€)*				
Energy bought @ 50 €/MWh	188 740.31	246 043.25	238 190.36	194 939.63	194 561.59
Surplus sold @ 10 €/MWh	–126 444.67	–141 952.35	–146 298.99	–136 286.05	–137 142.43
Cost of supplied local energy	*62 295.64*	*104 090.90*	*91 891.37*	*58 653.58*	*57 419.15*
Total cost <u>with</u> local regulation (a) + (b)	**246 399.25**	**225 657.63**	**212 404.26**	**171 936.61**	**177 412.84**
(c)	*Cost of ACE without local regulation (€)*				
Energy bought @ 100 €/MWh	409 669.61				
Surplus sold @ 5 €/MWh	–76 089.76				
Total cost <u>without</u> local regulation (c)	**333 579.85**				

If we assume that the OBP buys excess energy at 5 €/MWh and sells deficit at 100 €/MWh [30], then for the test dataset of 509 hours the cost of fully depending on the OBP (cost of the ACE without regulation) would be equal to 333.6 thousand € (76.1 thousand € income from sold energy and 409.7 thousand € expense for purchased energy) (Table 1.2, section (c)).

However, when local balancing energy is ordered in accordance with the optimised parameters as presented before, the overall costs decrease notably (Table 1.2, section (a) & (b)). For simplicity's sake, the prices of local balancing bids are assumed to be always cleared at 50 €/MWh for upward and 10 €/MWh for downward regulation and perfect liquidity is implied. In all cases with local balancing operations, the total imbalance costs diminish by a factor of 1.35 to 1.94 (depending on the selected max. number of activations) compared to the case with no local regulation. The lowest cost is achieved with 4 and 5 activations (171.9 and 177.4 thousand € respectively). Even with only 1 activation the cost with local regulation is 246.4 thousand € which is significantly lower than without local regulation (333.6 thousand €).

1.4. Summary

The numerical simulations of balancing activations based on the parameters optimised using historical time series affirmed the generalisability of the results, since in most of the cases the average absolute ACE was close to the forecast error. Additionally, this confirms improved ACE forecasting techniques to be a promising avenue for further research as any enhancements there can be expected to notably improve the efficiency of balancing operations. Furthermore, as currently the balancing parameter optimisation tool tends to postpone regulation to later part of the ISP when forecasts are more accurate, perfected early prediction abilities would allow for more even balancing operations throughout the ISP.

For the dataset considered in this study, 4 and 5 were identified as the maximum number of activations during the ISP equal to one hour that can provide the most efficient balancing. While the case with 3 maximum activations did provide a small overall ACE, the aforementioned cases were superior in terms of the utilised balancing energy and estimated cost.

While our tool can still be expanded to incorporate the merit order of balancing bids, the initial simplified economic calculations already point to noticeable financial gains from a more active local balancing in the Baltic power system and decreased reliance on regulation from the Russian power system, especially with the OBP's balancing energy pricing policy in place at the time of the study.

Even disregarding the financial aspects, the evolution of the common Baltic balancing market is well underway after its launch at the beginning of 2018. Similar trends are ongoing throughout Europe as the TSOs need to adapt the recently established European Commission guidelines on electricity balancing and devise their AOFs for more efficient power system balancing. Thus this study proves to be of significant relevance in the light of the changing balancing market landscape in Europe. The initial results of this study have informed some of the decisions of the Baltic TSOs in the development of their common balancing market. Moreover, this is also important as the Baltic countries strive to desynchronise from the IPS/UPS by 2025.

2. MODELLING OF DR-ENABLED ELECTRIC HEATING

2.1. Motivation and background

Dissemination of intermittent renewable energy sources (RES) such as wind, wave and solar power presents new challenges for the power systems. To reduce the curtailment of renewables and efficiently accommodate the distributed and variable RES across the power system, energy storage has become a necessity. Various forms of energy storage include mechanical energy storage (hydropower, compressed air, flywheel), electrochemical batteries, power to gas storage, electric and magnetic energy storage (capacitors and supercapacitors, superconducting materials) and thermal energy storage.

While there are mature and long-known technologies for large-scale energy storage such as pumped-storage hydropower, which is the most used storage option in the power sector worldwide, many efforts are devoted to the development of small-scale energy storage primarily for use in the residential sector. One of such technologies is smart electric thermal storage with household appliances for space heating and hot water heating [38]. It is a sensible heat storage system [39] which consumes electricity and is able to store it in the form of thermal energy for a long time to be used later just when it is needed. Thus the power demand of the heating system is decoupled from the time of thermal energy end-use by the domestic customer.

Electric thermal storage heaters have been in use for decades especially in countries where two-tariff electricity pricing is applied to households. Conventional thermal storage heaters had limited controllability due to relatively low heat retention rate. However, for the newest generation of smart electric thermal storage (SETS) system, the heat retention rate is significantly improved, and the recent advances of information and communication technologies have allowed a significant technological development of the storage heaters. SETS devices are now equipped with smart control at the aggregate electric power system level while ensuring that individual household space and water heating end-use requirements are maintained [38]. It allows to decouple the electricity demand from the expected heat output and deliver electricity to the SETS virtually at any time while consuming the heat at any other time when it is needed. Consequently, the whole electricity supply chain, including generation, transmission, distribution and consumption, can potentially benefit from SETS.

SETS can provide overall societal benefits such as cost savings to the customers and RES curtailment reduction, whereas the aggregated load can offer a number of services to the power system such as demand shifting and demand response, ancillary services (frequency response, reserves provision), congestion management and deferral of capital investments into the network.

It is estimated that by retrofitting all existing night storage heaters in the EU, SETS could introduce a controllable load of 55 GW (37 GW for all traditional night storage heaters and 18 GW for hot water) and, consequently, save 7.4 TWh of heating energy per year and avoid 3 million tons of CO_2 emissions per year compared to conventional storage heaters [40].

While the SETS technology and appliances are in place already [38], the power systems are not yet in a position to integrate them, and there are various ongoing studies on how to facilitate

this process. One of the problems to be solved includes co-optimisation of the electricity system scheduling together with requirements of the electric heating demand [39]. The modelling and optimisation environment for electrical power systems should endogenously represent the local small-scale thermal storage devices, including their technical characteristics and thermal energy end-use requirements.

To assess the potential cost savings to the customers when using SETS with dynamic pricing under conditions of a liberalised electricity market, the variable electricity prices need to be considered with appropriate temporal resolution (e.g., hourly resolution for the Nord Pool day-ahead market prices). Consequently, thermal energy end-use should also be modelled with an hourly resolution.

This section is focused on modelling the residential heating energy demand. We propose an approach based on physical experiments and virtual simulations to obtain the equivalent thermal characteristics of the building which can then be used for modelling the thermodynamics of the building under different weather conditions.

The approach presented here served as a basis for our further studies involving physical experiments in different buildings in Latvia to derive their thermal characteristics and heating energy requirements. The consumption of individual buildings can then be scaled to a national aggregate level. The aggregated electric load of local small-scale thermal storage will be integrated into the overall power system models to assess the impact of SETS on power system planning, unit commitment and dispatch of energy and reserves, distribution network congestion etc. Main results from this impact assessment are presented in Chapter 3. Furthermore, the heat demand modelling results have been also used for cost-benefit assessment of demand response from SETS from the end-user point of view in Chapter 0.

The scientific work presented in Chapters 2 and 3 took place during 2015–2018 as part of the RealValue project which received funding from the European Union's Horizon 2020 research and innovation programme under grant agreement No 646116.

2.1.1. Smart electric thermal storage technology

SETS is a decentralised space heating and hot water system with energy storage and up to 20% efficiency gains compared to traditional night storage heaters [38]. It consists of electric space heating radiators with an insulated thermal mass for storing heat (Fig. 2.1) and a hot water cylinder (Fig. 2.2).

SETS space heaters contain a highly insulated solid thermal energy storage core of bricks which enables the conversion of electrical energy into thermal energy for use at a later time [38]. The heat is released into the room by radiation and convection. Modern dynamic electric storage heaters are equipped with a fan which blows warm air from the core of the heater into the room. This allows for a more precise heat distribution control as compared to conventional static storage heaters without a fan blower [39].
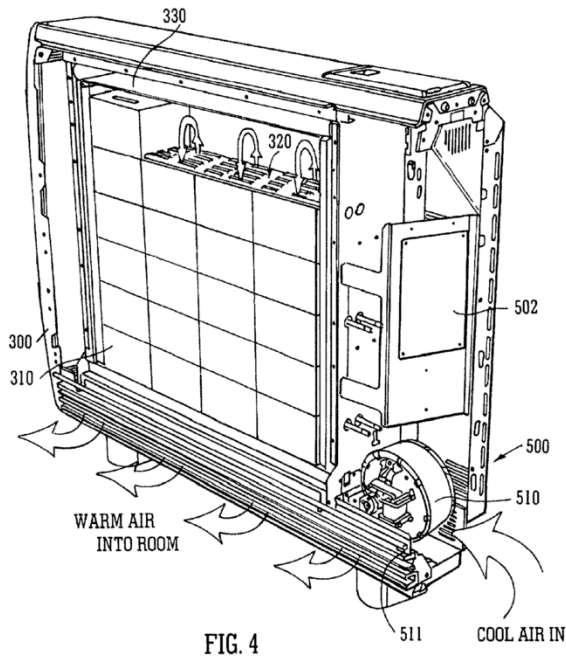
Fig. 2.1. SETS for space heating [38].
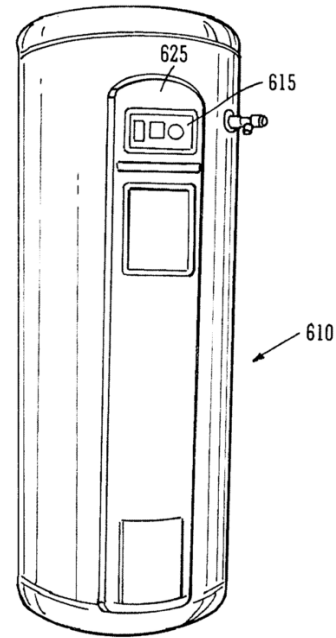
Fig. 2.2. SETS for hot water heating [38].

Recent developments of material and electronic control technologies have enabled storage heaters to provide the householder with time and temperature control comparable with direct electric heating technologies. Additionally, these devices can be managed remotely so that they can be charged flexibly at a time when it best suits the electricity system without jeopardising householder comfort [38].

The application range of dynamic electric storage heaters with a fan is typically 2–7 kW with a storage capacity of 16–56 kWh per charge cycle. The application range of static electric storage heaters is typically 0.75–3 kW with a storage capacity of 8–24 kWh. The maximum core temperature is about 700 °C [39].

SETS water cylinders use the same basic principle, except that the energy is stored in water rather than a solid medium. Both systems share the same communications and control architecture and can therefore be managed in a unified manner [40].

SETS includes advanced electronic command and control capabilities such as an automated input control with adaptive learning function to determine how much heat will be needed on a particular day while accounting for prevailing weather conditions. This daily energy requirement is calculated using an algorithm based on the residual stored energy, the rate of change in room temperature after the evening heating period, as well as user-programmed heating requirements. SETS uses ICT to enable flexible tariff regimes, to support integration of renewable energy resources at any time, allowing time of use tariff schemes to be integrated into the operation of SETS [40].

SETS facilitates the decoupling of energy production from energy consumption so that renewable energy can be converted into heat and offers control over when this heat is released. This allows low carbon space heating and hot water to be deployed when the end-user desires it [40].

2.1.2. Review of building heat demand modelling approaches

Mathematical models for simulating building energy systems and consumption can be either theoretical or experimental [41]. Theoretical models are described by mathematical equations derived from physical laws, whereas experimental models are devised empirically by measuring input and output signals of the system and evaluating the system's response.

Modelling structure for any energy system consists of three main blocks: input variables, output variables and the system itself (Fig. 2.3) [41]. While modelling it is necessary to determine one of these three building blocks when adequate information about the other two blocks is available. Consequently, the energy models are classified as white-box, black-box or grey-box models.
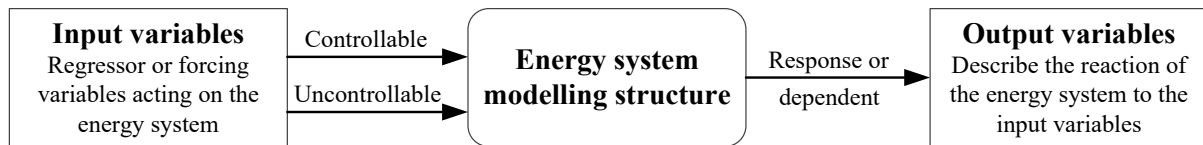
Fig. 2.3. Modelling structure of a building energy system [41].

White-box models are highly accurate and use a forward approach to predict the output variables based on a detailed structure and parameters of the model subjected to specific input variables [41]. To employ this approach, it is assumed that all the thermal and geometric building characteristics are well-known, which is usually the case for building design but is much more difficult and expensive to obtain for already existing buildings [42].

Black-box models use a data-driven approach to develop the model based on the knowledge of the input and output data acquired through experiments [41]. Black-box approaches often employ statistical or machine learning to derive a prediction model from a database, e.g. actual or forecasted energy consumption of a building [42]. When experimental data is obtained within the building, it is done either in an intrusive or a non-intrusive manner [41].

Grey-box or **hybrid modelling** involves formulating a physical model and identifying important and aggregated parameters and characteristics by a statistical analysis which requires a high level of expertise [41]. Whereas black-box models do not need a detailed description of the building geometry, instead they require a large amount of training data over an exhaustive period of time. In contrast, for grey-box models, a small amount of data for training is necessary with a rough description of the building geometry.

As opposite to white-box and grey-box models the results of which can be interpreted in physical terms, black-box model results can be difficult to interpret in physical terms [42], [43]. However, automatic parameter estimation using a black-box model has a significant advantage over white-box models in having a small setup cost and little computational effort [44].

In this study, we employ an experimental black-box modelling approach by using the outdoor temperature and heating consumption of the building as input data and the room temperature as output data. Based on this data, thermal parameters of the building are obtained

which are then used to estimate the heating consumption under different weather conditions at various time scales, e.g., hourly, daily, weekly or yearly.

This approach is also referred to as a data-driven inverse problem whereby the physical characteristics of a building are acquired given the actual performance data [45]. That is a classical formulation known as parameter estimation or system identification problem [46]. The building is considered as a black box the characteristics of which are derived from temperature measurements and energy consumption data [45]. Mathematically, the thermodynamics of the building can be described by a differential equation with unknown parameters. Using the measured values of input and output, the best or optimal estimate of these parameters is obtained.

A similar approach is implemented in [47], where a model of the space heating and cooling load is proposed to study its behaviour during cold load pickup after a power outage. The model is able to capture the thermal characteristics of a house at a thermostat without modelling all the details of the house. Since a detailed simulation model for the house thermodynamics used traditionally for the thermal design studies of the building is not practical for modelling a system-level heating load, the authors have minimised the data and computation requirements while making maximum use of the available data. Yet, the model is accurate enough for the study of cold load pickup. The parameters for the model can be obtained very easily through simple measurements: the authors use only the thermal characteristics as observed at the thermostat, i.e., the room temperature. A simple model is derived based on the assumption that the thermostat condenses building thermal characteristics (including the effects of weather conditions and resident lifestyle) into two variables – on-duration for heating and off-duration for cooling between to setpoints of the thermostat. The parameters of the model are obtained through simple experiments by turning the heater off and on for a definite time and measuring the temperature at the thermostat. Finally, after additional simplifications and approximations, all the dynamic characteristics of the house are summarised into a single parameter (harmonic constant), which is independent of weather and internal heat source. To find this constant, only the on/off-durations are required.

The objective of [47] has been to provide a quantitative method to predict the magnitude and duration of the overload following an outage. We suggest that a similar approach can be used to model the various effects on the power system of dissemination of a large amount of smart electric thermal storage appliances.

2.2. Methodology

2.2.1. Thermal model based on electrical analogy

For modelling thermodynamics of buildings, RC-diagrams are often used based on electrical analogy where each element of the building can be represented with resistors and capacitors as lumped parameters [48]–[52]. Such thermal network models have advantages of simplicity, transparency and low computational effort [49]. Theoretically, the simplest network might consist of one resistance and one capacitor [45]. However, this is practically and

physically unrealistic, therefore usually more elements are used. For example, [49]–[51] use second-order models that describe construction elements by three resistances and two capacitances. In [51], this reduced-order model is devised from a 20th-order model through nonlinear constrained optimisation and is given preference over an even simpler first-order model since the latter showed considerable performance differences from the high-order model, unlike the second-order model. This approach is further improved in [49] by using a multi-objective function search algorithm and reporting a large number of results for various construction elements.

For this study, we devised a simplified thermal network model presented in Fig. 2.4 which is suitable for inverse modelling to obtain equivalent thermal parameters in a computationally efficient way. Resistances represent heat transfer by conduction, whereas capacitances stand for thermal mass which reflects the ability of a material or a combination of materials to store energy. The model is developed in MATLAB Simscape (Fig. 2.5) which enables creation of models of physical systems and simulation of their thermal performance using MATLAB Simulink.
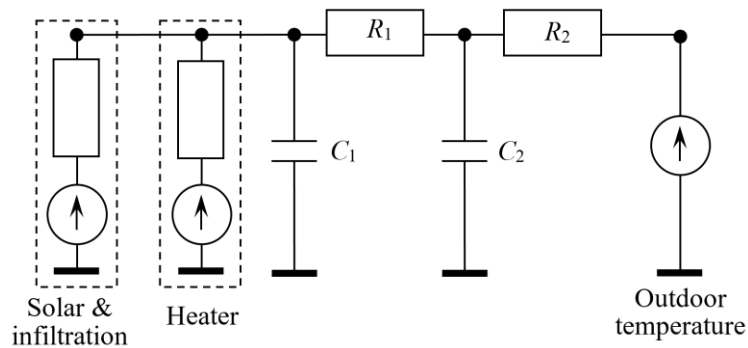
Fig. 2.4. Building thermal network used for inverse modelling.
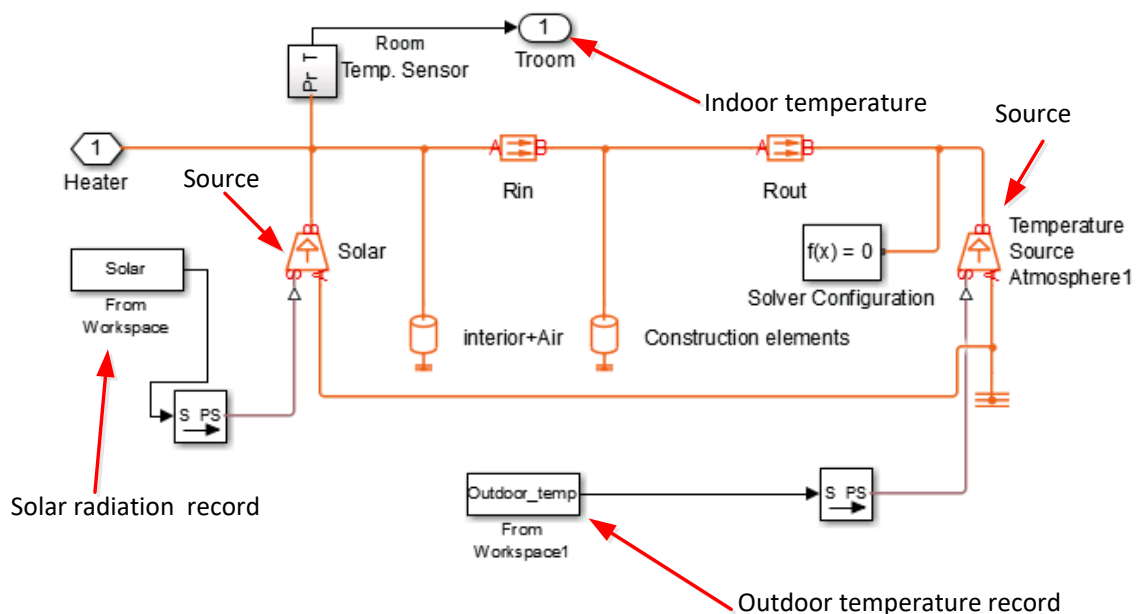
Fig. 2.5. Building thermal model in MATLAB Simscape.

2.2.2. Model parameter estimation

To obtain the equivalent thermal network parameters for each building of interest, first of all, model parameter identification was performed. Equivalent thermal parameters R_1, R_2, C_1 and C_2 (Fig. 2.4) were estimated according to the algorithm shown in Fig. 2.6. Model parameters were generated randomly employing Monte Carlo sampling and then applied to the simplified thermal network for simulation. The output of the model (energy consumption) was compared with measurements of virtual or physical experiments using mean square error as the error measure. The sampling was repeated for 100^n times, where $n = 4$ is the number of unknown parameters. The parameters which provided the most accurate performance of the model were saved. This approach involves a partial enumeration with a high accuracy thanks to the Monte Carlo random sampling, which allows selecting a result close to the global minimum avoiding local minima. The model with its tuned parameters can then be used for building heating energy demand modelling at the individual and aggregate level.
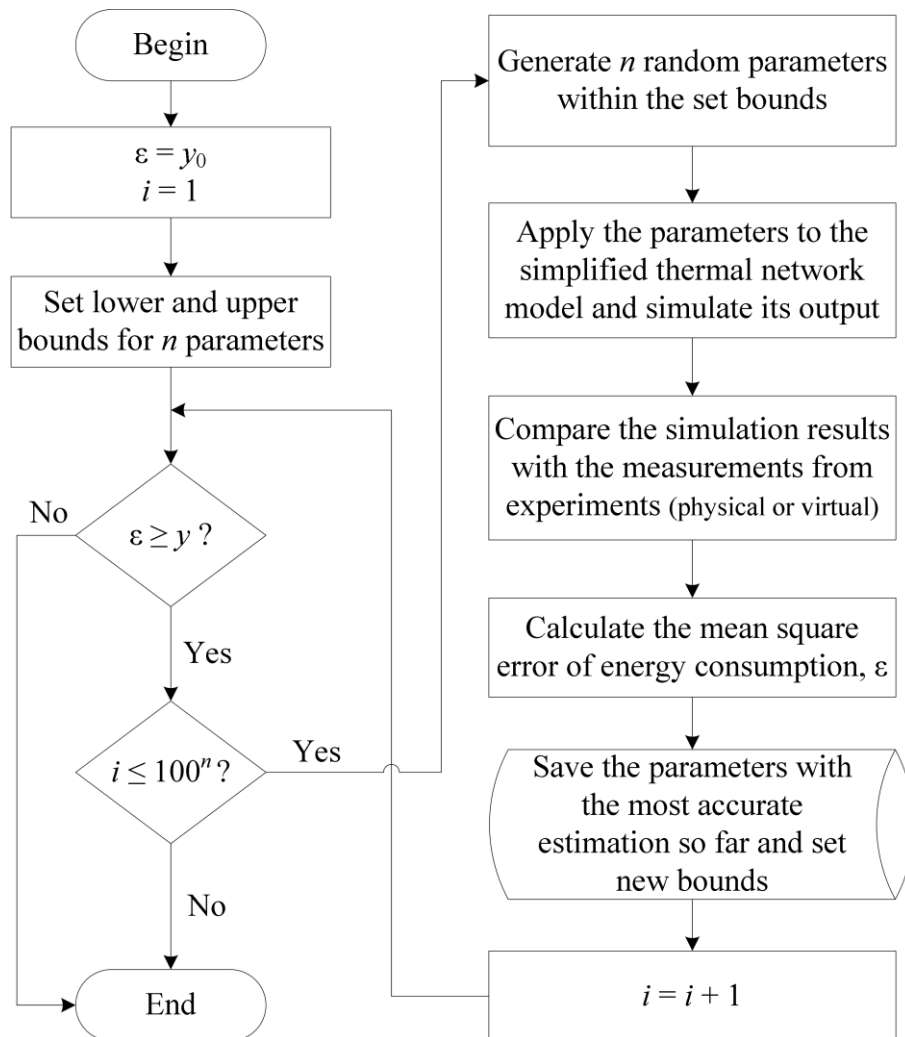
Fig. 2.6. Flowchart for parameter estimation of the thermal network.

2.2.3. Validation of model performance

The proposed building heat demand modelling approach was validated via virtual and physical experiments. Virtual experiments involved comparison of the proposed model simulation results to two more complex models, whereas physical experiments were carried out in a real residential house allowing to identify its thermal parameters to compare the building's actual (measured) and simulated thermal performance.

Virtual experiments

To estimate equivalent building parameters for the model in Fig. 2.4, we performed several virtual experiments employing a more complicated model represented in Fig. 2.7 to simulate the thermal dynamics of three different buildings. We should note that, at this stage, we assumed there are no heat losses and gains from infiltration or solar radiation.
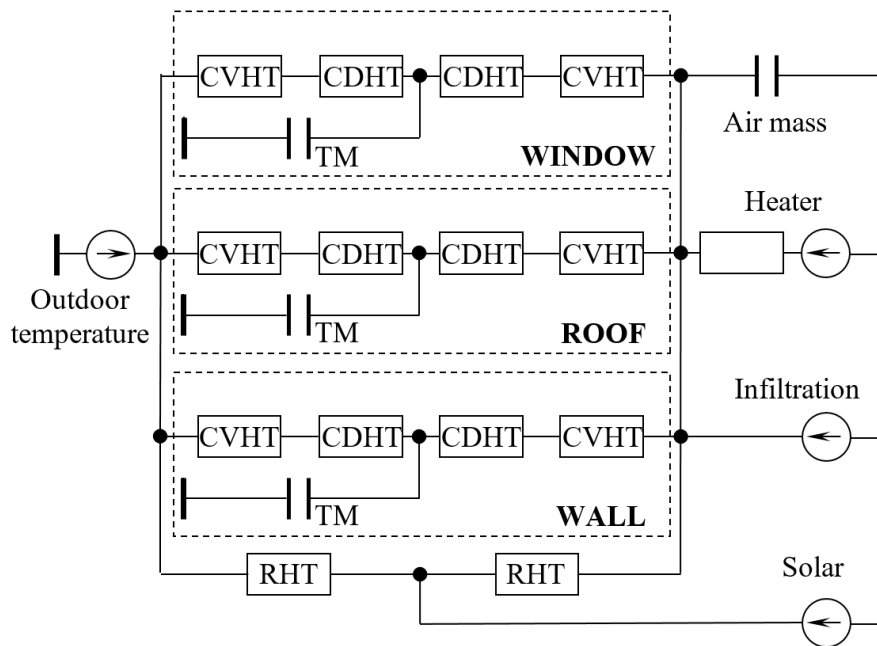
Fig. 2.7. The complex thermal network used for virtual experiments[2].

For the virtual experiments, we selected **three types of buildings** with the same geometry, but different insulation levels (House 1 having the least insulation and House 3 with the best insulation; all the parameters of buildings are presented in Table 2.1).

First, we used the complex model (Fig. 2.7) to simulate the performance of each building and obtain its heat demand under different weather conditions. Using the data of outside temperature, heat demand and room temperature obtained from simulations of the complex model, we then estimated the equivalent thermal network parameters for the simplified building model (Fig. 2.4).

---

[2] CVHT – convective heat transfer, CDHT – conductive heat transfer, RHT – radiative heat transfer, TM – thermal mass.

Table 2.1. Building parameters for virtual experiments

Parameter	Building Construction Element		
	Walls	*Windows*	*Roof*
Area (m²)	320	6	601
Thickness (m)	0.2	0.01	0.2
Convective heat transfer coefficient with indoor air (W/(m²·K))	24	25	12
Convective heat transfer coefficient with atmosphere (W/(m²·K))	34	32	38
Specific heat capacity (J/(kg·K))	835	840	835
House 1			
Thermal conductivity (W/(m·K))	0.038	0.78	0.035
Mass (kg)	122 880	162	3845
Density (kg/m³)	1920	2700	32
House 2			
Thermal conductivity (W/(m·K))	0.0038	0.0078	0.0035
Mass (kg)	122 880	243	7680
Density (kg/m³)	1920	4050	64
House 3			
Thermal conductivity (W/(m·K))	0.0019	0.0038	0.00185
Mass (kg)	245 760	486	38450
Density (kg/m³)	3840	8100	320

Fig. 2.8 illustrates the performance errors of the simplified model for House 1 with estimated parameters at the outside temperature of 0 °C. While there is no energy consumption error at the outside temperature of 0 °C, the accuracy significantly decreases up to an error of 9% at other outside temperatures which were not used for parameter estimation of the model.

Consequently, we expanded the range of experiments for parameter estimation with more outside temperatures, namely: –10, –5, 5 and 10 °C. Model performance errors with the estimated parameters for House 2 and 3 are presented in Fig. 2.9–Fig. 2.11.

As shown in Fig. 2.9–Fig. 2.10, energy consumption errors for House 2 are zero at those outside temperatures which were used for parameter estimation (circle markers). At other temperatures (diamond labels) errors tend to increase for longer simulations of energy consumption (compare Fig. 2.10 for 72 hours versus Fig. 2.9 for 48 hours).

For House 3, errors were zero for energy consumption over 48 hours, while the errors increased for a simulation of 150 hours (Fig. 2.11). These errors are mostly due to the delay or advance of the signal representing the thermodynamics of the house in relation to the actual signal (Fig. 2.12).
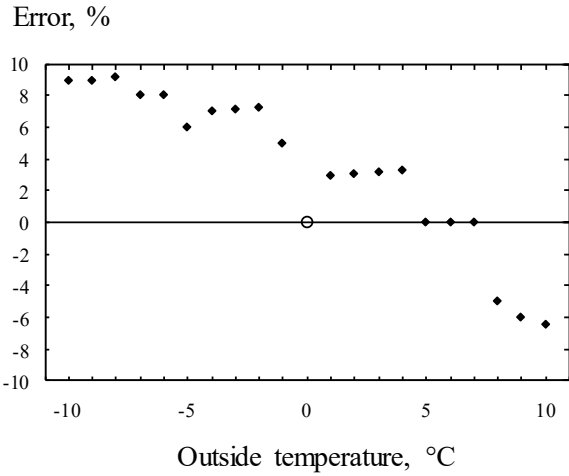
Error, %

Fig. 2.8. Energy consumption errors for House 1 at different outside temperatures for model with parameters estimated at the outside temperature of 0 °C (circle marker).
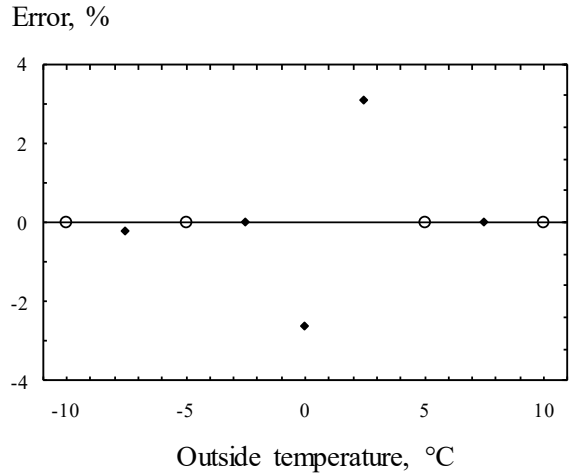
Error, %

Fig. 2.9. Energy consumption errors for House 2 over 48 h at different outside temperatures for model with parameters estimated at the outside temperature of –10, –5, 5 and 10 °C (circle mark.).
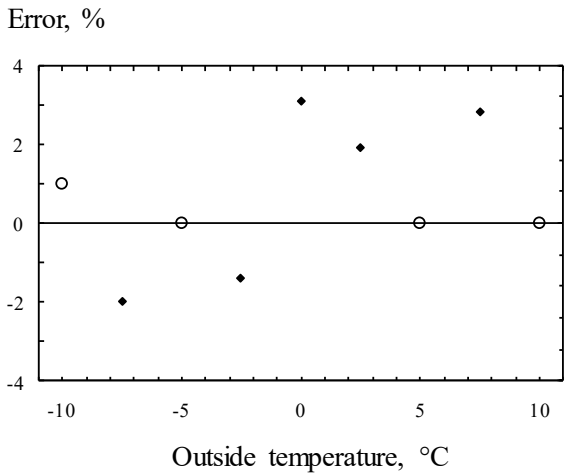
Error, %

Fig. 2.10. Energy consumption errors for House 2 over 72 h at different outside temperatures for model with parameters estimated at the outside temperature of –10, –5, 5 and 10 °C (circle markers).
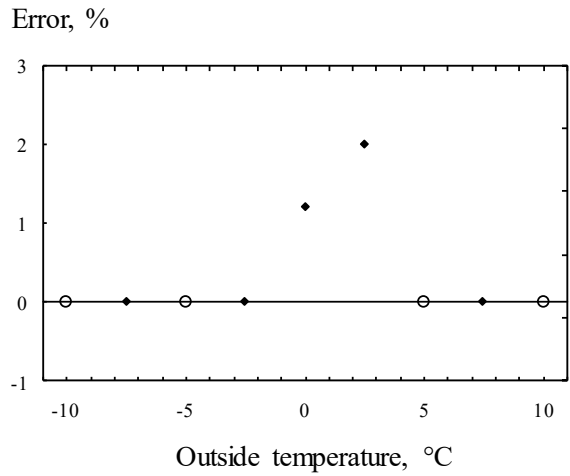
Error, %

Fig. 2.11. Energy consumption errors for House 3 over 150 h at different outside temperatures for model with parameters estimated at the outside temperature of –10, –5, 5 and 10 °C (circle mark.).
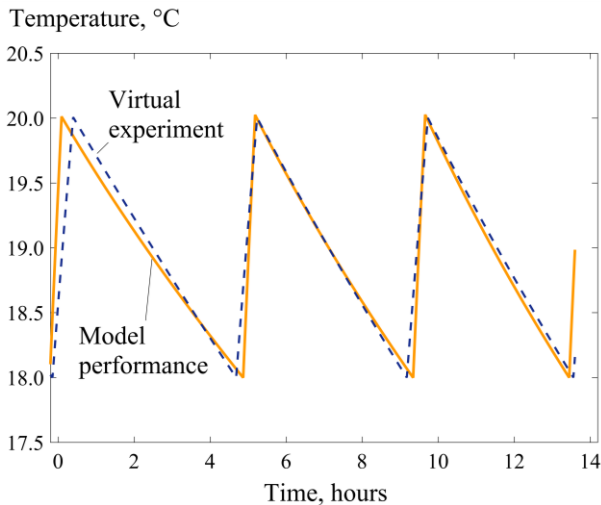
Temperature, °C

Fig. 2.12. Virtual experimental data of room temperature and the corresponding model performance as estimated for a constant outside temperature of 0 °C.

Finally, for validation of our simplified model, we also compared its performance to an even more complex **EnergyPlus-calibrated model**. This was possible thanks to our partners from University College Dublin (namely, Assoc. Prof. Donal P. Finn and PhD William J.N. Turner) within the RealValue project who provided us building simulation results obtained with their developed thermal network model. This more complex RC model (Fig. 2.13) is based on [52] with a few modifications.

The complex model presents one of the residential building archetypes (a mid-floor apartment) in Ireland initially developed in EnergyPlus simulation platform with a very high granularity of data [53]. Then, the reduced-order thermal network model (Fig. 2.13) was derived by calibration based on the detailed EnergyPlus archetype model output. Solar gains and ventilation losses were calculated based on weather data of one year with an hourly resolution. The reduced-order RC model is necessary for modelling the aggregated electric load of heaters with an affordable computational effort to integrate it into power system models and assess the large-scale impact of smart electric thermal storage.

Using the derived thermal network model, simulations were performed on it at the outside temperature of 0 °C. Fig. 2.14 shows the indoor air temperature dynamics for a single day. By using the output of the complex EnergyPlus calibrated model, we estimated the parameters for the corresponding simplified model (Fig. 2.4) and ran simulations on it at the same outside temperature. As shown in Fig. 2.14, the simplified model was able to replicate the temperature dynamics of the complex model with high accuracy. This implies that the simplified model should also be able to accurately model the heating demand characteristics of the building.
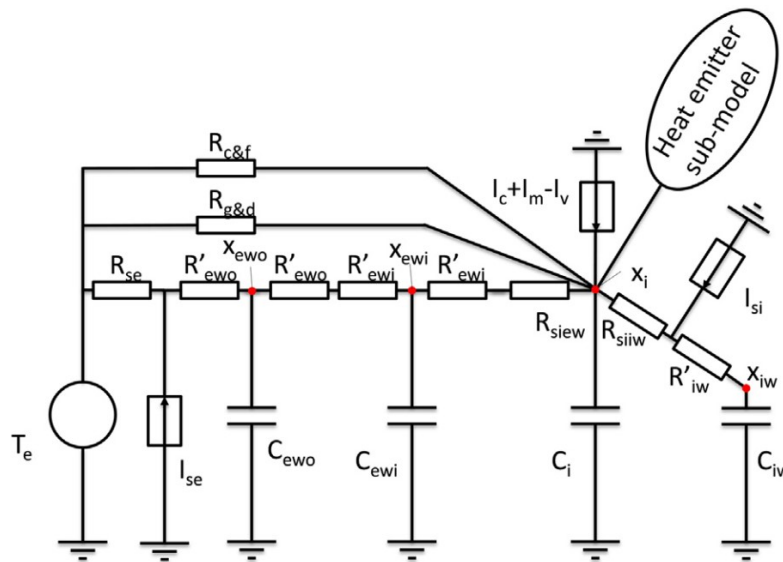
Fig. 2.13. The complex thermal network [52] used for comparison with the simplified model[3].

---

[3] C_{ewo}, C_{ewi} – thermal capacitance of the outer and inner portion of the external wall, respectively; C_i, C_{iw} – thermal capacitance of the inside zone of the building and the internal wall; I_c, I_m – cooking and metabolic heat gain; I_{se}, I_{si} – solar gain on external and internal building elements; I_v – heat exchange through ventilation (with external environment); $R_{c\&f}$, $R_{g\&d}$ – combined thermal resistance of ceiling and floor, glazing and doors; R'_{ewi}, R'_{ewo} – half of the thermal resistance of the inner and outer portion of the external wall; R'_{iw} – half of the thermal resistance of the internal wall; R_{se} – external surface resistance; R_{siew}, R_{siiw} – internal surface thermal resistance, external and internal wall; T_e – external temperature evolution; x_{ewo}, x_{ewi} – temperature of the outer and inner portion of the external wall; x_i – temperature of indoor environment; x_{iw} – temperature of the internal wall.
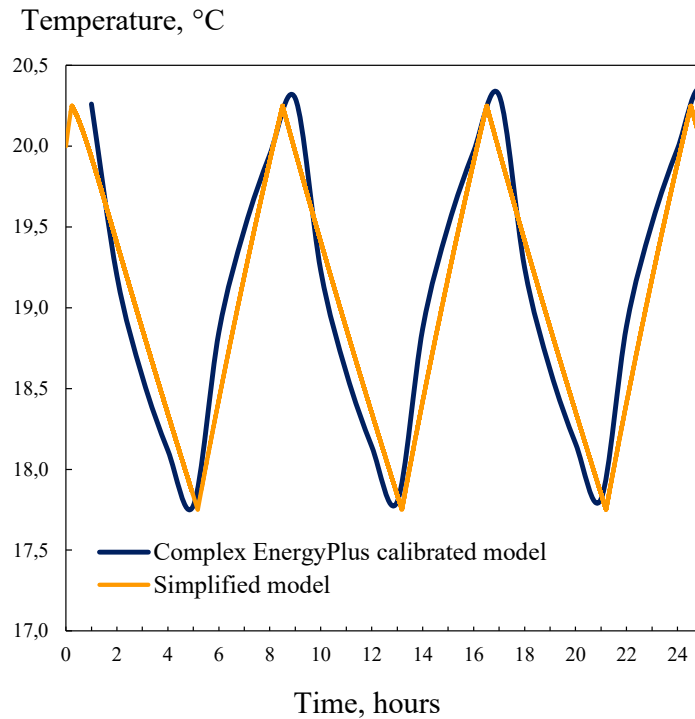
Fig. 2.14. Comparison of room temperature as per the complex EnergyPlus calibrated model and the simplified model.

Physical experiments

Additionally, we conducted a physical experiment on a real residential building by measuring its room temperature and the corresponding outside temperature during heating and cooling of the building (i.e., with the heater turned on or off). As previously, we used the measured inside temperature and information on the outside temperature to estimate the thermal characteristics of the building. Fig. 2.15 shows a comparison of the actual and estimated indoor temperature during a physical experiment on March 13–16, 2016 when the building was let to cool for two days and then heated. It can be observed that the derived model exhibits high accuracy as compared to the experimental data. The mean average percentage error for indoor temperature estimation was 4.44%.

The results for model validation for the same building (March 17–March 25, 2016) are presented in Fig. 2.16 allowing to conclude that the overall model performance is good. Until hour 114 and from hour 138–162, the building was let to cool down, while during the remaining time (hour 114–138 and 162–190) it was heated. Each day there was some solar irradiation which contributed to the heating of the building even with the heating equipment turned off. This shows the importance of considering solar gains.

The derived model enables us to calculate the heating consumption of the building during the whole heating season. For example, consumption during the 2015/2016 heating season was estimated as 86.52 kWh per square meter when solar gains are considered. Without solar gains, heating consumption is 92.3 kWh per square meter. The heating demand for various types of buildings will be used to elaborate the national-scale model.
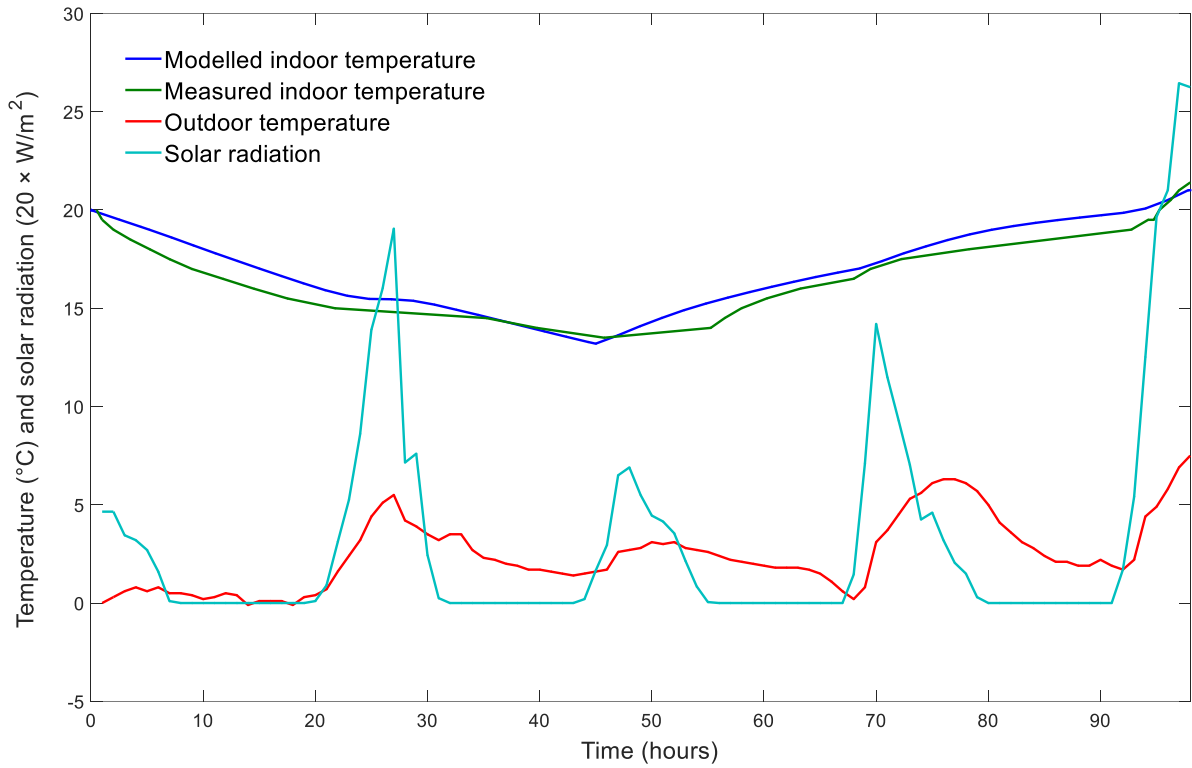
Fig. 2.15. Physical experiment data of room temperature and the corresponding model performance (March 13–16, 2016).
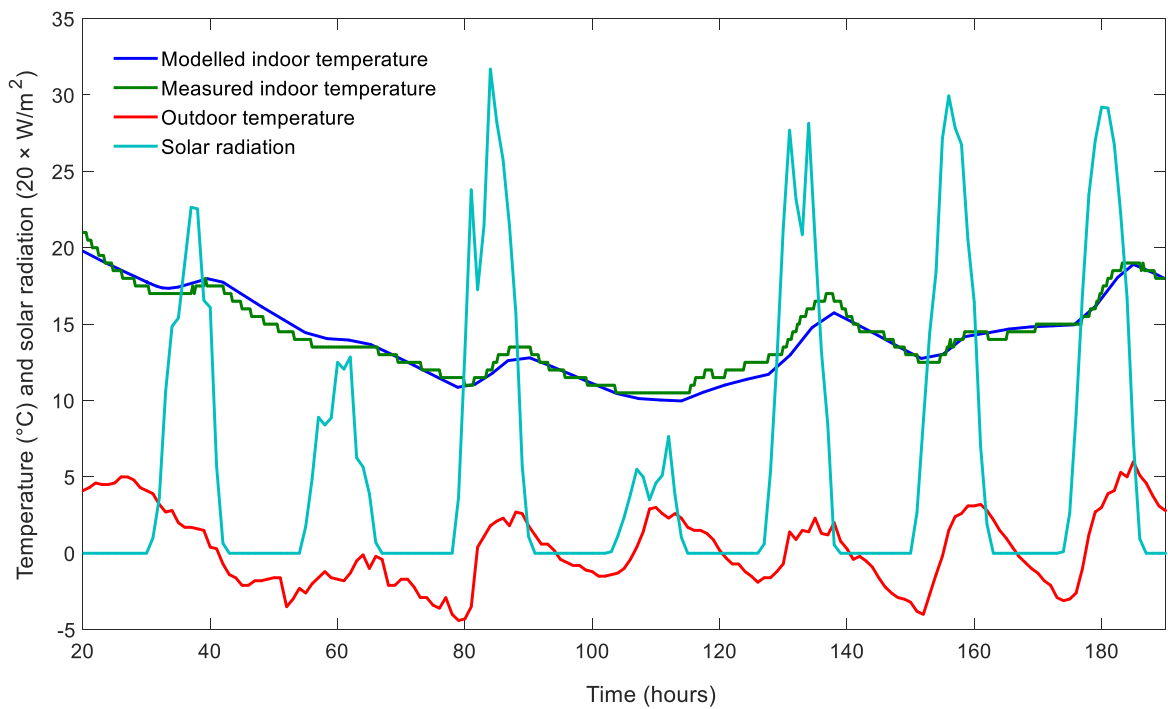
Fig. 2.16. Observed/modelled indoor temperature and weather conditions (March 17–March 25, 2016).

54

2.2.4. Building thermal performance simulation

Building models with the estimated equivalent thermal parameters were then used to simulate their thermal performance in MATLAB Simulink (Fig. 2.17). 'House Thermal Network' in Fig. 2.17 stands for the thermal model shown before in Fig. 2.4.

To simulate the thermal performance of each building, we input a heating schedule based on comfort requirements of the residents comprising a temperature setpoint and an hourly on/off profile reflecting the periods when heating is or is not required. This type of comfort control mimics the operation of SETS that were used for trials in Latvia within the RealValue project. For simulations, different comfort requirements were used based on the end-user type and building occupancy. The simulation can be run for any period of interest, e.g., 24 hours (one day) or 8760 hours (one year).

The model simulation then outputs the space heating demand and the indoor temperature as hourly time series to be used in further modelling efforts.
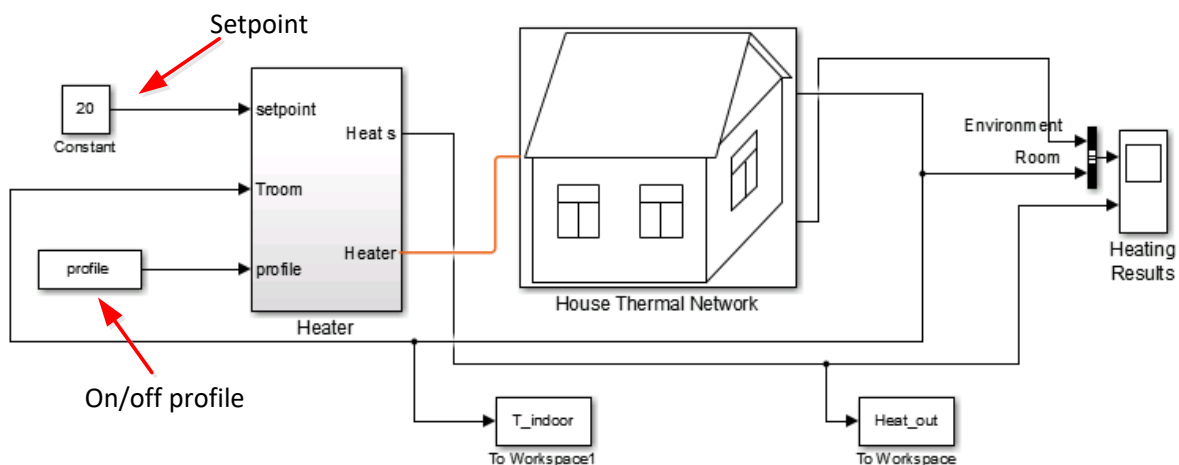
Fig. 2.17. Model for simulation of building thermal performance in MATLAB Simulink.

2.3. Results and discussion

2.3.1. Space heat demand time series development

Based on the methodology presented before, models for several buildings have been developed. The validated models were used to estimate the heating demand over a year using the hourly outdoor temperature and solar radiation. Fig. 2.18 shows the modelled room temperature and heat demand time series for a detached wooden house of 70 m^2 in 2016. Given a setpoint of 20 °C and 20-hour comfort profile daily, the simulated annual heat demand is 11.13 MWh with an average of 159 kWh/m^2. The highest heat demand occurs in January (hour 0–744) which coincides with the coldest weather of the year. During the hottest days in summer the room temperature often exceeds the setpoint of 20 °C, since the cooling system of the building is not being modelled. Conversely, we can also observe that additional heat is required a few times in summer when cold weather occurs. The developed model enables calculation of

hourly heat demand time series with different comfort profiles and occupancy patterns. For example, the annual heat demand for the same building with 19 °C setpoint and 17-hour comfort profile is 10.28 MWh (7.6% less than in the previous case).
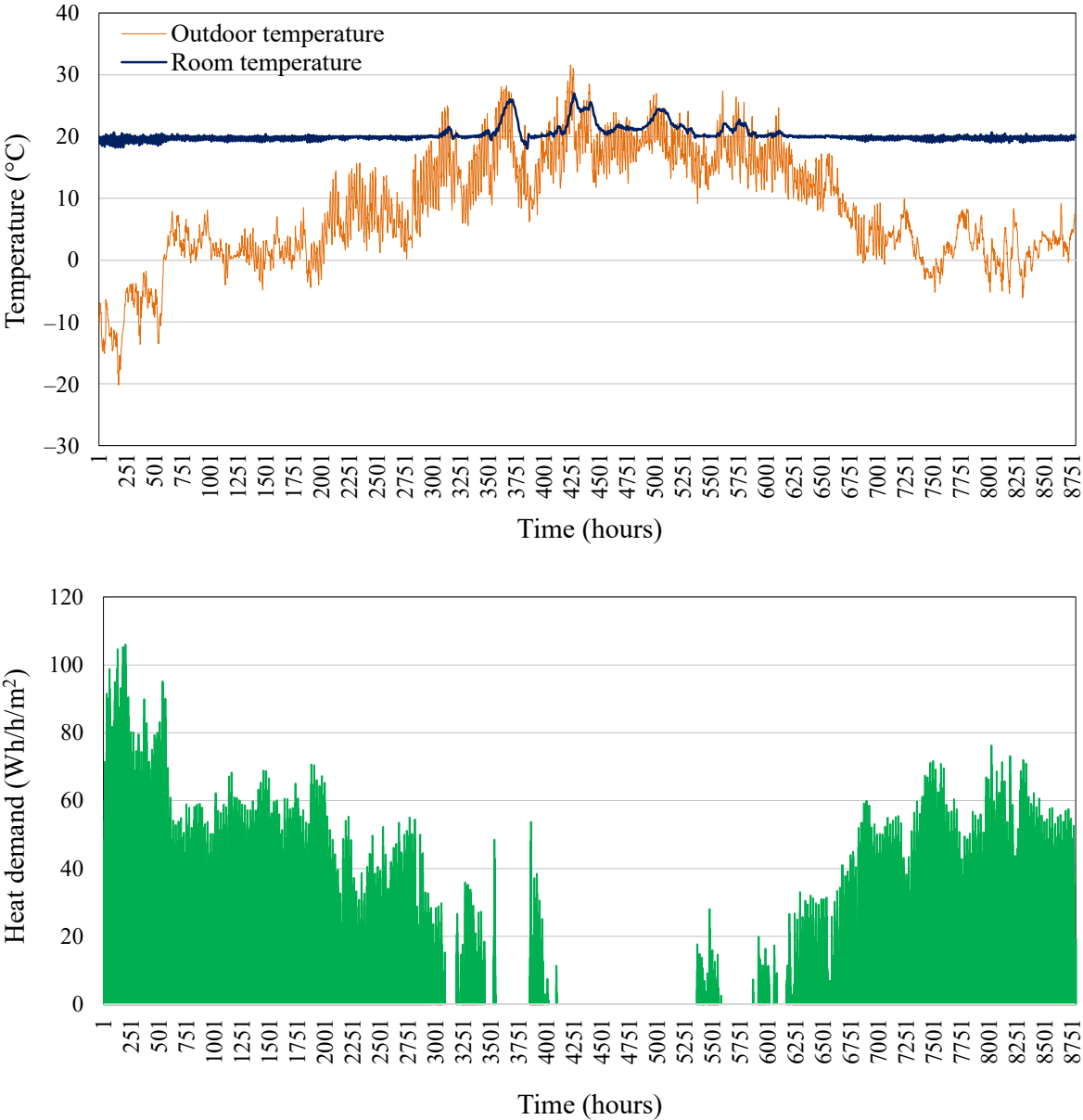
Fig. 2.18. Heat demand of a single-family wooden house in 2016 (20-hour comfort profile daily with 20 °C setpoint).

Heat requirements of industrial buildings have also been modelled, and Fig. 2.19 demonstrates heat demand for a distribution network substation where smart electric thermal storage (SETS) has been installed for space heating. The setpoint of heating is 14 °C based on the ambient temperature requirements for the control equipment installed at the substation. This temperature is to be maintained all the time. The estimated annual heat demand is 6.59 MWh in 2016 with an average of 67 kWh/m².
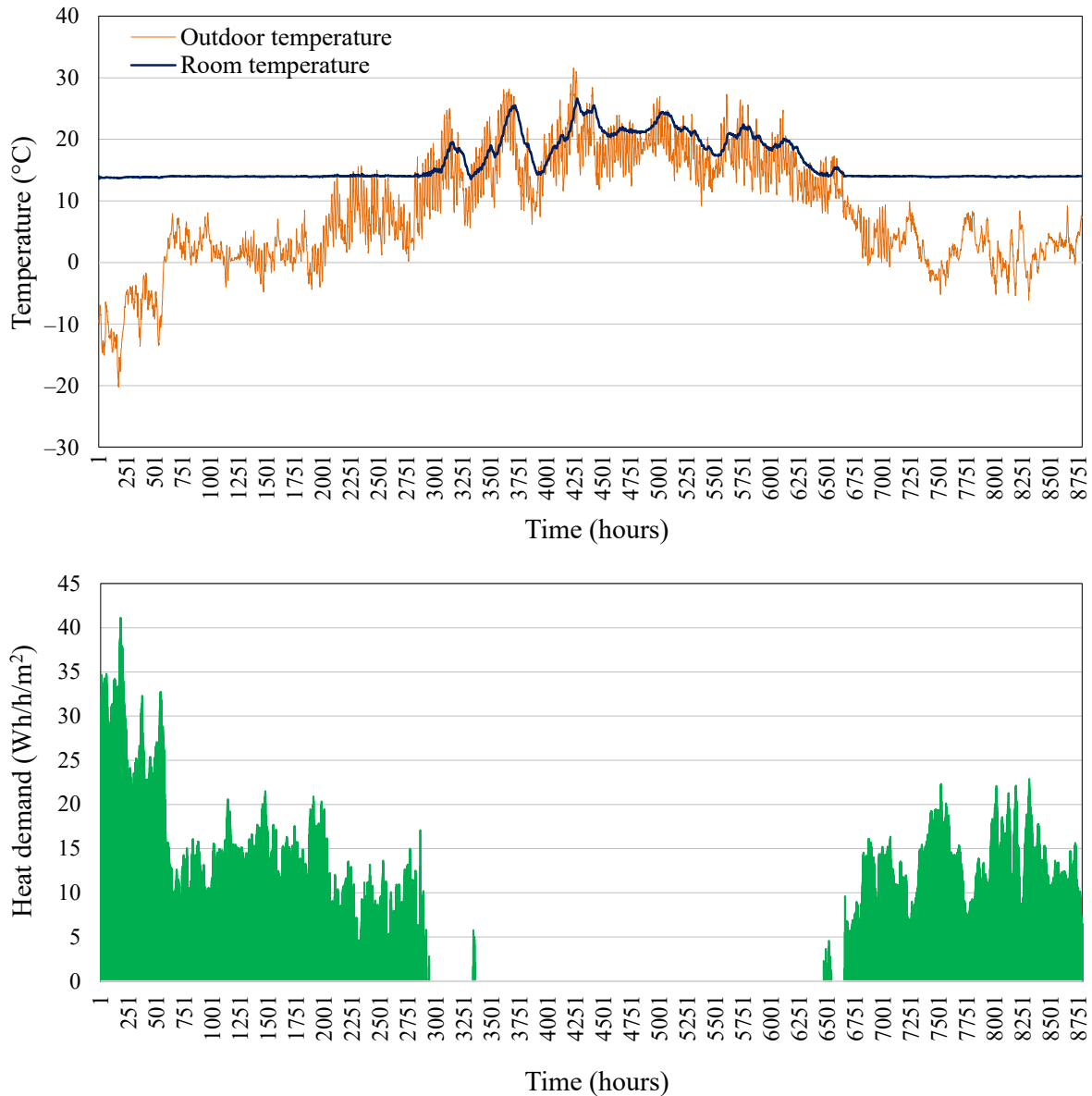
Fig. 2.19. Heat demand of a substation in 2016 (24-hour comfort profile with 14 °C setpoint).

2.3.2. Representation of heat demand in power system models

Using the experimental data measured in different houses, it is possible to derive thermal characteristics for various types of buildings. Thus, we are able to calculate the heating demand of representative individual buildings and extrapolate it to a national scale to further assess the impact of a large amount of smart electric thermal storage appliances on the power system. The heat demand obtained from thermal modelling is then incorporated into distribution grid and power system models presented in Chapter 3 where the impact of large-scale SETS deployment on the distribution grid and power system operation in Latvia is assessed. The derived heat demand is primarily included in the distribution network model for congestion management (Section 3.2). Namely, for each end-user of the representative distribution feeder, a heat demand profile is assigned based on the user type and occupancy profile. The heat demand is then translated into electricity consumption which forms an additional load, which is a supplement

to the existing base load. This is motivated by the fact that electrical heating is currently barely used in Latvia. As a next step, this load is distributed across the day based on different objectives as described in Section 3.2.6 (e.g. load variance minimisation, minimisation of energy cost or minimisation of cost of losses). This enables computing the power flow for the representative distribution feeder and obtaining the load at the low-voltage side of the 330/110 kV transformer. For power system modelling at the national scale (Section 3.3) however, the hourly load of the transformer obtained from the distribution grid modelling is upscaled based on the assumptions and scenarios regarding the total base load in Latvia in the selected years of study (2020, 2030 and 2050).

2.4. Summary

A simplified thermal network based on electrical analogy developed using data on indoor and outdoor temperature, solar irradiation and heat consumption. Equivalent thermal parameters of the simplified model were obtained through inverse black-box modelling. For validation of the method, virtual and physical experiments were conducted, and performance of the simplified thermal network model was compared to two more complex RC models (including the EnergyPlus calibrated RC model developed by the RealValue consortium members at UCD) and measurements in an existing building. It was concluded that the simplified and computationally efficient model was able to replicate the thermal dynamics of the complex models and the building with sufficient accuracy (for example, the mean absolute temperature difference as estimated with the simplified model vs the complex RC model developed by UCD was 0.24 °C, and for the experimentally measured vs modelled temperature for an existing building it was 0.84 °C). Thus, the derived heat demand can be used for further modelling of SETS impact on different power system operation aspects. The selected inverse modelling method is also motivated by the limited data availability on the Latvian building stock and its future forecasts and to benefit from real-world operational data obtained through the physical trials of SETS in Latvia within the RealValue project.

Different types of buildings were modelled through physical experiments or using data collected by the aggregator from the RealValue project trial sites. During the physical experiments, the heating equipment was switched off for several hours and consequently turned back on to obtain the cooling and heating curve for the building. Meanwhile, indoor and outdoor temperature, heat consumption and solar radiation measurements were taken either on-site or from the national meteorology centre (LEGMC, 2017). Part of the data was used for model identification, while the rest was employed for verification. Simulations were performed with MATLAB Simulink and Simscape.

Consequently, the developed building models are used to estimate the hourly heat demand over the year depending on the outdoor temperature and solar irradiation for different types of buildings. Based on the type of building or end-user, different occupancy profiles and comfort settings (i.e. heating schedule and setpoints) are assigned to it and accounted for when estimating the heat demand, thus capturing different consumption patterns of thermal energy.

3. VALUE ESTIMATION OF SETS AS A DR-ENABLED RESOURCE

3.1. Motivation and background

While smart electric thermal storage (SETS)[4], being an advanced and DR-enabled technology, could potentially bring significant advantages to the power system, it does not come without a cost, such as an increase of electric consumption (if SETS is to replace other types of heating sources) and changes of the load curve possibly contributing to grid congestion risks and increase of grid losses, increased bills for electricity etc. It has been identified that a major challenge for flexible demand response is the lack of understanding of its potential benefits due to a lack of methodologies for the quantification of costs and benefits [54]. Therefore, this section presents the methodology we developed for an overall cost-benefit assessment of **SETS impact on the power system operation until 2050**. For the study, we use various EU and national-level future scenarios and updated models simulating different aspects of power system operation developed in the Institute of Power Engineering of RTU to assess the benefits SETS might bring from two perspectives, the **power system** at large and, on a smaller scale, a **representative distribution feeder network** which also enables capturing cost-saving benefits individual households might experience. This study was performed during 2015–2018 within the RealValue project and is based on the Latvian power system, including the electricity market, characteristics at that time. The results of the study served as input to several RealValue deliverables approved by the European Commission.

The analysis of SETS impact is implemented by envisioning partial **electrification of heating supply in Latvia** at various penetration levels. In the baseline, the heating electrification is carried out with direct resistive heating (DRH) devices having no energy storage abilities or smart control whatsoever. The study is conducted for years 2020, 2030 and 2050, although most of the focus is put on 2030 since the 2020 is too soon for any major breakthroughs in SETS adoption in Latvia to actually take place, whereas 2050 is too far in the future for the conclusions drawn to have high reliability.

The approach chosen for the impact assessment of SETS on the Latvian power system is motivated by the heating technologies currently used in the residential sector and the data that is available for heat demand modelling at the national scale. As indicated in [55], 69% of the Latvian population or 64% of all dwellings are served by central heating (it comprises mainly district heating in cities and some local central heating). The second most common type of heating is stove or fireplace heating used by 29% of the population and in 32% of all dwellings. These results closely correlate with the share of multi-apartment buildings and detached houses in the housing stock since district heating is the most popular type of heating in apartments, but stoves and fireplaces are mostly used in rural individual houses. Unfortunately, central heating is not further detailed in the available statistics and thus it includes both district heating and local central heating. Local central heating, in general, can be used in detached buildings and

---

[4] For more details on SETS operation refer to section 2.1.1.

multi-apartment buildings alike. Only 3–4% of dwellings use other types of heating (including electric) as the main heating source. The Central Statistical Bureau of Latvia does not provide a further breakdown for the other types; however, it can be concluded that the share of electric heating in Latvia is negligible. Moreover, electric thermal storage heating is not used almost at all. Nevertheless, 26.7% of dwellings use electric water heaters. As a result, for the purposes of assessment of SETS impact on the Latvian power system, SETS equipment for space heating is modelled as an additional electric load rather than a replacement of existing electric heating appliances. The objective is to estimate the impact of partial heating electrification on the Latvian power system in various scenarios and by different technologies (e.g., SETS and direct resistive heaters) for the selected years of study (2020, 2030 and 2050).

Regarding data availability for **heat demand** modelling, there is a limited amount of information on detailed thermal characteristics of buildings in Latvia and their classification based on the actual building thermal performance that could be used for devising accurate building archetypes and upscaling them to the national level. Besides, it was found that there are no forecasts available on the future housing stock. Given the unavailability of data to be used for the secondary research and since carrying out such study as a primary research effort within the RealValue project was out of scope for the Latvian case study, a data-driven approach was selected for thermal modelling of buildings as already introduced in Chapter 2. Moreover, the choice of methodology was also motivated by the physical demonstration of SETS in 50 trial objects in Latvia managed by RTU during which it was planned to obtain detailed operational data of the installed heating equipment via the aggregator employed for the RealValue trials. The available data from the aggregator includes comfort requirements of end-users, heat consumption, room temperature etc. The derived heat demand was then translated into electric consumption of SETS to be used as input for power system modelling.

3.2. Modelling of SETS impact on the distribution grid

3.2.1. Introduction

The Latvian distribution system is operated almost exclusively by a single operator, Sadales tīkls AS. The distribution grid comprises 110/20/10/6 kV and 20/10/6/0.4 kV transformer substations and lines of voltage levels 20 kV, 10 kV, 6 kV, 1 kV and 0.4 kV. The overall length of distribution lines is about 94 000 km [56], of which 70% are overhead power lines (0.4 kV: 37500 km; 20 kV: 29200 km) and 23% are 0.4 kV aerial cable lines (21 500 km). There are only 6500 km of 20/10/6 kV underground cable lines.

The total amount of energy demand in 2016 was 6465 GWh, of which about 25% was consumed by residential customers and the rest by the commercial and industrial sectors. Distribution losses amounted to 4.6% in 2016 [56]. The total capacity of the Latvian distribution network is 5892 MVA. These statistics allow evaluating the overall utilisation efficiency of the grid which is equal to 13%, indicating a relatively low usage.

The grid is widely spread across the country and highly branched with a relatively large number of distant customers that contribute to low overall usage efficiency. However, due to

the socio-economic trends, the largest share of the load is concentrated in cities, and urbanisation is continuing. Lately, a lot of efforts and investments have been devoted to improving reliability by reconstructing old lines and substations and enforcing automation of the network. The national roll-out of smart meters which has been ongoing since 2014 is to be completed by 2022. It is carried out by the distribution system operator (DSO) that installs the meters for all customers free of charge.

Given that electric heating is not currently widespread in Latvia [55], for distribution modelling to assess the impacts of SETS, partial electrification of heating is assumed and the power flow study is carried out based on the existing electric load (base load) supplemented by the additional heating load. The modelled impact of smart electric thermal storage (SETS) devices is compared to that of direct resistive heaters. This enables assessing the implications of heating electrification in general and that of the studied technologies in particular.

As another possibly competitive technology that can provide storage, residential electrochemical batteries are studied. It is assumed that the batteries are installed at the customer's site and thus provide load shifting possibilities, e.g. by storing cheap energy for later usage and reducing peak load. Usage of local battery storage along with direct resistive heaters is also examined.

Since heat demand accounts for a large share of overall energy requirements in Latvia (it being located in the Northern part of Europe and having a long heating season of about 200 days), it is important to evaluate how heating electrification might impact the power system, including the distribution grid, in terms of system peak load, losses, voltage and system load factor. To mitigate possible issues, different congestion management strategies are examined in this study.

3.2.2. Approach overview

The case study for the Latvian distribution grid, having a negligible share of electric heating, is designed to examine how partial heating electrification with varying penetration of SETS might impact the distribution network by comparing it to electric resistance heating without storage (conventional electric heating). While SETS converts electrical energy and stores it in the form of heat for later use, electrochemical batteries are analysed as another possibly competitive technology that is able to provide local small-scale storage.

The congestion management study is implemented to investigate different strategies of SETS control in order to accommodate the additional new load (electrified heating) within the existing distribution grid. The current base load of customers is used as one of the main input variables, whereas the additional electrical load (e.g., from SETS or batteries) is scheduled based on different objectives subjected to the network constraints and end-user comfort requirements.

The assessment is done through simulations of the electric load based on a large database of end-user loads from which a number of end-users are randomly chosen. Several heating control strategies are examined, and a simplified radial distribution network topology is modelled which allows drawing general conclusions on the potential impact of SETS. When

designing an actual network, the same modelling approach can be applied considering the specific topology and parameters of the grid and end-user characteristics.

The potential benefits and issues that might arise as a result of heating electrification with or without heat storage have been quantified and evaluated using several indicators, such as grid reinforcement needs, peak load, cost of distribution losses, and cost of electricity for heating.

3.2.3. Power flow

Balanced three-phase power flow calculation is carried out, starting with customer loads at the end of each 0.4 kV line and moving upwards the distribution system, up to the 110 kV transmission line and eventually obtaining the load of 330/110 kV transformer (Fig. 3.1). The power flow represents the energy flow per unit time. Within this case study, an hourly time step is used for all the calculations.

Distribution losses (0.4, 20 kV) are composed of line losses and transformer losses, whereas for the transmission part (110 kV) only line losses are calculated since the 330/110 kV transformer is not modelled.

Line losses due to the flow of active power (kW) and reactive power (kvar) are expressed as follows:

$$P_{\text{losses line}} = \frac{\left(P_{\text{load}}^2 + Q_{\text{load}}^2 \right)}{U_{\text{line}}^2 \cdot 1000} \cdot R_{0,T} \cdot l, \tag{3.1}$$

$$Q_{\text{losses line}} = \frac{\left(P_{\text{load}}^2 + Q_{\text{load}}^2 \right)}{U_{\text{line}}^2 \cdot 1000} \cdot X_0 \cdot l, \tag{3.2}$$

where P_{load} and Q_{load} – active (kW) and reactive (kvar) power consumed at the end of the line;

U_{line} – voltage at the beginning of the line (0.42 kV for 0.4 kV feeders, 22 kV for 20 kV line and 120 kV for 110 kV line);

X_0 – inductive reactance per unit of length of the line (Ω/km);

l – line length (km);

$R_{0,T} = R_0 \left[1 + \alpha \cdot (T - 20) \right]$ – line resistance (Ω/km), adjusted based on the temperature;

R_0 – conductor reference resistance at 20 °C (Ω/km);

T – ambient temperature (°C);

α – temperature coefficient of resistance (°C^{-1}).

110/20 kV and 20/0.4 kV transformer load (active and reactive power output at the low-voltage side of the transformer) is calculated by adding line losses and load at the end of the line for all lines (feeders) outgoing from the transformer:

$$P_{\text{tr.load}} = \sum_{\text{all feeders}} P_{\text{line}} = \sum_{\text{all feeders}} \left(P_{\text{losses line}} + P_{\text{load}} \right), \tag{3.3}$$

$$Q_{\text{tr.load}} = \sum_{\text{all feeders}} Q_{\text{line}} = \sum_{\text{all feeders}} \left(Q_{\text{losses line}} + Q_{\text{load}} \right), \tag{3.4}$$

where P_{line} and Q_{line} – active (kW) and reactive (kvar) power flow at the beginning of the line.

For the 110 kV voltage level, power flow calculation at the beginning of the line (i.e., the load of the 330/110 kV transformer) is slightly different from the lower voltage levels:

$$P_{\text{line,110}} = P_{\text{losses line}} + P_{\text{load}} + \Delta P_{\text{cor}} \cdot l, \tag{3.5}$$

$$Q_{\text{line,110}} = Q_{\text{losses line}} + Q_{\text{load}} - \Delta Q_{\text{c}} \cdot l, \tag{3.6}$$

where ΔP_{cor} and ΔQ_{c} – corona losses (kW/km) and the reactive power injected due to the transmission line capacitance (kvar/km), respectively.

Active power losses of the transformer:

$$P_{\text{losses tr.}} = \Delta P_{\text{tr. no-load}} \cdot n_{\text{tr.}} + \frac{1}{n_{\text{tr.}}} \cdot \Delta P_{\text{tr. load}} \frac{\left(P_{\text{tr.load}}^2 + Q_{\text{tr.load}}^2 \right)}{S_{\text{tr.rated}}^2}, \tag{3.7}$$

where $\Delta P_{\text{tr. no-load}}$ – no-load (core) losses of the transformer (kW);

$\Delta P_{\text{tr. load}}$ – load (winding) losses of the transformer (kW);

$S_{\text{tr.rated}}$ – rated power of transformer (kVA);

$n_{\text{tr.}}$ – number of transformers installed at the substation.

Reactive power losses of the transformer:

$$Q_{\text{losses tr.}} = \frac{S_{\text{tr.rated}}}{100} \left(n_{\text{tr.}} \cdot I_{\text{no-load \%}} + \frac{1}{n_{\text{tr.}}} \cdot U_{\text{short-circ.\%}} \frac{P_{\text{tr.load}}^2 + Q_{\text{tr.load}}^2}{S_{\text{tr.rated}}^2} \right), \tag{3.8}$$

where $I_{\text{no-load \%}}$ – the percentage no-load current of the transformer (%);

$U_{\text{short-circ.\%}}$ – the percentage short-circuit voltage (%).

Active and reactive input power of the transformer is calculated by adding the transformer load and losses:

$$P_{\text{tr.input}} = P_{\text{tr.load}} + P_{\text{losses tr.}}, \tag{3.9}$$

$$Q_{\text{tr.input}} = Q_{\text{tr.load}} + Q_{\text{losses tr.}}. \tag{3.10}$$

Finally, we can summarise all active power flows to obtain the active load of 330/110 kV transformer:

$$P_{\text{330/110 tr.load}} = P_{\text{line,110}} = \sum_{\text{all lines}} P_{\text{losses line}} + \sum_{\text{all transf.}} P_{\text{losses tr.}} + \Delta P_{\text{cor}} \cdot l + P_{\text{total base}} + P_{\text{total heat}}, \tag{3.11}$$

where $P_{\text{total base}}$ and $P_{\text{total heat}}$ – total base load of end-users excluding electric heating (kW) and the total heating demand of end-users (kW) that is supplied by electric heating devices, respectively.

Similarly, the reactive load of the 330/110 kV transformer is

$$Q_{330/110 \text{ tr.load}} = Q_{\text{line,}110} = \sum_{\text{all lines}} Q_{\text{losses line}} + \sum_{\text{all transf.}} Q_{\text{losses tr.}} - \Delta Q_c \cdot l + Q_{\text{total base}} + Q_{\text{total heat}} . \quad (3.12)$$

Thus, the total load of end-users comprises the base and the heating load:

$$P_{\text{total load}} = P_{\text{total base}} + P_{\text{total heat}} , \quad (3.13)$$

Line current (A):

$$I_{\text{line}} = \frac{S_{\text{line}}}{U_{\text{line}}\sqrt{3}} = \frac{\sqrt{P_{\text{line}}^2 + Q_{\text{line}}^2}}{U_{\text{line}}\sqrt{3}} . \quad (3.14)$$

Voltage deviation (voltage drop at the end of each line) is calculated based on the active and reactive power flow at the beginning of the line:

$$\delta U = \frac{\left(P_{\text{line}} \cdot R_{0,T} + Q_{\text{line}} \cdot X_0\right) \cdot l}{U_{\text{line}}} , \quad (3.15)$$

$$\delta U_\% = \frac{\delta U}{U_{\text{rated}}} \cdot 100\% . \quad (3.16)$$

where δU – voltage deviation (kV);

$\delta U_\%$ – relative voltage drop (%).

3.2.4. SETS devices

SETS device for space heating is modelled with its rated parameters: input power for charging, P_{input} (kW), storage capacity, E (kWh), and input/output power for boost, P_{boost} (kW), which provides immediate additional heating if enough heat has not been stored. That can occur during cold spells when the daily required heat demand cannot be stored by SETS because of their limited storage capacity. The efficiency of SETS is assumed to be equal to 1, given that all the dissipated heat from the device is still used for space heating.

The specific SETS characteristics used in the study are based on the Quantum QM100 model with 2.2 kW input rating and 15.4 kWh storage capacity [57]. SETS are installed based on an average specific capacity of 150 W per 1 m² of electrically heated floor space obtained from specifications [58] and deemed most appropriate for the Latvian case study, which translates to 1.05 kWh/m² of energy storage.

The required hourly heat demand, $P_{\text{heat req.}}$ (kWh/h), is obtained from building models. Then for distribution grid modelling purposes, the total daily heat consumption is obtained by adding the hourly values:

$$P_{\text{total heat}} = \sum_{\text{all hours}} P_{\text{heat req.}} . \quad (3.17)$$

The hourly consumption of electrical energy for charging of SETS and boost is then obtained through day-ahead optimisation based on different objectives (see Section 3.2.6), so

that the total energy stored plus the energy provided by boost is no less than required. The boost element is switched on only if the daily heat demand is larger than the storage capacity of the device. It is assumed that the optimised charging schedule is able to satisfy the comfort requirements of users, given that SETS are usually charged over the night while heat is typically required during the day.

3.2.5. Competing technologies

Resistive heater

The direct resistive heater is modelled as a device the heat output of which coincides with power consumption from the grid. Additionally, the hourly heat output is equal to the heat demand derived from building models. Consequently, the total daily heat demand is the same as for SETS. The installed capacity of resistive heaters is assumed equal to that of SETS for comparability purposes between both types of equipment. Thus, resistive heaters alone form a set of uncontrollable load as opposed to SETS, the charging of which can be controlled based on different objectives. However, the operation of resistive heaters together with batteries is also studied. In that case, some load shifting may be possible depending on the operation of batteries as discussed later.

Battery

The main difference between batteries and SETS lies in their purpose of use and capabilities. The SETS devices decouple electricity consumption for heating from the actual heating demand only and provide the ability to charge based on external signals. In contrast, the batteries provide load shifting options to the residence in general, not constrained solely to heating appliances. Given sufficient control by the aggregator for instance, however, the battery operational strategy can also be optimised based on external signals, e.g., electricity hourly price.

The battery energy storage system (BESS) is modelled with its rated parameters: maximum input/output power, $P_{\text{BESS}}^{\max}$ (kW), energy capacity, C_{BESS} (kWh), and round-trip efficiency, η_{BESS}. As a full discharge of batteries is not recommended in order to prevent their quick deterioration, depth of discharge (DOD) and maximum discharge time ($D_{\max}$) can be constrained such that

$$DOD = \frac{E_{\text{BESS}}}{C_{\text{BESS}}} = \frac{P_{\text{BESS}} \cdot d}{P_{\text{BESS}}^{\max} \cdot D_{\max}} = \frac{d}{D_{\max}},$$ (3.18)

where E_{BESS} – energy discharged from the storage system (kWh);

d – discharge time [59].

As the overarching modelling is implemented with an hourly resolution, the same time step is applied for batteries.

The battery is not modelled based on a particular product available to consumers but is rather stylised instead. The battery is assumed to be Li-ion with a 90% DoD limit and a round-trip efficiency of 0.9.

3.2.6. Objective functions

To assess distribution grid performance and load characteristics with different congestion management strategies, several objectives are considered for an optimal charge and discharge strategy of SETS and BESS. The results of optimisation will also be used as input for the overall power system benefit assessment introduced in Section 3.3.

The three SETS control strategies analysed are:
(1) load factor maximisation;
(2) heating cost minimisation;
(3) cost of losses minimisation.

An additional comparison is made with a battery energy storage system operating in coordination with direct resistive heating for the added benefits of heating cost reduction for electrically-heated end-users.

Load variance minimisation

To minimise load variance or to level out the daily load profile, the following objective is formulated for the operation of SETS space heaters and water cylinders to be solved for each day separately:

$$f_1 = \frac{1}{T} \sum_{t=1}^{T} \left[\left(P_{\text{base}}^t + P_{\text{heat}}^t \right) - P_{\text{avg}} \right]^2 \rightarrow \min, \qquad (3.19)$$

where T – optimisation horizon;

t – time step (one hour);

P_{base}^t – the given power consumed by the base load during hour t (kWh/h);

P_{heat}^t – the hourly power to be optimised consumed by heating equipment;

P_{avg} – the hourly average power consumption comprising the base load and heating, averaged over 24 hours of the day.

For the hourly consumption of heating equipment, it is assumed that a fraction of all devices is being charged each hour so that it adds up to the total heat demand per day:

$$\sum_{t=1}^{T} P_{\text{heat}}^t = P_{\text{total heat}}. \qquad (3.20)$$

Additionally, the hourly charging power of SETS is constrained by the total installed capacity:

$$0 \le P_{\text{heat}}^t \le P_{\text{input}} \quad \forall t \in T. \qquad (3.21)$$

Note that the daily average power

$$P_{\text{avg}} = \frac{1}{T} \sum_{t=1}^{T} \left(P_{\text{base}}^t + P_{\text{heat}}^t \right) = \frac{1}{T} \left(\sum_{t=1}^{T} P_{\text{base}}^t + P_{\text{total heat}} \right), \tag{3.22}$$

where P_{base}^t – the base load, derived from the end-user database;

$P_{\text{total heat}}$ – the total daily heat demand provided by the building models.

Thus, P_{avg} is a constant for each day.

The optimisation problem is subjected to SETS parameters and heating requirements. Additionally, the total load is constrained by the rated transformer loading, the line current is constrained based on the thermal ratings of the line and the voltage deviation is constrained by the allowable limits in Latvia: +10/–15% [60].

As has been shown by [61], minimising load variance can be equivalent to minimising feeder energy losses, which is exactly true if the feeder is a single branch with all loads connected at the end of the line. Moreover, it follows from the findings of [61] that minimising load variance is equivalent to maximising load factor for a large penetration of the additional load from heating when peak loads exceeding the base load are unavoidable. Thus, for larger penetrations of electric heating, this objective can be replaced by load factor maximisation which leads to a linear objective function.

Both for this and the following optimisation problems, different levels of heating electrification were considered (i.e., 5, 10, 20%). Furthermore, where relevant, we use the same scenario assumptions as detailed in Section 3.3.2 and Table 3.6, namely for the future projections of electricity prices and demand development trends over time.

In the case of BESS, it is used together with direct resistive heating at the same penetration level as SETS and with the same installed capacity and input power for charging as SETS. For comparability purposes, the batteries are limited to only cover electric heating demand supplied by DRH with no ability to affect the other components of consumer's electric demand and no option to feed power back to the grid. Accordingly, self-consumption operation mode was assumed for BESS. For optimal operation strategy of BESS based on load variance minimisation, the following objective is formulated:

$$f_2 = \frac{1}{T} \sum_{t=1}^{T} \left[\left(P_{\text{base}}^t + P_{\text{heat}}^t + P_{\text{BESS}}^t \right) - P_{\text{avg}} \right]^2 \rightarrow \min, \tag{3.23}$$

where P_{base}^t and P_{heat}^t – the active power consumed by the base load and by resistive heaters during hour t (kWh/h);

P_{BESS}^t – the optimisation variable having a positive or negative value representing the actual charging or discharge power of BESS during hour t (kWh/h), subjected to its maximum power rating.

Now, P_{avg} is the hourly average power consumption from the grid composed of the base load, the heating load and BESS:

$$P_{\text{avg}} = \frac{1}{T} \sum_{t=1}^{T} \left(P_{\text{base}}^t + P_{\text{heat}}^t + P_{\text{BESS}}^t \right). \tag{3.24}$$

The power of BESS is constrained by its maximum input/output rating:

$$-P_{\text{BESS}}^{\max} \le P_{\text{BESS}}^t \le P_{\text{BESS}}^{\max} \quad \forall t \in T , \qquad (3.25)$$

and the hourly charging and discharging power values of BESS over the day sum up to zero, meaning that all the energy charged needs to be consumed during the same day:

$$P_{\text{BESS}}^{\text{charge}} \cdot \eta_{\text{BESS}} + P_{\text{BESS}}^{\text{discharge}} = 0 ; \qquad (3.26)$$

$$P_{\text{BESS}}^{\text{charge}} = \sum_{t=1}^{T} P_{\text{BESS}}^t \text{ for } P_{\text{BESS}}^t > 0 ; \qquad (3.27)$$

$$P_{\text{BESS}}^{\text{discharge}} = \sum_{t=1}^{T} P_{\text{BESS}}^t \text{ for } P_{\text{BESS}}^t \le 0 . \qquad (3.28)$$

Obviously, the total stored energy at any moment must not exceed the energy capacity of BESS:

$$\sum_{t=1}^{T} P_{\text{BESS}}^t \le C_{\text{BESS}} \text{ for } \forall T = [1, 24]. \qquad (3.29)$$

Minimisation of energy cost

To minimise the cost of heating for customers, the following objective is solved for optimal SETS charging each day:

$$f_3 = \sum_{t=1}^{T} P_{\text{heat}}^t \cdot c^t \cdot h \to \min , \qquad (3.30)$$

where c^t – the electricity market price (€/kWh) which is the time-variable component of the final price the customer pays;

h – time step, equal to one hour;

P_{heat}^t – the optimisation variable subject to:

$$\sum_{t=1}^{T} P_{\text{heat}}^t = P_{\text{total heat}} , \qquad (3.31)$$

$$0 \le P_{\text{heat}}^t \le P_{\text{input}} \quad \forall t \in T . \qquad (3.32)$$

For the case of BESS, energy cost minimisation function for the end-users is as follows:

$$f_4 = \sum_{t=1}^{T} \left(P_{\text{base}}^t + P_{\text{heat}}^t + P_{\text{BESS}}^t \right) \cdot c^t \cdot h \to \min , \qquad (3.33)$$

where P_{BESS}^t – the optimisation variable subject to the same constraints as for the objective function f_2 before.

A positive value of P_{BESS}^t represents charging of BESS and adds to the cost, while a negative value of P_{BESS}^t for discharging reduces the cost of energy during the hour t, since less energy is drawn from the grid than without BESS.

Minimisation of cost of losses

Similarly, as for the cost of heating for end-users, the cost of distribution losses can be minimised assuming that the distribution operator pays for losses to the transmission operator based on the total amount of lost energy multiplied by the market price, c^t.

For comparison, power flow with and without heating electrification is being calculated to compare losses and other indicators, such as load factor and cost, in both cases.

3.2.7. Representative feeders

A simplified radial distribution network topology (Fig. 3.1) is modelled to draw general conclusions on the potential impact of SETS and compare that to other possibly competing technologies. When designing an actual network, the same modelling approach can be applied considering the specific topology of the grid and end-user characteristics.

Main components of the modelled network are as follows:

- 110 kV line;
- 110/20 kV transformer;
- 20 kV feeders;
- 20/0.4 kV transformers;
- 0.4 kV feeder lines;
- end-user loads.

The representative feeder network part presented in the assessment results consists of 9 0.4 kV feeder lines and a total of 402 end-users (both detached dwellings and apartments, business and public buildings) as shown in Fig. 3.1. The list of consumers considered can be found in Appendix 4, Table A4.7. The non-heating electrical load for the different consumer types is obtained from a previously summarised anonymised data library [62] and scaled according to scenario assumptions. Unlike all other input time series used in the Latvian case study, this hourly data was collected in 2012.

Particular attention has been drawn to the representation of the end-user load. Real-world historical data is used to model the base load which characterises common types of end-users in Latvia (for an example see Fig. 3.2). This data has been collected from smart meter measurements of end-user consumption with an hourly resolution for the whole year of 2012 and includes several types of end-users, such as multi-apartment buildings, detached buildings, commercial and industrial customers, public buildings etc. [63]. A random number of different types of end-users has been selected and assigned to each of the nine feeders (Fig. 3.1) to form the total electrical base load.

For power flow calculations, common parameters of lines and transformers representative of the Latvian distribution system have been chosen.
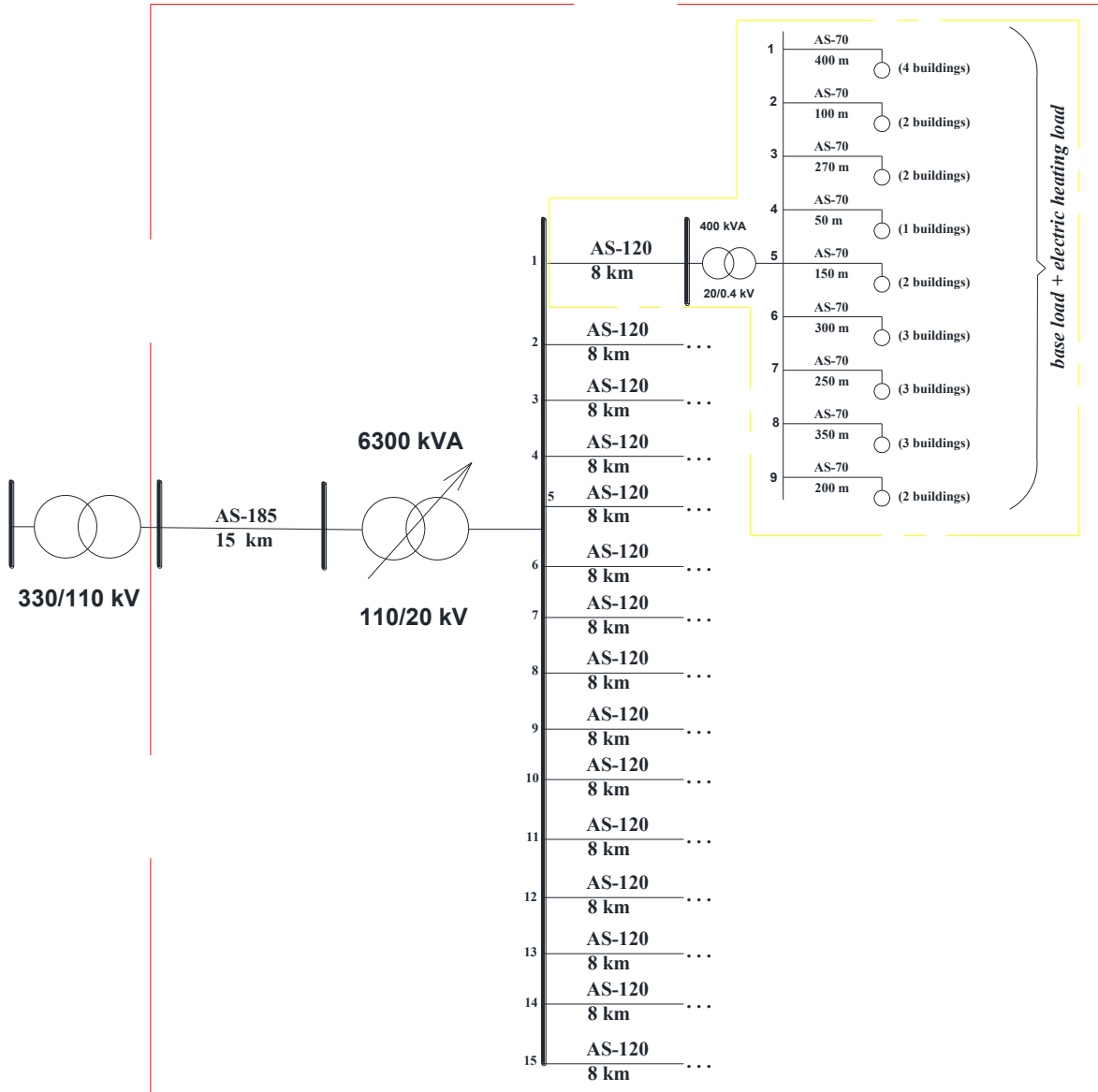
Fig. 3.1. Topology of the modelled feeder network (framed).
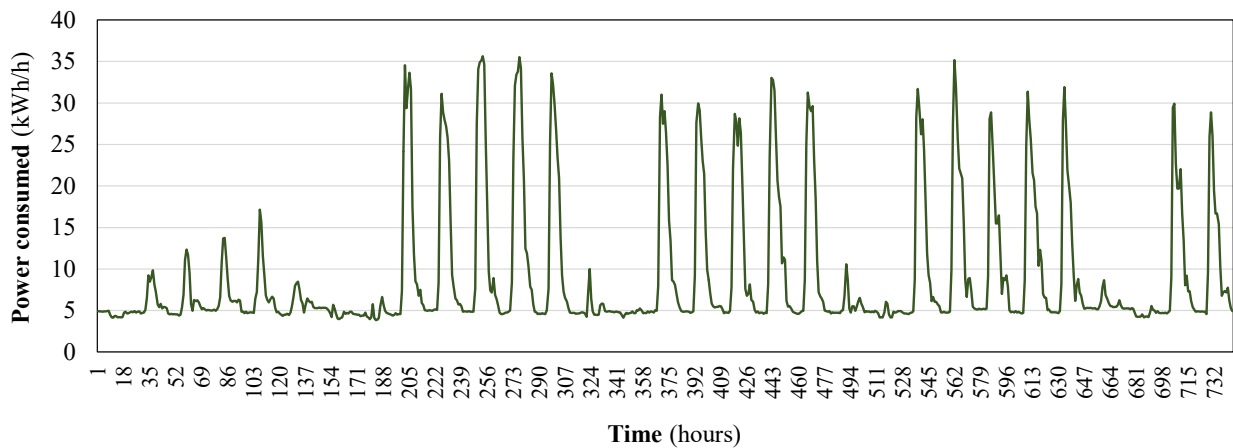
Fig. 3.2. Load profile for a school in January.

Some important assumptions made within this study which may not exactly align with the real world are stated below.

- Whereas detailed hourly comfort requirements and heating schedules are accounted for within the building models, for SETS operation within the distribution grid the hourly heat demands are translated into a daily total consumption. An assumption is made that comfort requirements will still be met since SETS are mostly charged during the night with all the studied control strategies, while the largest heat demand typically occurs later during the day.

- Based on data availability, electrical loads of end-users from the year 2012 are used to simulate the base load. However, for the evaluation of SETS potential other years need to be studied. Therefore, the load time series of 2012 is to be aligned with the other input data (ambient temperature, electricity prices) by time-shifting it as necessary, so that, e.g. weekdays and holidays are matched between the time series, given that electric loads exhibit high time-dependence. Additionally, for modelling of future scenarios, the load data is scaled based on assumptions on future trends.

3.2.8. Results and discussion

The results from the representative feeder network modelling for the Latvian case study comprise various metrics across the scenarios, heating electrification and SETS scheduling strategies analysed. The total number of combinations modelled is equal to 216 = 6 scenarios × 3 study years × 3 heating electrification levels × 4 (3 SETS strategies and reference DRH). However, only select results will be presented in this section to maintain readability. The other results will nevertheless inform the overall conclusions.

Firstly, let us consider the **grid reinforcement** needs caused/prevented by the various SETS strategies and the conventional direct resistive heating in Table 3.1. In this section, the focus is put on the study years **2020** and **2030**.

The numbers in columns labelled 'Feeders w/ line reinf.' refer to the percentage of feeders that require line reinforcement due to the added electrical heating load. In the model, the assumed wire is currently AS-35, aluminium steel reinforced conductor with 35 mm^2 cross-section. The other columns labelled 'Transf. reinf. needed' show a binary (0/1) on whether the 20/0.4 kV and 110/20 kV transformers in the network need upgrades due to the added electric heating load.

We can easily see that direct resistive heaters do not overload the transformers but cause some issues with line thermal ratings at high heating electrification levels. The SETS (1) charging strategy (load factor maximisation) alleviates almost all of these problems except in two of the displayed scenarios. Charging strategy (3) and, more so, strategy (2), however, cause additional issues in the grid due to excessive peaks. On the other hand, the reference heating electrification case (DRH) does not actually require many new investments in the grid. This signifies the historically oversized grids with low utilisation efficiency which, indeed, is generally the case in Latvia [64].

Table 3.1. Grid reinforcement needs in the representative feeder network in selected scenarios

Scenario	DRH		SETS – (1) load factor max.		SETS – (2) heating cost min.		SETS – (3) losses cost min.	
	Feeders w/ line reinf. (%)	Transf. reinf. needed (0/1)	Feeders w/ line reinf. (%)	Transf. reinf. needed (0/1)	Feeders w/ line reinf. (%)	Transf. reinf. needed (1/0)	Feeders w/ line reinf. (%)	Transf. reinf. needed (1/0)
2020_Base_2%	0%	0	0%	0	0%	0	0%	0
2020_DSM_2%	0%	0	0%	0	0%	0	0%	0
2020_Base_10%	0%	0	0%	0	44%	0	44%	0
2020_DSM_10%	0%	0	0%	0	33%	0	0%	0
2020_Base_20%	33%	0	11%	0	67%	1	67%	1
2020_DSM_20%	33%	0	0%	0	67%	1	44%	0
2030_Base_2%	0%	0	0%	0	0%	0	0%	0
2030_DSM_2%	0%	0	0%	0	67%	1	0%	0
2030_Base_10%	22%	0	0%	0	56%	1	44%	0
2030_DSM_10%	0%	0	0%	0	44%	0	0%	0
2030_Base_20%	33%	0	11%	0	67%	1	67%	1
2030_DSM_20%	33%	0	0%	0	67%	1	44%	0

Table 3.2 summarises some noteworthy results from the ***Base* scenario** for the year **2020**. The **load factor maximisation strategy** as a coordinated control of SETS seems to be the most overall beneficial in terms of trade-offs to the distribution grid operator and end-users because it provides significant peak load reductions, somewhat reasonable decreases in the electricity bills (for electrified heating) and also decreased cost of energy losses in the distribution grid.

The heating and losses cost reductions are expressed in terms of € per dwelling heated by SETS, but there were also some public and business buildings in the representative feeder setup that can be electrically heated, so the reader should be advised the term 'dwelling' here refers not only to households.

Table 3.2. Impact of SETS charging strategies on the grid losses and heating costs, *Base* scenario, 2020

Heating strategy	SETS – (1) load factor max.			SETS – (2) heating cost min.			SETS – (3) losses cost min.		
Heating electrification	2%	10%	20%	2%	10%	20%	2%	10%	20%
Peak load reduction (kW)	11.1	46.6	178.3	–27.6	–267.7	–513	12.1	–144.2	–455.6
%	1.94	7.53	21.91	–4.84	–43.25	–63.05	2.12	–23.30	–55.99
Cost of heating decrease (€/dw.)	64.66	29.66	18.66		121.58		114.45	98.94	82.64
%	16.80	7.70	4.85		31.59		29.73	25.70	21.47
Cost of losses decrease (€/dw.)	9.20	5.57	5.13	11.95	5.52	–2.63	13.00	10.59	10.15
%	32.76	16.99	13.24	42.56	16.84	–6.79	46.32	32.29	26.20

Also, it is crucial to point out that only the energy component of end-consumer electricity bills is considered here, which constitutes roughly 20–30% of the final bill in Latvia [65]. Renewables levies, taxes, transmission and distribution tariffs comprise the remaining part.

The second charging strategy (**heating cost min.**) is not a coordinated control, at least not in the sense that the SETS devices in the different houses affect each other's operation. The control in SETS – (2) strategy is solely price-based. As a consequence, all the devices strive to charge when the price is the lowest, resulting in vastly increased peak loads (which are now shifted in time). Since the scope of the distribution grid model is limited to one representative feeder network, it was assumed the operation of SETS within this network could not affect the overall electricity price in the system.

The third charging strategy, **cost of losses** (incurred by the DSO) **minimisation**, also results in increased peak load in 10% and 20% heating electrification scenarios. In retrospect, the SETS – (3) strategy could have been augmented with constraints on permissible peak load increase.

The following Table 3.3, Table 3.4 and Table 3.5 dwells deeper in some other scenarios, particularly the *Demand-side measures (DSM)* scenario for 2020 and, correspondingly, the *Base* and *DSM* scenarios for 2030. The **DSM scenario** shows an improved ability of SETS to decrease the peak load in the representative feeder network. However, this is likely due to the way the scenario is implemented. The reference electric heating (direct resistive) is not subjected to any demand-side measures, rather it is added to a system where the rest of electric load has already been smoothened. As a result, the DRH use causes quite pronounced peaks which the SETS can then reduce. The monetary savings, however, are more than halved. For instance, in the *Base* scenario (Table 3.2) SETS can reduce the electric heating costs in dwellings by 31.59% (cost reduction strategy), while in the *DSM* scenario they are decreased only by 16.04% (Table 3.3). The same differences between the *Base* and *DSM* scenario can be observed in the **2030** case (Table 3.4 and Table 3.5). Compared to the 2020 scenarios however, 2030 shows improved benefits from SETS in almost all metrics. Realistically, the 2030 study is more relevant to Latvia, as 2020 is too soon for any noteworthy SETS introduction to take place in Latvia.

Table 3.3. Impact of SETS charging strategies on the grid losses and heating costs, *DSM* scen., 2020

Heating strategy	SETS – (1) load factor max.			SETS – (2) heating cost min.			SETS – (3) losses cost min.		
Heating electrification	**2%**	**10%**	**20%**	**2%**	**10%**	**20%**	**2%**	**10%**	**20%**
Peak load reduction (kW)	10.9	89.1	188.2	–43.8	–256.5	–500.8	12.1	–64.8	–35.9
%	**2.52**	**16.25**	**23.34**	**–10.12**	**–46.78**	**–62.10**	**2.80**	**–11.82**	**–4.45**
Cost of heating decrease (€/dw.)	25.43	9.33	4.76		60.79		53.91	36.17	26.52
%	**6.71**	**2.46**	**1.26**		**16.04**		**14.23**	**9.54**	**7.00**
Cost of losses decrease (€/dw.)	3.62	2.34	2.96	4.57	–4.28	–15.49	5.61	4.03	4.47
%	**14.01**	**7.68**	**8.17**	**17.71**	**–14.05**	**–42.79**	**21.73**	**13.25**	**12.35**

Table 3.4. Impact of SETS charging strategies on the grid losses and heating costs, *Base* scenario, 2030

Heating strategy	SETS – (1) load factor max.			SETS – (2) heating cost min.			SETS – (3) losses cost min.		
Heating electrification	2%	10%	20%	2%	10%	20%	2%	10%	20%
Peak load reduction (kW)	11.2	51.5	150.3	–23.3	–263.4	–516.3	12	–108.9	–154.6
%	**1.73**	**7.42**	**17.60**	**–3.61**	**–37.94**	**–60.46**	**1.86**	**–15.68**	**–18.11**
Cost of heating decrease (€/dw.)	76.13	38.32	23.63		138.78		131.18	115.79	97.98
%	**17.33**	**8.72**	**5.38**		**31.58**		**29.85**	**26.35**	**22.30**
Cost of losses decrease (€/dw.)	12.26	7.64	6.65	15.74	8.40	–0.91	17.05	13.98	13.13
%	**33.84**	**18.36**	**13.75**	**43.46**	**20.19**	**–1.89**	**47.07**	**33.59**	**27.13**

Table 3.5. Impact of SETS charging strategies on the grid losses and heating costs, *DSM* scenario, 2030

Heating strategy	SETS – (1) load factor max.			SETS – (2) heating cost min.			SETS – (3) losses cost min.		
Heating electrification	2%	10%	20%	2%	10%	20%	2%	10%	20%
Peak load reduction (kW)	10.9	75.1	188.3	–41.7	–258.2	–502.4	12	–77.8	–48.5
%	**2.23**	**12.78**	**22.27**	**–8.52**	**–43.95**	**–59.41**	**2.45**	**–13.24**	**–5.74**
Cost of heating decrease (€/dw.)	30.61	11.88	6.22		69.39		62.81	43.44	32.15
%	**7.08**	**2.75**	**1.44**		**16.04**		**14.52**	**10.04**	**7.43**
Cost of losses decrease (€/dw.)	4.90	3.01	3.57	2.37	–3.85	–16.68	7.48	5.28	5.56
%	**14.71**	**7.82**	**7.91**	**7.11**	**–9.99**	**–36.94**	**22.48**	**13.69**	**12.32**

Another potentially competing small scale energy storage option was analysed concerning heating electrification, **electrochemical batteries**. For comparability purposes, the batteries were limited to only cover electric heating demand supplied by DRH with no ability to affect the other components of consumer's electric demand and no option to feed power back to the grid. The operating strategy imposed on the batteries is most closely tied to the heating cost reduction. However, it had an additional requirement to respect the transformer ratings in the feeder network, so it performed a coordinated control from the DSO perspective, avoiding transformer reinforcements. Due to significantly higher specific costs of batteries compared to SETS, it was deemed more realistic to assume smaller kWh capacities for the batteries than the SETS devices. For instance, the retail price of the QM100 model with 15.4 kWh storage capacity is £832.63 in the UK market or roughly 944.53 €. This translates to about 61.33 €/kWh while battery prices are notably higher, e.g. the PowerWall costs about 360 €/kWh [66] without the additional hardware (i.e., inverter) and installation costs. However, the capital costs of

battery storage are expected to keep falling. It is suggested the capital costs of utility-scale batteries could reach even mere 165 €/kWh by 2025 (assuming a low price trajectory) [67].

The operating strategy imposed on the batteries is most closely tied to the heating cost reduction. However, it had an additional requirement to respect the transformer ratings in the feeder network, so it performed a coordinated control from the DSO perspective, avoiding transformer reinforcements. Due to significantly higher specific costs of batteries compared to SETS, it was deemed more realistic to assume smaller kWh capacities for the batteries than the SETS devices. For instance, the retail price of the QM100 model with 15.4 kWh storage capacity is £832.63 in the UK market or roughly 944.53 €. This translates to about 61.33 €/kWh while battery prices are notably higher, e.g. the PowerWall costs about 360 €/kWh [66] without the additional hardware (i.e., inverter) and installation costs. However, the capital costs of battery storage are expected to keep falling. It is suggested the capital costs of utility-scale batteries could reach even mere 165 €/kWh by 2025 (assuming a low price trajectory) [67].

The batteries considered in our analysis have storage capacity sufficient for 4 hours of operation. On kW basis, we modelled the batteries with two different sizes. The batteries in the model are implied to be of a residential scale, but the modelled control strategy envisions aggregation at the feeder level. Consequently, their sizing is decided based on the aggregated heating demand at each feeder. Two different battery system sizes are considered for each feeder: for size 1, the battery output power is selected to cover one-fourth of the maximum hourly heat demand; for size 4, the battery power is selected to be sufficient to provide all the heat demand (via DRH) during the coldest hour of the year.

While batteries do seem to provide more significant specific electricity cost reductions compared to SETS (Fig. 3.3), it might at least partially be explained by the notably lower storage capacities (e.g., 76 kWh of battery storage (size 1) vs 363 kWh of SETS in the 10% case for the *Base* scenario). An effect can be observed for SETS where the specific benefits decrease with higher installed storage capacities of SETS and the same appears to be true for the batteries. If we compare the two considered battery system sizes, the system with four times increased storage capacity already shows diminishing benefits per kWh (Fig. 3.3).
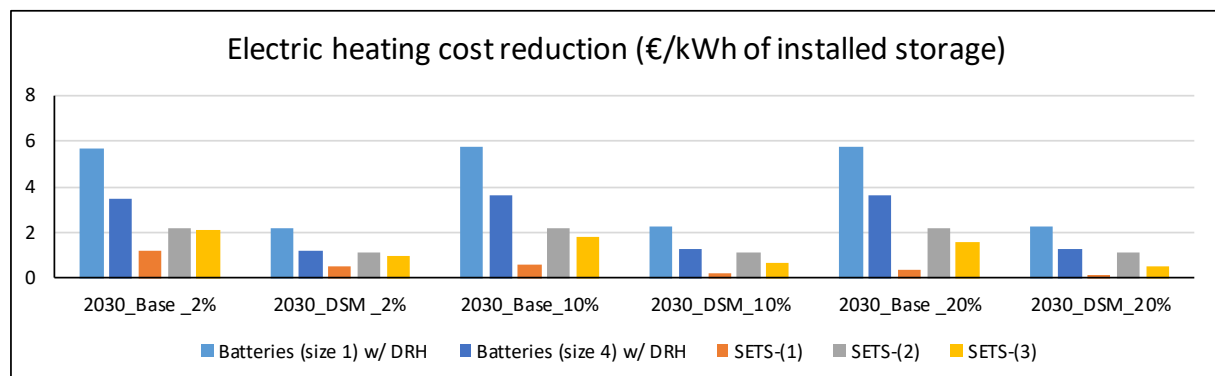
Fig. 3.3. Electric heating cost reduction with batteries combined with DRH and SETS with various control strategies (the difference to the DRH baseline is displayed).

The following Fig. 3.4 compares the ability of batteries and SETS to decrease the costs of losses in the feeder network from heating electrification compared to the DRH baseline.

Notably, at large electrification levels, the batteries and price-following decentralised SETS can slightly increase the costs of losses. They also can significantly increase peak loads and generally act contrary to the desired goal from the DSO perspective – congestion management and grid investment deferral. SETS with the coordinated strategy (1) (load factor maximisation) do seem to offer the best trade-off between end-users' desire to decrease their bills and DSO's wish to have less need for additional grid reinforcements in the scenario of widespread heating electrification. It can, however, prove to be challenging to establish a fair compensation mechanism if the owners of SETS were to delegate some control over their devices to an aggregator who schedules charging based on the distribution grid parameters.
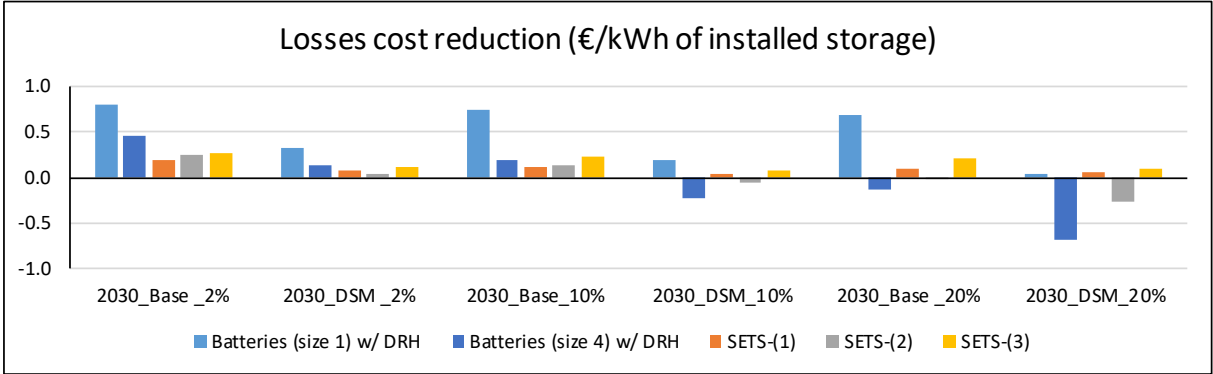
Fig. 3.4. Reduction of losses in the grid incurred by electrifying heating with batteries combined with DRH and SETS with various control strategies (the difference to the DRH baseline is displayed).

3.3. Modelling of SETS impact on the power system

3.3.1. Introduction

The present-day Latvian power system is characterised by a large share of electricity production from hydropower resources, in particular, the three cascaded plants on the Daugava River with the total installed capacity of 1580 MW. The other major local sources of electricity are the two combined heat and power plants in the city of Riga (1025 MW), which provide district heating energy for most of the consumers on the right bank of the city. However, their schedule is very dependent on the heating demand. Together these five sources comprise about 86% of the total installed capacity in Latvia [31], and they are owned by the same company, Latvenergo AS. This situation is a remnant of the previous setup of the strictly regulated and monopolised Latvian power system before liberalisation begun in 2007 [68].

Since mid-2013, the most electrical energy produced and consumed in Latvia is traded in the Nord Pool day-ahead market [69]. The interconnections to neighbouring countries play an important role in the efficiency of the wholesale market. Currently (in 2018), the Latvian power system is well connected to the Lithuanian system, but connections to Estonia are still insufficient [3]. There are also interconnections to the Russian and Belarusian power systems although no day-ahead trade takes place using these links. These connections are currently only used for balancing the Baltic power systems [70]. This too will expectedly seize by 2025 as

desynchronisation from the Integrated/Unified Power System (IPS/UPS) of Russia and Belarus has been decided on [71]. The first steps towards this have already been taken with the launch of the common Baltic balancing market at the beginning of 2018 [6].

Impact assessment of SETS deployment on the Latvian power system provides for an interesting case research as, even though climatic conditions in winters there are quite harsh and heating demand comparatively high, electric heating has not really caught on in Latvia [55]. Furthermore, thermal-electric storage heating technology, an advanced version of which is the subject of this study, is virtually unknown.

3.3.2. Outline of future scenarios & modelling assumptions

Most of the input data are taken from the *EU Reference Scenario 2016* [72] for the 2020 and 2030 cases and *e-Highway* sensitivities [73] for the 2050 case study. This includes main annual power system statistics such as electricity generation and installed capacity by source, annual electricity consumption and peak demand.

Using the *Reference Scenario* as a base, some additional sensitivities have been devised for **2020** and **2030** as relevant for the particular case study and modelling tools employed (Table 3.6). Firstly, some scenarios are developed which differ from the *Base* scenario with diverse price projections assumed (*High Price*, *Medium Price*, *Low Price* and *Volatile Price*). Additionally, *Demand-side measures* scenario envisions a power system where the typical load (and price) curve has become smoother in nature primarily thanks to implicit demand response and other measures, technological advancements and public awareness which increase the adoption of smart technologies and users' willingness to utilise them. Another differing sensitivity is the *Heating demand reduction* scenario which envisions significantly reduced heating energy demand in Latvia due to energy efficiency measures.

Table 3.6. List of main scenarios for modelling of 2020 and 2030

Scenario	Main assumptions
Base	annual el. price change +1.5%
Medium prices	annual el. price change +3.0%
High prices	annual el. price change +4.5%
Low prices	annual el. price change –0.5%
Volatile prices	*Base* scenario with an additional 1.5% chance for any particular hour to experience a tenfold price reduction
Demand-side measures	*Base* scenario with a 50% smaller standard deviation of hourly electricity price and demand timeseries to lessen the price spread and smoothen the load curve
Heating demand reduction	annual heating demand change –1.5%

For **2050**, due to the increased level of uncertainty in the longer-run perspective, five self-contained scenarios have been identified, taken from the e-Highway project [73]. This European FP7 project, undertaken by several European TSOs, developed the five following scenarios representing different developments of demand, storage, cross-border power exchange and generation capacities: *Large-Scale RES, 100% RES* [electricity], *Big & Market* (high GDP growth and market-based energy policies), *Fossil & Nuclear* (large fossil fuel deployment with CCS and nuclear electricity), *Small & Local*. In contrast to 2020 and 2030 study years, all 2050 scenarios assume a constant annual price increase of 1.5%.

Some adjustments have been made also according to the "Ten Year Network Development Plan" of the transmission system operator [74]. A major departure from the *Reference Scenario* has been made in regard to nuclear power developments. The original scenario envisions the construction of a nuclear power plant in Lithuania. However, since a consultative referendum decision in 2014 rejected this prospect [75], this has become extremely unlikely, and thus any nuclear capacities have been excluded from the models for 2030. However, those 2050 scenarios which did envision nuclear capacities in the region have been left unchanged.

The 2020 and 2030 scenarios do not envision significant growth of wind and solar capacities in Latvia, which corresponds fairly well to the current day situation in the Latvian power system where only about 2% of electrical energy annually is produced using wind resources [76] and new improvements in the near future are unlikely since no subsidies or state support are currently offered for the construction of any new renewable energy generation plants [77] and new support policies are still under development.

Electric production time series are taken from the ENTSO-E Transparency platform [78] and the public database of the Latvian TSO for the year 2016 as a base, upscaling to the scenario requirements as necessary. Demand time series are taken from the Nord Pool database [79] for the system-scale model and from a database of different consumer profiles [62] for the distribution-scale model. Temperature data necessary for heating demand approximation for the CHP plants [80] or the electrically heated houses is acquired from the national meteorological service [81].

Transmission capacity projections follow the announced plans by the Latvian TSO, Augstsprieguma tīkls AS, namely, the construction of new interconnector to Estonia in 2020 [82], refurbishment of the current cross-border transmission lines by 2025 [83] and the disconnection from the IPS/UPS in 2025. The possible increase of Estonian–Latvian net transmission capacity (NTC) [84] due to higher reserves volume can be estimated based on the data kindly provided by the Latvian and Estonian TSOs (Augstsprieguma tīkls AS and Elering).

Historical electricity price data is collected from the Nord Pool database. The same source was used to collect and analyse interconnector unavailability data which is an important factor in the Latvian case study due to the significant role the cross-border links have in the operation and clearing of the wholesale electricity market in Latvia. The Swedish–Lithuanian interconnection NordBalt is assumed to have undergone reconstruction in its weak points [71] to enable more stable operation than currently observed. Consequently, historical unavailability data from a similar DC undersea cable (EstLink-2) has been used for the reliability of the link instead of the NordBalt historical data during its initial unstable operation.

3.3.3. Approach overview

The power system-scale benefit modelling employed for the Latvian case study combines the various tools and approaches developed by the Institute of Power Engineering during the implementation of RealValue project (2015–2018) and even before that. It also closely intertwines with the distribution grid model described in Section 3.2 (i.e., the DG model feeds electrical heating time series data to the system model), which, in its turn, uses the heat demand derived from building thermal modelling in Chapter 2. The overall setup for modelling SETS impact on the Latvian power system is illustrated in Fig. 3.5.

The geographical scope of the model covers Latvia and Lithuania, whereas heating electrification is carried out only in Latvia (i.e., no SETS in Lithuania and the benefits are also expressed solely from the Latvian power system point of view).

The SETS compared to DRH brings two beneficial effects captured by the model:

- decoupling heat demand from electricity consumption (i.e., **energy arbitrage**);
- **provision of reserves** to the power system due to SETS remote controllability.

The energy arbitrage effect of SETS impacts the electricity prices in the system decreasing the total costs incurred by all the electricity consumers. However, the reserves provided by SETS enable increasing the NTC of the Estonian–Latvian interconnection which can result in more effective electricity market operation in the region, also affecting the wholesale prices in some hours.

Hydroelectric and small cogeneration plants' generation data is obtained by scaling historical data. While this might seem counterintuitive, especially for the small cogeneration plants, it does reflect the actual situation in Latvia where the renewables' support system in place does not encourage the owners of biomass/biogas cogeneration plants to follow market signals. Instead, all the electricity produced by these plants is procured by a public trader. This system is obviously suboptimal from a market point of view, but as a result, the small cogeneration plants generally opt for a very uniform operation which, on the other hand, is good for operational efficiency.

The major cogeneration plants, Riga CHP-1 and Riga CHP-2, however, are modelled in detail by integrating the RTU's in-house developed scheduling tool OptiBidus-TEC.

The devised Latvian power system model employs, in its first iteration, the hourly wholesale electricity price as an exogenous variable which is then endogenously reprocessed in the following iterations when finding the market equilibrium. The first stage in the model adds electrified heating (DRH) to 2%, 10% and 20% of the total heated space (this is assumed to generally equal the same proportion of the total heating demand). The increased demand results in higher marginal prices and demand covered by either activating more expensive price-setting plants or increased imports if there is import capacity unused. In the following steps, the electrification is carried out by SETS instead which have optimised charging patterns enabling the system to benefit from energy arbitrage. Finally, by assuming the SETS are able to quickly react to TSO signals on reserve activation, the net transfer capacity of the interconnectors between market areas can be increased closer (but not fully) to the total transfer capacity, which

enables increased imports if the import of energy is indeed able to provide cheaper electricity than the assumed local price-setter for the particular hour.
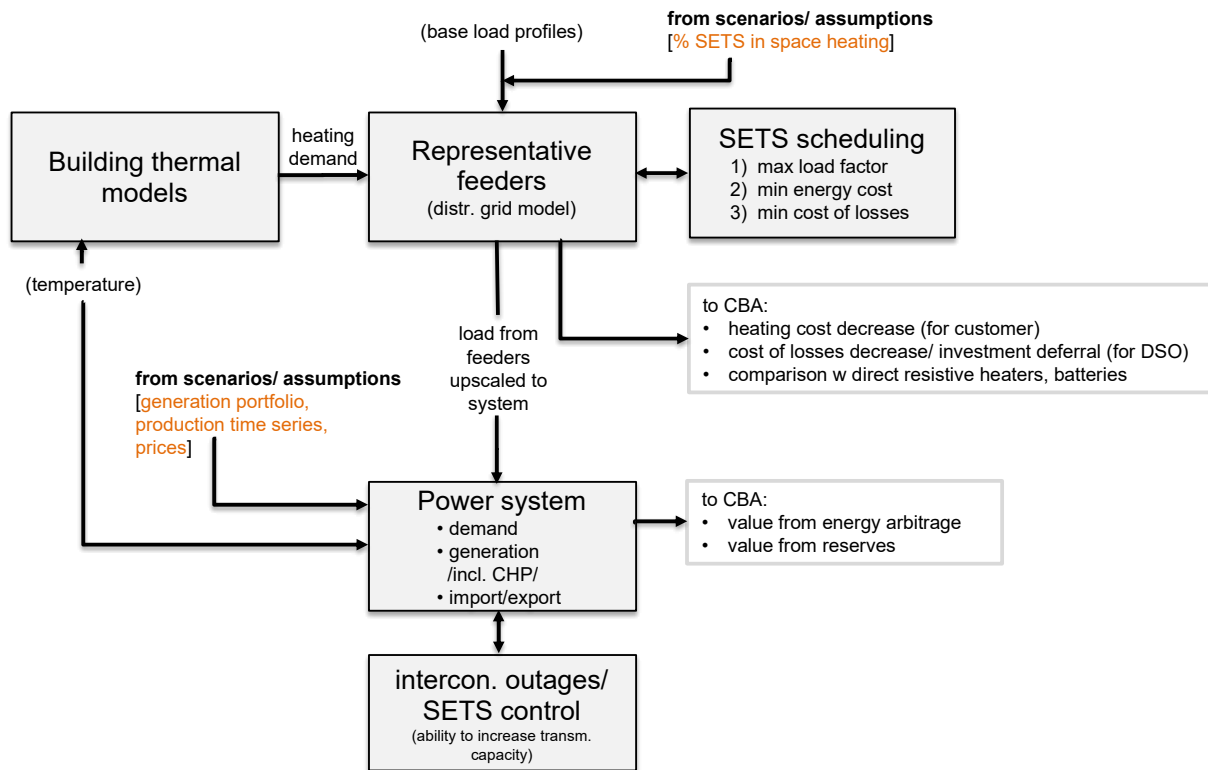
Fig. 3.5. Overall setup for SETS impact modelling.

3.3.4. Main steps of the power system benefit assessment

The operation of the power system benefit assessment model can be summarised by three main steps:

1) hourly timeseries preparation for the input;
2) multi-iteration calculation of electricity wholesale price decrease (in hourly resolution);
3) assessment of the annual benefits incurred.

Each step is described in more detail in the subsequent sections while the overall block diagram of the algorithm is illustrated in Appendix 5.

Input timeseries preparation

To prepare the timeseries for input, the following actions are taken.

- Scaling the historical timeseries of **demand** (in Latvia, Lithuania and Estonia) and **generation** by type of source (in Latvia and Lithuania) to match the scenario-dependent annual demand/generation with a constraint to avoid exceeding the peak demand or total installed generation capacity of a type of generation in any hour of the year. This is achieved by a MATLAB script specifically designed to perform iterative timeseries scaling while satisfying two principal constraints: (1) the annual sum must be equal (or less, but only if equal is impossible) to the target sum, (2) the value at any particular hour must be less or equal to the hourly maximum.

- Special consideration is given for preparing the timeseries for **Riga CHP plants** schedules – use is made of a software model developed at the Institute of Power Engineering of RTU – OptiBidus-TEC, which can calculate the cogeneration schedules of the Riga CHP plants (with hourly ambient temperature used as input).

- In terms of **interconnection capacities** and **cross-border market flows**, the flows to Belarus and Kaliningrad are assumed to be the same in 2020 as in 2016, but for 2030 and 2050 they are assumed to be null (due to the desynchronisation). The flows to/from Poland and SE4 area are recalculated with a specially designed MATLAB script which takes into account the generation and demand changes in Poland and Sweden in the *EU Reference Scenario 2016* and *e-Highway* scenarios, as well as the assumptions on interconnector capacities; also for these flows, 2016 is considered as the base year. Note: Estonian-Latvian interconnection serves as a balancing point in the model, i.e., flow in it is calculated by the model.

- Thereby, the **net transfer capacity** (NTC) in hourly resolution is a particularly important input timeseries. Furthermore, it is included in the model in two ways – the "normal NTC", which is the NTC value used by Nord Pool (in practice it is the smallest value from the NTC calculated by the Latvian TSO and the Estonian TSO); and the "increased NTC", which is the value calculated by the Estonian TSO. The hourly values of these parameters for 2016 were obtained from the respective TSOs. The future values are obtained by scaling according to the scenario-based, assumed future values.

- The hourly timeseries for **DRH** (for the reference cases) and **SETS electricity consumption** are obtained by scaling the respective hourly consumption patterns from the distribution grid model. Particularly for SETS we use the optimised charging strategy (1), i.e., load factor maximisation.

Electricity market price estimation

For estimation of the electricity wholesale market price, we use a stylised model which calculates the price in four iterations, subsequently updating it as required. For the years 2020 and 2030, six different electricity price subscenarios (Table 3.6) are devised under each main heating electrification scenario (2%, 10% and 20%) – both for *electrification with DRH* (used as reference case) and *heating with SETS*. For all 2050 scenarios, however, a constant annual price increase of 1.5% is assumed. These scenario-based prices are devised in the 1st iteration and then updated in the following ones. For identifying the benefits brought by SETS, we estimate the electricity price at each subscenario both for DRH and SETS cases.

The main steps of the algorithm for estimation of the hourly price are as follows for each subscenario.

- **1st market price iteration**. Prices for Latvia ($\Pi_{LV}^{approx.1}$) and Estonia ($\Pi_{EE}^{approx.1}$) are assumed to have the same variation profile as in 2016, but they are scaled or modified according to the annual price subscenario (Table 3.6).

- **1st market flow estimation**. The theoretical market flow in the EE–LV interconnection is calculated disregarding NTC constraints, i.e., as the arithmetic balance in Latvia/Lithuania with Estonian import as the balancing point:

$$P_{\text{EE-LV}}^{\text{approx.1}} = P_{\text{demand,LV}}^{\text{base}} + P_{\text{demand,LT}}^{\text{base}} - P_{\text{generation,LV}} - P_{\text{generation,LT}} - \sum_{n=1}^{N} P_{\text{interc.,LT},n} \cdot \qquad (3.34)$$

- **2$^{\text{nd}}$ market price iteration**. Firstly, those hours when the demand in LV+LT ($P_{\text{demand,LV}}^{\text{base}} + P_{\text{demand,LT}}^{\text{base}}$) increases (hour-to-hour) are identified. Secondly, hours when the price in LV ($\Pi_{\text{LV}}^{\text{approx.1}}$) increases (hour-to-hour) are identified. Thirdly, those hours where the previous two conditions hold true are selected, and linear regression employing the least squares' method is performed to obtain a coefficient reflecting the average dependence of market price increase as a function of demand increase, i.e.,

$$\Delta\Pi_{\text{LV, incr.}} = a \cdot \Delta P_{\text{demand,LV+LT, incr.}} \cdot \qquad (3.35)$$

Next, for hours when the 1$^{\text{st}}$ market flow approximation falls within the normal NTC constraint ($P_{\text{EE-LV}}^{\text{approx.1}} \leq P_{\text{norm.NTC}}$), the 2$^{\text{nd}}$ market price approximation equals the 1$^{\text{st}}$ approximation. Conversely, for the other hours (where $P_{\text{EE-LV}}^{\text{approx.1}} > P_{\text{norm.NTC}}$), more expensive generation has to (implicitly) be activated to maintain market balance, thereby the 2$^{\text{nd}}$ market price approximation is

$$\Pi_{\text{LV}}^{\text{approx.2}} = \Pi_{\text{LV}}^{\text{approx.1}} + a \cdot \left(P_{\text{EE-LV}}^{\text{approx.1}} - P_{\text{norm.NTC}} \right). \qquad (3.36)$$

I.e., the market flow which would have exceeded the normal NTC, would cause other (more expensive) sources to be utilised.

- Now, the **additional electric consumption** introduced by SETS or DRH is added to the base consumption.
- **3$^{\text{rd}}$ market price iteration** is performed separately for the SETS and DRH subcases. The electric load timeseries of heating equipment are added to the base consumption. Following that, the previously identified linear regression coefficient is utilised to update the hourly market prices:

$$\Pi_{\text{LV,SETS}}^{\text{approx.3}} = \Pi_{\text{LV}}^{\text{approx.2}} + a \cdot P_{\text{SETS}}; \qquad (3.37)$$

$$\Pi_{\text{LV,DRH}}^{\text{approx.3}} = \Pi_{\text{LV}}^{\text{approx.2}} + a \cdot P_{\text{DRH}}. \qquad (3.38)$$

- Now, we investigate **the option to increase the NTC** available to the market up to the theoretical maximum NTC ($P_{\text{max.NTC}}$) thanks to utilising the fast controllability of SETS devices. However, we assume the NTC can only be increased if there is available scheduled SETS load to be disconnected in case of emergency, and only by 95% of the available SETS load & not exceeding $P_{\text{max.NTC}}$, i.e.,

$$P_{\text{incr.NTC}} = \min\left(P_{\text{norm.NTC}} + 0.95 \cdot P_{\text{SETS}}, P_{\text{max.NTC}} \right). \qquad (3.39)$$

Then, we can identify the hours when such NTC increase could bring benefits in the form of reduced electricity wholesale market prices. The respective hours must meet the following three conditions:

$$P_{\text{EE-LV}}^{\text{approx.2}} > P_{\text{norm.NTC}}, \tag{3.40}$$

where
$$P_{\text{EE-LV}}^{\text{approx.2}} = P_{\text{EE-LV}}^{\text{approx.1}} + P_{\text{SETS}}; \tag{3.41}$$

$$\Pi_{\text{LV,SETS}}^{\text{approx.3}} > \Pi_{\text{EE}}^{\text{approx.1}}; \tag{3.42}$$

$$P_{\text{incr.NTC}} > P_{\text{norm.NTC}}. \tag{3.43}$$

- In the **4th market price iteration** we only recalculate the price for the hours where an NTC increase (with SETS as reserve providers) would be both possible and necessary, thus resulting in a reduced price:

$$
\begin{aligned}
\Pi_{\text{LV,SETS}}^{\text{approx.4}} &= \Pi_{\text{LV,SETS}}^{\text{approx.3}} - \frac{P_{\text{demand,EE}}}{P_{\text{demand,LV}}^{\text{base}} + P_{\text{SETS}}} \cdot \left(\Pi_{\text{LV,SETS}}^{\text{approx.3}} - \Pi_{\text{EE}}^{\text{approx.1}} \right) \cdot \\
&\quad \cdot \frac{\min\left(P_{\text{EE-LV}}^{\text{approx.2}}, P_{\text{incr.NTC}} \right) - P_{\text{norm.NTC}}}{P_{\text{EE-LV}}^{\text{approx.2}} - P_{\text{norm.NTC}}}.
\end{aligned}
\tag{3.44}
$$

Here, if the NTC available for market transactions is increased, the prices in Estonia and Latvia tend to equalise (i.e., by increasing in the former and reducing in the latter). The last component of the equation ensures that they can be even only if the increased NTC constraint is not violated; if the constraint is active, the prices tend to but do not become fully equal. The equation also ensures that the ability of the additional flow from Estonia (and thus, implicitly, from Scandinavia) to reduce the prices in Latvia is proportional to the demand in both countries.

Power system benefit assessment

Finally, it is possible to assess the benefits obtained in the form of wholesale market price reduction.

Price reduction due to smart SETS scheduling via price arbitrage (compared to the reference case with DRH):

$$\Delta\Pi_{\text{SETS,sched.}} = \Pi_{\text{LV,DRH}}^{\text{approx.3}} - \Pi_{\text{LV,SETS}}^{\text{approx.3}}. \tag{3.45}$$

Price reduction due to increased system reserves (i.e., thereby increased NTC):

$$\Delta\Pi_{\text{SETS,res.}} = \Pi_{\text{LV,SETS}}^{\text{approx.3}} - \Pi_{\text{LV,SETS}}^{\text{approx.4}}. \tag{3.46}$$

The total price reduction obtained because of SETS (scheduling and reserves):

$$\Delta\Pi_{\text{SETS,full}} = \Pi_{\text{LV,DRH}}^{\text{approx.3}} - \Pi_{\text{LV,SETS}}^{\text{approx.4}}. \tag{3.47}$$

By multiplying the price timeseries with the consumption timeseries, it is possible to express the obtained benefit in terms of the overall (country-wide) annual electricity purchase cost reduction at the wholesale level.

3.3.5. Results and discussion

Results for 2020

Since electricity cost reduction benefits in the Latvian case study are explored in a twofold manner, the results for each of the study years are presented first by their components (benefits from arbitrage and reserves) and afterwards in a summarised way. All costs and benefits are expressed per annum.

Table A4.1 in the appendix compiles the results regarding the electricity cost savings from SETS arbitrage (i.e., optimised scheduling) at various heating electrification levels. The benefits are identified in comparison to a reference case where heating electrification is carried out with DRH at the same penetration level. In all the scenarios summarised, a trend can be established where the electricity cost decrease from SETS arbitrage increases in both absolute and relative terms with larger heating electrification. For example, 3.78 M€ (0.48%) savings for the 2% penetration, 10.10 M€ (1.09%) for the 10% and 18.75 M€ (1.46%) for the 20% penetration in the *Base* scenario.

However, this effect can primarily be explained by the main peculiarity of the Latvian power system in contrast to the other countries studied in the RealValue project, namely, the currently minuscule prevalence of electric space heating [55]. This fact is reflected in the modelling assumptions by implementing both the baseline DRH and controllable SETS as an additional electrical load which is added to the demand data from *Reference Scenario 2016* (2020, 2030) and *e-Highway* (2050). In other words, heating electrification inevitably significantly increases the overall electricity costs, thereby, understandably, the opportunity to diminish this cost increase by the deployment of SETS is greater when the electrification itself is more noteworthy. For instance, in the *Base* scenario, the total electricity costs for the year 2020 with DRH are larger by about 38% if we compare the 20% and 2% electrification cases.

Indeed, if we instead analyse the arbitrage benefits relative to the total annual energy consumption of SETS or their installed energy storage capacity, the trend reverses and, with larger penetrations, the specific benefit actually decreases. In the *Base* case, it is 1.21 €/kWh, 0.65 €/kWh and 0.60 €/kWh of installed SETS for the 2%, 10% and 20% penetration scenarios respectively. This is true for all the scenarios considered for 2020 except for the *Demand-Side Measures* scenario, where the smallest specific benefit from arbitrage is found at the 10% case. Curiously, as can be seen in Fig. 3.6, while the specific benefit nearly halves if heating electrification is increased from 2% to 10%, further increase to 20% diminishes the savings from SETS arbitrage per kWh of installed storage by merely about 6–9.4% depending on the scenario, except for *Demand-side measures* scenario.

In regard to scenario differences, it can be seen that the scenarios based on different price future development assumptions (*Medium*, *High* and *Low prices*) provide generally very similar results, where they differ in absolute numbers in correspondence to the underlying projections. The *Volatile prices* scenario, however, does manage to capture higher cost decreases from arbitrage since there are more and better-defined hours controllable load like SETS can exploit where the electricity day-ahead price is significantly lower than the mean.

The *Demand-side measures* and *Heating demand reduction* scenarios, on the other hand, do show decreased SETS arbitrage value in absolute terms. Moreover, in the former, the value is reduced significantly (i.e., by a factor of 2.5, 2.0 and 1.4 in the 2%, 10% and 20% cases respectively, whereas, in the latter, the decrease in savings is however fairly small at only about a factor of 1.1). It is interesting to note that in the *Base* and *Heating demand reduction* scenarios, the specific benefit per kWh of SETS installed (Fig. 3.6) is almost the same even though the installed storage differs notably (e.g., 3 131 MWh in the *Base* and 2 943 MWh in the *Heating demand reduction* scenario at 2% penetration.
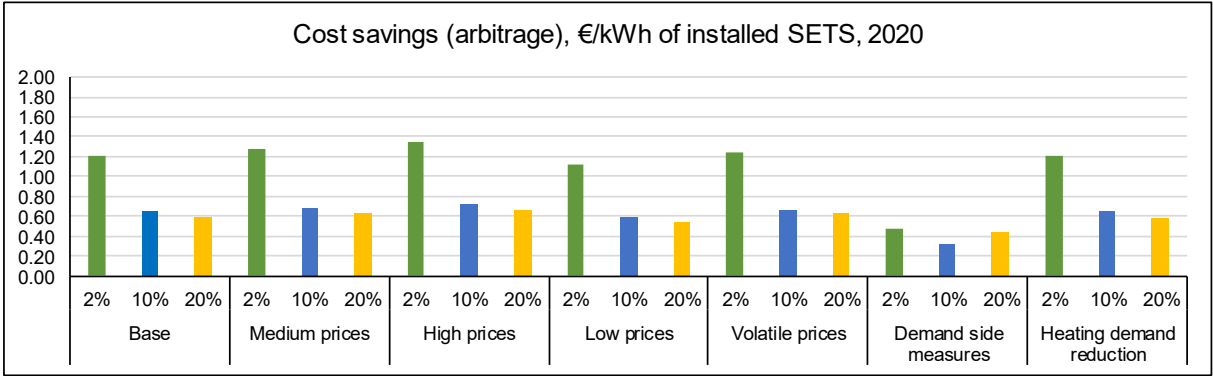
Fig. 3.6. Cost savings from SETS arbitrage per kWh of installed storage, 2020.

Compared to the value extracted from SETS arbitrage, the electricity cost decreases brought by SETS participation in reserve provision are notably smaller. The results for the year 2020 summarised in Table A4.2 in the Appendix show that, relative to the total electricity costs in Latvia, SETS as a contributor in reserve provision can provide cost reductions ranging from 0.01% to 0.03% in the 2% penetration case, 0.06–0.17% in the 10% penetration case and 0.30–0.44% in the 20% penetration case.

Benefit from reserves comprises roughly 2.83%, 12.92% and 22.34% of the total electricity cost reductions brought by SETS in the *Base* scenario for the 2%, 10% and 20% penetration cases respectively. Unlike in arbitrage (Fig. 3.6), the reserve provision has greater specific benefit the more SETS there are in the system (Fig. 3.7). For instance, in the *Base* scenario, the cost savings from SETS reserves are 0.04 €/kWh, 0.10 €/kWh and 0.17 €/kWh of installed SETS storage in the various penetration levels.

Once again, the *Demand-side measures* scenario shows to be an exception as the abovementioned trend is not really in effect in this case. The other alternative demand-side flexibility measures implicitly modelled in this scenario seem to have a hardly generalisable and predictable effect on SETS value, apart from the obvious implication that the value of a particular flexibility provider (e.g., SETS) decreases when the demand side as a whole has become more price-sensitive and manageable.
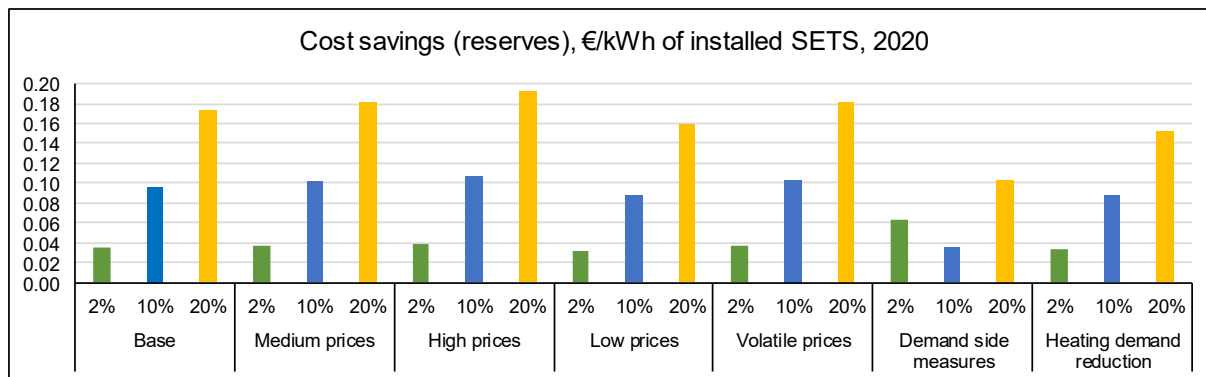
Fig. 3.7. Cost savings from SETS reserves per kWh of installed storage, 2020.

Table 3.7 combines both avenues of SETS beneficial contributions to the power system studied in the Latvian case study for the year 2020. It can be concluded from the various scenarios that SETS value somewhat depends on the underlying heating demand assumptions, but even more so from the characteristics and flexibility of the other electrical load and the marginal costs of price-setting generators. In terms of benefits from SETS penetration, the 2% case offers the highest savings in the electricity system, whereas if the penetration is 10% or more, the specific benefit is greatly diminished (Fig. 3.8).

It could also be useful to express the cost reduction brought by SETS in other comparable terms. For instance, in the scenarios analysed for 2020, the benefit ranges for the 2%, 10% and 20% penetrations are 33.10–85.26 €/dwelling, 21.59–50.79 €/dwelling and 33.69–52.88 €/dwelling or if expressed per units of SETS deployed in the country: 8.28–21.31 €/device, 5.40–12.70 €/device and 8.42–13.22 €/device. A note should be made here on another peculiarity of the Latvian case study. We assumed SETS could be installed not only in detached houses and apartments but also in some public and industrial buildings, which is an assumption derived from the physical demonstration of SETS technology in the Latvian trial within the RealValue project. The average heating space of a dwelling/house in the model translates to roughly 60.25 m^2.

Finally, the Latvian case study for the year 2020 can be concluded by observing the price-reducing effects of SETS in the day-ahead electricity wholesale market. Table 3.8 compiles the average hourly electricity price in the various scenarios and penetration levels. The weighted average price is also included (weighted against the hourly consumption in Latvia). While the average price decrease due to SETS is fairly small (0.01%, 0.16% and 0.42% for the 2%, 10% and 20% penetration levels), the weighted average decreases more noticeably (0.49%, 1.25% and 1.88% respectively) as can be seen in Fig. 3.9. This very well exemplifies the positive effect from SETS energy storage and scheduling abilities, i.e., moving heating-related electrical load away from the peak price periods thus smoothening the overall load curve.

Table 3.7. Total electricity costs and total cost savings from SETS in Latvia, 2020

Scenario	Heating electrifica-tion	Total costs, M€	Cost savings, M€	Cost savings, %	Cost savings, €/kWh of installed SETS	Cost savings, €/device of SETS
Base	2%	792	3.89	0.49%	1.24	19.15
	10%	930	11.60	1.25%	0.74	11.41
	20%	1 283	24.14	1.88%	0.77	11.88
Medium prices	2%	837	4.11	0.49%	1.31	20.23
	10%	982	12.25	1.25%	0.78	12.05
	20%	1 356	25.51	1.88%	0.81	12.55
High prices	2%	882	4.33	0.49%	1.38	21.31
	10%	1 035	12.91	1.25%	0.82	12.70
	20%	1 428	26.88	1.88%	0.86	13.22
Low prices	2%	733	3.60	0.49%	1.15	17.70
	10%	860	10.72	1.25%	0.68	10.55
	20%	1 186	22.32	1.88%	0.71	10.98
Volatile prices	2%	786	4.01	0.51%	1.28	19.75
	10%	929	12.04	1.30%	0.77	11.85
	20%	1 291	25.28	1.96%	0.81	12.44
Demand-side measures	2%	763	1.68	0.22%	0.54	8.28
	10%	899	5.49	0.61%	0.35	5.40
	20%	1 096	17.12	1.56%	0.55	8.42
Heating demand reduction	2%	791	3.68	0.47%	1.25	19.26
	10%	919	10.81	1.18%	0.73	11.31
	20%	1 256	21.69	1.73%	0.74	11.35
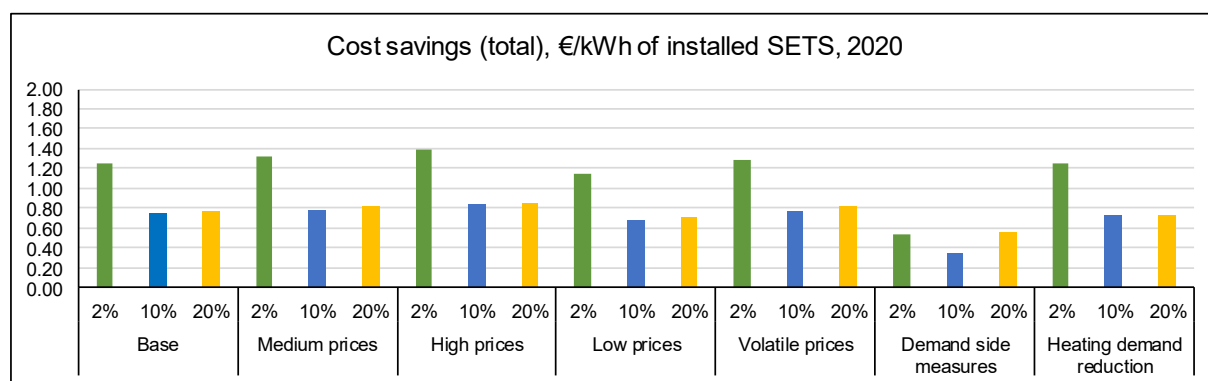
Fig. 3.8. Total costs savings from SETS per kWh of installed storage, 2020.

Table 3.8. Average electricity day-ahead price in the Latvian bidding area, 2020

Scenario	Heating electrifi-cation	Average electricity day-ahead price			Weighted average electricity day-ahead price		
		with DRH	with SETS	reduction	with DRH	with SETS	reduction
Base	2%	39.82	39.82	0.01%	41.89	41.68	0.49%
	10%	43.56	43.50	0.15%	46.13	45.55	1.25%
	20%	48.24	48.06	0.37%	51.20	50.24	1.88%
Medium prices	2%	42.08	42.07	0.01%	44.26	44.04	0.49%
	10%	46.03	45.96	0.15%	48.74	48.13	1.25%
	20%	50.97	50.78	0.37%	54.10	53.08	1.88%
High prices	2%	44.33	44.32	0.01%	46.63	46.40	0.49%
	10%	48.50	48.42	0.15%	51.35	50.71	1.25%
	20%	53.70	53.51	0.37%	57.00	55.93	1.88%
Low prices	2%	36.82	36.81	0.01%	38.72	38.53	0.49%
	10%	40.28	40.22	0.15%	42.64	42.11	1.25%
	20%	44.60	44.44	0.37%	47.34	46.45	1.88%
Volatile prices	2%	39.49	39.49	0.02%	41.55	41.34	0.51%
	10%	43.48	43.41	0.16%	46.08	45.48	1.30%
	20%	48.46	48.28	0.38%	51.52	50.51	1.96%
Demand-side measures	2%	39.80	39.79	0.03%	40.34	40.25	0.22%
	10%	43.57	43.54	0.06%	44.59	44.31	0.61%
	20%	48.27	48.15	0.26%	50.49	49.70	1.56%
Heating demand reduction	2%	39.77	39.76	0.01%	41.83	41.63	0.47%
	10%	43.28	43.23	0.13%	45.79	45.25	1.18%
	20%	47.68	47.53	0.31%	50.49	49.61	1.73%
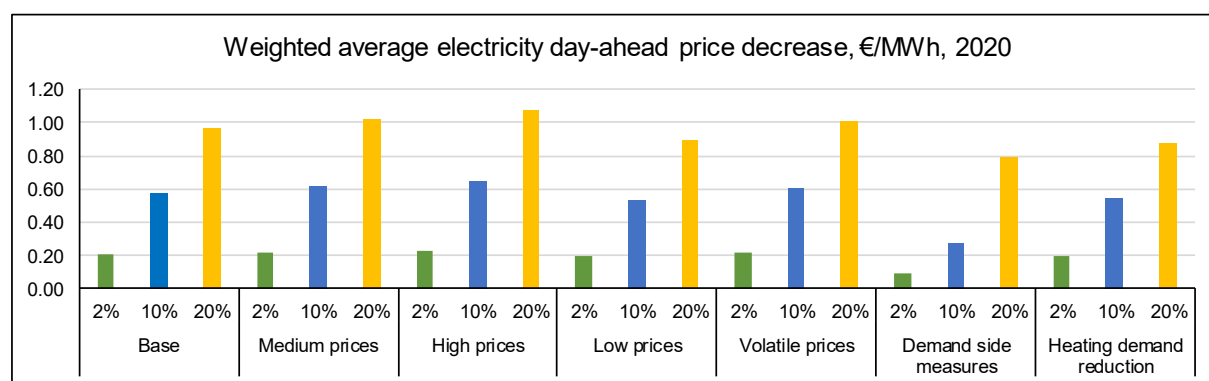
Fig. 3.9. Electricity price decrease in the Latvian bidding area with SETS.

Results for 2030

At first glance, the results from the study year 2030 show some obvious differences from the 2020 results. Firstly, the cost savings brought by SETS arbitrage are overall greater. In the *Base* scenario, they have grown by 0.57 M€, 1.58 M€ and 3.37 M€ for the various penetration levels. This also translates to improved savings per kWh of installed SETS: a 0.18 €/kWh, 0.10 €/kWh and 0.11 €/kWh increase respectively. However, the previously observed tendency for the specific benefit from arbitrage to decrease as the level of penetration rises is also seen here (Table A4.3 in the Appendix).

In the 2030 results, we can observe much greater variation in arbitrage benefits depending on price assumptions (*Medium*, *High* and *Low price* scenarios) compared to 2020. It is, however, primarily a consequence of the model setup and the fact that the price uncertainties considered here grow larger the further in future we project.

The *Demand-side measures* scenario, on the other hand, is similar to the 2020 case as it shows significantly lesser cost savings than the *Base* scenario as can be well seen in Fig. 3.10. More particularly, the specific benefit decreases from 1.39 €/kWh, 0.75 €/kWh, 0.71 €/kWh to 0.54 €/kWh, 0.36 €/kWh, 0.49 €/kWh for the various penetration levels. Again, the previous conclusion can be reiterated so that demand without any demand-side measures applied shows greater potential for cost decrease with SETS scheduling abilities than demand which is already smoother.

Contrary to the 2020 study year, the 2030 case shows more significantly decreased overall SETS arbitrage value in the *Heating demand reduction* scenario compared to the *Base* scenario. If the overall heating demand decreases as projected in the scenario, the cost savings from arbitrage decrease by 0.83 M€, 2.28 M€, 5.71 M€ a year, or in relative terms: 0.09 pp., 0.17 pp., 0.34 pp. However, since the deployment of SETS (installed storage) decreases from 3 131 MWh, 15 654 MWh, 31 308 MWh to 2 473 MWh, 12 367 MWh, 24 733 MWh (2%, 10%, 20% penetration cases respectively), the arbitrage benefits expressed per unit of installed storage are actually fairly similar in the *Base* and *Heating demand reduction* scenarios as can be seen in Fig. 3.10.
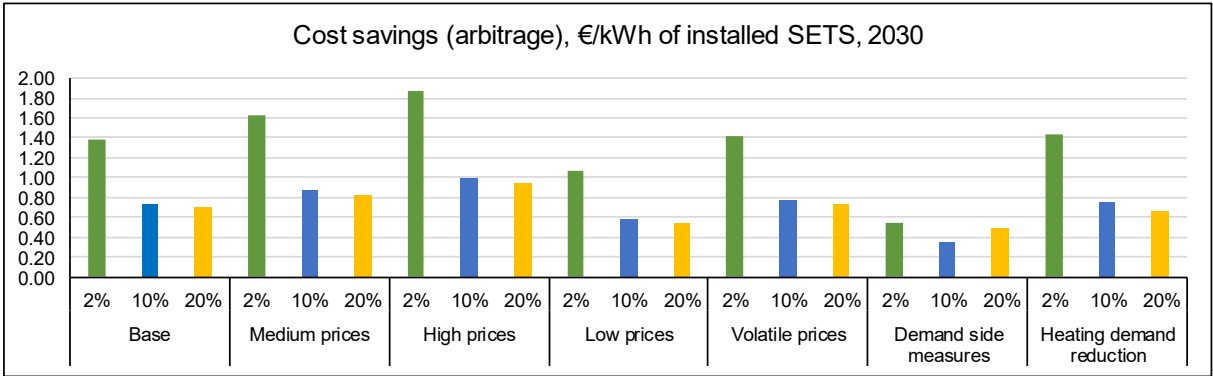
Fig. 3.10. Cost savings from SETS arbitrage per kWh of installed storage, 2030.

The other value stream of SETS considered in the Latvian case study, reserves, brings a decidedly smaller contribution to the overall cost savings in the 2030 study year than in 2020. Table A4.4 in Appendix 4 summarises these results, and it can be seen that for the 2%

penetration level SETS actually has so minuscule reserve value that for all intents and purposes it can be considered to be zero. For the 10% penetration case, it is also very small not even exceeding 0.01% of the total electricity costs in the system. Only for the 20% penetration case, the reserve value reaches about 0.12% of the total electricity costs, but that, of course, is also a very small benefit.

The reason for the tremendously diminished reserves' value of SETS can be pinpointed to major reinforcements of the transmission grid, particularly the interconnector between Estonia and Latvia, expected to be conducted by 2020 and 2025. As a result, the transmission capacity between these countries almost doubles from 2020 to 2030 study year (i.e., the TTC increases from 1000 MW to about 1900 MW). Due to this fact and the capacity/production assumptions from *Reference scenario 2016*, there are significantly fewer hours during the year when the interconnector is congested, meaning that there is close to no value from covering some of the reserve requirements in the Latvian power system with controllable SETS.

Fig. 3.11 illustrates the small specific benefits from SETS as a contributor to reserves (in the scenarios where applicable).
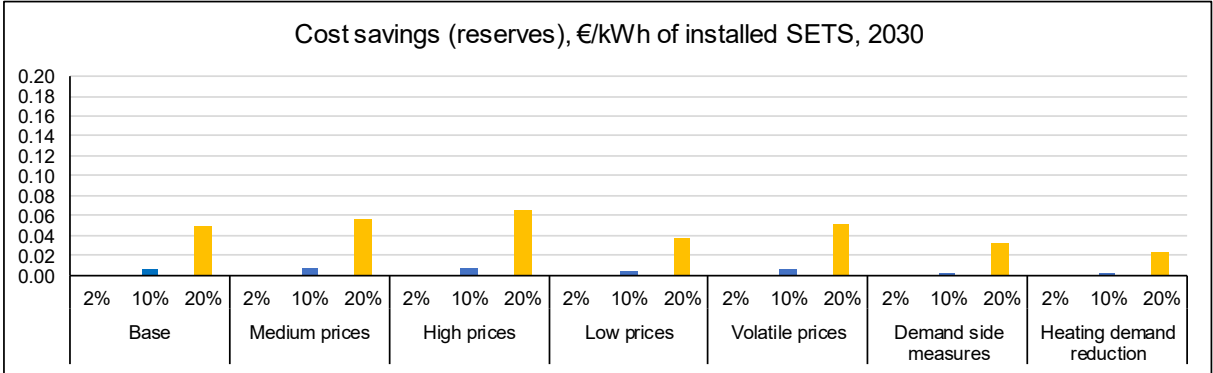
Fig. 3.11. Cost savings from SETS reserves per kWh of installed storage, 2030.

At last, Table 3.9 summarises the total benefits of electricity cost reduction offered by heating electrification with SETS in 2030. Fig. 3.12 illustrates visually the penultimate column of the table which is the total cost savings expressed per kWh of SETS storage installed in the system.

On the surface, there is only minor difference from Fig. 3.10 due to the minuscule benefits from reserves. Nevertheless, the conclusion can be made, comparing the total savings in 2030 to those of 2020, that despite the drawback in reserve provision, the overall electricity cost-saving effects of SETS have improved in both magnitude and benefit per installed storage capacity or device of SETS. Across the scenarios, this improvement is most prominent with the 2% penetration level and ranges up to 7.53 €/device (*High prices* scenario). There are, however, some exceptions. In the *Low prices* scenario, the benefit per device actually decreases in 2030 regardless of the SETS penetration level. Furthermore, it also diminishes in the *Base*, *Volatile Prices*, *Demand-side measures* and *Heating demand reduction* scenarios for the 20% penetration (the largest decrease is equal to 2.04 €/device).

Table 3.9. Total electricity costs and total cost savings from SETS in Latvia, 2030

Scenario	Heating electrifica-tion	Total costs, M€	Cost savings, M€	Cost savings, %	Cost savings, €/kWh of installed SETS	Cost savings, €/device of SETS
Base	2%	931	4.35	0.47%	1.39	21.41
	10%	1 087	11.77	1.08%	0.75	11.58
	20%	1 312	23.64	1.80%	0.76	11.63
Medium prices	2%	1 093	5.11	0.47%	1.63	25.13
	10%	1 276	13.82	1.08%	0.88	13.59
	20%	1 540	27.75	1.80%	0.89	13.65
High prices	2%	1 254	5.86	0.47%	1.87	28.84
	10%	1 464	15.86	1.08%	1.01	15.60
	20%	1 768	31.85	1.80%	1.02	15.67
Low prices	2%	716	3.35	0.47%	1.07	16.46
	10%	835	9.05	1.08%	0.58	8.90
	20%	1 009	18.17	1.80%	0.58	8.94
Volatile prices	2%	921	4.46	0.48%	1.43	21.96
	10%	1 082	12.12	1.12%	0.77	11.92
	20%	1 315	24.61	1.87%	0.79	12.10
Demand-side measures	2%	898	1.70	0.19%	0.54	8.37
	10%	1 051	5.58	0.53%	0.36	5.49
	20%	1 274	16.36	1.28%	0.52	8.05
Heating demand reduction	2%	923	3.53	0.38%	1.43	21.97
	10%	1 044	9.44	0.90%	0.76	11.75
	20%	1 213	16.98	1.40%	0.69	10.57
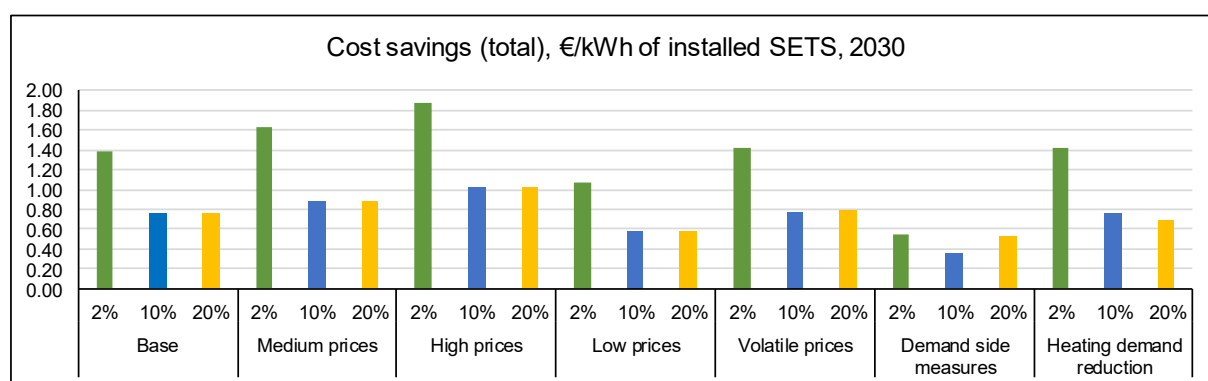
Fig. 3.12. Total costs savings from SETS per kWh of installed storage, 2030.

It should be noted that neither in the 2020 nor 2030 scenarios there was any wind curtailment in the Latvian power system. However, it is not surprising as it already follows from the capacity and production assumptions. *Reference scenario 2016* does not project drastic increases in intermittent renewable capacities in Latvia in either of these years, but nearby European countries where it might prove to be a problem were out of the model scope.

Table 3.10 enables us to consider the effects SETS devices have on the electricity wholesale day-ahead price in both average and weighted average terms. Fig. 3.13 illustrates the difference in particular. Similarly to 2020, the larger the heating electrification level, the better SETS can decrease the electricity price if the reference electrification medium is DRH. While the average hourly price itself changes only barely (by 0.09% maximum), the weighted average experiences much more impactful reductions (by up to 1.88%) which is very beneficial to all the electricity consumers but might not necessarily be a good sign to electricity producers, especially those who do not have much flexibility in their production scheduling.

Table 3.10. Average electricity day-ahead price in the Latvian bidding area, 2030

Scenario	Heating electrifi-cation	Average electricity day-ahead price			Weighted average electricity day-ahead price		
		with DRH	with SETS	difference	with DRH	with SETS	difference
Base	2%	44.70	44.70	0.00%	46.99	46.77	0.47%
	10%	48.79	48.79	0.01%	51.63	51.07	1.08%
	20%	53.92	53.87	0.09%	58.06	57.01	1.80%
Medium prices	2%	52.45	52.45	0.00%	55.15	54.89	0.47%
	10%	57.26	57.26	0.01%	60.59	59.93	1.08%
	20%	63.28	63.22	0.09%	68.13	66.91	1.80%
High prices	2%	60.21	60.21	0.00%	63.30	63.00	0.47%
	10%	65.73	65.73	0.01%	69.55	68.80	1.08%
	20%	72.63	72.57	0.09%	78.21	76.80	1.80%
Low prices	2%	34.35	34.35	0.00%	36.12	35.95	0.47%
	10%	37.50	37.50	0.01%	39.68	39.25	1.08%
	20%	41.44	41.40	0.09%	44.62	43.82	1.80%
Volatile prices	2%	44.23	44.23	0.00%	46.48	46.26	0.48%
	10%	48.56	48.55	0.01%	51.38	50.81	1.12%
	20%	53.97	53.91	0.10%	58.17	57.09	1.87%
Demand-side measures	2%	44.70	44.70	0.00%	45.30	45.22	0.19%
	10%	48.82	48.82	0.00%	49.94	49.67	0.53%
	20%	53.97	53.93	0.08%	56.36	55.64	1.28%
Heating demand reduction	2%	44.48	44.48	0.00%	46.76	46.58	0.38%
	10%	47.72	47.72	0.00%	50.36	49.91	0.90%
	20%	51.77	51.75	0.03%	55.28	54.51	1.40%
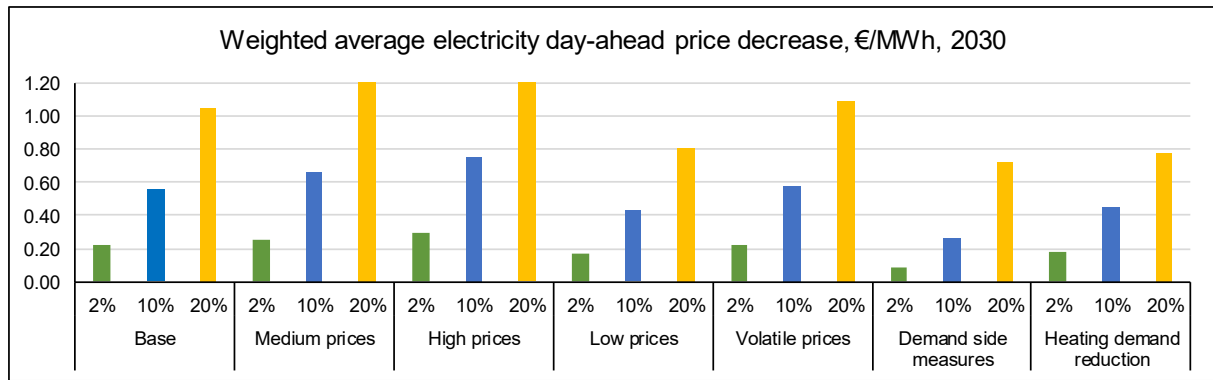
Fig. 3.13. Electricity price decrease in the Latvian bidding area with SETS.

Due to possible generation developments in the Lithuanian power system, a special scenario was considered for the study year of 2030. The Kruonis pumped storage hydropower plant which currently has four hydroelectric units with the total installed capacity of 900 MW is considering adding a fifth unit rated at 225 MW [85]. This would increase the total input and output power of the plant, but not its energy storage capability (i.e., upper reservoir capacity). As a consequence, we constructed an additional scenario which is based on the *Base* scenario only differing in additional 225 MW pumped storage capacity in Lithuania.

Table 3.11, Table 3.12 and Fig. 3.14 summarise this supplementary scenario titled *Additional Pumped Storage* in comparison to the *Base* scenario. The first observable effect is the almost complete elimination of any remaining value for SETS in reserve provision (there is some residual nonzero benefit in the 20% penetration case, but it is nevertheless negligible). The savings brought by arbitrage are also diminished but to a relatively minor extent. When comparing the cost reductions caused by SETS as a percentage of the total electricity costs, additional pumped storage capacity decreases SETS contribution by about 0.02 pp., 0.03 pp. and 0.11 pp. for 2%, 10% and 20% penetrations respectively. In absolute terms, this translates to a 0.09 M€, 0.22 M€ and 0.92 M€ diminishment in SETS value at system scale.

To conclude the 2030 analysis, it can be established that with all the other assumptions remaining the same, additional 225 MW in pumped storage capacity result in completely negated SETS value in reserves and somewhat diminished value in arbitrage.

Table 3.11. Total electricity costs and cost savings from SETS,
Additional Pumped Storage sensitivity, 2030

Scenario	Heating electrifica-tion	Total costs, M€	Cost savings, M€	Cost savings, %	Cost savings, €/MWh of total cons.	Cost savings, €/MWh of SETS cons.	Cost savings, €/kWh of inst. SETS
Base	2%	931	4.35	0.47%	0.22	14.04	1.39
	10%	1 087	11.77	1.08%	0.56	7.60	0.75
	20%	1 312	23.64	1.80%	1.05	7.63	0.76
Additional Pumped Storage	2%	939	4.26	0.45%	0.21	13.75	1.36
	10%	1 104	11.55	1.05%	0.54	7.45	0.74
	20%	1 344	22.72	1.69%	1.00	7.33	0.73

Table 3.12. Electricity cost savings from SETS arbitrage and reserves, *Additional Pumped Storage* sensitivity, 2030

Scenario	Heating electrifica-tion	Cost savings, M€ (arbitrage)	Cost savings, M€ (reserves)	Cost savings, % (arbitrage)	Cost savings, % (reserves)	Cost savings, €/kWh of installed SETS (arbitrage)	Cost savings, €/kWh of installed SETS (reserves)
Base	2%	4.35	0.00	0.47%	0.00%	1.39	0.00
	10%	11.68	0.09	1.07%	0.01%	0.75	0.01
	20%	22.12	1.52	1.69%	0.12%	0.71	0.05
Additional Pumped Storage	2%	4.26	0.00	0.45%	0.00%	1.36	0.00
	10%	11.55	0.00	1.05%	0.00%	0.74	0.00
	20%	22.71	0.02	1.69%	0.00%	0.73	0.00
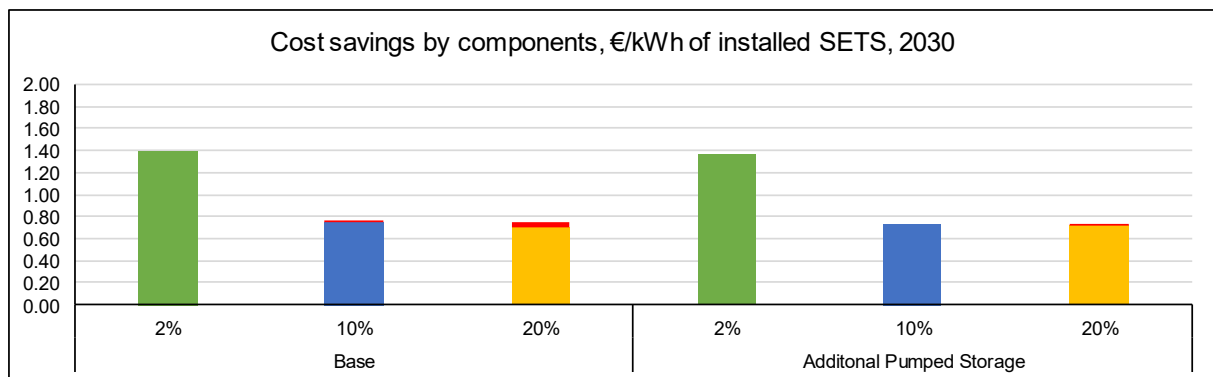
Fig. 3.14. Costs savings (by components) from SETS per kWh of installed storage, 2030.

Results for 2050

The *e-Highway* sensitivities for the 2050 study year were also analysed from the same two vehicles of electricity cost savings as in the previous two study years – arbitrage and reserves.

The 2050 scenarios differ from 2020 and 2030 assumptions most importantly by majorly increased renewable generation, especially intermittent sources like wind and solar. Of course, modelling so far in the future must be taken with a grain of salt, nevertheless the results obtained here might provide some valuable insights.

The annual electricity demand also is notably higher in the 2050 scenarios than in either of the prior study years. The benefits from arbitrage are lower in relative terms (savings versus total costs) but quite higher in absolute values or per units of SETS consumption or capacity (Fig. 3.15). Table A4.5 in the Appendix summarises the benefit from arbitrage in various metrics.

From the five scenarios compared, *Small & Local* finds the least specific value from SETS per kWh of installed capacity, whereas, in the *Large Scale RES* scenario, the specific arbitrage value is the highest. In general, the cost savings brought from SETS arbitrage range from 0.17% to 0.89% of the total electricity costs in Latvia or from 0.74 €/kWh to 1.88 €/kWh of installed SETS depending on the scenario and penetration level.

A somewhat interesting result is the fact that the specific value per installed SETS storage varies between the scenarios for the 2% and 10% heating electrification levels, while for the 20% penetration the specific benefit ends up at about 0.74–0.75 €/kWh of installed SETS.
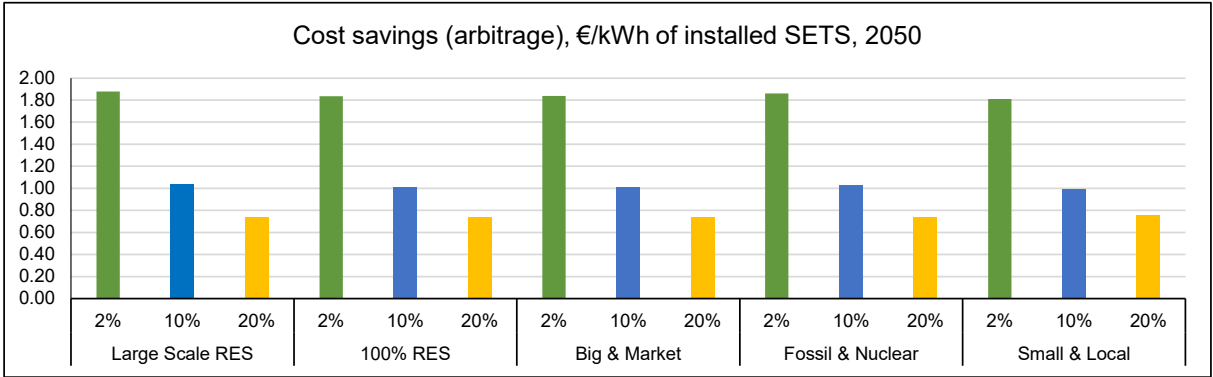
Fig. 3.15. Cost savings from SETS arbitrage per kWh of installed storage, 2050.

The other source of value, reserve provision, varies a lot across the scenarios and no discernible trend can be identified. However, some value from reserves is present in most of the scenarios albeit very small. A conclusive exception is the *Small & Local* scenario where no value from SETS as a reserves' provider could be identified (Fig. 3.16).

The Latvian power system in the *e-Highway* scenarios is supposed to be a net exporter and well-integrated transmission-wise with the other countries in the region. The geographically limited scope of the model employed for the Latvian case study might prove to be insufficient in finding some hidden untapped value streams in conditions so very detached from the contemporary situation in Latvia.
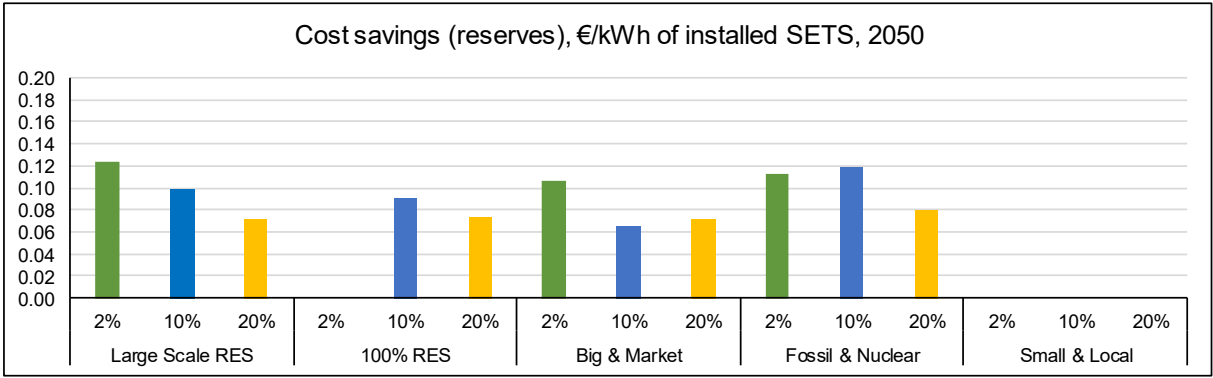
Fig. 3.16. Cost savings from SETS reserves per kWh of installed storage, 2050.

The total cost reductions from SETS in the 2050 study year are summarised in Table 3.13 with Fig. 3.17 illustrating the savings per kWh of installed SETS. The results are unfortunately quite hard to interpret given the large disconnect in the time-scale from the modelled year, but, in brief, SETS do seem to still provide value in the form of overall electricity cost reduction even in 2050. Objectively, however, one has to keep in mind that decidedly more advanced flexibility providing technologies could be developed and deployed in the following 30 years. Furthermore, the characteristics of SETS itself might change markedly in the future.

Table 3.13. Total electricity costs and total cost savings from SETS, 2050

Scenario	Heating electrification	Total costs, M€	Cost savings, M€	Cost savings, %	Cost savings, €/kWh of installed SETS	Cost savings, €/device of SETS
Large Scale RES	2%	3 492	6.27	0.18%	2.00	30.83
	10%	3 662	17.78	0.49%	1.14	17.49
	20%	3 886	25.41	0.65%	0.81	12.50
100% RES	2%	2 845	5.75	0.20%	1.84	28.26
	10%	3 016	17.24	0.57%	1.10	16.96
	20%	3 243	25.39	0.78%	0.81	12.49
Big & Market	2%	2 979	6.09	0.20%	1.94	29.95
	10%	3 150	16.87	0.54%	1.08	16.60
	20%	3 376	25.25	0.75%	0.81	12.42
Fossil & Nuclear	2%	3 329	6.18	0.19%	1.97	30.40
	10%	3 499	17.94	0.51%	1.15	17.65
	20%	3 723	25.59	0.69%	0.82	12.59
Small & Local	2%	2 235	5.67	0.25%	1.81	27.87
	10%	2 408	15.54	0.65%	0.99	15.29
	20%	2 641	23.61	0.89%	0.75	11.61
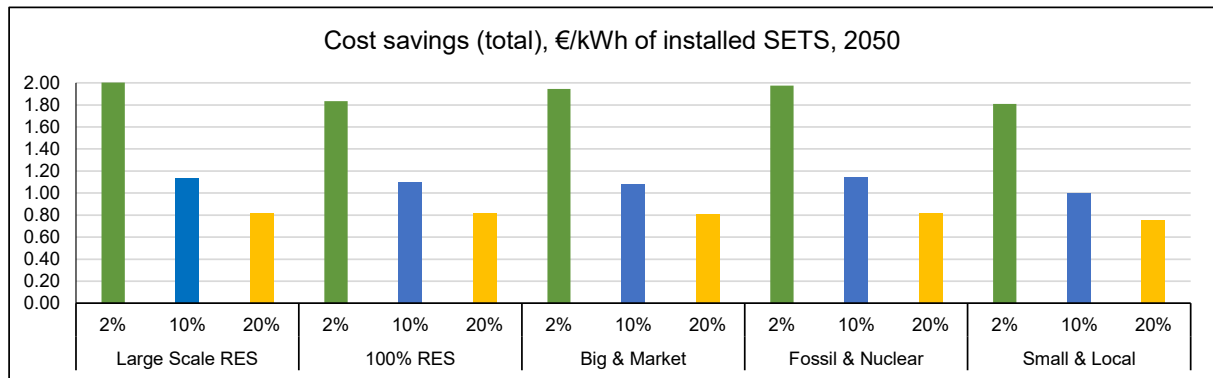
Fig. 3.17. Total costs savings from SETS per kWh of installed storage, 2050.

3.4. Summary

To investigate the impact of local small-scale thermal electric storage on the low voltage distribution network congestions, a model representing general characteristics of the Latvian distribution grid and typical electrical loads of end-users has been developed. Since the share of customers currently using electric heating as their main heat source is negligible in Latvia, partial electrification of heating with SETS or direct resistive heaters is examined. Accordingly, it allows evaluation of the consequences such electrification implies.

To mitigate the possible issues, several congestion management strategies have been studied that strive to either minimise daily load variance, decrease overall losses or minimise the cost of heating for customers.

The output from the distribution modelling efforts was used as input to the overall power system benefit assessment model simulating the impacts of large-scale SETS deployment in Latvia for the study years of 2020, 2030 and 2050 employing a number of future projection scenarios.

The partial electrification of heating assumed in this study might not necessarily be the best approach in developing new multi-energy systems in Latvia. The increased demand resulting from the electrification does induce notably higher electricity costs in the system, especially in the 10% and 20% cases. However, evidently, these cost increases can be somewhat alleviated if the electrification is carried out with smart electric thermal storage instead of direct resistive heating. Depending on the scenario and assumed penetration, these savings can amount to 0.47–1.96% of the total costs, or 4.35–25.28 M€/annum in absolute numbers for the 2020 and 2030 study years.

Most of the value SETS bring comes from their smart storage ability, i.e., mostly charging in times when the electricity price/demand is lower and discharging whenever the heating energy is required which allows avoiding electricity consumption at the usual peak times. However, this also exemplifies that SETS contribution to system benefits can be expected to be lower if the peak/off-peak characteristics of the overall demand curve have become less pronounced due to other developments on the demand-side of the power system. This expectation was indeed confirmed by the *Demand-side measures* sensitivity. Improvements in thermal efficiency/ heat demand reduction measures also signify lesser deployment of SETS devices and diminished benefit from them. The benefit from each SETS unit installed also decreases the more of them are deployed in the system.

Additionally, the smart control and web connection of SETS devices enable them to be used in reserve provision to the power system. This was another value stream of SETS identified in the Latvian case study. However, due to significant improvements to the interconnection capacities, these benefits decreased majorly from 2020 to 2030. Furthermore, if an additional 225 MW pumped storage expansion project was to be followed through (the likelihood of which is currently uncertain though), the benefits from SETS reserves in 2030 would be nearly completely negated.

The 2050 sensitivities again do show some savings from SETS as a reserve provider (except in the *Small & Local* scenario). However, the arbitrage benefits have almost halved compared to the 2020 and 2030 scenarios. All the 2050 sensitivities do show a power system very contrasting to contemporary Latvia with uncharacteristically high deployments of wind and solar power generators. On the other hand, the 2050 results should be taken for what they are, an informative what-if study, as opposed to robust future projections.

From the distribution grid operator's perspective, partial heating electrification does bring the risk of congestion and increased need for investments to avoid it. However, coordinated scheduling of SETS does serve well in alleviating most of these concerns as shown in the representative feeder study in Section 3.2.8. Furthermore, it also aids in decreasing the cost of

losses for the DSO and reasonably reduced electricity bills to the end-consumers when compared to the baseline of electrification with DRH. However, some caution is necessary because if the control of SETS is not coordinated for grid benefit but only follows the electricity price signal to decrease the end-user bills to a minimum, it causes massive issues to the distribution grid in terms of peak power, load factor and necessary grid reinforcements.

Finally, from the results presented in this study, the 2030 scenarios with 2% penetration could be selected as the most insightful and relevant. The reason for this is the unlikelihood of any SETS deployment in Latvia by 2020 (during the time of study in 2018, this or any other similar technology was not even directly sold in Latvia) and the very overambitious goals of the 10% and 20% electrification which would unlikely happen naturally and would require policy intervention to be actually fulfilled. Thus, we will use the 2030 2% results for the cost-benefit assessment that follows.

In terms of benefits compared to a system with DRH, the SETS devices offer a potential total electricity cost reduction in the range of 0.54–1.87 €/kWh/annum of installed SETS storage (among the 2030 2% sensitivities). Additionally, the distribution grid model shows that coordinated smart control strategy could reduce the cost of losses to the DSO by 0.08–0.20 €/kWh/annum and end-user electricity bills by 0.50–1.24 €/kWh/annum expressed per kWh of installed SETS. If the end-users were to schedule their SETS solely based on price signals, they could achieve specific electricity cost reduction in the range of 1.13–2.25 €/kWh/annum, but with some congestion risk to the distribution grid (albeit minor compared to the 10% and 20% cases).

The average household modelled in the Latvian case study would require four SETS devices with the total storage of 61.6 kWh. The cost of the devices would be equal to about 3800 € [57] and additionally, expenses for the gateways and installation. In the reference case, a price search shows an equivalent DRH system could have prices varying in a very broad range, illustratively, about 50–600 €. If we assume approximately equal installation costs and 200 € for the SETS gateway, the SETS devices would have a cost differential of about 55.19–64.12 €/kWh.

It is evident that the benefits neither from the system, the distribution grid nor the end-user perspective do not seem to be high enough to cover the expenses in a reasonable timeframe and justify heating electrification to be carried out with SETS. However, the possibility exists that some potential revenue streams have not been considered in this case study. Additionally, a more precise cost-benefit analysis would very much depend on the business model assumed since there are several conceivable ways how both, the costs and incurred savings could be distributed among the energy chain actors and business parties. Nevertheless, the results presented do seem to suggest that some form of financial subsidies or support would be necessary for the end-users to install SETS.

Finally, it is useful to observe the comparison of SETS benefits brought to the power system in terms of overall cost savings as compared to DRH in various countries that were modelled by different partners in the RealValue project (Table 3.14). Though each country case had a different approach based on the local characteristics and available modelling tools and, more so important, very different starting levels for the uptake of SETS (or electrical heating) as a heating source at all, the results are of roughly the same scale and fairly comparable among

each other. More details on the country-specific case studies and underlying assumptions can be found in [86].

Table 3.14. Comparison of operating cost savings[5] (per kWh of installed SETS) for selected penetrations of SETS in each of the country case studies

	Ireland (6% SETS v DR)		Finland (20% SETS v DR[6])		Latvia (2% SETS v DR)		Germany (1.6% SETS v DR)		Germany (1.6% SETS v NETS[7])	
	2020	2030	2020	2030	2020	2030	2020	2030	2020	2030
Base	2.25	1.57	1.20	2.43	1.24	1.39	1.80	1.74	0.28	0.38
High Fuel Price	3.55	3.02	1.52	1.69	1.38	1.87				0.52
Low Fuel Price	2.01	1.51	0.70	1.61	1.15	1.07				

---

[5] Operating cost savings only – i.e., for Ireland this does not include capacity value, and for Germany these reflect results from the dispatch model.
[6] 20% SETS in Finland refers to 20% of electrically heated detached homes or approximately 4.4% of the housing stock by floor area.
[7] Non-smart night-time electric thermal storage heaters traditionally use in Germany.

4. ECONOMIC ASSESSMENT OF RESIDENTIAL-SCALE DR

4.1. Motivation and background

The EU had already set itself ambitious targets for decarbonisation and climate change mitigation, but on June 2018 a move was made to raise the aspirations even higher by envisioning a 32% share of renewable energy in the total consumption within the EU by 2030 [87]. However, the increasing adoption of renewable energy resources poses new challenges to successful and reliable operation of electric power systems. Some of the issues created by increased penetration of distributed and renewable energy sources (especially solar and wind) within power systems are caused by the stochastic nature of their energy production, i.e., frequency control and balancing issues, also power quality problems, which affect both power system real-time operation and the planning of future developments on the distribution grid as well as the transmission network level [88], [89].

While solutions to the emerging issues can be sought on the power generation, transmission or distribution side, the demand side also offers promising measures for mitigating the increasing stochasticity of power system operation [14]. Demand response (DR) has been identified as a particularly attractive tool power system operators could use for system control and management by offering incentives to consumers via so-called **explicit DR** where the DR asset owner is remunerated in either a classic direct control/interruptible load program or from an ancillary service/capacity market [12], [90], [91]. Furthermore, indirect encouragement of consumers to adapt their behaviour for overall power system benefit by their voluntary exposure to electricity real-time prices or some other price-based programs via **implicit DR** can bring some effect in coupling consumption patterns to generation availability [92], [93].

There are several benefits DR can bring to the system, e.g., provision of ancillary services, contingency management, price volatility reduction, investment cost deferral etc. [14], [91], [37]. While, in general, this topic is widely studied in recent literature in the context of the ongoing transition to the Smart Grid paradigm [12], there is nevertheless still some uncertainty in terms of DR implementation. Small individual loads do not have much influence on the overall system operation, hence their control has to be aggregated to reach the required minimum balancing power bid size. This is usually done by an aggregator which is an entity that pools together the flexibility resources of several consumers and offers them to a marketplace or an operator directly [95].

While the reserve and regulating power markets do offer new and exciting possibilities for small consumers to participate in developing DR markets, the insufficiently clear rules regarding resource aggregation provide an apparent obstacle [14], [96]. Luckily, the situation is improving and policy-makers and power system operators throughout Europe are working on more efficient utilisation of potential DR resources. For instance, it is increasingly viewed as an important and underutilised asset in the Baltic region [97] that could help to improve the energy independence and diversify the flexibility resources offered on the Baltic balancing market [98]. Moreover, the EU Clean Energy Package also calls for the involvement of demand-side resources in all electricity markets.

How widespread DR implementation can influence the operation of electric power systems is a subject already extensively studied in the literature. While there are some associated risks identified (e.g., pronounced rebound effects with time-varying electricity prices [99]), most sources come to the conclusion that DR programs have the capability to reduce the overall power supply costs [100]–[103]. However, the economic effect of DR on the DR asset owners (i.e., householders or businesses with flexible load) is paid somewhat less attention to, some notable work being presented in [103]–[107]. Furthermore, in some cases, current market structures and incentives seemingly either fail to provide meaningful economic benefit to DR asset owners or only result in minuscule profitability [93], [96], [108], [109].

On the one hand, for electricity end-users to become interested in DR provision, they need to be aware of the potential benefit they can gain. On the other hand, proper incentives need to be introduced for customers to participate in DR programs. However, the modelling of DR operation required for economic feasibility evaluation is quite complicated. An important issue which should not be neglected is load recovery when consumers change their consumption patterns in the hours following a DR event [110]. Another peculiarity arises when modelling the flexibility potential of a consumer and uncertainties related to it [111]. Uncertainty is also a factor concerning the stochastic behaviour of prices in electricity markets and system imbalances. To that end, Monte Carlo simulations have proven to be an effective approach to handle modelling uncertainties [112]. Based on the above-mentioned considerations, a bespoke tool was developed to aid the potential DR providers in assessing the benefits from their participation in a DR program or electricity market.

4.2. Methodology

For assessment of DR economic potential from the DR asset owner's perspective, a software tool was developed using the MATLAB scripting environment [113]. The tool, *DR Assess*, establishes the potential economic benefit the owners of controllable load assets might achieve should they agree to participate in a DR program, for example, by having their load remotely reduced or increased to meet system balancing needs, thus providing explicit DR. Development of *DR Assess* tool was commissioned by the Latvian TSO, "Augstsprieguma tīkls" AS, within the research contract work "Development of mathematical models for economic assessment of demand-side flexibility resources and activation optimisation of balancing reserves". Elaboration of *DR Assess* took place during 2017/2018.

The main computational principle of this software lies in a Monte Carlo simulation-based approach for modelling the activations of DR and the related cash flows within a full year of the asset's operation. Consequently, the output of the model is in the form of probability distributions instead of one deterministic result as implying absolute certainty would be unreasonable when considering future processes.

The sequence of operations performed during a model run can be broadly summarised by the following steps:
1) day-ahead electricity market price scenario generation;
2) balancing market liquidity and price scenario generation;

3) balancing activation simulation carried out according to the consumer model and the generated scenarios;
4) annual economic assessment of DR profitability.

The tool is implemented via a number of software modules which are described in more detail in the following subsections.

4.2.1. Input module

The overall setup of the model is based on the expected market conditions for DR operation in the Baltic states. The input settings necessary to run the developed assessment model are primarily divided into four categories.

I. Firstly, there are parameters which provide an <u>economic description of the DR asset and contractual conditions</u> of its owner:

- asset **service life** (years) which serves as the timeframe for the NPV and IRR calculation;
- **discount rate** – the annual percentage decrease in the future value of the calculated benefits (note: in this application, it is assumed that [discount rate] ≈ [interest rate] – [price inflation] to consider both the discount (interest) rate and electricity price inflation);
- **capital expenditure** (CAPEX) to enable asset's participation in system balancing (€), e.g., remote control hardware or software, broadband installation etc.;
- annual **fixed operating expenditure** (F-OPEX) to maintain the DR provision ability (€), e.g., additional bandwidth maintenance, related service fees etc.;
- **variable operating expenditure** (V-OPEX) arising from DR operations. This parameter allows reflecting the cost for shifted production process or cost of comfort loss. To better accommodate each specific case study, the user can indicate this cost in one of the three different approaches:
  - **€/kWh (of DR affected load)** – an energy volume-based expense which depends on the amount of consumption changed due to DR disregarding the energy recovery process occurring after DR;
  - **€/kWh (of unrecovered load)** – an energy volume-based expense which depends on the amount of consumption <u>not recovered</u> following a DR event (unrecovered load occurs if the recovery factor is other than 1);
  - **€/activation** – an energy-independent expense based solely on the number of times the DR has been activated;
- **minimum balancing price** for consumption reduction and **maximum balancing price** for consumption increase (either fixed €/MWh or % from the energy purchase price) – parameters to establish the bid price limits of the DR asset's participation in the balancing market;
- a binary variable to establish if the owner of the DR asset itself is a **balance responsible party** (BRP) or not, which significantly changes how the cash flows are modelled. In short, a BRP purchases electricity at wholesale and has to ensure that the actual

consumption matches the planned as close as possible, else imbalance settlements have to be made. On the contrary, a non-BRP consumer pays only for the actually consumed (metered) energy and does not need to compensate any imbalance;

- an option to select how the **energy purchase price** (€/MWh) is modelled:
  - only day-ahead price Π_{da}^t (available for both a BRP and a non-BRP),
  - day-ahead with markup in the form $k_1 \cdot \Pi_{da}^t + k_2$ (available for both a BRP and a non-BRP),
  - fixed price derived from the simulated mean day-ahead price plus a markup: $k_1 \cdot \sum_{t=1}^{T} \Pi_{da}^t \big/ T + k_2$ (available only for a non-BRP),
  - scenario-independent general fixed price (available only for a non-BRP);
- optional **transfer price** which is the price the DR asset **aggregator** pays to the balance responsible supplier for causing an imbalance in its portfolio in case of load reduction. This setting is only available if the DR asset owner is a non-BRP;
- **share of the TSO payment** for load reduction which is passed on to the DR asset owner (%); implying that the rest of the remuneration is received by the aggregator, BRP or another unspecified party.

II. Secondly, a <u>technical description of the DR asset's hourly load and its flexibility</u> has to be provided. This can be done either for a typical day or a typical week if applicable and with up to four distinct profiles to capture seasonality (i.e., the modelled year can be divided in four three-month periods).

As the DR activations are modelled with an hourly resolution, the most important parameters here are:

- the maximum permitted **number of DR events** in a day or week;
- the minimum **time distance** between any two DR events (hours);
- load **flexibility direction** for balancing (reduce, increase, both);
- minimum and maximum **duration of a DR event** (hours);
- maximum duration before **load recovery** (hours);
- load recovery **factor** (coefficient, where 1 implies that all the load reduced/increased during a DR event has to be recouped (increased/reduced) in the following hours.

The meaning of these settings is better explained in Fig. 4.1, where green colours denote a DR event and red – the recovery.
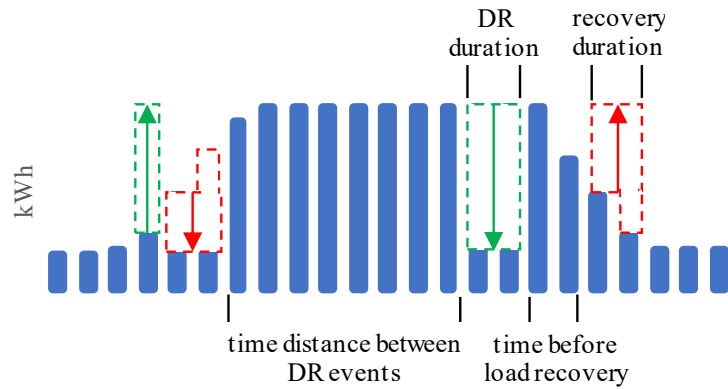
Fig. 4.1. Explanation of some of the DR modelling terms used.

Note that the distance between two events is the time between the end of last recovery and beginning of the next DR activation. The area ratio between the green and red figures depends on the recovery factor, which can be selected different for the load increase and load reduction DR events. The **hourly load profile** with hourly **upwards** and **downwards flexibility** concludes the full technical description of the DR asset.

III. Thirdly, there are settings concerning the <u>generation of day-ahead price scenarios</u> (Fig. 4.2):

- expected **mean price** (€/MWh) for the normally distributed hours;
- expected **ratio** between the mean **weekday** and **holiday** price;
- expected **ratio** between the mean **day** and **night** price (night defined as 22:00–6:00);
- expected **minimum price** (€/MWh);
- expected **maximum price** (€/MWh) for the normally distributed hours.

For each scenario, these parameters are drawn from a **normal distribution**. Two more parameters ensure that the resulting price distributions more closely follow the **skewness with right tail** traditionally observed in electricity wholesale spot prices:

- percentage of hours where **peaks outside the normal distribution** occur;
- the expected **maximum of such peaks** (€/MWh).

All the above-mentioned parameters for price generation additionally have **individually selectable standard deviations** to ensure better controllability of the price scenario generation mechanism.

	Expected value		Std dev
MEAN 99.5%	34.34	€/MWh	10%
MEAN weekday / MEAN holiday	1.22		10%
MEAN day / MEAN night	1.38		10%
MIN 100%	3	€/MWh	10%
MAX 99.5%	130	€/MWh	10%
MAX 100%	200	€/MWh	10%
% of hours with PEAKS	0.5%		10%

Fig. 4.2. Settings for DA price scenarios (screenshot from *DR Assess*).

IV. Finally, certain input parameters are needed to model the <u>balancing market scenarios</u>:

- **expected balancing market liquidity** (percentage of hours within a year when the power system operator seeks to activate the manual frequency restoration reserves (mFRR); in general, the balancing market can have demand for either upward or downward balancing or no demand for balancing within an hour);

- upper and lower **bounds of the market liquidity** to ensure that in none of the scenarios generated the liquidity is drawn from outside this range;

- **ratio of negative imbalance hours** from all the hours with system balancing.

For those hours when balancing is required, the balancing price scenarios are drawn based on the previously generated day-ahead prices. The additional settings controlling the generation of balancing price scenarios are:

- the expected **ratio** of hourly **balancing price vs day-ahead price** separately for negative and positive system imbalance;

- probability of **extraordinarily high** balancing price **peaks**;

- the maximum **ceiling** for extraordinary balancing prices (€/MWh).

4.2.2. Day-ahead price scenario generation

The input parameters described in the previous subsection related to the day-ahead prices are used to generate a pre-selected number of hourly day-ahead price scenarios for a whole year. The day-ahead price generation algorithm proceeds as follows.

1. From a normal distribution, draw price generation settings for each particular scenario (mean, min, max, ratios etc.) using the expected values and standard deviations read from the input parameters.

2. For each scenario s, ensure that the drawn mean, min and max settings are not contradictory.

3. For each hour category within each scenario, calculate a coefficient $k_{..}^s$ necessary to enforce the weekday/holiday and day/night ratios ($R_{w/h}^s$ and $R_{d/n}^s$) for weekday nights (4.1), weekday daytime (4.2), holiday nights (4.3) and holiday daytime (4.4) where $\Pi_{da}^{s,avg}$ is the drawn mean day-ahead price in scenario s:

$$k_{w,n}^s = \frac{R_{w/h}^s \cdot \Pi_{da}^{s,avg} \Big/ \left(2/7 + 5/7 \cdot R_{w/h}^s\right)}{1/3 + 2/3 \cdot R_{d/n}^s};\tag{4.1}$$

$$k_{w,d}^s = R_{d/n}^s \cdot \frac{R_{w/h}^s \cdot \Pi_{da}^{s,avg} \Big/ \left(2/7 + 5/7 \cdot R_{w/h}^s\right)}{1/3 + 2/3 \cdot R_{d/n}^s}\tag{4.2}$$

$$k_{h,n}^s = \frac{\Pi_{da}^{s,avg} \Big/ \left(2/7 + 5/7 \cdot R_{w/h}^s\right)}{1/3 + 2/3 \cdot R_{d/n}^s};\tag{4.3}$$

$$k_{h,d}^s = R_{d/n}^s \cdot \frac{\Pi_{da}^{s,avg} \Big/ \left(2/7 + 5/7 \cdot R_{w/h}^s\right)}{1/3 + 2/3 \cdot R_{d/n}^s}.\tag{4.4}$$

4. For each hour t in each scenario s, generate day-ahead price $\Pi_{\text{da}}^{s,\text{avg}}$ (4.5), while ensuring it does not violate scenario minimum and maximum restrictions (4.6):

$$\Pi_{\text{da}}^{s,t} = \max\left[N\left(k_t^s, \frac{\Pi_{\text{da}}^{s,\text{avg}} - \Pi_{\text{da}}^{s,\text{min}}}{3} \right), \Pi_{\text{da}}^{s,\text{min}} \right]; \tag{4.5}$$

$$\Pi_{\text{da}}^{s,t} = \min\left[\Pi_{\text{da}}^{s,t}, \Pi_{\text{da}}^{s,\text{norm max}} \right]. \tag{4.6}$$

5. Smoothen the generated time series with a moving average filter with a span of five elements (hours).
6. Enforce the expected mean on the smoothened price:

$$\Pi_{\text{da}}^{s,t} = \frac{\Pi_{\text{da}}^{s,t} \cdot \Pi_{\text{da}}^{\text{exp,avg}}}{\displaystyle\sum_{s=1}^{S}\left(\sum_{t=1}^{T} \frac{\Pi_{\text{da}}^{s,t}}{S \cdot T} \right)}. \tag{4.7}$$

7. Finally, in each scenario, for $k_{\text{extra peak}}^s$ (%) of hours add an increased price event:

$$\Pi_{\text{da}}^{s,t} = \Pi_{\text{da}}^{s,t} + \Pi_{\text{da}}^{s,\text{extra max}} - \Pi_{\text{da}}^{s,\text{norm max}}. \tag{4.8}$$

4.2.3. Balancing market liquidity and price scenario generation

The balancing market liquidity and price scenarios are generated as follows.
1. For each scenario, draw the balancing market liquidity (% of hours where TSO might request DR) parameter from a normal distribution.
2. Ensure that the drawn values respect the upper and lower bounds; if they do not, replace the value with the violated bound.
3. Since the model runs with hourly resolution, each hour when there is a demand in the balancing market has to be assigned either direction – upwards or downwards balancing.
4. Generate upwards and downwards balancing prices for each hour in each scenario:

$$\Pi_{\text{bal, up}}^{s,t} = \Pi_{\text{da}}^{s,t} \cdot \min\left(1, N\left(R_{\text{up/da}}, \left(R_{\text{up/all}} - 1 \right) \big/ 3 \right)\right); \tag{4.9}$$

$$\Pi_{\text{bal, dwn}}^{s,t} = \Pi_{\text{da}}^{s,t} \cdot \max\left(1, N\left(R_{\text{dwn/da}}, \left(1 - R_{\text{dwn/all}} \right) \big/ 3 \right)\right). \tag{4.10}$$

5. Combine the two timeseries for each scenario as per the hourly imbalance direction to obtain one balancing timeseries per scenario.
6. Add the extraordinarily high balancing price peaks according to the probability set in the Input module.

4.2.4. Balancing activation simulation

When all the required day-ahead electricity market price and balancing market scenarios have been generated, they can be paired to simulate the activation of balancing reserves. All the created Monte Carlo scenarios are assigned equal realisation probabilities.
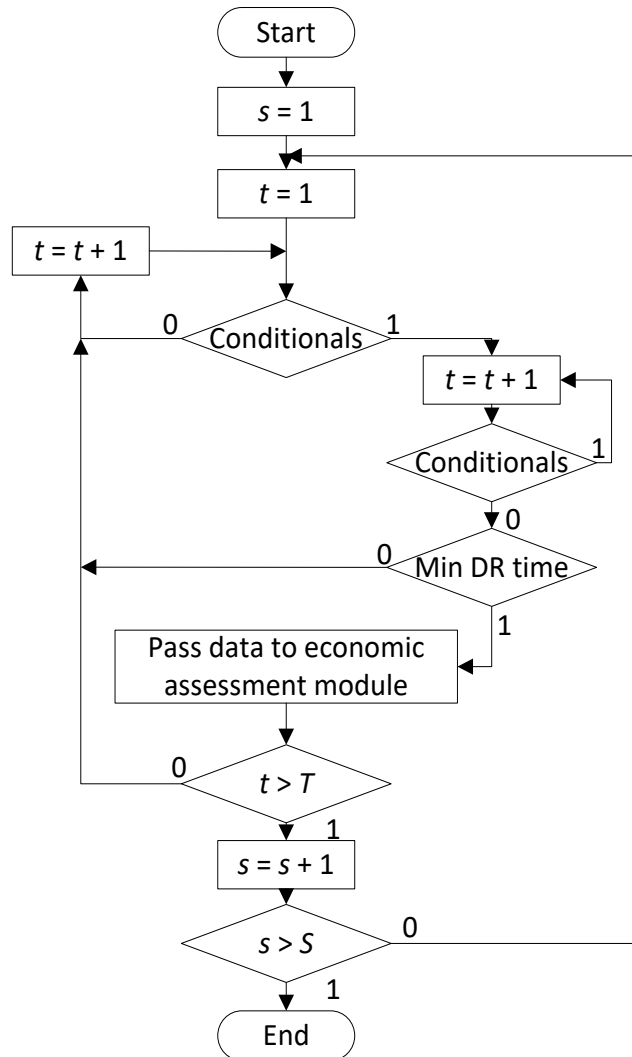
Fig. 4.3. Simplified visualisation of the DR activation simulation algorithm.

The purpose of this module is identifying the hours when the modelled DR asset can participate in balancing and when the energy recovery post-DR takes place. The program iterates through each scenario sequentially checking each hour to test if activation conditions are met. The overall DR activation simulation algorithm in a simplified manner is summarised in Fig. 4.3.

In the **first conditional test block**, all of these conditions have to be met:

- the minimum time distance since the previous DR activation is respected;
- the number of DR activations in the current day/week does not exceed the limit;
- there is demand for balancing reserves in the system coinciding with the direction the DR asset owner is willing to provide services in (load reduction/increase);

- the DR asset has flexibility in the particular direction during the particular hour;
- the balancing price falls within the DR asset's bid limits;
- there is enough flexibility in the following hours for DR energy recovery while respecting the max duration before load recovery constraint (only relevant if the load recovery factor is nonzero).

During the subloop with the **second conditional block**, it is tested if the duration of the DR event can be increased to more hours (the same conditions are checked with an additional test against the max duration of a DR event variable). Finally, it is checked whether the potential DR event duration meets the minimum limit.

Afterwards, if a DR event has been identified, information about it is passed on to the economic assessment module.

4.2.5. Short-term economic assessment

The formulae (4.11)–(4.16) are used to calculate the cash flows associated with a simulated DR event. They depend on the direction of the DR-induced load change and the balance responsibility status of the DR asset owner. The benefit is derived by contrasting the cash flows with and without DR. Beforehand, however, the energy purchase price timeseries are produced as mentioned in Section 4.2.1.

Variable tDR denotes the set of hours when the DR event takes place and, consequently, $trec$ denotes the set of hours when the recovery takes place. Since, theoretically, the DR event and recovery can span multiple hours, the multiplications in the following equations are implied to be matrix operations.

<u>Benefit from load reduction</u> if the DR asset owner is a <u>BRP</u> is composed from the income from the sold balancing energy (at balancing prices) and expenditure for recovery energy (at balancing prices):

$$B_{\mathrm{BRP}}^{\mathrm{red.}} = E_{\mathrm{DR}}^{s,tDR} \times \Pi_{\mathrm{bal}}^{s,tDR} - E_{\mathrm{rec}}^{s,trec} \times \Pi_{\mathrm{bal}}^{s,trec}. \tag{4.11}$$

<u>Note</u>: in equations (4.11)–(4.24) the variables $E_{\mathrm{DR}}^{s,tDR}$ and $E_{\mathrm{rec}}^{s,trec}$ contain the **absolute values** of the DR and recovery energy respectively, i.e., they do not contain information on the process direction, which instead is handled by heuristically choosing the appropriate equation. This is an effect of the program realisation and the mathematical description could easily be transformed to be more general. Nevertheless, the reader should be advised that the respective variables for demand response energy (4.12) and recovery energy (4.13) can be generally expressed as:

$$E_{\mathrm{DR}}^{s,tDR} = \frac{1+d}{2} \cdot \left| E_{\mathrm{DR.incr.}}^{s,tDR} \right| + \frac{1-d}{2} \cdot \left| E_{\mathrm{DR.red.}}^{s,tDR} \right|, \tag{4.12}$$

$$E_{\mathrm{rec}}^{s,trec} = \frac{1+d}{2} \cdot \left| E_{\mathrm{rec.incr.}}^{s,trec} \right| + \frac{1-d}{2} \cdot \left| E_{\mathrm{rec.red.}}^{s,trec} \right|, \tag{4.13}$$

where $d = -1$ for load reduction DR event and $d = 1$ for load increase DR event.

Benefit from load increase for a BRP depends on the expense for the procured balancing energy during the DR event and income from sold balancing energy during the recovery:

$$B_{\text{BRP}}^{\text{incr.}} = -E_{\text{DR}}^{s,tDR} \times \Pi_{\text{bal}}^{s,tDR} + E_{\text{rec}}^{s,trec} \times \Pi_{\text{bal}}^{s,trec} . \tag{4.14}$$

For a DR asset owner who is <u>not balance responsible</u>, the <u>benefit from load reduction</u> derives from the income from sold balancing energy, savings from load reduction during the DR event (at retail purchase price since, unlike BRP, the owner has no obligation to balance their portfolio) and expense for recovery energy (at purchase price):

$$B_{\text{nonBRP}}^{\text{red.}} = E_{\text{DR}}^{s,tDR} \times \left(\Pi_{\text{bal}}^{s,tDR} + \Pi_{\text{pp}}^{s,tDR} \right) - E_{\text{rec}}^{s,trec} \times \Pi_{\text{pp}}^{s,trec} . \tag{4.15}$$

Finally, for a <u>non-BRP</u>, the <u>load increase</u> cash flow components are the expense for procured balancing energy (at balancing price) and the savings from load reduction in the recovery phase (at purchase price):

$$B_{\text{nonBRP}}^{\text{incr.}} = -E_{\text{DR}}^{s,tDR} \times \Pi_{\text{bal}}^{s,tDR} + E_{\text{rec}}^{s,trec} \times \Pi_{\text{pp}}^{s,trec} . \tag{4.16}$$

The benefit from load reduction and/or increase is contrasted to the fixed and variable OPEX to establish the overall benefit from participation in DR in each scenario throughout the whole year.

Furthermore, for the ease of understanding the different cash flow sources, additional effort was made to partition and represent graphically the total net annual revenue in four main components listed below (for an illustration of this division see Fig. 4.32 and Fig. 4.33):

1) *balancing market* → the benefit arising directly from the balancing market (i.e., the received payment for the balancing energy or the difference in costs of purchasing electricity normally vs at the balancing prices). Expressions for load reduction (4.17) and load increase (4.18) DR:

$$B^{\text{red., bal. mar.}} = \left(\Pi_{\text{bal}}^{s,tDR} - a \cdot \Pi_{\text{pp}}^{s,tDR} \right) \times E_{\text{DR}}^{s,tDR} , \tag{4.17}$$

$$B^{\text{incr., bal. mar.}} = \left(\Pi_{\text{pp}}^{s,tDR} - \Pi_{\text{bal}}^{s,tDR} \right) \times E_{\text{DR}}^{s,tDR} , \tag{4.18}$$

where the binary variable a denotes the BRP status of the DR asset owner (1 = yes and 0 = no);

2) *saved energy* → the benefit (or expense) arising from the efficiency increase (or decrease) observed during demand response events. Expressions for load reduction (4.19) and load increase (4.20) DR:

$$B^{\text{red., s. en.}} = \left(1 - k_{\text{rec}}^{\text{red.}} \right) \cdot E_{\text{DR}}^{s,tDR} \times \Pi_{\text{pp}}^{s,tDR} , \tag{4.19}$$

$$B^{\text{incr., s. en.}} = \left(k_{\text{rec}}^{\text{incr.}} - 1 \right) \cdot E_{\text{DR}}^{s,tDR} \times \Pi_{\text{pp}}^{s,tDR} ; \tag{4.20}$$

3) *price fluctuation* → the benefit (or expense) arising from the price differentials during the recovery phase compared to the time of the DR event. Expressions for load reduction (4.21) and load increase (4.22) DR:

$$B^{\text{red., p. fluct.}} = \left(\Pi_{\text{pp}}^{s,tDR} - a \cdot \Pi_{\text{bal}}^{s,trec} - (1-a) \cdot \Pi_{\text{pp}}^{s,trec} \right) \times E_{\text{DR}}^{s,tDR} \cdot k_{\text{rec}}^{\text{red.}} , \tag{4.21}$$

$$B^{\text{incr., p. fluct.}} = \left(a \cdot \Pi_{\text{bal}}^{s,trec} - (1-a) \cdot \Pi_{\text{pp}}^{s,trec} - \Pi_{\text{pp}}^{s,tDR} \right) \times E_{\text{DR}}^{s,tDR} \cdot k_{\text{rec}}^{\text{incr.}} , \tag{4.22}$$

where coefficient $k_{\text{rec}}^{\text{red.}}$ and $k_{\text{rec}}^{\text{incr.}}$ is the load recovery factor after DR activation;

4) *F+V OPEX* → the fixed (input) and variable (calculated according to the selected OPEX type) operating expenses related to participation in DR (C_{opex});

5) *total* → the sum of the previous four revenue and cost components (*balancing market + saved energy + price fluctuation – F+V OPEX*):

$$B^{\text{sum}} = B^{\text{red., bal. mar.}} + B^{\text{red., s. en.}} + B^{\text{red., p. fluct.}} + B^{\text{incr., bal. mar.}} + B^{\text{incr., s. en.}} + B^{\text{incr., p. fluct.}} - C_{\text{opex}} . \tag{4.23}$$

Important note on the influence of the TSO payment share coefficient, k_{share}, and transfer price settings. If the TSO payment share coefficient setting is below 100% and/or the selected transfer price is nonzero for a non-BRP, the compensation received by the asset owner for load reduction DR (income from sold balancing energy) is decreased as follows:

$$E_{\text{DR}}^{s,tDR} \times \Pi_{\text{bal}}^{s,tDR} \rightarrow E_{\text{DR}}^{s,tDR} \cdot k_{\text{share}} \times \left(\Pi_{\text{bal}}^{s,tDR} - \Pi_{\text{transf}}^{s,tDR} \right) . \tag{4.24}$$

This transformation accordingly changes the variable $\Pi_{\text{bal}}^{s,tDR}$ in equations (4.11), (4.15) and (4.17) .

4.2.6. Long-term economic assessment

The modelling outcome from the one-year run is extrapolated to further years for the whole service life of the DR asset (*y* years) by applying the previously selected discount rate *d*. Several widely used investment assessment metrics are calculated in this step, such as the net present value (NPV), internal rate of return (IRR) and payback period (PP).

The **NPV** calculation is carried out according to:

$$NPV = -CAPEX + \sum_{y=1}^{\substack{\text{asset} \\ \text{service life}}} \frac{B_y^{\text{sum}}}{(1+d)^y} . \tag{4.25}$$

The **IRR** is found by solving the $NPV = 0$ equation for the discount rate *d* as the variable.

The **PP** is found by increasing the *NPV* equation's iterand *y* up to a point where the *NPV* first becomes **positive**.

Note: it is assumed the initial investments (CAPEX) are made at year 0 and the asset starts participating in DR at year 1.

Once the long-term assessment is finalised, the calculation results are summarised and output to figures and data tables.

The tool *DR Assess* has been used for the economic assessment of DR-enabled smart electric heating, assessment of the influence of flexibility modelling parameters as well as for

analysis of the impact of implicit DR on the provision of explicit DR. The results are presented in three distinct case studies below.

4.3. Case study I: participation of residential DR in balancing market

This section presents the first case study performed with the *DR Assess* tool. The model tackles uncertainties in electricity market prices and system imbalance by employing Monte Carlo simulations. While the model provides vast customizability options, this case study is focused on the potential demand response benefits for a particular type of consumer with smart electric thermal storage. It is found that participation of DR in the balancing market can be economically feasible for the asset owner, but on the condition that sufficient proportion of the balancing remuneration is shared with the owner by the aggregator.

4.3.1. Assumptions

The case study aims to apply our developed software tool for the economic assessment of smart electric thermal storage (SETS) participation in DR. The subject of the study is a hypothetical household having five SETS devices at their disposal with 2.2 kW input power and 15.4 kWh storage capacity each. The owner is not balance responsible and is willing to participate in both upward and downward DR (which requires the SETS equipment to never be disconnected from the outlet and the gateway). We assume the asset service life is 15 years, discount rate – 3%, CAPEX – 200 € (to cover gateway costs) and annual F-OPEX – 20 € (service and other related costs). For simplicity sake, it is implied for now the householder purchases electricity at wholesale price. It is also assumed that the aggregator passes on to the DR asset owner the full amount of TSO payments for load reduction (however, the effect of this assumption will be explicitly addressed).

In regard to the **load profile and flexibility,** we set a maximum number of 14 DR activations per week but do not restrict the time between them. In this study, we do not allow for multi-hour DR events. Maximum duration before load recovery is set to 12 hours and the recovery factor is set to 0.9 both for load reduction and increase (this implies some energy savings in case of load reduction and some wasted energy in case of increase).

The seasonal heating demand data is derived from building thermal modelling presented in Chapter 2, where it was seen that the overall heating demand in summer, spring and autumn is approximately 10%, 50% and 20% of the winter demand respectively. Consequently, we assume that, in summer, there is one SETS unit that charges 2..5 hours a day, can be disconnected anytime during the charging and another unit can be turned on whenever necessary.

In autumn, one SETS unit charges for the full seven hours but can be disconnected at request; the other remaining units can be switched to charging when necessary. In winter, four of the five units are in full operation; in spring – two, in either case, the operational units can be switched off and any idle units – set to charge.

An example of the load profile and flexibility settings for a winter week is shown in Fig. 4.4. By default, the SETS is designed to charge during the first seven hours of the day (00:00–06:59) at 0.8 pu[8] power (since only four of the five units are used). During the charging hours, it has some flexibility in both directions: load increase by 0.2 pu, decrease by 0.8 pu. Starting from hour 8, only the load increasing flexibility remains.

The actual load profile, however, depends on the DR events experienced (if any) and the subsequent recovery after DR. This is illustrated by weekly charts in Fig. 4.5 and daily charts in Fig. 4.6.
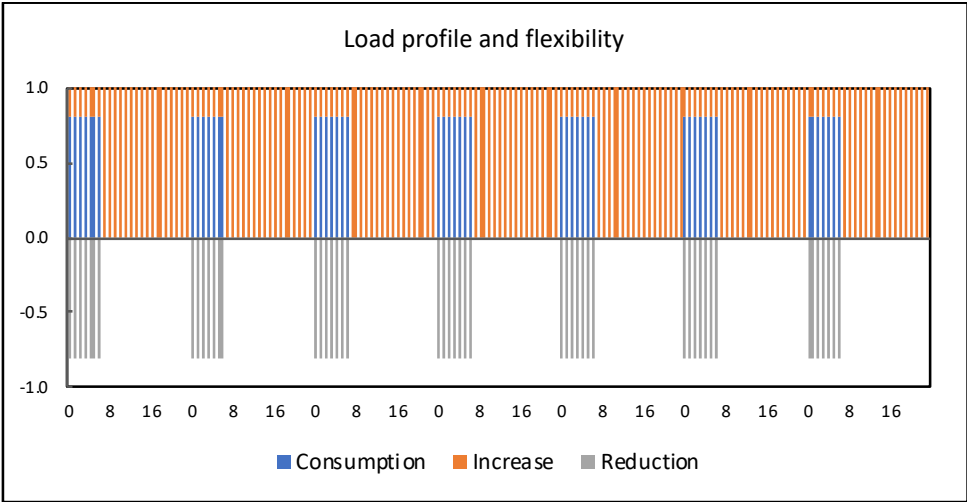
Fig. 4.4. Load profile and flexibility settings for SETS in a winter week (vertical axis: power, pu; horizontal axis: hour of day).
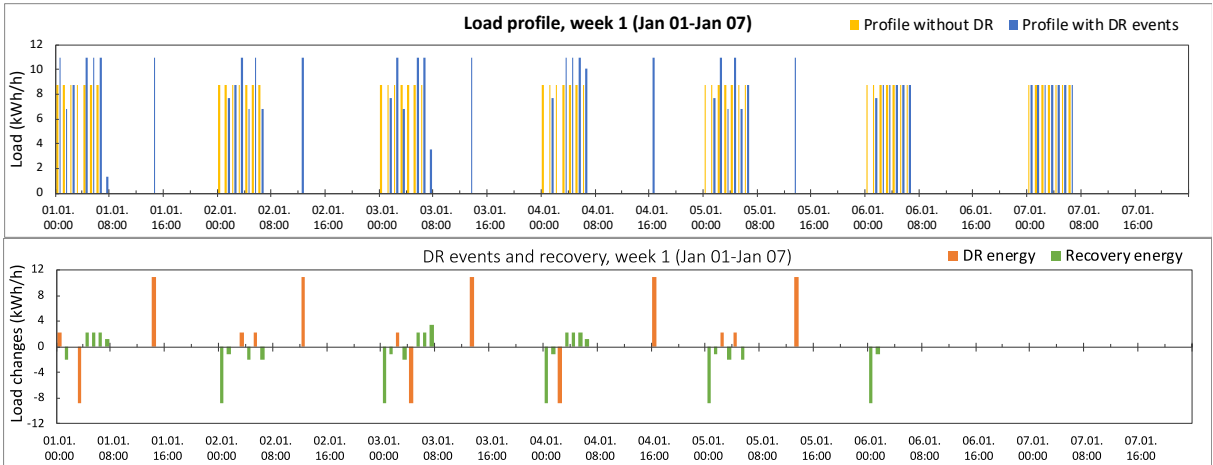
Fig. 4.5. Simulated load profile with/without DR and DR events of SETS in a selected week.

---

[8] pu – per unit from the rated power. In this case, 0.8 pu = 0.8 x 2.2 x 5 = 8.8 kW.
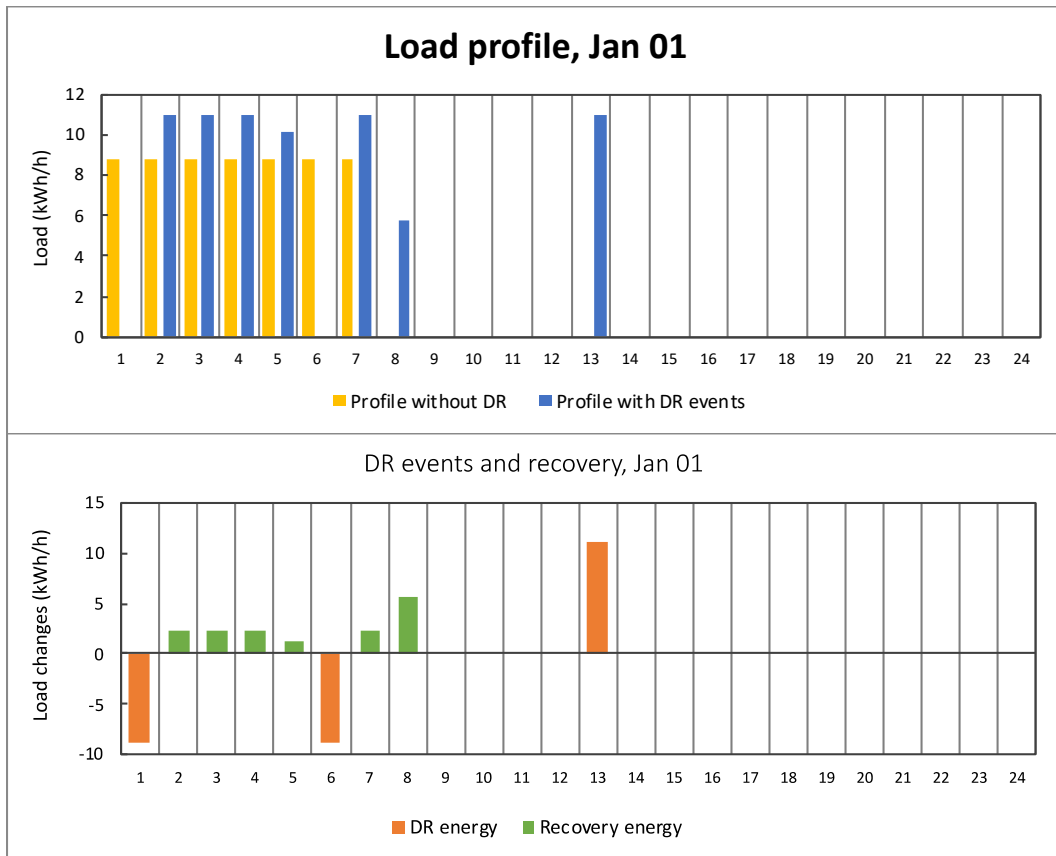
Fig. 4.6. Simulated actual load profile and DR events of SETS in a selected day.

The **day-ahead price** scenario generation settings for this case study were derived from the analysis of the Nord Pool Latvian bidding area prices during the period of 01.06.2017–31.05.2018. Expected mean price for 99.5% of hours is 37.75 €/MWh, expected maximum price for 99.5% of hours – 119.5 €/MWh, expected ratio between the mean weekday and holiday prices – 1.25, expected ratio between mean daytime and nighttime prices – 1.44, expected minimum price – 1.59 €/MWh, expected rare maximum – 255 €/MWh. A total of 1000 price scenarios are generated.

The balancing scenario settings were derived from the common Baltic balancing market data (the market was launched on 01.01.2018). The expected balancing market liquidity is 64.97%, the ratio of negative vs positive imbalance hours – 0.44, the expected balancing price during positive system imbalance – 0.58 pu from the day-ahead price, the expected balancing price during negative system imbalance – 1.49 pu from the day-ahead price. Zero extraordinary balancing price events are assumed.

The generated hourly day-ahead market and balancing prices across all the thousand scenarios are summarised in Fig. 4.7.
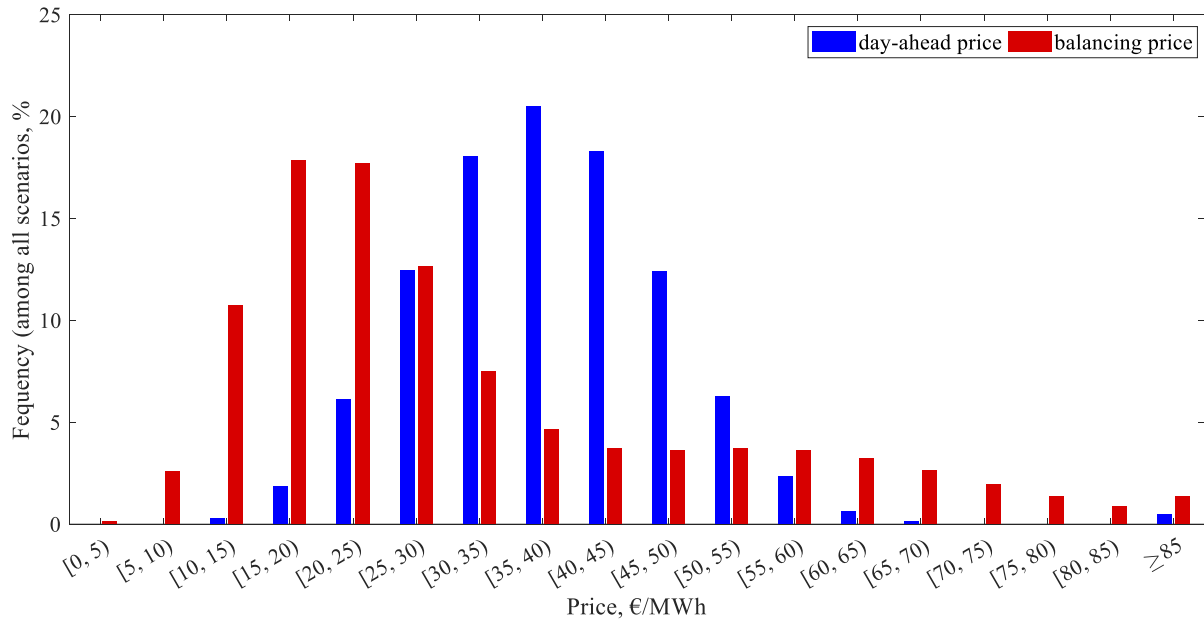
Fig. 4.7. Day-ahead and balancing market price histograms.

4.3.2. Results and discussion

Though the simulation results imply there have been much more DR activations for load increase than for load reduction (on average, 452 times for increase and 199 for reduction, see Fig. 4.8), Fig. 4.9 suggests that the reduction operations have been overall more economically beneficial (scenario average of 46.50 € vs 12.71 €). This is also reflected in the specific benefit in respect to provided DR energy – on average, mere 3.92 €/MWh for increase vs 49.80 €/MWh for reduction (Fig. 4.8). It can primarily be explained by two factors, the additional positive cash flow component in case of load reduction (Fig. 4.9) and the initially assumed load recovery factor 0.9 for both directions, which implied that load increase DR is slightly wasteful in terms of energy consumption.
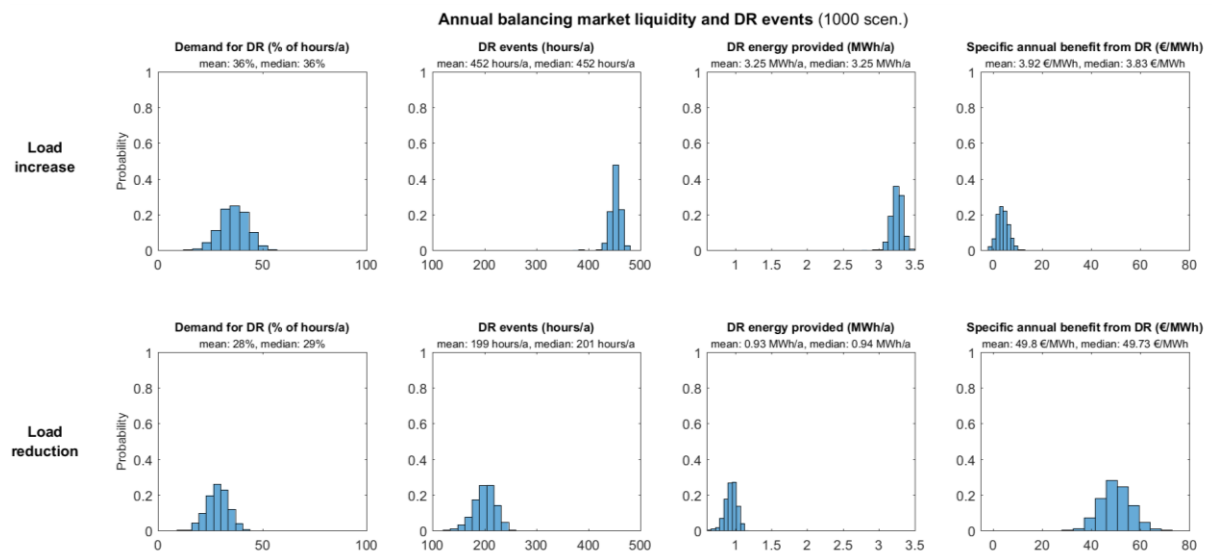
Fig. 4.8. Summary of the annual demand for DR, simulated DR events and benefit thereof.

114

While the average NPV is at 268.10 €, Fig. 4.9 and Fig. 4.10 nevertheless show that there are some scenarios (3.6%) where the NPV is still negative at the end of the selected service life (15 years). The average IRR is 17.56%. The average payback period is thus 7.23 years while the median is 6 years, which signals that the outlier scenarios are likely skewing the mean. Indeed, Fig. 4.11 shows that some of the outlier scenarios have not reached payback even by year 20.

Nevertheless, while an expectable 268.10 € benefit accumulated during a 15-year period is not necessarily very enticing for a whole household to allow remote control of their heating equipment, this result does serve as valuable first insight in the assessment of the economical potential of participation in explicit DR on a dwelling level.

A note should be made, however, that the initial assumption of a household in Latvia exclusively heated by SETS devices is not strictly realistic since even conventional electric heating which could be replaced is not currently widespread in Latvia and SETS is on a significantly higher price range than conventional heaters. If the SETS device costs were also included in DR CAPEX calculations, payback would not be possible.
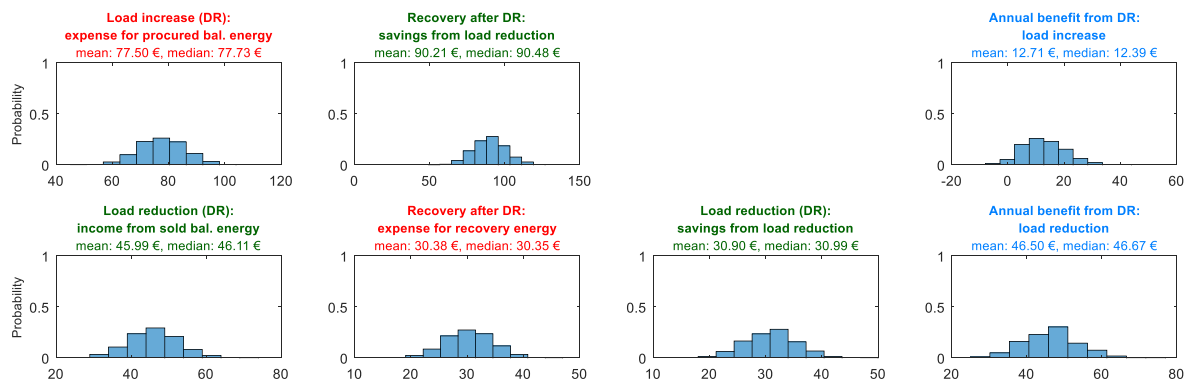
Fig. 4.9. Economic assessment for a single modelled year.
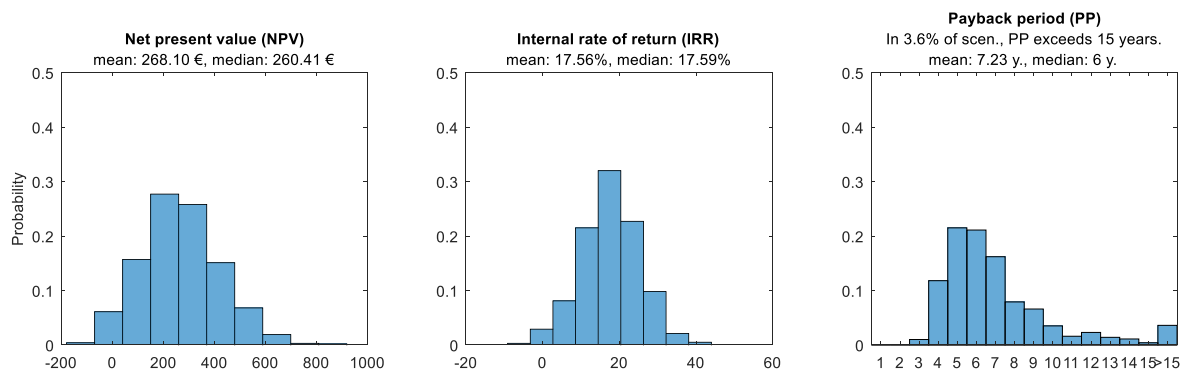
Fig. 4.10. Long-term economic assessment for the asset service life (15 years).
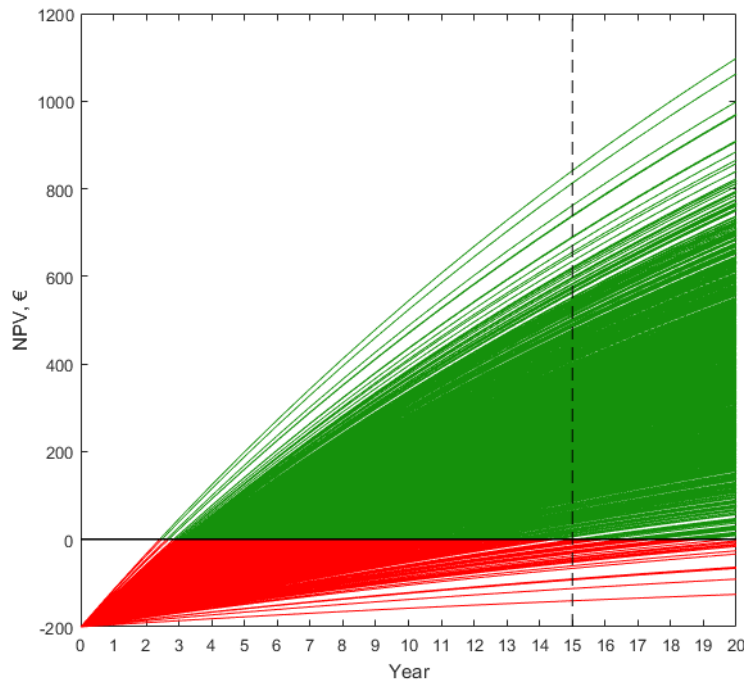
Fig. 4.11. Cumulative cash flows in all the simulated scenarios.

Impact of the payment sharing on SETS DR feasibility

Additionally, the assumption that 100% of the TSO payment for load reduction is received by the DR asset owner is objectionable. To alleviate this limitation of the study, we completed several additional model runs with all the same input data only varying the share coefficient. The results from the repeated runs are summarised in Table 4.1. Evidently, the share of TSO payment the DR asset owner receives has to be higher than 50% for the participation in an explicit DR program to be economically meaningful.

Table 4.1. Effect of benefit-sharing on DR feasibility

TSO payment share passed to the DR asset owner	Long-term assessment parameter			
	NPV, €	*IRR, %*	*PP, years mean / med.*	*% of scenarios where payback not achieved*
100%	268.10	17.56	7.2 / 6	0.0
90%	209.37	14.57	8.5 / 7	0.0
80%	149.28	11.32	11.2 / 8	0.0
70%	101.08	8.57	15.1 / 10	0.7
60%	35.43	4.37	22.9 / 13	2.0
50%	–6.85	1.47	30.0 / 16	3.4

4.4. Case study II: sensitivity analysis of DR resource modelling parameters

To incentivise residential-scale customer participation in explicit DR, it has to be possible to provide them with a sufficiently accurate assessment of the potential economic benefits they might gain from it. However, such an assessment necessarily requires good knowledge of the technical flexibility of the consumption and parameters characterising it. To that end, the

116

authors of [111] offer an empirical methodology to obtain a full probabilistic characterisation of residential consumers' flexibility. Their approach is based on quantile regression, but the findings suggest that there is potentially very high variability between different individual flexibility profiles. Furthermore, it is strongly dependent on factors like the number of occupants, baseline consumption and even the education level of consumers.

A flexibility indicator to be extracted from aggregate residential customer load patterns is proposed in [114]. It is found there that the flexibility levels become more prominent with a decrease in customer aggregation. The authors of [107] also propose a specific parameter – flexibility ratio, which represents the average degree of flexibility in shifting an appliance within its operating time window. These studies, as well as [105], [106], [109] strive in favour of a stochastic approach to demand flexibility assessment and DR modelling.

In this case study, the *DR Assess* tool is used to analyse the impact of various flexibility characteristics and constraints. It is found that some of them significantly affect the results, whereas others have minuscule influence. The case study analysis, based on a typical consumption profile of a DR resource able to reduce its load on-demand, allows concluding that a householder without significant thermostatic loads has relatively small economic benefit from participation in explicit DR.

One of the main assumptions (and input parameters in *DR Assess* tool) in modelling a specific DR resource is the load **recovery factor**. In this study, it is defined as the ratio between the recovered energy and the DR energy. Essentially, this expresses energy savings (or conversely, efficiency losses) the customer achieves as a result of providing DR. Thus, the impact this setting has on the simulations is evident and it is not warranted to perform sensitivity analysis on it. The impact of several other flexibility modelling settings is, however, worth assessing. Therefore, **sensitivity analysis** is performed for the following settings:

- the minimum time distance between DR events;
- the maximum time before load recovery;
- the maximum number of DR events in a week;
- the minimum duration of a DR event;
- the maximum duration of a DR event;
- consumption flexibility (the percentage change of the hourly consumption which can be incurred due to DR activation or post-DR recovery).

The sensitivity analysis is carried out by repeated model runs wherein all the case study input data and model settings remain unchanged, except for the parameter to be analysed, which is, instead, varied in a certain range. The impact of each parameter is thus assessed by comparing the simulation results, both the total economic benefit from DR and the specific benefit per unit of energy served in DR.

4.4.1. Assumptions

Statistical parameters for **day-ahead price** scenario generation are derived from the historical prices in the Latvian bidding area of Nord Pool during the last 12 months at the time of performing these calculations – 01.11.2017–31.10.2018. Price scenarios are generated based

on the following indicators: minimum price 1.59 €/MWh, the 99.5th percentile 100.06 €/MWh, maximum price 255.03 €/MWh, mean of the values up to the 99.5th percentile 45.81 €/MWh, mean ratio of weekday and weekend prices 1.21, mean ratio of daytime and nighttime prices 1.39. Subsequently, these are set as the scenario expected values with a 10% standard deviation for all of them.

The balancing market liquidity and balancing price generation settings are derived from the statistics of the common Baltic balancing market from 01.01.2018 until 31.10.2018. Expected balancing market liquidity for mFRR is 63.08% (i.e., demand for mFRR is expected in 63.08% of hours per year), ratio of hours with negative vs positive system imbalance 0.49, expected ratio of the day-ahead price vs balancing price at positive system imbalance (surplus) is 0.64 and at negative system imbalance (shortage) 1.87.

Furthermore, we assume that the **DR asset** owner is exposed to a dynamic retail tariff equal to the day-ahead price and affixed renewable support, trade commission and grid tariff components amounting to a total of 62.91 €/MWh fixed addition to the varying day-ahead price. Besides that, a value-added tax (21%) is applied to the total sum of tariff components. Moreover, being a residential customer, the DR asset owner itself is not a balance responsible party.

Since the subject of this study is not a particular DR-enabled technology, we utilise an anonymised aggregated load profile of residential end-users from smart meter data library [62]. Since the *DR Assess* tool allows for the representation of four distinct weekly load profiles, we generate different load profiles with the mean hourly consumption values (Fig. 4.12) and scale them to a maximum hourly consumption of 2 kWh, representative of an average-sized residential household in Latvia.
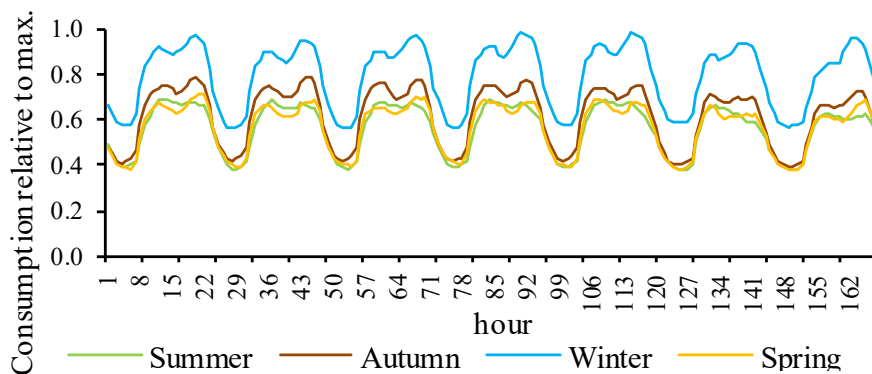
Fig. 4.12. Weekly consumption profiles in different seasons.

The flexibility at each hour is set in a simplistic manner by selecting a percentage from the hourly consumption which can be reduced for DR or increased for load recovery, the latter of which is constrained by the maximum consumption. Thus, instead of simulating specific home appliances (e.g., large thermostatic loads), we assume some flexibility in the overall consumption profile. Unlike the previous case analysis, this study only considers load reduction DR, as it is a more realistic scenario for householder-scale DR. Thus, a portion of the total load is considered delayable. Furthermore, 10% energy savings during explicit DR activation are

assumed, or, in other words, the recovery factor is set to 0.9, implying that not all of the consumption reduced during DR has to be recouped afterwards. This way we can model an effect resembling both load shifting and shedding, respecting the consumer flexibility bounds.

4.4.2. Results and discussion

Base case

For the base case, let us test how profitable such an explicit DR program for power system balancing (mFRR) would be to a consumer with the assumed load (Fig. 4.12) and seemingly adequate flexibility modelling settings: minimum time distance between DR events – 0 (unconstrained); maximum time before load recovery – 12 hours; maximum number of DR events in a week – 14; minimum duration of a DR event – 1 hour; maximum duration of a DR event – 1 hour; consumption flexibility – 5%. The results of a model run with 1000 Monte Carlo simulations are summarised by probability distributions in Fig. 4.13 and Fig. 4.14.
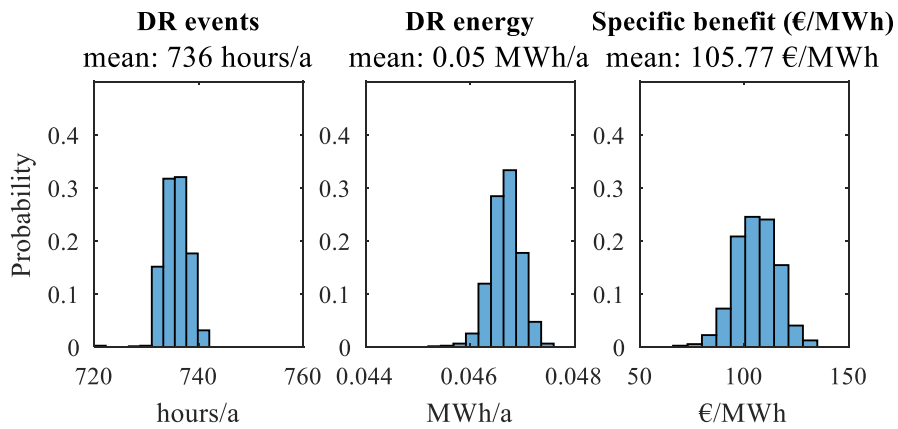
Fig. 4.13. Probability distributions of simulated DR activations (*base case*).
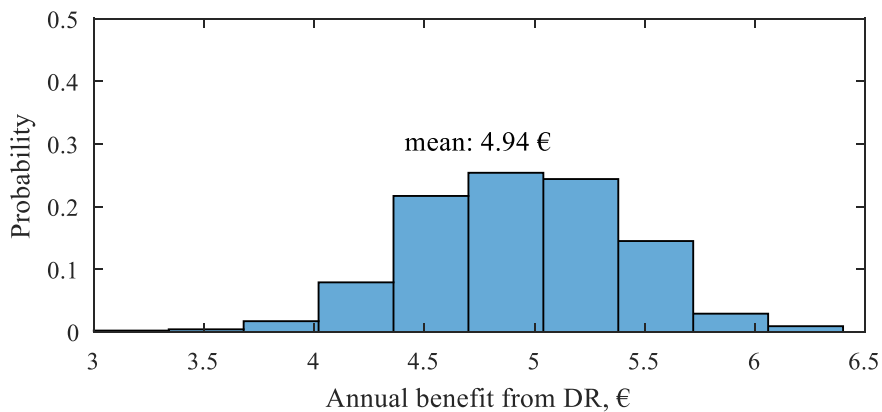
Fig. 4.14. Probability distribution of the DR asset owner's annual benefit (*base case*).

Evidently, in the base case, participation in explicit DR program provides a very small benefit to the DR-enabled asset's owner. Furthermore, this calculation does not account for any variable or capital expenditure necessary to implement and maintain the DR capability. However, this is in line with some previous studies where the benefit from DR to residential

load was estimated in single digits (e.g., 1 €/annum for 2% load shifting or 6.5 €/annum for 15% load shifting in [93]).

Furthermore, the energy provided to the TSO for balancing purposes is fairly small with the mean being only about 50 kWh annually. However, while such an amount of energy, of course, does not noticeably aid in power system balancing, the prior assumption was that this is only a part of a larger aggregated mFRR offer to the TSO. The scope of this case study envisions to look at the flexibility modelling and DR economic assessment issue strictly from the householder point of view, i.e., in a disaggregated manner.

Sensitivity analysis

Results of the sensitivity analysis are summarised in Fig. 4.15 to Fig. 4.20, wherein the points corresponding to the base case are marked by a red cross. The average annual benefit in the simulated scenarios is portrayed with a blue line, whereas the average specific benefit per unit of energy served as DR for power system balancing is illustrated with an orange line.

Evidently, increasing the required minimum time distance between two explicit DR activations tends to decrease the annual benefit obtainable (Fig. 5). However, this effect is not so pronounced with the constraint values from 0 to 5 hours (with corresponding resulting benefit from 4.97 € to 4.88 €), beyond which the profitability starts to decrease more obviously. This can seemingly be explained by two factors. Firstly, the actual number of DR activations also decreases rapidly if the constraint is above 5, thus resulting in less total energy served in DR. Secondly, as the average specific benefit line portrays, the DR energy becomes less valuable the higher the constraint is. In fact, two distinct cases can be observed: if the minimum time distance constraint is in the range of [0; 5], the average specific benefit is roughly 106.00 €/MWh, whereas in the range [9; 24] it is about 102.29 €/MWh.
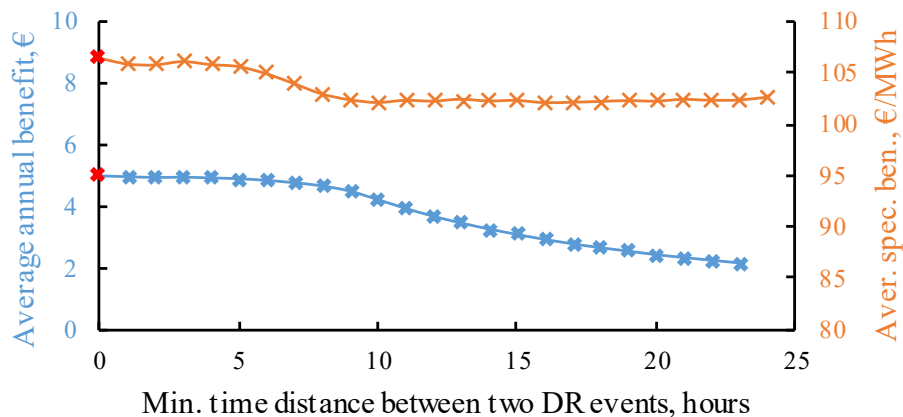
Fig. 4.15. Sensitivity of model results to min time between DR events.

As can be seen in Fig. 4.16, the constraint for the maximum time before load recovery does not have a noticeable effect on either of the simulation result indicators. This is likely explained by the fact that the modelled consumption mostly always had sufficient flexibility in the direction opposite to DR in the next few hours following the DR event. Thus, the recovery effect could always start right after the DR event itself. In fact, this suggests that this constraint should be redefined to limit the time for completion of the recovery effect as opposed to the

beginning of it. This would likely be far more useful in DR flexibility modelling, but a further study is necessary to confirm this assertion.
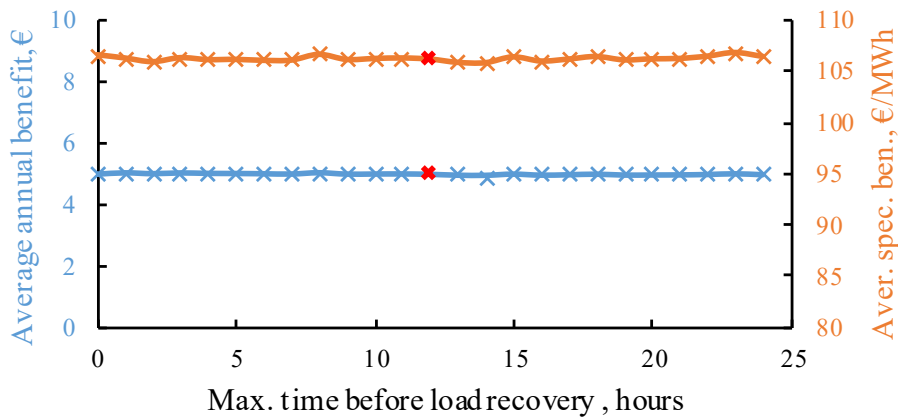
Fig. 4.16. Sensitivity of model results to max time before recovery.

On the other hand, the next parameter analysed, the maximum number of DR events in a week, shows a lot clearer and straightforward picture (Fig. 4.17). Indeed, the more DR activations are allowed, the more remuneration is received resulting in an almost linear curve for the annual benefit. Evidently, this constraint is always active in the simulations, effectively designating the number of activations to be modelled. This arises from the fact that almost every modelled activation provides a net positive benefit even if it is minuscule. If variable costs were taken into account and reflected in the bid price, the activations would be performed less often.

The specific benefit per unit of DR energy served (Fig. 4.17) also rises with a higher maximum number of DR events allowed in a week. However, it seemingly saturates at about 4 events a week already. If relatively few activations are allowed, the likelihood increases of them being carried out in suboptimal time.
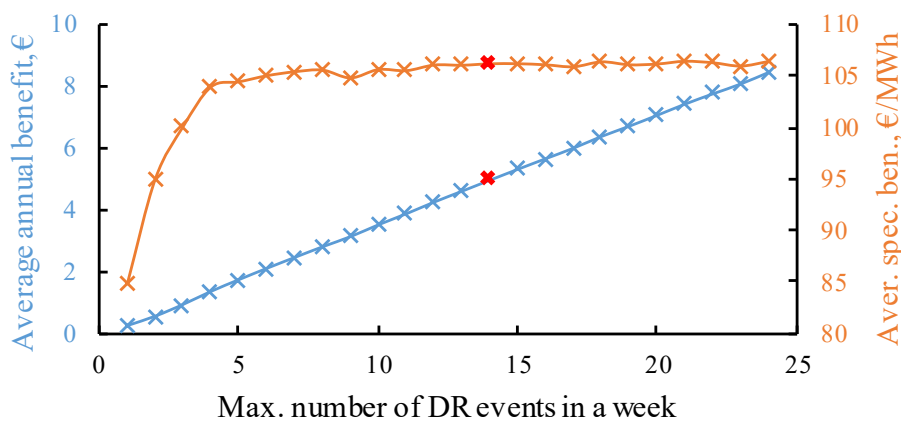
Fig. 4.17. Sensitivity of model results to max activations a week.

The impact of the next two parameters, minimum and maximum duration of a DR event, is summarised in the surface charts, Fig. 4.18 and Fig. 4.19. It should be noted however that values of these constraints exceeding 1 are not realistic in the Baltic balancing market mFRR framework, but instead can denote hypothetical future purpose-specific flexibility markets for long-duration DR. Evidently, the most profitable case is when the minimum constraint is set to

2 hours and the maximum to 5 (Fig. 4.18). Conversely, the specific benefit is the highest when the minimum constraint is set to 1 and the maximum to 5 (Fig. 4.19). On the one hand, the wide temporal range of the DR event duration allows to increase the prospective profitability of DR; however, the longer a DR event is, the longer also the recovery period will be exposing the asset owner to more price volatility risks. The minimum DR event duration of 2 hours provides the best overall benefit likely because it balances the aforementioned long duration price variability risks with the overall higher DR energy that can be served compared to the case where the minimum duration is 1 hour but the number of activations per week limit remains the same. Thus, higher amounts of balancing energy provided by DR result in improved overall benefit despite lower specific benefit per balancing energy provided.
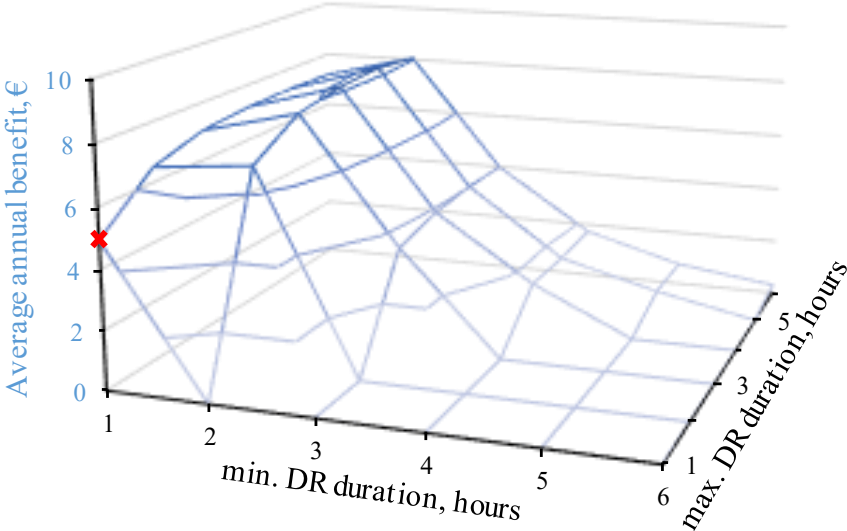
Fig. 4.18. Annual benefit depending on DR event duration constraints.
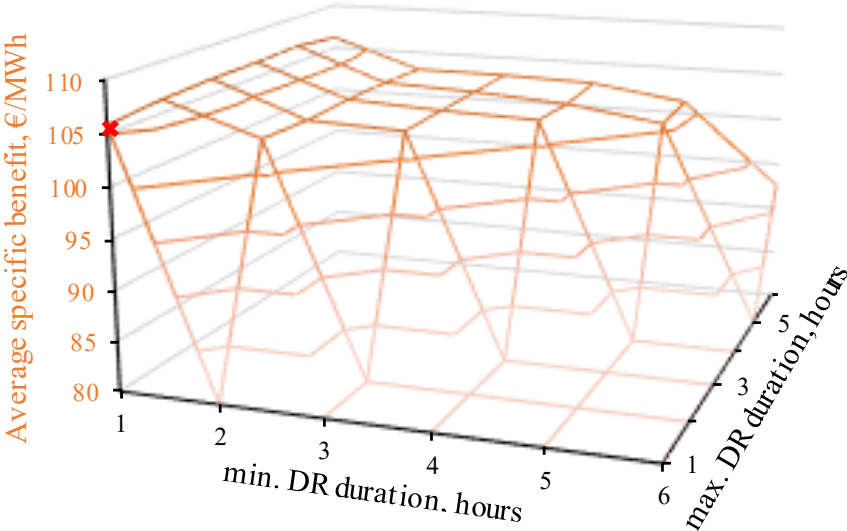
Fig. 4.19. Specific benefit depending on DR event duration constraints.

Finally, the last flexibility modelling parameter analysed, the percentage of total consumption offered to DR, shows a nearly linear characteristic (Fig. 4.20). It follows that the more flexibility a DR-ready consumer offers, the more overall profitability they can expect. Of course, flexibility above the 5–15% mark is hardly realistic for a household, unless a significant part of their consumption comes from large thermostatic loads (e.g., electric heating) that have controllability potential. Nevertheless, these results being as expected aids in validating the overall performance of the model.
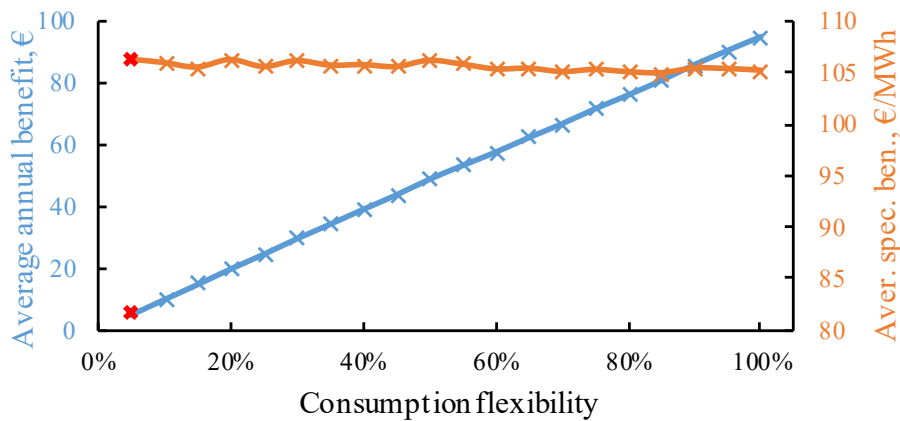
Fig. 4.20. Sensitivity of model results to consumption flexibility.

4.5. Case study III: analysis of the potential benefits from participation in explicit and implicit DR

Participation of DR in ancillary services (i.e., explicit DR), which was the focus of two previous case studies, is not the only way to benefit from load controllability. Implicit DR, when consumers voluntarily adjust their consumption according to external price signals (e.g., optimising load schedule as per hourly electricity prices), can also provide notable benefit [93], and the entry barriers are significantly smaller, e.g., no definitive need for aggregation. Technical capability to reschedule load and incentivising tariff structure are the only requirements for implicit DR.

Therefore, the final case study performed with the *DR Assess* tool is focused on analysing the profitability of participation in both explicit and implicit DR from the perspective of the owner of flexible load assets on a householder level. Furthermore, it is tested whether price-based optimisation of the flexible consumption schedule negatively affects the ability and profitability of participation in explicit DR, particularly focusing on the balancing market. The investigation, based on DR-enabled smart electric thermal storage heaters, allows concluding that implicit DR does not necessarily hinder the ability to provide ancillary services to the power system. Instead, it adds a supplemental benefit to the asset owner. Besides, an investigation on the "optimal" number of Monte Carlo scenarios to be used is carried out and some considerations regarding the bidding strategy of the DR asset owner are provided.

4.5.1. Methodology for assessing the benefit from implicit DR

For assessment of the potential benefit obtainable from participation in **explicit DR** programs for system balancing, the methodology introduced in section 4.2 is employed. The benefits from explicit DR thus are calculated using equations (4.11)–(4.24). However, it is reasonable to assume that a consumer possessing some amount of consumption flexibility would primarily be interested in taking advantage of the time-varying electricity prices. For this purpose, the DR economic potential assessment model has been enhanced with the ability to assess also the benefit from **implicit DR** (i.e., purchasing electricity at dynamic hourly prices which are known the day before) as shown in Fig. 4.21.

Electricity day-ahead price scenario generation
⇩
Day-ahead rescheduling
⇩
Balancing market liquidity & price scenario generation
⇩
Balancing activation simulations
⇩
Annual economic assessment
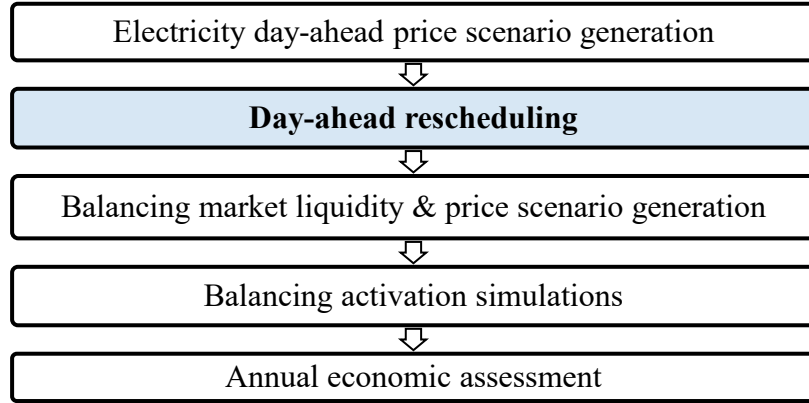
Fig. 4.21. *DR Assess* algorithm structure with implicit DR.

In essence, sequential day-ahead optimisation is performed for the whole year with the objective to minimise electricity purchase costs:

$$\sum_{t=1}^{24} \left(E_{\text{cons}.t}^{\text{unopt.}} + \Delta E_t \right) \cdot \Pi_{\text{ret}.t} \rightarrow \min, \tag{4.26}$$

subject to

$$E_{\text{flex}.t}^{\min} \leq \Delta E_t \leq E_{\text{flex}.t}^{\max}, \tag{4.27}$$

$$\sum_{t=1}^{24} \Delta E_t = 0, \tag{4.28}$$

where $E_{\text{cons}.t}^{\text{unopt.}}$ – the original, unoptimised energy consumption at hour t;

ΔE_t (the optimisation variable) – the change in hourly consumption for cost minimisation;

$\Pi_{\text{ret}.t}$ – electricity retail price at hour t, and $E_{\text{flex}.t}^{\min}$;

$E_{\text{flex}.t}^{\max}$ – the lower (load reduction) and upper (load increase) bounds on the available consumption flexibility at each hour.

The constraint (4.28) ensures that the total daily consumption remains unchanged. The optimisation problem (4.26)–(4.28) is clearly linear and can be solved with a simple linear programming approach. For that, the MATLAB interior-point algorithm is used (with a switch

to the slightly more time consuming dual-simplex algorithm for the edge cases the previous algorithm fails to resolve).

When the day-ahead price-based rescheduling is modelled, the flexibility profiles available for balancing are readjusted accordingly before performing explicit DR activation simulations. The overall consumption flexibility bounds remain the same, while the load profile is changed as per the results of the price-based optimisation. The annual benefit from implicit DR is estimated by contrasting the consumed electricity costs with and without rescheduling. For both explicit and implicit DR, the resulting annual benefit is obtained in the form of probability distributions, since it accounts for all scenario results. Thus, the scenario mean is the expected benefit.

4.5.2. Required number of scenarios

The results of the model and their credibility strongly depend on the number of Monte Carlo simulations performed. However, evaluating a high number of scenarios can demand significant computational resources. Thus, a compromise between precision and evaluation time has to be found.

Fig. 4.22 illustrates the differences in results of model runs with a varied number of scenarios (ten runs with each number to distinctly illustrate the dispersion of results). The green dots represent the deviation of each model result (expected benefit) from the overall average. The violet line, however, represents the mean calculation time of the runs.
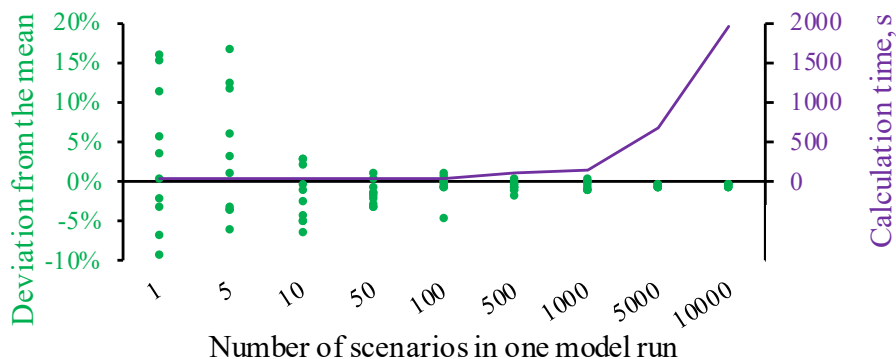
Fig. 4.22. Trade-off between calculation time and precision.

Evidently, 1000 scenarios are sufficient. They provide satisfactory low deviations (the highest value within the test runs – 1.31%) while still providing reasonable computational time (~153 seconds on an ordinary desktop computer). More simulations need significantly higher computational effort.

4.5.3. Assumptions for the case study

The case study is based on **thermostatic load**, which has been identified in the literature as one of the most promising load types for residential DR applications [115]–[117]. Particularly, we model **smart electric thermal energy storage devices** (introduced in Chapter 2) able to receive external control signals (e.g., from an aggregator). The rated input power of each device

is 2.2 kW, and, similarly to case study I, we assume a household with five units installed. The default behaviour (no gateway connection) envisions electricity consumption (i.e., storing thermal energy) in the first hours of each day, as the good thermal insulation of heaters allows the heat to be released when necessary throughout the day. Variable OPEX is disregarded in this study, but fixed OPEX is set to 20 € per annum.

Four different consumption and flexibility profiles for a week are used in the study to capture seasonal differences (the year is divided into four 3-month seasons). Heat energy demand is derived from building thermal modelling results in Riga, Latvia, suggesting that the average heat demand in spring is about 50% of the winter load, autumn – 20%, summer – 10%. In terms of flexibility, we assume that any idle heater units can be turned on and any working units switched off for one hour up to 14 times a week if there is enough flexibility in the opposite direction for recovery to be completed within the next 12 hours. Summer is an exception – we assume that only one additional heater unit can be turned on for load increase DR. The model has hourly resolution, and DR event duration is also set to one hour. The recovery effect is characterised by $k_{\text{rec}}^{\text{incr.}} = 0.9$ and $k_{\text{rec}}^{\text{red.}} = 0.9$, i.e., load increase DR results in slightly wasted energy, whereas load reduction DR manifests some energy savings.

The **day-ahead price** scenario generation is based on statistics in the Latvian price area of Nord Pool (01.11.2017–31.10.2018) and is summarised in Table 4.2. A 10% standard deviation is set to these parameters during scenario generation.

Table 4.2. Day-ahead price scenario expected parameters

Day-ahead price scenario parameter	Expected value
Minimum price	1.59 €/MWh
Mean price (for 99.5% of hours)	45.81 €/MWh
Maximum price (for 99.5% of hours)	100.06 €/MWh
Maximum price (for 100% of hours)	255.03 €/MWh
Mean weekday and weekend price ratio	1.21
Mean daytime and nighttime price ratio	1.39

Parameters for **balancing market** scenarios are derived from the common Baltic balancing market data (01.01.2018–31.10.2018) and summarised in Table 4.3. The parameters from both tables are used to generate scenarios as per the algorithm described in Section 4.2.

Table 4.3. Balancing market scenario expected parameters

Balancing liquidity and price scenario parameter	Expected value
Balancing market liquidity (hours w demand for DR)	63.08%
Negative vs positive hourly system imbalance ratio	0.49
Balancing vs day-ahead price (at positive imbalance)	0.64
Balancing vs day-ahead price (at negative imbalance)	1.87

The owner of the flexible load purchases electricity for its regular consumption at a **dynamic retail price** defined as $\Pi_{\text{ret}.t} = 1.21 \cdot \left(\Pi_{\text{DA}t} + 62.91 \right)$ which is a representative electricity retail tariff in Latvia at the time of conducting this study (November 2018) composed of the hourly day-ahead wholesale price $\Pi_{\text{DA}t}$, trade commission (4.20 €/MWh), mandatory procurement component (14.63 €/MWh), distribution tariff (44.08 €/MWh) and a 21% value-added tax on top. The consumption-independent or fixed monthly components of the tariff have been disregarded, as they would not be affected by DR.

For comparability, all the calculations within this study have been performed using the same 1000 scenarios for the day-ahead and balancing market (i.e., they have been generated only once). The distributions of the hourly prices generated are summarised in Fig. 4.23.
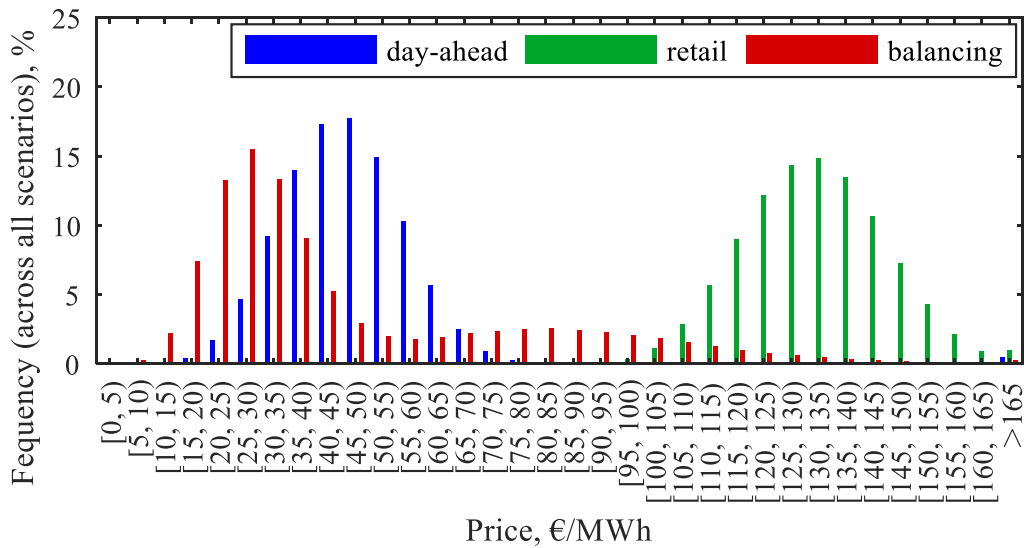
Fig. 4.23. Histogram of electricity prices.

4.5.4. Results and discussion

Considerations regarding the bidding strategy

As already mentioned in Section 4.2.1, the *DR Assess* input module contains a series of settings related to the economic description of the DR asset. This also includes defining the balancing market price thresholds at which the DR asset owner is willing to provide its services: namely, the minimum balancing price the owner wants to receive for consumption reduction (upward regulation) and the maximum balancing price it is willing to pay for consumption increase (downward regulation). Both constraints can be defined either as a fixed price (€/MWh) or as a fraction of the energy purchase price at the same hour. In practice, these constraints would be adhered to by submitting respective price-dependent bids to the balancing market.

Market participant bidding strategy within the common Baltic balancing market framework implies that, in most cases, the marginal market price a DR asset owner may receive for up-regulation is higher than the day-ahead price, while the balancing price for down-regulation is usually lower than the day-ahead price at the same hour. Nevertheless, the possible bid price

range a DR asset owner may offer to the market is broad enough. Moreover, for the DR service to be profitable, it is also important to consider the related cost due to the rebound effect during the recovery period that may follow after a DR event. Therefore, selecting the "optimal" bidding strategy for a DR asset is not a straightforward task and involves a number of different uncertainties. To tackle this, we start with using the *DR Assess* tool to determine the recommended bid price limits. Afterwards, the selected settings will be used as an input for the specific case study.

To assess what is a reasonable maximum balancing price for load-increase DR and minimum balancing price for load-reduction DR, we perform several model runs varying these parameters. Each type of explicit DR is modelled separately and two ways to select the bid price are considered – as a fixed price and as a retail price-dependent bid (Fig. 4.24–Fig. 4.27).

Evidently, with the assumption of no DR-induced variable OPEX and the retail price significantly exceeding the balancing price (Fig. 4.23), it is reasonable to set the maximum balancing price for load-increase DR activation equal to about 30% of the time-varying retail price (Fig. 4.24) or roughly 40 €/MWh (Fig. 4.25) if a fixed bid price is envisioned.
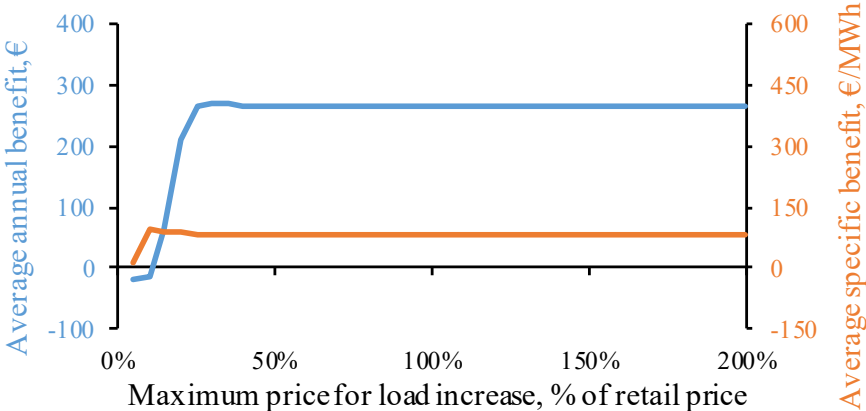
Fig. 4.24. Profitability of load-increase DR per varied bid price (% from retail price).
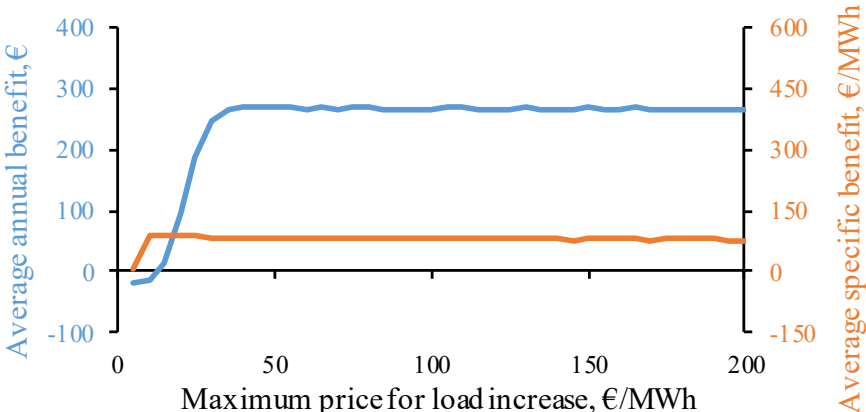
Fig. 4.25. Profitability of load-increase DR per varied bid price (fixed).

The load-reduction DR analysis presents a more peculiar situation. It follows from Fig. 4.26 and Fig. 4.27 that there is no benefit in constraining the minimum balancing price for load reduction. Although the specific benefit (disregarding fixed OPEX) per MWh of energy served

in DR is the highest at about 105% of the time-varying retail price or 200 €/MWh if a fixed bid is considered, the actual average annual benefit in these cases is close to zero or even negative if fixed OPEX is considered. This is explained by the very low explicit DR activity with these constraints. For instance, load-reduction DR is activated on average 2.7 times per annum with the 105% constraint, whereas in the unconstrained case it amounts to 472.5 times, thus the overall profitability is higher in the latter case despite significantly lower specific benefit.
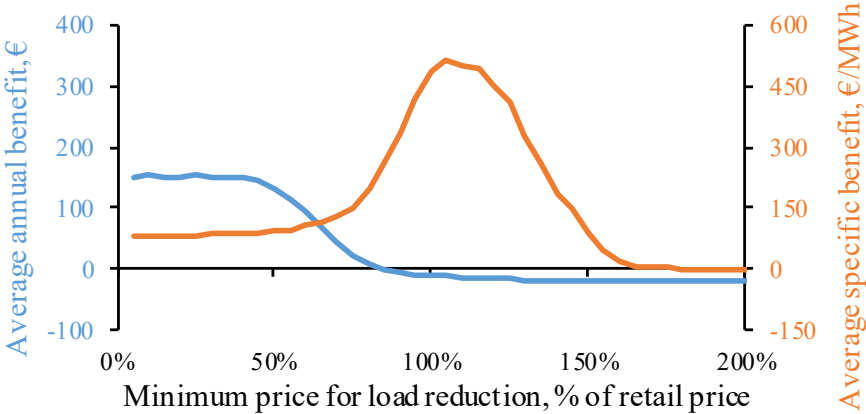
Fig. 4.26. Profitability of load-reduction DR per varied bid price (% from retail price).
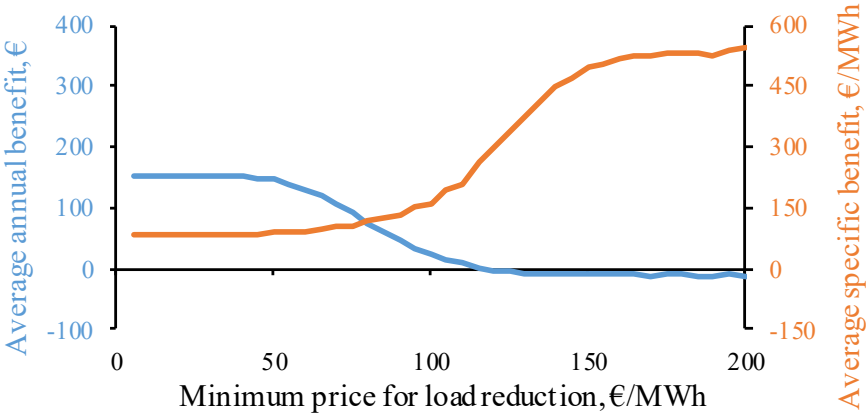
Fig. 4.27. Profitability of load-reduction DR per varied bid price (fixed).

However, if the variable OPEX induced by DR activations is taken into account, the selection of appropriate balancing price constraints for DR activation is not so straightforward anymore. Fig. 4.28 and Fig. 4.29 examines the effects of price constraint settings at various levels of variable OPEX.

Evidently, in this case study, the maximum balancing price constraint for load increase (Fig. 4.28) should be reduced when the variable OPEX is higher (e.g., to 35 €/MWh at V-OPEX of 40 €/MWh or to 30 €/MWh at V-OPEX of 70 €/MWh).
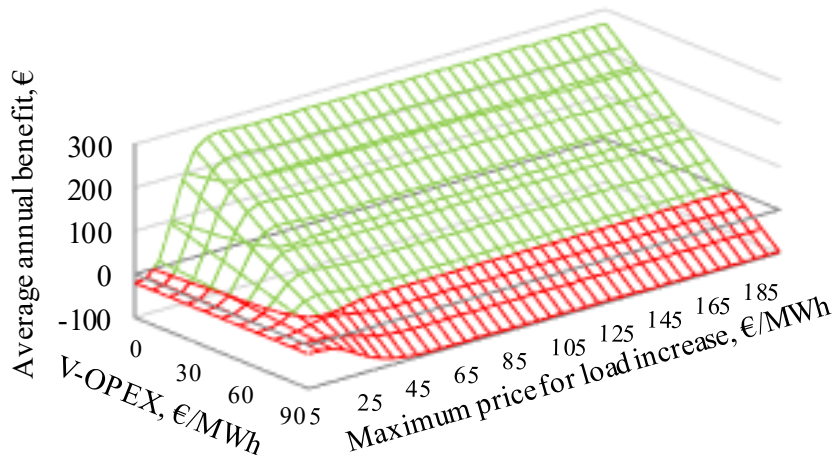
Fig. 4.28. Load-increase DR profitability per varied bid price & V-OPEX.

Similarly, the minimum balancing price for load-reduction DR (Fig. 4.29) becomes more relevant as the variable OPEX increases (e.g., 30 €/MWh at V-OPEX of 40 €/MWh or 70 €/MWh at V-OPEX of 70 €/MWh). With an accurately selected constraint, it is even possible to achieve marginal profitability at V-OPEX of 90 €/MWh (if the balancing price constraint is set to 85 €/MWh).

Since in the case study to follow the V-OPEX is disregarded, the bidding strategy is set to a 40 €/MWh ceiling for load increase and remains unconstrained for load reduction.
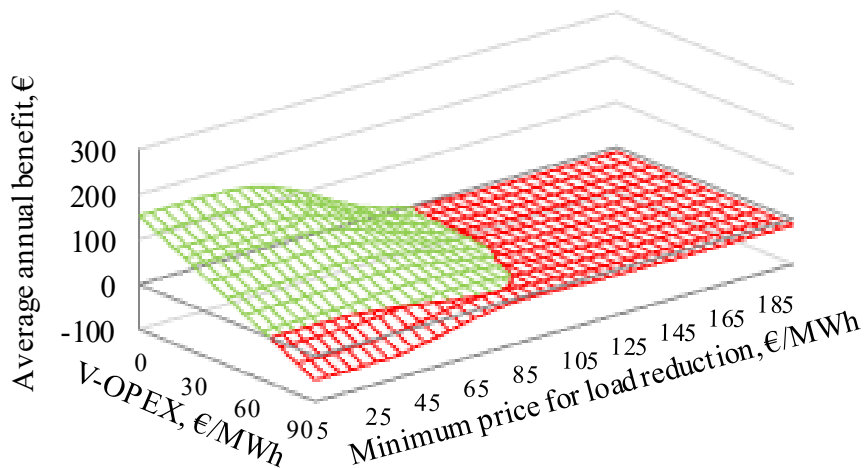
Fig. 4.29. Load-reduction DR profitability per varied bid price & V-OPEX.

Case study

This subsection presents the case study results of using smart electric thermal storage heaters for implicit and explicit DR, based on the assumptions detailed in Section 4.5.3 and employing the previously selected bid price settings for explicit DR provision in the balancing market. For comparison purposes, let us carry out two model runs. Firstly, with only explicit DR for power system balancing, assuming aggregated DR capability to participate in the mFRR market in the Baltics, and, secondly, with additional implicit DR implemented by price-based rescheduling of the consumption on a day-ahead basis, before participation in the balancing market.

Fig. 4.30 summarises the modelled scenario results in terms of the positive and negative annual cash flow positions incurred due to explicit DR activations for a case where the initial consumption has not been price-optimised. When compared to the same indicators for a case where there has been a day-ahead rescheduling performed beforehand (Fig. 4.31), three main implications can be inferred.

Firstly, the benefit from implicit DR is well comparable to that from explicit DR (e.g., 74.67 € from rescheduling, 336.16 € from balancing DR). Secondly, implicit DR does not negatively affect the profitability of participation in explicit DR but supplements it instead. Thirdly, the cash flow components directly dependent on the hourly retail price are most affected by the day-ahead rescheduling.
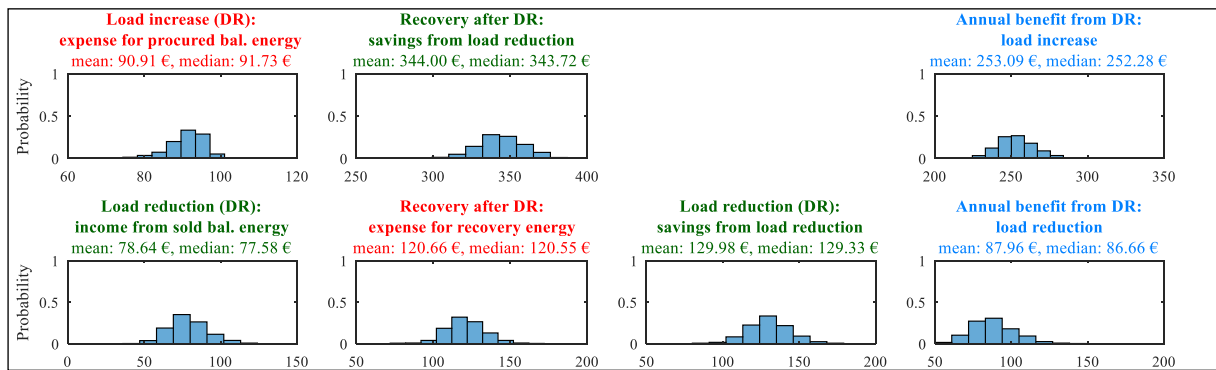
Fig. 4.30. Probability histograms of the modelled cash flow positions (red – positive, green – negative, blue – total) without day-ahead rescheduling.
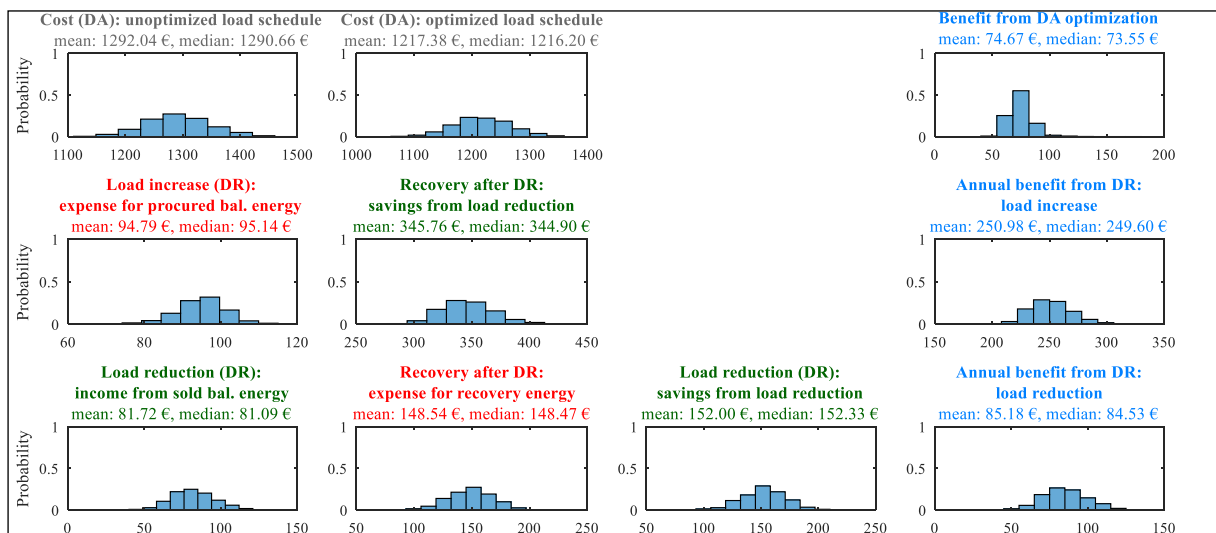
Fig. 4.31. Probability histograms of the modelled cash flow positions (red – positive, green – negative, blue – total) with day-ahead rescheduling.

The same overall explicit DR benefit can also be expressed by its different components defined in (4.17)–(4.22). Fig. 4.32 and Fig. 4.33 provides the mean values (mathematical expectation) of these indicators.

While the mean overall annual benefit from explicit DR is slightly decreased (from 321.05 € to 316.15 €) if day-ahead optimisation has been performed beforehand, the actual income from the balancing market is increased in the second case. However, it has been offset by the notably

131

higher negative effect of the price variation component. It can be explained by the greater likelihood for the recovery effect post load-reduction DR to take place during high-price hours since the initial pre-DR consumption is already placed at the cheapest hours in the second case. This becomes even more evident if we study the statistics of the modelled DR activations summarised in Table 4.4.

Even though the total number of annual DR events has decreased (from 653 to 540 events) when the underlying consumption pattern of electric thermal storage heaters has been optimised, the sum amount of energy delivered for system balancing has actually increased (from 4.17 MWh to 4.56 MWh). Presumably, this is because post-optimisation there are some hours with remaining flexibility only in one direction, and thus there are overall fewer hours when either directional DR is possible. However, the amount of flexibility in terms of energy in one direction is higher. The specific benefit per unit of energy served in explicit DR, however, is also decreased, notably so for demand reduction DR events.

If the asset owner were to incur notable variable OPEX due to energy served in explicit DR (e.g., loss of productivity, value of comfort lost etc.), the difference between both cases might become starker; however, this assertion remains to be studied. Some other significant assumptions that could influence the results is the balance responsibility of DR asset owner and prospective compensation to its retailer (for both, we assumed none), and it is also presumed that the payments to/from balancing market are equal to the respective balancing market price. If the DR asset owner were to pay additional taxes or share the benefit with its aggregator, the resulting profit would certainly be less.
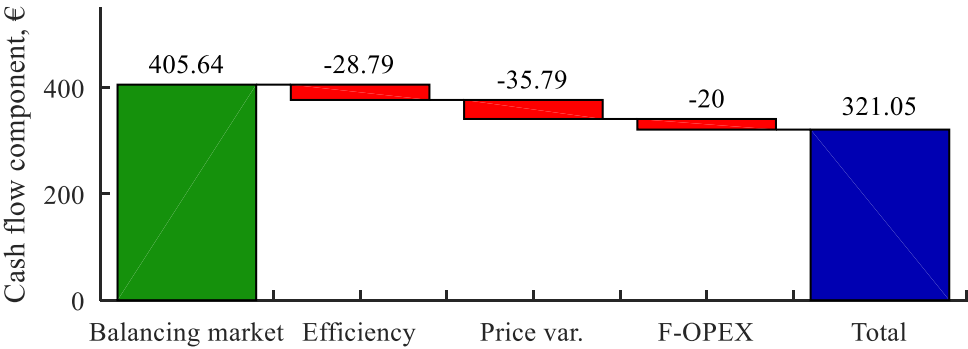
Fig. 4.32. Breakdown of the mean total benefit from explicit DR (original schedule).
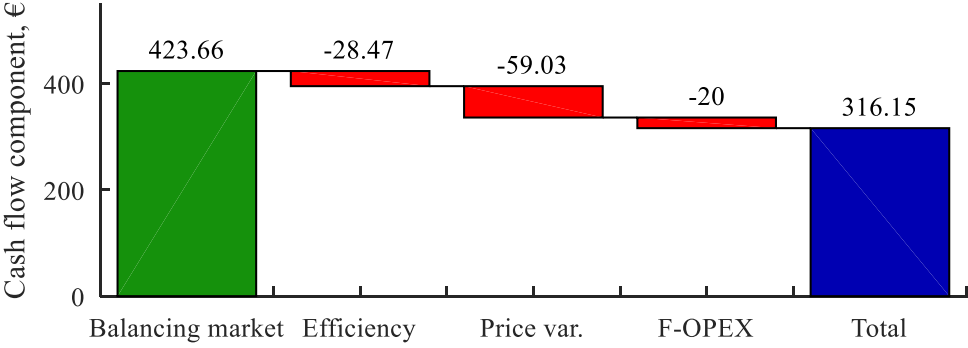
Fig. 4.33. Breakdown of the mean total benefit from explicit DR (optimised schedule).

Table 4.4. Mean annual values of the modelled DR events

Case	DR events		DR Energy, MWh		Specific benefit, €/MWh	
	increase	*reduction*	*increase*	*reduction*	*increase*	*reduction*
original schedule	431	222	3.13	1.04	80.95	84.60
optimised schedule	386	154	3.26	1.30	76.97	65.44

4.6. Summary

The developed Monte Carlo simulation-based DR economic assessment tool *DR Assess* has proven to be useful in providing a preliminary evaluation of the potential benefits a controllable load asset owner might gain by participating in the power system balancing via an explicit DR program and, additionally, by optimising its load schedule based on the day-ahead market prices (i.e., implicit DR). However, the model employed requires quite detailed knowledge of the technical characteristics of the DR asset, especially in regard to its available flexibility with an hourly resolution. In general, the results are assumption-sensitive, thus any output should not be viewed independently of the input.

The DR economic assessment model also allows studying the benefit from explicit DR by its components – balancing payment, efficiency increase (or decrease), and hourly price variations if a dynamic retail tariff is used. While the last two components provided a negative effect in some of the case studies, albeit the sum cash flow remained positive in all cases, thus rewarding the DR asset owner with financial benefits.

The results from **case study I** signal that electric thermal storage devices can recoup the additional investments necessary to make them DR-ready, but only if more than 50% of the load reduction remuneration is passed on to the asset owner. In fact, the stochastic output of the model shows that even at 100% remuneration, there is a small probability that the payback period could exceed the asset service life. Realistically, however, such a full payment sharing is unlikely as the aggregation service provider also needs incentives for its operation.

The flexibility modelling parameter sensitivity analysis carried out in **case study II** aids in validating the developed DR economic assessment tool and its capability to inform potential residential-scale DR participants on the potential activity and profitability from taking part in an explicit DR program. Moreover, this study confirms the importance of accurate selection of the parameter values describing the available flexibility of the consumption profile or particular flexible assets.

Metrics like the available flexibility within an hour, the maximum number of DR events in a certain time horizon and the minimum time distance between two subsequent DR activations have to be selected particularly carefully as they majorly affect the model results. On the other hand, the maximum time before the beginning of recovery has proven to be inconsequential to the simulations and should instead be replaced by a constraint limiting the maximum time before the recovery has to be completed.

When the flexibility parameters are set to reasonable assumptions, it can be inferred that a residential-scale DR participant with a typical load profile, subject to electricity retail prices akin to the Latvian market and capable to participate in Baltic power system balancing (via an

aggregator), can receive some annual benefit from explicit DR. However, with consumption flexibility of about 5%, the economic benefit is barely noticeable (about 5 € annum) and might not even offset the technical costs of DR readiness implementation and maintenance. Indeed, a householder with a typical standard consumption pattern without significant thermostatic load is not well incentivised to participate in explicit DR.

Furthermore, the **case study III** analysis of smart electric thermal storage devices as an asset for explicit DR allows to draw the conclusion that being subjected also to implicit DR by means of price-based consumption rescheduling does not impede the overall profitability of explicit DR. While the parameters of DR activations and related cash flows do change, the sum benefit remains similar in both cases. Moreover, the exposure to implicit DR itself adds notable supplemental benefit to the overall profitability of DR-enabled smart electric thermal storage heaters. It was also demonstrated how the *DR Assess* tool can be used for identification of reasonable bidding price selection for explicit DR activation for system balancing purposes. Evidently, for load reduction, activation price constraints are not strictly necessary as long as the variable OPEX induced by DR is minuscule.

In conclusion, a more realistic DR economic feasibility assessment would require near perfect beforehand knowledge of the contractual setup between the DR asset owner, aggregator, BRP, TSO and other potentially linked parties. However, the regulatory and market framework for DR aggregators in Latvia is still under development. To that end, the *DR Assess* tool allows modelling a variety of different setups which enables studies on finding the most suitable business case for a particular application. It could also be used by policy-makers to analyse the potential implications for the involved parties of different regulatory conditions.

Further studies should aim to expand the DR assessment model to consider other potential markets and forms of explicit DR where residential-scale customers might theoretically participate in an aggregated form since currently the model is focused solely on an mFRR product-based balancing market.

CONCLUSIONS

1. The assessment of benefits obtainable from demand response and results of the balancing process optimisation confirm the hypothesis of the Doctoral Thesis. The proposed solutions have proven to be able to increase the flexibility of the power system and improve its operational efficiency.

2. The developed methodology and software tool, *AOF parameter search*, for optimising the activation process of balancing resources within the common Baltic balancing market framework allows significantly reducing the Baltic area control error, thus promoting cost-effectiveness and energy-independence of the Baltic power systems. The proposed solution is relevant for the common Baltic balancing market, which was established in 2018. Furthermore, in the upcoming years, it can aid the Baltic transmission system operators not only in the planned synchronisation with the Continental Europe network but also in implementing the European Commission guidelines on electricity balancing. To that end, the developed *AOF parameter search* tool can serve as one of the components for the Activation Optimisation Function stipulated in these guidelines.

3. Power system and end-user benefits from employment of demand response have been assessed based on the example of smart electric thermal storage (SETS) as a DR-enabled innovative technology. Results show that, compared to conventional (direct resistive) heating, SETS can provide cost savings both to the Latvian power system as a whole and to individual end-users. Most of the value comes from their smart storage ability. However, the benefit from each SETS unit decreases the more units are deployed in the system. The value of SETS in the power system also reduces if the spread of daily load curve (and electricity prices respectively) diminishes as it lessens the savings obtainable from energy arbitrage.

4. Additional value stream of SETS identified in the Thesis is reserve provision to the power system. However, in the future, this value can be expected to decrease with improvements of interconnections between Latvia and Estonia and, additionally, with introduction of additional storage capacities in the Baltic power system.

5. If partial electrification of heating is envisioned in Latvia, potential distribution grid congestion risks can be significantly alleviated through coordinated scheduling of SETS as demonstrated in the representative feeder study. This also allows decreasing the cost of losses for the DSO and reducing the electricity bills for the end-consumers. In contrast, uncoordinated control of SETS can contribute to peak power rise, hence it should be avoided.

6. Notwithstanding the benefits identified in the case study for Latvia, the investment cost of the particular technology considered (SETS) is still too high for the end-user to have a positive total cash flow. Therefore, novel business models (e.g., service-based) and new revenue streams (e.g., capacity payments for DR provision) would be required for this specific technology to become financially attractive to end-users.

7. The developed Monte Carlo simulation-based tool, *DR Assess*, provides a probabilistic assessment of the economic feasibility of DR provision from its asset owner point-of-view.

It allows considering uncertainties of electricity markets and can be applied for different types of DR assets, provided their flexibility profile is known. The tool, being able to study the effects of both implicit or explicit DR, can be particularly useful for prospective Baltic balancing market entrants by providing them with a comprehensive and reliable cost-benefit assessment.

8. Case studies performed with the *DR Assess* tool in the Doctoral Thesis were focused on residential-scale DR. It was shown that its profitability is highly dependent on the share of remuneration passed to the DR asset owner by the aggregator and is even more so dependent on the flexibility settings for a particular DR asset. Furthermore, it can be concluded that implicit DR adds supplemental benefit to explicit DR provision.

9. Future studies should aim towards investigating additional value streams for demand response to become more attractive and towards studying additional emerging market frameworks where the value of DR could be unlocked. Furthermore, the potential of industrial demand response should be examined together with the related cash flows.

REFERENCES

[1]   "Memorandum of Understanding on the Baltic Energy Market Interconnection Plan," 2009. [Online]. Available: https://ec.europa.eu/energy/sites/ener/files/documents/2009_bemip_mou_signed.pdf. [Accessed: 18-Sep-2018].

[2]   "Baltic Energy Market Interconnection Plan. Final report," 2009. [Online]. Available: https://ec.europa.eu/energy/sites/ener/files/documents/2009_11_25_hlg_report_170609 _0.pdf. [Accessed: 18-Sep-2018].

[3]   BEMIP, "Baltic Energy Market Interconnection Plan. 5th progress report," 2013. [Online]. Available: https://ec.europa.eu/energy/sites/ener/files/documents/20140225_5rd_bemip_progress_ report.pdf. [Accessed: 25-Apr-2018].

[4]   Arturs Purvins; Gianluca Fulli; Catalin Felix Covrig, "The Baltic Power System between East and West Interconnections," 2016.

[5]   Augstsprieguma tīkls AS, "Technical scenario for Baltic grid sinchronisation approved in Brussels," 2018. [Online]. Available: http://ast.lv/en/events/technical-scenario-baltic-grid-synchronisation-approved-brussels. [Accessed: 18-Sep-2018].

[6]   Augstsprieguma tīkls AS, "Baltic TSOs launch a common Baltic balancing market from 2018," 2017. [Online]. Available: http://www.ast.lv/en/events/baltic-tsos-launch-common-baltic-balancing-market-2018. [Accessed: 02-Feb-2018].

[7]   G. Junghans, A. Silis, K. Marcina, and K. Ertmanis, "Role of Balancing Markets in Dealing with Future Challenges of System Adequacy Caused by Energy Transmission," *Latv. J. Phys. Tech. Sci.*, vol. 57, no. 3, pp. 48–56, Jun. 2020.

[8]   H. Holttinen, A. Tuohy, M. Milligan, V. Silva, S. Müller, and L. Soder, "The Flexibility Workout," *IEEE Power Energy Mag.*, vol. 11, no. 6, pp. 53–62, 2013.

[9]   N. O′Connell, P. Pinson, H. Madsen, and M. O′Malley, "Benefits and challenges of electrical demand response: A critical review," *Renew. Sustain. Energy Rev.*, vol. 39, pp. 686–699, Nov. 2014.

[10]   "UCTE Operation Handbook. Appendix 1: Load-frequency Control and Performance." [Online]. Available: https://www.entsoe.eu/fileadmin/user_upload/_library/publications/entsoe/Operation_ Handbook/Policy_1_Appendix _final.pdf. [Accessed: 17-Sep-2018].

[11]   J. Machowski, J. W. Bialek, and J. R. Bumby, *Power System Dynamics: Stability and Control*, 2nd ed. John Wiley & Sons, Ltd., 2008.

[12]   N. Good, K. A. Ellis, and P. Mancarella, "Review and classification of barriers and enablers of demand response in the smart grid," *Renew. Sustain. Energy Rev.*, vol. 72, pp. 57–72, May 2017.

[13]   Smart Grid Task Force, "Regulatory Recommendations for the Deployment of Flexibility - EG3 REPORT," 2015.

[14]   N. G. Paterakis, O. Erdinç, and J. P. S. Catalão, "An overview of Demand Response: Key-elements and international experience," *Renew. Sustain. Energy Rev.*, vol. 69, pp. 871–891, 2017.

[15]   CIGRE, *Short-term flexibility in power systems: drivers and solutions*. Paris, 2020.

[16]   SEDC, "Explicit Demand Response in Europe Mapping the Markets 2017," 2017.

[17]   J. Villar, R. Bessa, and M. Matos, "Flexibility products and markets: Literature review," *Electr. Power Syst. Res.*, vol. 154, pp. 329–340, Jan. 2018.

[18]   X. Lu, K. Li, H. Xu, F. Wang, Z. Zhou, and Y. Zhang, "Fundamentals and business model for resource aggregator of demand response in electricity markets," *Energy*, vol. 204, p. 117885, Aug. 2020.

[19] M. Muratori, B.-A. Schuelke-Leech, and G. Rizzoni, "Role of residential demand response in modern electricity markets," *Renew. Sustain. Energy Rev.*, vol. 33, pp. 546–553, May 2014.

[20] J.-H. Kim and A. Shcherbakova, "Common failures of demand response," *Energy*, vol. 36, no. 2, pp. 873–880, Feb. 2011.

[21] M. Shafie-khah, P. Siano, J. Aghaei, M. A. S. Masoum, F. Li, and J. P. S. Catalao, "Comprehensive Review of the Recent Advances in Industrial and Commercial DR," *IEEE Trans. Ind. Informatics*, vol. 15, no. 7, pp. 3757–3771, Jul. 2019.

[22] C. A. Cardoso, J. Torriti, and M. Lorincz, "Making demand side response happen: A review of barriers in commercial and public organisations," *Energy Res. Soc. Sci.*, vol. 64, p. 101443, Jun. 2020.

[23] B. Dupont, K. Dietrich, C. De Jonghe, A. Ramos, and R. Belmans, "Impact of residential demand response on power system operation: A Belgian case study," *Appl. Energy*, vol. 122, pp. 1–10, Jun. 2014.

[24] F. Shariatzadeh, P. Mandal, and A. K. Srivastava, "Demand response for sustainable energy systems: A review, application and implementation strategy," *Renew. Sustain. Energy Rev.*, vol. 45, pp. 343–350, May 2015.

[25] S. Paiho, H. Saastamoinen, E. Hakkarainen, L. Similä, R. Pasonen, J. Ikäheimo, M. Rämä, M. Tuovinen, and S. Horsmanheimo, "Increasing flexibility of Finnish energy systems—A review of potential technologies and means," *Sustain. Cities Soc.*, vol. 43, pp. 509–523, Nov. 2018.

[26] M. Barbero, C. Corchero, L. Canals Casals, L. Igualada, and F.-J. Heredia, "Critical evaluation of European balancing markets to enable the participation of Demand Aggregators," *Appl. Energy*, vol. 264, p. 114707, Apr. 2020.

[27] P. Kohlhepp, H. Harb, H. Wolisz, S. Waczowicz, D. Müller, and V. Hagenmeyer, "Large-scale grid integration of residential thermal energy storages as demand-side flexibility resource: A review of international field studies," *Renew. Sustain. Energy Rev.*, vol. 101, pp. 527–547, Mar. 2019.

[28] European Commission, *Commission Regulation (EU) 2017/2195 of 23 November 2017 establishing a guideline on electricity balancing*. 2017.

[29] "Feasibility study regarding cooperation between the Nordic and the Baltic power systems within the Nordic ENTSO-E pilot project on electricity balancing," 2014. [Online]. Available: http://www.ast.lv/files/ast_files/balansesana/STUDY REPORT-Nordic - Baltic cooperation in Electricity Balancing_112014_final.pdf.

[30] Pöyry Management Consulting (UK) Ltd, "Baltic's balance management model study and harmonisation plan towards EU energy markets model (including Nordic-Baltic balancing cooperation). A report to Elering," 2016. [Online]. Available: https://elering.ee/sites/default/files/attachments/Pöyry uuring.pdf.

[31] Augstsprieguma tīkls AS, "Annual statement of transmission system operator for the year 2016," 2017. [Online]. Available: http://ast.lv/files/ast_files/gadaparskzinoj/TSO_Annual_Statement_2016.pdf. [Accessed: 28-Apr-2018].

[32] ENTSO-E, "First Edition of the Bidding Zone Review: First Draft," 2018.

[33] M. Haberg and G. Doorman, "A stochastic mixed integer linear programming formulation for the balancing energy activation problem under uncertainty," in *2017 IEEE Manchester PowerTech*, 2017, pp. 1–6.

[34] P. Havel, P. Filas, and J. Fantik, "Simulation-based optimization of ancillary services," in *2008 5th International Conference on the European Electricity Market*, 2008, pp. 1–5.

[35] J. Novak, P. Chalupa, and V. Bobal, "Automatic controller for cost-optimal power

balance control," in *2010 9th International Conference on Environment and Electrical Engineering*, 2010, pp. 222–225.

[36] M. P. Garcia and D. S. Kirschen, "Forecasting system imbalance volumes in competitive electricity markets," in *IEEE PES Power Systems Conference and Exposition*, 2004, pp. 1115–1122.

[37] S. Lu, Y. V. Makarov, A. J. Brothers, C. A. McKinstry, S. Jin, and J. H. Pease, "Prediction of power system balancing requirement and tail event," in *IEEE PES T&D*, 2010, pp. 1–7.

[38] A. McDonald, "Thermal Storage Device," US 2015/0055941 (A1), 2015.

[39] J.-M. Durand, M. J. Duarte, and P. Clerens, "Joint EASE/EERA recommendations for a European Energy Storage Technology Development Roadmap towards 2030," 2013.

[40] J. Raadschelders, F. Sikkema, and B. in 't Groen, "Potential for Smart Electric Thermal Storage. Contributing to a low carbon energy system," Arnhem, 2013.

[41] V. S. K. V. Harish and A. Kumar, "A review on modeling and simulation of building energy systems," *Renew. Sustain. Energy Rev.*, vol. 56, pp. 1272–1292, Apr. 2016.

[42] A. Foucquier, S. Robert, F. Suard, L. Stéphan, and A. Jay, "State of the art in building modelling and energy performances prediction: A review," *Renew. Sustain. Energy Rev.*, vol. 23, pp. 272–288, Jul. 2013.

[43] G. Reynders, J. Diriken, and D. Saelens, "Quality of grey-box models and identified parameters as function of the accuracy of input and observation signals," *Energy Build.*, vol. 82, pp. 263–274, Oct. 2014.

[44] J. L. M. Hensen and R. Lamberts, *Building Performance Simulation for Design and Operation*. Spon Press, 2011.

[45] A. Rabl, "Parameter Estimation in Buildings: Methods for Dynamic Analysis of Measured Energy Use," *J. Sol. Energy Eng.*, vol. 110, no. 1, pp. 52–66, 1988.

[46] J. V. Beck and K. J. Arnold, *Parameter Estimation in Engineering and Science*. John Wiley & Sons, 1979.

[47] S. Ihara and F. C. Schweppe, "Physically based modeling of cold load pickup," *IEEE Trans. Power Appar. Syst.*, vol. PAS-100, no. 9, pp. 4142–4150, 1981.

[48] G. Fraisse, C. Viardot, O. Lafabrie, and G. Achard, "Development of a simplified and accurate building model based on electrical analogy," *Energy Build.*, vol. 34, no. 10, pp. 1017–1031, Nov. 2002.

[49] C. P. Underwood, "An improved lumped parameter method for building thermal modelling," *Energy Build.*, vol. 79, pp. 191–201, Aug. 2014.

[50] A. P. Ramallo-González, M. E. Eames, and D. A. Coley, "Lumped parameter models for building thermal modelling: An analytic approach to simplifying complex multi-layered constructions," *Energy Build.*, vol. 60, pp. 174–184, May 2013.

[51] M. M. Gouda, S. Danaher, and C. P. Underwood, "Building thermal model reduction using nonlinear constrained optimization," *Build. Environ.*, vol. 37, no. 12, pp. 1255–1265, Dec. 2002.

[52] N. Good, L. Zhang, A. Navarro-Espinosa, and P. Mancarella, "High resolution modelling of multi-energy domestic demand profiles," *Appl. Energy*, vol. 137, pp. 193–210, 2015.

[53] O. Neu, B. Sherlock, S. Oxizidis, D. Flynn, and D. Finn, "Developing building archetypes for electrical load shifting assessment: Analysis of Irish residential stock," in *CIBSE ASHRAE Technical Symposium*, 2014, pp. 1–19.

[54] G. Strbac, "Demand side management: Benefits and challenges," *Energy Policy*, vol. 36, no. 12, pp. 4419–4426, 2008.

[55] N. Ritter, Z. Broka, L. Grandell, G. Koreneff, O. Neu, C. O'Dwyer, and L. Simila, "H2020 RealValue D6.2 Market review report: socio-economic & housing trends in

selected countries," 2016. [Online]. Available: https://ec.europa.eu/research/participants/documents/downloadPublic?documentIds=08 0166e5ad302011&appId=PPGMS. [Accessed: 29-Jun-2020].

[56] AS "Sadales tīkls," "AS 'Sadales tīkls' gada pārskats 2016," 2017. [Online]. Available: https://www.sadalestikls.lv/files/newnode/parskati/ST__2016_gada_parskats.pdf.

[57] Glen Dimplex, "Quantum Heater," 2018. [Online]. Available: https://www.dimplex.co.uk/product/quantum-heater. [Accessed: 05-Apr-2018].

[58] Glen Dimplex, "Introducing the Quantum heating system," 2015. [Online]. Available: www.glendimplexireland.com/.../20276446_Quantum_Main_Brochure_Sep14_v4.pdf. [Accessed: 10-Nov-2017].

[59] E. Telaretti, M. Ippolito, and L. Dusonchet, "A Simple Operating Strategy of Small-Scale Battery Energy Storages for Energy Arbitrage under Dynamic Pricing Tariffs," *Energies*, vol. 9, no. 1, 2016.

[60] Latvian Standard, "LVS EN 50160:2010 Voltage characteristics of electricity supplied by public electricity networks," 2010.

[61] E. Sortomme, M. M. Hindi, S. D. J. MacPherson, and S. S. Venkata, "Coordinated charging of plug-in hybrid electric vehicles to minimize distribution system losses," *IEEE Trans. Smart Grid*, vol. 2, no. 1, pp. 186–193, 2011.

[62] A. Sauhats, L. Petrichenko, S. Beryozkina, and N. Jankovskis, "Stochastic planning of distribution lines," in *2016 13th International Conference on the European Energy Market (EEM)*, 2016, pp. 895–899.

[63] N. Jankovskis, "Viedo tehnoloģiju izmantošanas paņēmieni Latvijas sadales tīklos," Rīgas Tehniskā universitāte, 2016.

[64] E. Karnītis, "Electricity Supply in Latvia: Objective and Subjective Aspects (in Latvian)," *Econ. Bus.*, vol. 20, pp. 81–89, 2010.

[65] D. Bride and A. Zvaigzne, "Electricity Market Development in Latvia," *J. Soc. Sci.*, vol. 1, no. 8, pp. 5–19, 2016.

[66] Tesla, "Powerwall," 2018. [Online]. Available: https://www.tesla.com/powerwall. [Accessed: 28-Apr-2018].

[67] W. J. Cole, C. Marcy, V. K. Krishnan, and R. Margolis, "Utility-scale lithium-ion storage cost projections for use in capacity expansion models," in *2016 North American Power Symposium (NAPS)*, 2016.

[68] European Commission, "State Aid SA.43140 (2015/NN) – Latvia Support to renewable energy and CHP," Brussels, 2017.

[69] Nord Pool, "Baltic power market completed with successful opening of Latvian bidding area," 2013. [Online]. Available: https://www.nordpoolgroup.com/message-center-container/newsroom/exchange-message-list/2013/Q2/No-332013---Baltic-power-market-completed-with-successful-opening-of-Latvian-bidding-area/. [Accessed: 28-Apr-2018].

[70] Z. Broka, K. Baltputnis, A. Sauhats, G. Junghāns, L. Sadoviča, and V. Lavrinovičs, "Towards Optimal Activation of Balancing Energy to Minimize Regulation from Neighboring Control Areas," in *2018 15th International Conference on the European Energy Market (EEM)*, 2018, pp. 1–5.

[71] E. Tuohy, T. Jermalavičius, A. Bulakh, N. Theisen, J. Vainio, A. Petkus, H. Bahşi, and Y. Tsarik, "The Geopolitics of Power Grids – Political and Security Aspects of Baltic Electricity Synchronization," Tallinn, 2018.

[72] European Commission, "EU Reference Scneario 2016 – Energy, transport and GHG Emissions – Trends to 2050," 2016. [Online]. Available: https://ec.europa.eu/energy/sites/ener/files/documents/ref2016_report_final-web.pdf. [Accessed: 28-Apr-2018].

[73] e-Highway 2050 Consortium, "Modular Development Plan of the Pan-European Tranmission System 2050. Deliverable 2.1 Data sets of scenarios for 2050," 2014.

[74] Augstsprieguma tīkls AS, "Power Transmission System Development Plan 2018-2027 [in Latvian]," 2017. [Online]. Available: http://www.ast.lv/en/content/power-transmission-system-development-plan. [Accessed: 28-Apr-2018].

[75] A. Krupavicius, "The 2014 Referendum in Lithuania," *East Eur. Q.*, vol. 43, no. 1, pp. 129–136, 2015.

[76] Central Statistical Bureau of Latvia, "Annual Energy Statistics," 2016. [Online]. Available: http://data.csb.gov.lv/pxweb/lv/vide/vide__ikgad__energetika/?tablelist=true&rxid=cd cb978c-22b0-416a-aacc-aa650d3e2ce0. [Accessed: 28-Apr-2018].

[77] M. Rubins and I. Pilvere, "Development of Renewable Energy Policy in Latvia," in *International Conference "Economic Science for Rural Development,"* 2018, pp. 281–291.

[78] ENTSO-E, "Transparency Platform," 2018. [Online]. Available: https://transparency.entsoe.eu/. [Accessed: 28-Apr-2018].

[79] Nord Pool, "Historical Market Data," 2018. [Online]. Available: https://www.nordpoolgroup.com/historical-market-data/. [Accessed: 28-Apr-2018].

[80] R. Petrichenko, K. Baltputnis, A. Sauhats, and D. Sobolevsky, "District heating demand short-term forecasting," in *2017 IEEE International Conference on Environment and Electrical Engineering and 2017 IEEE Industrial and Commercial Power Systems Europe (EEEIC / I&CPS Europe)*, 2017, pp. 1–5.

[81] LVĢMC, "Meteorological Data [in Latvian]," 2016. [Online]. Available: https://www.meteo.lv/meteorologija-datu-meklesana/?nid=461. [Accessed: 28-Apr-2018].

[82] Augstsprieguma tīkls AS, "Latvia - Estonia third interconnection," 2018. [Online]. Available: http://www.ast.lv/en/transmission-network-projects/latvia-estonia-third-interconnection. [Accessed: 28-Apr-2018].

[83] Augstsprieguma tīkls AS, "Reconstruction of the existing Latvia - Estonia 330kV interconnections," 2017. [Online]. Available: http://www.ast.lv/en/transmission-network-projects/reconstruction-existing-latvija-estonia-330kv-interconnections. [Accessed: 28-Apr-2018].

[84] Elering AS, Augstsprieguma tīkls AS, and Litgrid UAB, "Terms, Conditions and Methodologies on Cross-Zonal Capacity Calculation, Provision and Allocation within the Baltic States and with the 3rd Countries," 2015. [Online]. Available: https://prelive.elering.ee/sites/default/files/public/Elektriturg/20150911_Baltic_CCCA _Rules_for_submission_to_NRAs_for_signing_final.pdf. [Accessed: 28-Apr-2018].

[85] Lietuvos Energija, "Kruonis Pumped Storage Power Plant Expansion," 2017. [Online]. Available: https://gamyba.le.lt/en/activities/projects/kruonis-pumped-storage-power-plant-expansion. [Accessed: 05-Jan-2018].

[86] C. O'Dwyer, M. B. Anwar, J. Dillon, M. Bakhtvar, G. Buttitta, C. Andrade Cabrera, K. Baltputnis, Z. Broka, J. Kozadajevs, A. Sauhats, T. Rasku, J. Kiviluoma, W.-P. Schill, and A. Zerrahn, "H2020 Realvalue D3.6 Cost Benefit Analysis of SETS and Alternative Local Small-Scale Storage Options," 2018. [Online]. Available: https://ec.europa.eu/research/participants/documents/downloadPublic?documentIds=08 0166e5bb1b5de4&appId=PPGMS. [Accessed: 29-Jun-2020].

[87] European Commission, "Europe leads the global clean energy transition: Commission welcomes ambitious agreement on further renewable energy development in the EU," 2018. .

[88] T. J. Hammons, "Integrating renewable energy sources into European grids," *Int. J.*

Electr. Power Energy Syst., vol. 30, no. 8, pp. 462–475, Oct. 2008.

[89] J. a. P. Lopes, N. Hatziargyriou, J. Mutale, P. Djapic, and N. Jenkins, "Integrating distributed generation into electric power systems: A review of drivers, challenges and opportunities," *Electr. Power Syst. Res.*, vol. 77, no. 9, pp. 1189–1203, Jul. 2007.

[90] SEDC, "Explicit and Implicit Demand-Side Flexibility Complementary Approaches for an Efficient Energy System Explicit and Implicit Demand-Side Flexibility: Complementary Approaches for an Efficient Energy System," no. September, 2016.

[91] M. H. Albadi and E. F. El-Saadany, "A summary of demand response in electricity markets," *Electr. Power Syst. Res.*, vol. 78, no. 11, pp. 1989–1996, Nov. 2008.

[92] M. H. Albadi and E. F. El-Saadany, "Demand Response in Electricity Markets: An Overview," in *2007 IEEE Power Engineering Society General Meeting*, 2007, pp. 1–5.

[93] N. Prüggler, "Economic potential of demand response at household level—Are Central-European market conditions sufficient?," *Energy Policy*, vol. 60, pp. 487–498, Sep. 2013.

[94] M. Behrangrad, "A review of demand side management business models in the electricity market," *Renew. Sustain. Energy Rev.*, vol. 47, pp. 270–283, Jul. 2015.

[95] L. Gkatzikis and I. Koutsopoulos, "The Role of Aggregators in Smart Grid Demand Response Markets," *IEEE J. Sel. Areas Commun.*, vol. 31, no. 7, pp. 1247–1257, 2013.

[96] A. Rautiainen, J. Koskela, O. Vilppo, A. Supponen, M. Kojo, P. Toivanen, E. Rinne, and P. Jarventausta, "Attractiveness of demand response in the Nordic electricity market — Present state and future prospects," in *2017 14th International Conference on the European Energy Market (EEM)*, 2017, pp. 1–6.

[97] L. Sadovica, K. Marcina, V. Lavrinovics, and G. Junghans, "Facilitating energy system flexibility by demand response in the baltics — Choice of the market model," in *2017 IEEE 58th International Scientific Conference on Power and Electrical Engineering of Riga Technical University (RTUCON)*, 2017, pp. 1–6.

[98] Augstsprieguma tīkls AS, Elering AS, and Litgrid UAB, "Demand response through aggregation - a harmonized approach in Baltic region," 2017.

[99] M. Muratori and G. Rizzoni, "Residential Demand Response: Dynamic Energy Management and Time-Varying Electricity Pricing," *IEEE Trans. Power Syst.*, vol. 31, no. 2, pp. 1108–1117, 2016.

[100] H. C. Gils, "Economic potential for future demand response in Germany – Modeling approach and case study," *Appl. Energy*, vol. 162, pp. 401–415, 2016.

[101] F. Wang, H. Xu, T. Xu, K. Li, M. Shafie-khah, and J. P. S. Catalão, "The values of market-based demand response on improving power system reliability under extreme circumstances," *Appl. Energy*, vol. 193, pp. 220–231, May 2017.

[102] G. Bianchini, M. Casini, A. Vicino, and D. Zarrilli, "Demand-response in building heating systems: A Model Predictive Control approach," *Appl. Energy*, vol. 168, pp. 159–170, 2016.

[103] A. Arteconi, D. Patteeuw, K. Bruninx, E. Delarue, W. D'haeseleer, and L. Helsen, "Active demand response with electric heating systems: Impact of market penetration," *Appl. Energy*, vol. 177, pp. 636–648, 2016.

[104] F. De Ridder, M. Hommelberg, and E. Peeters, "Demand side integration: four potential business cases and an analysis of the 2020 situation," *Eur. Trans. Electr. Power*, vol. 21, no. 6, pp. 1902–1913, Sep. 2011.

[105] E. Moreno, O. A. Gonzalez, and A. Pavas, "Demand flexibility assessment for residential customers," in *2017 IEEE Workshop on Power Electronics and Power Quality Applications (PEPQA)*, 2017, pp. 1–5.

[106] B. Neupane, L. Šikšnys, and T. B. Pedersen, "Generation and Evaluation of Flex-Offers from Flexible Electrical Devices," *Proc. Eighth Int. Conf. Futur. Energy Syst. - e-Energy*

'17, pp. 143–156, 2017.

[107] Z. Yahia and A. Pradhan, "Optimal load scheduling of household appliances considering consumer preferences: An experimental analysis," *Energy*, vol. 163, pp. 15–26, 2018.

[108] Z. Ma, J. Billanes, and B. Jørgensen, "Aggregation Potentials for Buildings—Business Models of Demand Response and Virtual Power Plants," *Energies*, vol. 10, no. 10, p. 1646, Oct. 2017.

[109] M. Brolin, "Aggregator trading and demand dispatch under price and load uncertainty," in *2016 IEEE PES Innovative Smart Grid Technologies Conference Europe (ISGT-Europe)*, 2016, pp. 1–6.

[110] D. T. Nguyen, M. Negnevitsky, and M. De Groot, "Modeling load recovery impact for demand response applications," *IEEE Trans. Power Syst.*, vol. 28, no. 2, pp. 1216–1225, 2013.

[111] M. Vallés, A. Bello, J. Reneses, and P. Frías, "Probabilistic characterization of electricity consumer responsiveness to economic incentives," *Appl. Energy*, vol. 216, no. September 2017, pp. 296–310, 2018.

[112] H. Janssen, "Monte-Carlo based uncertainty analysis: Sampling efficiency and sampling convergence," *Reliab. Eng. Syst. Saf.*, vol. 109, pp. 123–132, 2013.

[113] "MATLAB." The MathWorks Inc, Natick, Massachusetts.

[114] M. Waseem, I. A. Sajjad, L. Martirano, and M. Manganelli, "Flexibility assessment indicator for aggregate residential demand," in *2017 IEEE International Conference on Environment and Electrical Engineering and 2017 IEEE Industrial and Commercial Power Systems Europe (EEEIC / I&CPS Europe)*, 2017, pp. 1–5.

[115] J. L. Mathieu, M. Kamgarpour, J. Lygeros, G. Andersson, and D. S. Callaway, "Arbitraging Intraday Wholesale Energy Market Prices With Aggregations of Thermostatic Loads," *IEEE Trans. Power Syst.*, vol. 30, no. 2, pp. 763–772, Mar. 2015.

[116] V. Trovato, F. Teng, and G. Strbac, "Value of thermostatic loads in future low-carbon Great Britain system," in *2016 Power Systems Computation Conference (PSCC)*, 2016, pp. 1–7.

[117] A. M. Mathew and R. Menon, "Assessment of demand response capability with thermostatic loads in residential sector," in *2015 International Conference on Power, Instrumentation, Control and Computing (PICC)*, 2015, pp. 1–5.

APPENDICES

Structure of the overall algorithm of *AOF parameter search* tool
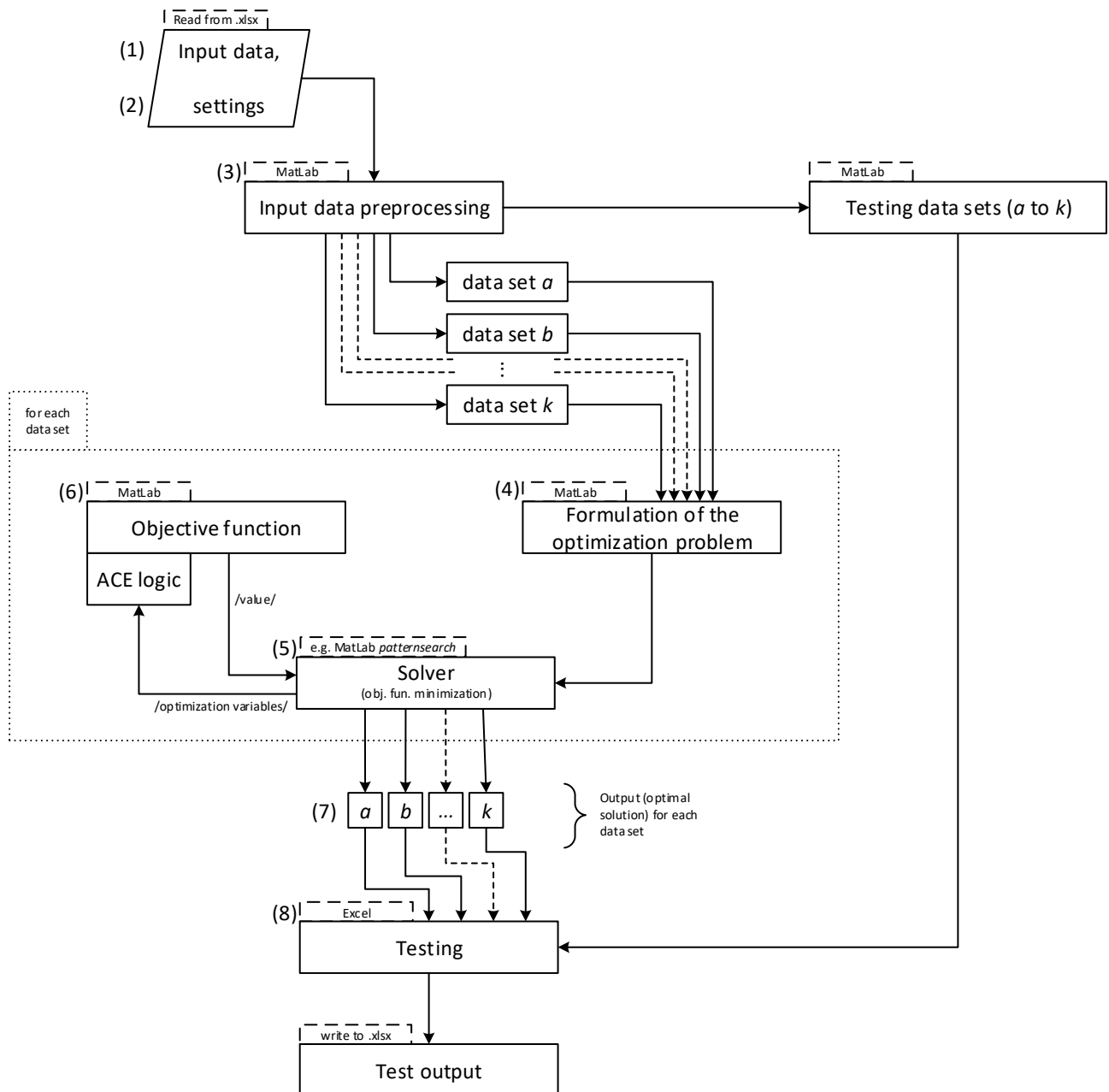
Continued on next page.

No	Step	Description
(1)	Input data	• ACE forecast in minute resolution

(2)	Settings	• max number of activations in an hour (set from 1 to 5)
		• preparation time (initial assumption: 2 min)
		• ramp rate (initial assumption: 20 MW/min)
		• lower and upper bounds on optimisation variables such as
		    ○ t^n_{min} (activation minute);
		    ○ c^n_{nb} (% of ACE forecast);
		    ○ ACE^n_{ign} (ignorance)
		      $\forall\, n \in [1;\ max\ numb.\ of\ act.]$

(3)	Data preprocessing	• check quality; apply filter
		• separation in datasets, for instance:
		    ○ weekdays → hours by type (up, down, stable);
		    ○ holidays → hours by type (up, down, stable)
		• additionally, separation in training and testing datasets

(4)	Formulation of the optim. problem	• format bounds and constraints to pass them to solver • feed objective function to solver
(5)	Solver	• objective function is non-convex, non-smooth; • use global search algorithms, e.g., *patternsearch* (multiple-start) to minimise the objective function

(6)	Objective function	• set of logical instruction;
		• variables: t^n_{min}; c^n_{nb}; ACE^n_{ign}
		• $\min\!\left(w_{1a}\sum ACE^{ISP}_{pos} + w_{1b}\sum\left|ACE^{ISP}_{neg}\right| + w_2\sum\left|E^{ISP}_{reg.s.}\right| + w_3\sum\left|P^{ISP}_{reg.o.}\right|\right)$
		    [primary goal] [penalty for overactive reg. / for large capacities]
		  w – weight coefficients (adjustable)
		• additional constraints (minimum time between activations, e.g., 10 min)

(7)	Output	• for each dataset
		    ○ t^n_{min} – minute when operator must check the necessity of regulation activation;
		    ○ c^n_{nb} – % of ACE forecast to be balanced if ignorance threshold is met at t^n_{min};
		    ○ ACE^n_{ign} – ignorance threshold for activation at t^n_{min}

(8)	Testing	• return of testing dataset with regulation activated according to the output parameters

Calculation of objective function within the *AOF parameter search* tool
(example for ISP of 1 hour)

Solver
(optimization variables from current iteration)

Settings

Preprocessed data set
(minute resolution)

t^n_{min} c^n_{nb} ACE^n_{ign} $\forall\, n \in [1;$ max numb. of activations]

Start

Number of hours = size(data set)/60

$Idx_{hour} = 0$

idx_{hour} < number of hours   *Outer loop*

0

1

$idx_{hour} = idx_{hour} + 1$

obj. fun. val. = obj. fun. val. + obj. fun. val.$_{hour}$

$Idx_{activation} = 0$

obj. fun. val.$_{hour}$ =

$$\left(w_{1a} \cdot \sum ACE^{hour}_{poz} + w_{1b} \sum |ACE^{hour}_{neg}| + w_2 \cdot \sum |E^{hour}_{reg}| + w_3 \cdot \sum |P^{hour}_{reg}| \right)$$

$idx_{activation}$ < max number of activations

0

Inner loop *

Import obj. fun. components for the current hour from the inner loop: ACE; ΣE_{reg}; ΣP_{reg}

1

$idx_{activation} = idx_{activation} + 1$

*

Regulation simulation logic

Pass obj. fun. value to solver; update variables; next solver iteration

Balancing activation/cancellation simulation logic for the AOF algorithm
with assumptions on preparation time and constant ramping (up and down) rate within each activation/cancellation

Main variables, sets and indices

size_ISP	number of minutes within the ISP
m	index (minute) from the set [1; *size_ISP*]
preparation	preparation time (minutes from the decision to activate/cancel to the beginning of its realisation (i.e., ramping))
ramp	ramping (up/down) rate (MW/min)
$ACE\_forc_{act\_minutes_n}$	base[9] forecast of the ACE for the ISP at minute $act\_minutes_n$ (MWh/h)
ACE_corr	ACE correction corresponding to the simulated balancing operations currently in effect (MWh/h)
numb_of_act	maximum number of activations (within an ISP)
n	index for the current activation/cancellation decision (1…*numb_of_act*)
$act\_minutes_n$	minute for activation/cancellation decision at activ. *n*
act_volume_n	percentage of the ACE forecast to be regulated against at activ. *n*
$tolerance_n$	ignorance level of the ACE forecast at activ. *n* (MWh/h)
r	index for realised balancing activations (needed for cancellation simulation)

Algorithm outline for each ISP

I.   Iterate through minutes *m* of the ISP (in real-time application case, read ACE forecast and perform calculations once each minute).

II. Check if minute *m* corresponds to any of the $act\_minutes_n$ values.

III. If so, check if the ACE forecast (absolute value) meets the ignorance threshold: $|ACE\_forc_m + ACE\_corr| \geq tolerance_n$.

IV. If it does and if there are previously ordered balancing operations currently active, compare their direction to the direction of the ACE_forc_m; if they are the same, perform Cancellation; update information on currently active balancing and *ACE_corr*.

V.   Compare once more if the updated ACE forecast (absolute value) meets the ignorance threshold: $|ACE\_forc_m + ACE\_corr| \geq tolerance_n$.

VI. If it does, perform Activation.

---

[9] I.e., ACE forecast without any balancing activations.

1. Activation

1.1. Necessary regulation **energy** at minute $act\_minutes_n$:

$$reg\_energy = -act\_volume_n \cdot \left(ACE\_forc_{act\_minutes_n} + ACE\_corr \right)$$

Corresponding **power**:

$$ordered\_power = \text{sign}(reg\_energy) \cdot ramp \cdot \left(size\_ISP - act\_minutes_n - preparation + 1 - \right.$$
$$\left. - \sqrt{\left(size\_ISP - act\_minutes_n - preparation + 1 \right)^2 - 120 \cdot \left| reg\_energy \right| / ramp} \right)$$

➢ If the radicand above is **negative**, the desired energy cannot be served within the remainder of the ISP, thus we calculate the maximum amount of energy that can be served (with account to the given ramp rate and preparation time):

$$reg\_energy = ramp / 120 \cdot \left(size\_ISP - act\_minutes_n - preparation + 1 \right)^2 \cdot \text{sign}(reg\_energy)$$
$$ordered\_power = ramp \cdot \left(size\_ISP - act\_minutes_n - preparation + 1 \right) \cdot \text{sign}(reg\_energy)$$

Update the **correction** of ACE forecast:

$$ACE\_corr = ACE\_corr + reg\_energy$$

1.2. If balancing has been ordered, **save information** about this activation in a separate set of variables with index *r* so that its cancellation can later be adequately simulated if necessary:
$ordered\_power_r$; $ord\_minutes_r$; reg_energy_r
(power; time of decision [input value]; expected energy)

2. Cancellation

As before, the time for the current activation/cancellation decision is denoted by $act\_minutes_n$, whereas r serves as an index for the previous balancing activations that can be potentially cancelled.

Amount of the balancing energy that <u>should be cancelled</u> at minute $act\_minutes_n$ is initially assumed to equal the forecasted ACE: $energy\_to\_cancel = ACE\_forc_{act\_minutes_n} + ACE\_corr$. However, at first we calculate the amount of energy that <u>can be cancelled</u> (*cancelable_energy*) in section 2.1. Then, in section 2.2, we compare that to the total amount of the redundant balancing energy to perform its full or partial cancellation.

Hereinafter, "ramping up" refers to moving towards the absolute value of the ordered power from zero regardless of its actual sign (i.e., activation), whereas "ramping down" refers to moving from the ordered power towards zero (i.e., cancellation). Hence why the direction of balancing energy and power is saved in a separate variable: $dir = \text{sign}(energy\_to\_cancel)$, and further calculations are done using the absolute values of power and energy.

2.1. For each of the previously ordered and currently active balancing activations r, calculate the maximum amount of energy that <u>can be cancelled</u> by the end of the ISP (MWh).

A. IF $\quad act\_minutes_n \leq |ordered\_power_r| / ramp + ord\_minutes_r - 1$

AND $\quad 2 \cdot act\_minutes_n + preparation - ord\_minutes_r \leq size\_ISP$

(still ramping up, but can fully ramp down)

THEN $\quad cancelable\_energy_r = \left(|reg\_energy_r| - ramp/60 \cdot (act\_minutes_n - ord\_minutes_r)^2 \right) \cdot dir$
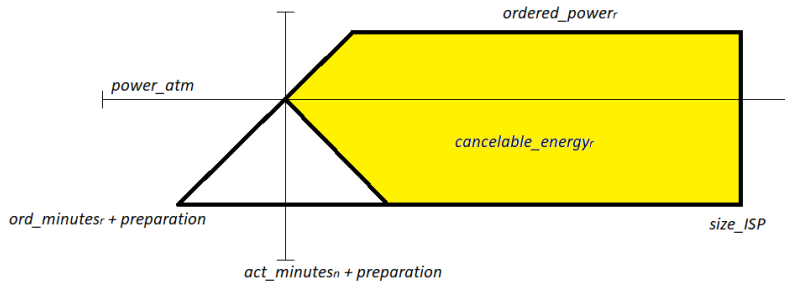
B. IF $\quad act\_minutes_n > |ordered\_power_r| / ramp + ord\_minutes_r - 1$

AND $\quad act\_minutes_n + preparation \leq size\_ISP - |ordered\_power_r|/ramp - 1$

(already ramped up, can ramp down to 0 within the ISP)

THEN $\quad cancelable\_energy_r = \Big(|ordered\_power_r| \cdot (size\_ISP - act\_minutes_n - preparation + 1)/60 -$
$$- ordered\_power_r^2 / (120 \cdot ramp) \Big) \cdot dir$$

150
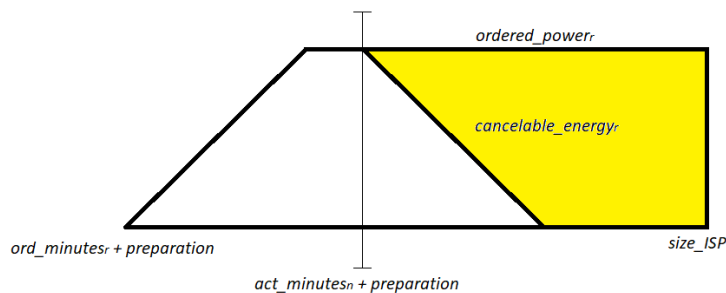
C. IF $act\_minutes_n > \left|ordered\_power_r\right| / ramp + ord\_minutes_r - 1$

AND $act\_minutes_n + preparation > size\_ISP - \left|ordered\_power_r\right| / ramp - 1$

(already ramped up, cannot ramp down to 0 within the ISP)

THEN $cancelable\_energy_r = ramp / 120 \cdot \left(size\_ISP - act\_minutes_n - preparation + 1\right)^2 \cdot dir$

ordered_power_r

cancelable_energy_r

ord_minutes_r + preparation

size_ISP

act_minutes_n + preparation
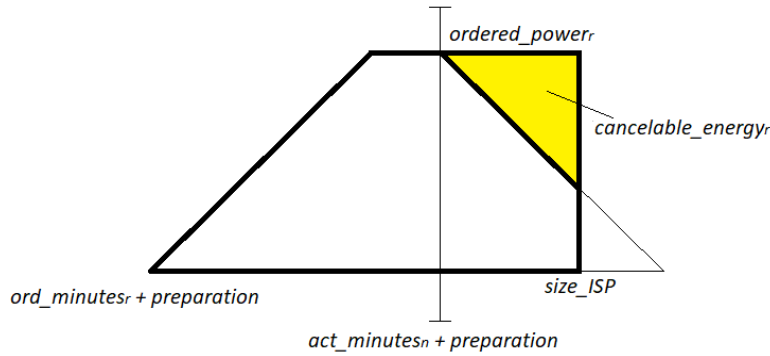
D. IF $act\_minutes_n \leq \left|ordered\_power_r\right| / ramp + ord\_minutes_r - 1$

AND $2 \cdot act\_minutes_n + preparation - ord\_minutes_r > size\_ISP$

(still ramping up, but cannot fully cancel anymore (extremely unlikely, but theoretically possible))

THEN $cancelable\_energy_r = \Big(\left|reg\_energy_r\right| - ramp / 60 \cdot \left(act\_minutes_n - ord\_minutes_r\right)^2 +$

$+ ramp \cdot \left(size\_ISP + ord\_minutes_r - 2 \cdot act\_minutes_n - preparation + 1\right)^2 / 120 \Big) \cdot dir$

power_atm

ordered_power_r

cancelable_energy_r

ord_minutes_r + preparation

size_ISP

act_minutes_n + preparation
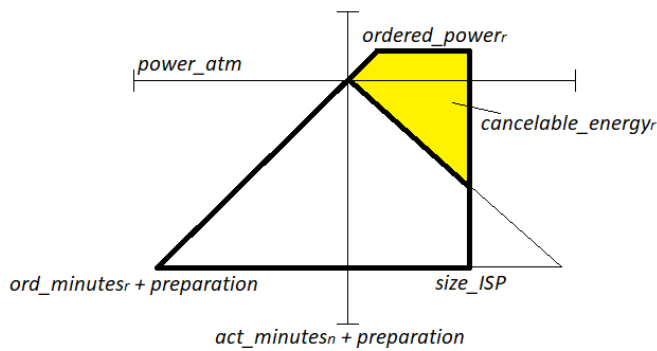
2.2. Compare the total **cancelable_energy** from all the active previous orders r to the needed amount of cancellation at $act\_minutes_n$, **energy_to_cancel**.

A. IF $\left|\text{sum}(cancelable\_energy)\right| \leq \left|energy\_to\_cancel\right|$, cancel everything and delete the data on currently active balancing orders. Update the ACE forecast correction:

$$ACE\_corr = ACE\_corr - \text{sum}(cancelable\_energy)$$

B. IF $\left|\text{sum}(cancelable\_energy)\right| > \left|energy\_to\_cancel\right|$, iterate through all the currently active balancing orders r, starting from the earlier activations, following this algorithm:

    I. $r = 1$

    II. IF $\left|cancelable\_energy_r\right| \leq \left|energy\_to\_cancel\right|$
       GO TO (III)
       ELSE GO TO (V)

    III. Fully cancel regulation r and readjust $energy\_to\_cancel$:
       $energy\_to\_cancel = energy\_to\_cancel - cancelable\_energy_r$

    IV. IF $r < R$ (where R is the number of active previous activations)
       THEN $r = r + 1$ AND GO TO (II)
       ELSE GO TO (VI)

    V. Simulate reg. power decrease: **Partial cancellation**.

    VI. Adjust the ACE forecast correction, ACE_corr, and activation data to reflect all cancelled energy and power, and return to invoking function.

2.3. Partial cancellation

$energy\_prim$ denotes the energy not delivered (i.e., cancelled) in MWh if ramping were to stop at minute $(act\_minutes_n + preparation)$; necessary to determine the subcase of partial cancellation.

$$
\begin{aligned}
energy\_prim = \Big[& \left(\left|ordered\_power_r\right| - ramp \cdot (act\_minutes_n - ord\_minutes_r) \right) / 60 \cdot \\
& \cdot \left(size\_ISP - act\_minutes_n - preparation + 1 - \right. \\
& \left. - \left(\left|ordered\_power_r\right| - ramp \cdot (act\_minutes_n - ord\_minutes_r) \right) / (2 \cdot ramp) \right) \Big] \cdot dir
\end{aligned}
$$

$power\_atm$ stands for the value of balancing power in MW at minute $(act\_minutes_n + preparation)$ as illustrated below:

$$power\_atm = \min\left\{ ramp \cdot (act\_minutes_n - ord\_minutes_r), \left|ordered\_power_r\right| \right\} \cdot dir$$
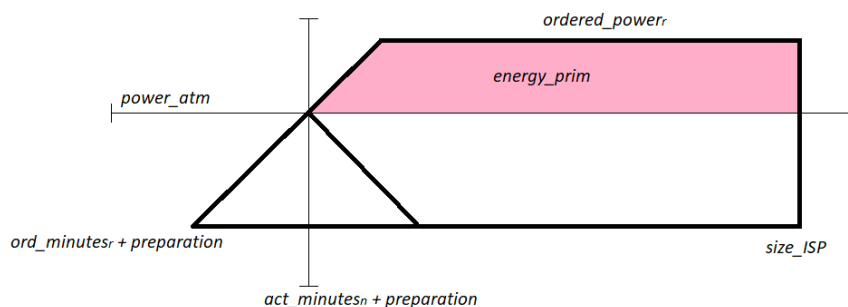
Determine the **subcase** of partial cancellation for the current cancellation decision n:

A. IF $\left| power\_atm \right| < \left| ordered\_power_r \right|$ AND $\left| energy\_prim \right| = \left| energy\_to\_cancel \right|$
(stop ramping and remain at current power)

THEN $power\_reduced = power\_atm$
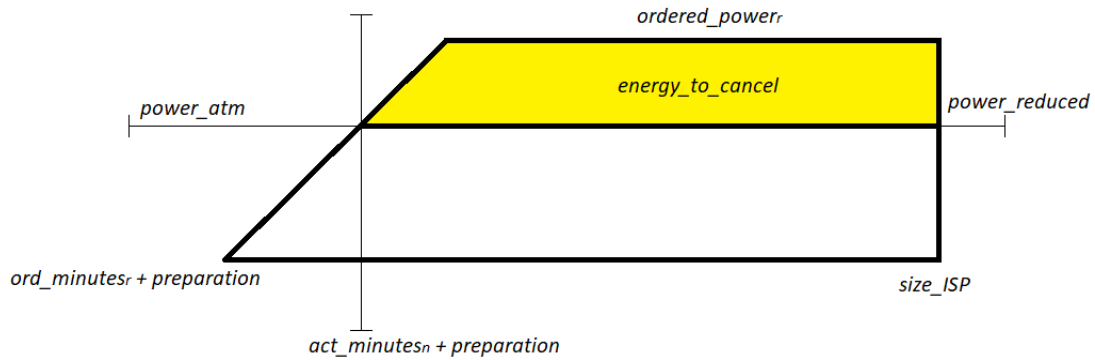
B. IF $\left| power\_atm \right| < \left| ordered\_power_r \right|$ AND $\left| energy\_prim \right| > \left| energy\_to\_cancel \right|$
(keep ramping, but to a lower power than initially ordered)

THEN

$$power\_corr = dir \cdot ramp \cdot \Big(size\_ISP - act\_minutes_n - preparation + 1 - $$
$$- \sqrt{\left(size\_ISP - act\_minutes_n - preparation + 1 \right)^2 - 120 \cdot \left(\left| energy\_prim \right| - \left| energy\_to\_cancel \right| \right) / ramp } \Big)$$

$$power\_reduced = power\_atm + power\_corr$$
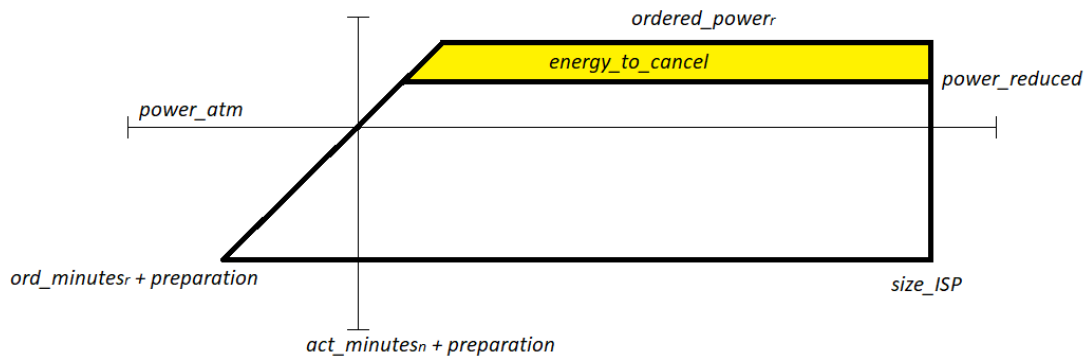
C. IF $power\_atm = ordered\_power_r$
(reduce power)

THEN

$$power\_corr = dir \cdot ramp \cdot \Big(size\_ISP - act\_minutes_n - preparation + 1 -$$
$$- \sqrt{\left(size\_ISP - act\_minutes_n - preparation + 1 \right)^2 - 120 \cdot |energy\_to\_cancel| / ramp} \Big)$$

$$power\_reduced = power\_atm - power\_corr$$

ordered_power$_r$ = power_atm
energy_to_cancel
power_reduced
ord_minutes$_r$ + preparation
size_ISP
act_minutes$_n$ + preparation
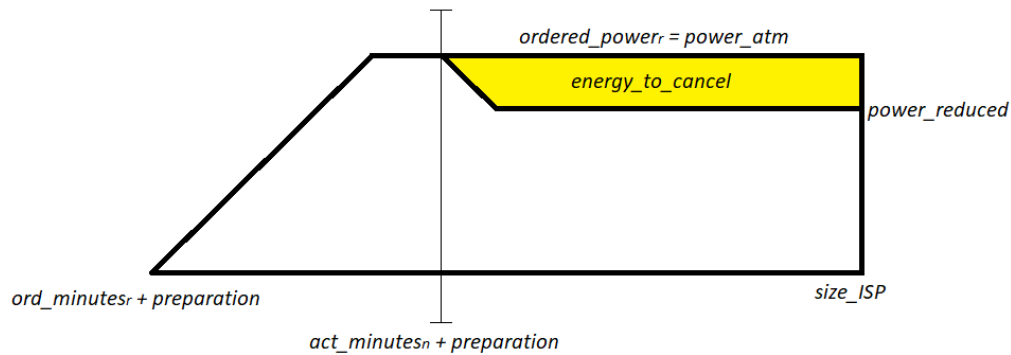
D. IF $|power\_atm| < |ordered\_power_r|$ AND $|energy\_prim| < |energy\_to\_cancel|$
(stop ramping up and partially ramp down)

THEN

$$power\_corr = dir \cdot ramp \cdot \Big(size\_ISP - act\_minutes_n - preparation + 1 -$$
$$- \sqrt{\left(size\_ISP - act\_minutes_n - preparation + 1 \right)^2 - 120 \cdot \left(|energy\_to\_cancel| - |energy\_prim| \right) / ramp} \Big)$$

$$power\_reduced = power\_atm - power\_corr$$

ordered_power$_r$
energy_to_cancel
power_atm
power_reduced
ord_minutes$_r$ + preparation
size_ISP
act_minutes$_n$ + preparation
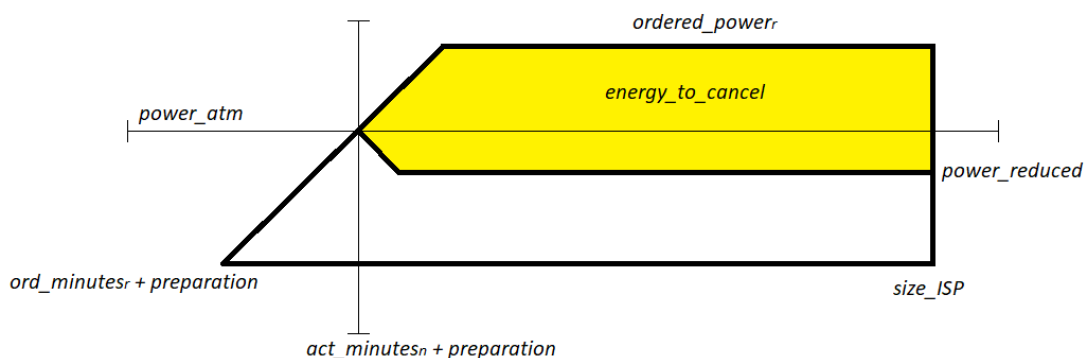
Finally, edit delivered/deliverable balancing energy to reflect the changed power state after partial cancellation of activation *r*:

$$reg\_energy_r = power\_reduced / 60 \cdot \Big(size\_ISP - ord\_minute_r - preparation + 1 -$$
$$- power\_reduced / (2 \cdot ramp) \Big)$$

154

3. Examples of calculation

Maximum power and energy at a given decision minute

size_ISP = 60 min
preparation = 2 min
ramp = 20 MW/min

act_minutes$_n$ = 45

Max reg_energy:

$$reg\_energy = ramp / 120 \cdot \left(size\_ISP - act\_minutes_n - preparation + 1\right)^2 \cdot \text{sign}\left(reg\_energy\right)$$

reg_energy = 32.67 MWh

Max ordered_power:

$$ordered\_power = ramp \cdot \left(size\_ISP - act\_minutes_n - preparation + 1\right) \cdot \text{sign}\left(reg\_energy\right)$$

ordered_power = 280.00 MW

Ordered power from a given regulation energy at a given decision minute

size_ISP = 60 min
preparation = 2 min
ramp = 20 MW/min

act_minutes$_n$ = 45
reg_energy$_r$ = 30.00 MWh

Power from reg_energy:

$$ordered\_power = \text{sign}\left(reg\_energy\right) \cdot ramp \cdot \Big(size\_ISP - act\_minutes_n - preparation + 1 -$$
$$-\sqrt{\left(size\_ISP - act\_minutes_n - preparation + 1\right)^2 - 120 \cdot |reg\_energy| / ramp}\Big)$$

ordered_power = 200.00 MW

155

Full cancellation (goal of calculation: cancellable energy)

2.1. A

size_ISP =	60 min	
preparation =	2 min	
ramp =	20 MW/min	

$$act\_minutes_n \leq \left|ordered\_power_r\right| / ramp + ord\_minutes_r - 1 \qquad \text{TRUE}$$

$$2 \cdot act\_minutes_n + preparation - ord\_minutes_r \leq size\_ISP \qquad \text{TRUE}$$

$act\_minutes_n$ =	33	
$ordered\_power_r$ =	195.85 MW	
$ord\_minutes_r$ =	25	
reg_energy_r =	95.00 MWh	
dir =	1	

$$cancelable\_energy_r = \left(\left| reg\_energy_r \right| - ramp / 60 \cdot \left(act\_minutes_n - ord\_minutes_r \right)^2 \right) \cdot dir$$

$$cancelable\_energy_r = \qquad 73.67 \text{ MWh}$$

size_ISP =	60 min
preparation =	2 min
ramp =	20 MW/min
$act\_minutes_n$ =	35
$ordered\_power_r$ =	195.85 MW
$ord\_minutes_r$ =	25
reg_energy_r =	95.00 MWh
dir =	1

$$act\_minutes_n > \left|ordered\_power_r\right|/ramp + ord\_minutes_r - 1 \qquad \text{TRUE}$$

$$act\_minutes_n + preparation \le size\_ISP - \left|ordered\_power_r\right|/ramp - 1 \qquad \text{TRUE}$$

$$cancelable\_energy_r = \left(\left|ordered\_power_r\right|\cdot\left(size\_ISP - act\_minutes_n - preparation + 1\right)\big/60 - ordered\_power_r^2\big/\left(120\cdot ramp\right)\right)\cdot dir$$

$$cancelable\_energy = \qquad 62.36 \text{ MWh}$$

$ord\_minutes_r + preparation$

$act\_minutes_n + preparation$

$ordered\_power_r$

$cancelable\_energy_r$

$size\_ISP$

157

2.1. C

size_ISP =	60 min
preparation =	2 min
ramp =	20 MW/min

$$act\_minutes_n > \left|ordered\_power_r\right|/ramp + ord\_minutes_r - 1 \qquad \text{TRUE}$$

$$act\_minutes_n + preparation > size\_ISP - \left|ordered\_power_r\right|/ramp - 1 \qquad \text{TRUE}$$

$act\_minutes_n$ =	48
$ordered\_power_r$ =	195.85 MW
$ord\_minutes_r$ =	25
reg_energy_r =	95.00 MWh
dir =	1

$$cancelable\_energy_r = ramp/120 \cdot \left(size\_ISP - act\_minutes_n - preparation + 1\right)^2 \cdot dir$$

cancelable_energy=   20.17 MWh

ordered_power$_r$

cancelable_energy$_r$

ord_minutes$_r$ + preparation

act_minutes$_n$ + preparation

size_ISP

2.1. D

size_ISP =	60 min			
preparation =	2 min			
ramp =	20 MW/min			

$$act\_minutes_n \leq \left|ordered\_power_r\right| / ramp + ord\_minutes_r - 1 \qquad \text{TRUE}$$

$$2 \cdot act\_minutes_n + preparation - ord\_minutes_r > size\_ISP \qquad \text{TRUE}$$

act_minutes$_n$ =	56
ordered_power$_r$ =	640.00 MW
ord_minutes$_r$ =	25
reg_energy$_r$ =	192.00 MWh
dir =	1

$$cancelable\_energy_r = \left(\left|reg\_energy_r\right| - ramp / 60 \cdot \left(act\_minutes_n - ord\_minutes_r\right)^2 + \right.$$
$$\left. + ramp \cdot \left(size\_ISP + ord\_minutes_r - 2 \cdot act\_minutes_n - preparation + 1\right)^2 / 120\right) \cdot dir$$

$$cancelable\_energy = \quad 2.33 \text{ MWh}$$
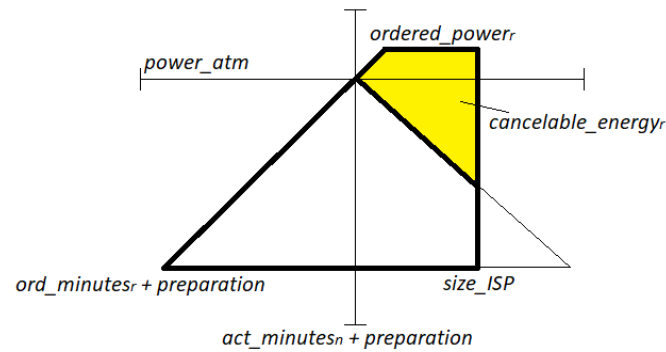
Partial cancellation (goal of calculation: reduced balancing power)

2.3. A

size_ISP =	60 min	energy_prim =	47.50 MWh
preparation =	2 min	power_atm =	100 MW
ramp =	20 MW/min		

$$\left| power\_atm \right| \; < \; \left| ordered\_power_r \right| \qquad \text{TRUE}$$

$act\_minutes_n$ =	30		
$ordered\_power_r$ =	208.41 MW		

$$\left| energy\_prim \right| \; = \; \left| energy\_to\_cancel \right| \qquad \text{TRUE}$$

$ord\_minutes_r$ =	25
reg_energy_r =	100.00 MWh
dir =	1

$$power\_reduced = power\_atm$$

power_reduced = 100 MW

energy_to_cancel = 47.50 MWh

$$energy\_prim = \Big[\big(\left| ordered\_power_r \right| - ramp \cdot \left(act\_minutes_n - ord\_minutes_r \right) \big) / 60 \cdot$$
$$\cdot \big(size\_ISP - act\_minutes_n - preparation + 1 \; -$$
$$- \big(\left| ordered\_power_r \right| - ramp \cdot \left(act\_minutes_n - ord\_minutes_r \right) \big) / \left(2 \cdot ramp \right) \big) \Big] \cdot dir$$

$$power\_atm = \min \big(ramp \cdot \left(act\_minutes_n - ord\_minutes_r \right), \left| ordered\_power_r \right| \big) \cdot dir$$

160

2.3. B

size_ISP =	60 min	energy_prim =	47.50 MWh
preparation =	2 min	power_atm =	100 MW
ramp =	20 MW/min		

$$\left|power\_atm\right| < \left|ordered\_power_r\right| \qquad \text{TRUE}$$

$act\_minutes_n$ =	30
$ordered\_power_r$ =	208.41 MW

$$\left|energy\_prim\right| > \left|energy\_to\_cancel\right| \qquad \text{TRUE}$$

$ord\_minutes_r$ =	25
reg_energy_r =	100.00 MWh
dir =	1

$$power\_corr = ramp \cdot \Big(size\_ISP - act\_minutes_n - preparation + 1 - \sqrt{\left(size\_ISP - act\_minutes_n - preparation + 1\right)^2 - 120 \cdot \left(\left|energy\_prim\right| - \left|energy\_to\_cancel\right|\right)/ramp} \Big) \cdot dir$$

energy_to_cancel =	30.00 MWh

power_corr = 37.42 MW

$$power\_reduced = power\_atm + power\_corr$$

power_reduced = 137.42 MW

$$energy\_prim = \Big[\left(\left|ordered\_power_r\right| - ramp \cdot \left(act\_minutes_n - ord\_minutes_r\right)\right)/60 \cdot$$
$$\cdot \left(size\_ISP - act\_minutes_n - preparation + 1 - \right.$$
$$\left. - \left(\left|ordered\_power_r\right| - ramp \cdot \left(act\_minutes_n - ord\_minutes_r\right)\right)/\left(2 \cdot ramp\right)\right) \Big] \cdot dir$$

$$power\_atm = \min\left(ramp \cdot \left(act\_minutes_n - ord\_minutes_r\right), \left|ordered\_power_r\right|\right) \cdot dir$$
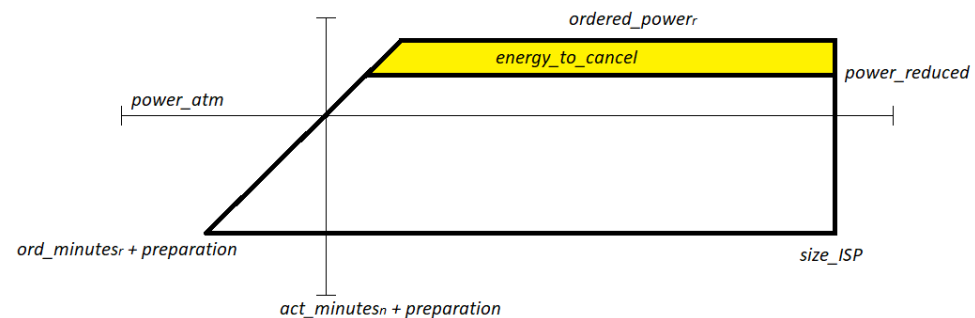
2.3. C

size_ISP =	60 min		
preparation =	2 min	power_atm =	208.41 MW
ramp =	20 MW/min		

$$\left| power\_atm \right| = \left| ordered\_power_r \right| \qquad \text{TRUE}$$

$act\_minutes_n$ =	40
$ordered\_power_r$ =	208.41 MW
$ord\_minutes_r$ =	25
reg_energy_r =	100.00 MWh
dir =	1

$$power\_corr = ramp \cdot \left(size\_ISP - act\_minutes_n - preparation + 1 - \sqrt{\left(size\_ISP - act\_minutes_n - preparation + 1 \right)^2 - 120 \cdot \left| energy\_to\_cancel \right| / ramp} \right) \cdot dir$$

energy_to_cancel =	30.00 MWh	power_corr =	110.93 MW

$$power\_reduced = power\_atm - power\_corr$$

power_reduced =	97.48 MW

$$power\_atm = \min \left(ramp \cdot \left(act\_minutes_n - ord\_minutes_r \right), \left| ordered\_power_r \right| \right) \cdot dir$$

162

2.3. D

size_ISP =	60 min	energy_prim =	47.50 MWh
preparation =	2 min	power_atm =	100 MW
ramp =	20 MW/min		

$$\left|power\_atm\right| < \left|ordered\_power_r\right| \qquad \text{TRUE}$$

$act\_minutes_n$ =	30
$ordered\_power_r$ =	208.41 MW
$ord\_minutes_r$ =	25

$$\left|energy\_prim\right| < \left|energy\_to\_cancel\right| \qquad \text{TRUE}$$

reg_energy_r =	100.00 MWh
dir =	1

$$power\_corr = ramp \cdot \left(size\_ISP - act\_minutes_n - preparation + 1 - \right.$$
$$\left. -\sqrt{\left(size\_ISP - act\_minutes_n - preparation + 1\right)^2 - 120 \cdot \left(\left|energy\_prim\right| - \left|energy\_to\_cancel\right|\right)/ramp} \right) \cdot dir$$

energy_to_cancel =   60.00 MWh   power_corr =   26.46 MW

$$power\_reduced = power\_atm - power\_corr$$

power_reduced =   73.54 MW

$$energy\_prim = \left[\left(\left|ordered\_power_r\right| - ramp \cdot \left(act\_minutes_n - ord\_minutes_r\right)\right)/60 \cdot \right.$$
$$\cdot \left(size\_ISP - act\_minutes_n - preparation + 1 - \right.$$
$$\left. \left. -\left(\left|ordered\_power_r\right| - ramp \cdot \left(act\_minutes_n - ord\_minutes_r\right)\right)/\left(2 \cdot ramp\right)\right)\right] \cdot dir$$
$$power\_atm = \min\left(ramp \cdot \left(act\_minutes_n - ord\_minutes_r\right), \left|ordered\_power_r\right|\right) \cdot dir$$
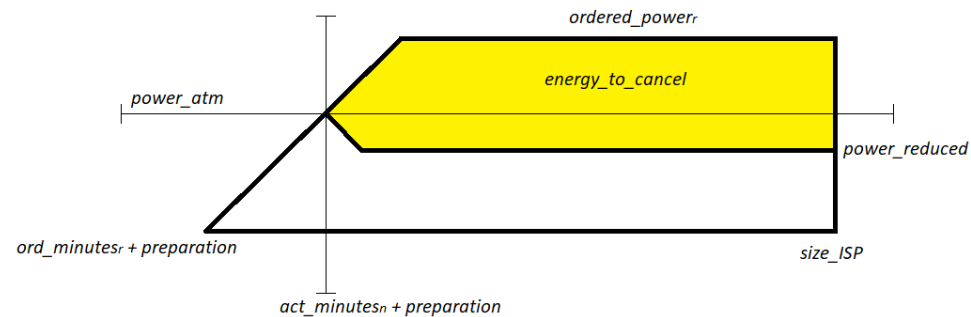
Additional results for SETS impact of power system

Table A4.1. Electricity cost savings from SETS arbitrage, 2020

Scenario	Heating electrifica-tion	Cost savings, M€	Cost savings, %	Cost savings, €/MWh of total consumption	Cost savings, €/MWh of SETS consumption	Cost savings, €/kWh of installed SETS
Base	2%	3.78	0.48%	0.20	12.20	1.21
	10%	10.10	1.09%	0.50	6.51	0.65
	20%	18.75	1.46%	0.75	6.05	0.60
Medium prices	2%	4.00	0.48%	0.21	12.89	1.28
	10%	10.67	1.09%	0.53	6.88	0.68
	20%	19.81	1.46%	0.79	6.39	0.63
High prices	2%	4.21	0.48%	0.22	13.58	1.34
	10%	11.24	1.09%	0.56	7.25	0.72
	20%	20.87	1.46%	0.83	6.73	0.67
Low prices	2%	3.50	0.48%	0.18	11.28	1.12
	10%	9.34	1.09%	0.46	6.02	0.60
	20%	17.34	1.46%	0.69	5.59	0.55
Volatile prices	2%	3.90	0.50%	0.21	12.57	1.24
	10%	10.43	1.12%	0.52	6.73	0.67
	20%	19.61	1.52%	0.78	6.33	0.63
Demand-side measures	2%	1.48	0.19%	0.08	4.79	0.47
	10%	4.94	0.55%	0.25	3.19	0.32
	20%	13.86	1.26%	0.64	4.47	0.44
Heating demand reduction	2%	3.58	0.45%	0.19	12.29	1.22
	10%	9.51	1.04%	0.47	6.53	0.65
	20%	17.23	1.37%	0.69	5.91	0.59

Table A4.2. Electricity cost savings from SETS reserves, 2020

Scenario	Heating electrifica-tion	Cost savings, M€	Cost savings, %	Cost savings, €/MWh of total consumption	Cost savings, €/MWh of SETS consumption	Cost savings, €/kWh of installed SETS
Base	2%	0.11	0.01%	0.01	0.36	0.04
	10%	1.50	0.16%	0.07	0.97	0.10
	20%	5.39	0.42%	0.22	1.74	0.17
Medium prices	2%	0.12	0.01%	0.01	0.38	0.04
	10%	1.58	0.16%	0.08	1.02	0.10
	20%	5.70	0.42%	0.23	1.84	0.18
High prices	2%	0.12	0.01%	0.01	0.40	0.04
	10%	1.67	0.16%	0.08	1.08	0.11
	20%	6.00	0.42%	0.24	1.94	0.19
Low prices	2%	0.10	0.01%	0.01	0.33	0.03
	10%	1.38	0.16%	0.07	0.89	0.09
	20%	4.99	0.42%	0.20	1.61	0.16
Volatile prices	2%	0.12	0.02%	0.01	0.38	0.04
	10%	1.61	0.17%	0.08	1.04	0.10
	20%	5.67	0.44%	0.23	1.83	0.18
Demand-side measures	2%	0.20	0.03%	0.01	0.64	0.06
	10%	0.54	0.06%	0.03	0.35	0.03
	20%	3.26	0.30%	0.15	1.05	0.10
Heating demand reduction	2%	0.10	0.01%	0.01	0.35	0.03
	10%	1.30	0.14%	0.06	0.89	0.09
	20%	4.46	0.36%	0.18	1.53	0.15

Table A4.3. Electricity cost savings from SETS arbitrage, 2030

Scenario	Heating electrifica-tion	Cost savings, M€	Cost savings, %	Cost savings, €/MWh of total consumption	Cost savings, €/MWh of SETS consumption	Cost savings, €/kWh of installed SETS
Base	2%	4.35	0.47%	0.22	14.04	1.39
	10%	11.68	1.07%	0.55	7.54	0.75
	20%	22.12	1.69%	0.98	7.14	0.71
Medium prices	2%	5.11	0.47%	0.26	16.48	1.63
	10%	13.71	1.07%	0.65	8.84	0.88
	20%	25.96	1.69%	1.15	8.37	0.83
High prices	2%	5.86	0.47%	0.30	18.92	1.87
	10%	15.74	1.07%	0.75	10.15	1.01
	20%	29.80	1.69%	1.32	9.61	0.95
Low prices	2%	3.35	0.47%	0.17	10.79	1.07
	10%	8.98	1.07%	0.43	5.79	0.57
	20%	17.00	1.69%	0.75	5.48	0.54
Volatile prices	2%	4.46	0.48%	0.23	14.40	1.43
	10%	12.03	1.11%	0.57	7.76	0.77
	20%	22.99	1.75%	1.02	7.42	0.73
Demand-side measures	2%	1.70	0.19%	0.09	5.49	0.54
	10%	5.57	0.53%	0.26	3.59	0.36
	20%	15.35	1.20%	0.68	4.95	0.49
Heating demand reduction	2%	3.53	0.38%	0.18	14.40	1.43
	10%	9.40	0.90%	0.45	7.67	0.76
	20%	16.41	1.35%	0.75	6.70	0.66

Table A4.4. Electricity cost savings from SETS reserves, 2030

Scenario	Heating electrification	Cost savings, M€	Cost savings, %	Cost savings, €/MWh of total consumption	Cost savings, €/MWh of SETS consumption	Cost savings, €/kWh of installed SETS
Base	2%	0.00	0.00%	0.00	0.00	0.00
	10%	0.09	0.01%	0.00	0.06	0.01
	20%	1.52	0.12%	0.07	0.49	0.05
Medium prices	2%	0.00	0.00%	0.00	0.00	0.00
	10%	0.11	0.01%	0.01	0.07	0.01
	20%	1.79	0.12%	0.08	0.58	0.06
High prices	2%	0.00	0.00%	0.00	0.00	0.00
	10%	0.12	0.01%	0.01	0.08	0.01
	20%	2.05	0.12%	0.09	0.66	0.07
Low prices	2%	0.00	0.00%	0.00	0.00	0.00
	10%	0.07	0.01%	0.00	0.05	0.00
	20%	1.17	0.12%	0.05	0.38	0.04
Volatile prices	2%	0.00	0.00%	0.00	0.00	0.00
	10%	0.09	0.01%	0.00	0.06	0.01
	20%	1.62	0.12%	0.07	0.52	0.05
Demand-side measures	2%	0.00	0.00%	0.00	0.00	0.00
	10%	0.01	0.00%	0.00	0.01	0.00
	20%	1.01	0.08%	0.04	0.33	0.03
Heating demand reduction	2%	0.00	0.00%	0.00	0.00	0.00
	10%	0.04	0.00%	0.00	0.03	0.00
	20%	0.56	0.05%	0.03	0.23	0.02

Table A4.5. Electricity cost savings from SETS arbitrage, 2050

Scenario	Heating electrifica-tion	Cost savings, M€	Cost savings, %	Cost savings, €/MWh of total consumption	Cost savings, €/MWh of SETS consumption	Cost savings, €/kWh of installed SETS
Large Scale RES	2%	5.88	0.17%	0.10	18.97	1.88
	10%	16.23	0.44%	0.26	10.47	1.04
	20%	23.15	0.60%	0.37	7.47	0.74
100% RES	2%	5.75	0.20%	0.12	18.54	1.84
	10%	15.81	0.52%	0.31	10.20	1.01
	20%	23.12	0.71%	0.44	7.46	0.74
Big & Market	2%	5.76	0.19%	0.11	18.57	1.84
	10%	15.85	0.50%	0.30	10.23	1.01
	20%	23.03	0.68%	0.42	7.43	0.74
Fossil & Nuclear	2%	5.83	0.18%	0.10	18.80	1.86
	10%	16.09	0.46%	0.28	10.38	1.03
	20%	23.08	0.62%	0.39	7.44	0.74
Small & Local	2%	5.67	0.25%	0.15	18.28	1.81
	10%	15.54	0.65%	0.39	10.03	0.99
	20%	23.61	0.89%	0.57	7.62	0.75

Table A4.6. Electricity cost savings from SETS reserves, 2050

Scenario	Heating electrificatio n	Cost savings, M€	Cost savings, %	Cost savings, €/MWh of total consumption	Cost savings, €/MWh of SETS consumption	Cost savings, €/kWh of installed SETS
Large Scale RES	2%	0.39	0.01%	0.01	1.25	0.12
	10%	1.55	0.04%	0.03	1.00	0.10
	20%	2.26	0.06%	0.04	0.73	0.07
100% RES	2%	0.00	0.00%	0.00	0.00	0.00
	10%	1.42	0.05%	0.03	0.92	0.09
	20%	2.28	0.07%	0.04	0.73	0.07
Big & Market	2%	0.33	0.01%	0.01	1.07	0.11
	10%	1.02	0.03%	0.02	0.66	0.06
	20%	2.22	0.07%	0.04	0.72	0.07
Fossil & Nuclear	2%	0.35	0.01%	0.01	1.14	0.11
	10%	1.85	0.05%	0.03	1.20	0.12
	20%	2.51	0.07%	0.04	0.81	0.08
Small & Local	2%	0.00	0.00%	0.00	0.00	0.00
	10%	0.00	0.00%	0.00	0.00	0.00
	20%	0.00	0.00%	0.00	0.00	0.00

Table A4.7. Types of buildings connected to the representative feeder network and their total heated space for the Latvian distribution grid study

Feeder No	Type of building	Heated space, m²
1	apartment building (31 ap.)	1550
	apartment building (27 ap.)	1275
	detached house	80
	detached house	80
2	apartment building (66 ap.)	3300
	detached house	120
3	small business	100
	detached house	200
4	apartment building (17 ap.)	850
5	apartment building (54 ap.)	2700
	apartment building (31 ap.)	1550
6	medium business	1000
	detached house	80
	apartment building (66 ap.)	3300
7	apartment building (27 ap.)	1275
	apartment building (17 ap.)	850
	public building	2060
8	small business	100
	detached house	200
	public building	800
9	small business	50
	apartment building (54 ap.)	2700

Algorithm of power system benefit assessment from SETS

```
                    ( Start )

              ┌──────────────────┐        ┌─────────────────────────────────────┐
              │ Base timeseries  │◄───────│  Exogenous time series              │
              │ preprocessing    │        │  • ENTSO-E Transparency Platform     │
              └──────────────────┘        │  • Nord Pool                         │
                                          │  • LVĢMC                             │
              ┌──────────────────┐        │  • AST                               │
              │ s = 1...23       │        │  • Elering                           │
              │ (for each        │        │  • Optibidus-TEC                     │
              │  scenario)       │        └─────────────────────────────────────┘
              └──────────────────┘

              ┌──────────────────┐        ┌─────────────────────────────────────┐
              │ Prepare scenario │◄───────│  Scenario data                       │
              │ input timeseries │        │  • Distribution grid modelling results│
              └──────────────────┘        │  • EU REF 2016                       │
                                          │  • e-Highway2050                     │
              ┌──────────────────┐        │  • AST                               │
              │ t = 1...8760     │        └─────────────────────────────────────┘
              │ (for each hour)  │
              └──────────────────┘

              ┌──────────────────┐
              │ 1st price        │
              │ iteration        │
              │ (scaled input    │
              │  price)          │
              └──────────────────┘
```

1st price iteration
(scaled input price)

Estimate market flow EE–LV
Eq. (3.34)

Linear regression to find coefficient a
Eq. (3.35)

$P_{EE\text{-}LV}^{approx.1} > P_{norm.NTC}$?   0

1

2nd price iteration
Eq. (3.36)

2nd price iteration
(same as 1st)

Add SETS load

Add DRH load

3rd price iteration
Eq. (3.38)

3rd price iteration
Eq. (3.37)

Update market flow
Eq. (3.41)

Calculate increased NTC
Eq. (3.39)

Eq. (3.40) &
Eq. (3.42) &
Eq. (3.43)

0

1

4th price iteration
(same as 3rd)

4th price iteration
Eq. (3.44)

Calculate benefit from
SETS scheduling
Eq. (3.45)

Calculate benefit from
SETS reserves
Eq. (3.46)

Calculate full benefit
from SETS
Eq. (3.47)

(End)